

**STRUCTURE-FUNCTION RELATIONSHIPS IN
SERINE HYDROXYMETHYLTRANSFERASE**

A THESIS SUBMITTED TO

THE UNIVERSITY OF MYSORE, MYSORE,

FOR THE DEGREE OF

DOCTOR OF PHILOSOPHY

IN

BIOCHEMISTRY

BY

BHAVANI B. S.

DEPARTMENT OF PROTEIN CHEMISTRY AND TECHNOLOGY

CENTRAL FOOD TECHNOLOGICAL RESEARCH INSTITUTE

MYSORE - 570020, INDIA

MAY, 2009

DECLARATION

I hereby declare that the thesis entitled “**Structure-Function Relationships in Serine Hydroxymethyltransferase**” which is submitted herewith for the degree of **Doctor of Philosophy in Biochemistry** to the **University of Mysore, Mysore** is the result of research work done by me in the Department of Protein Chemistry and Technology, Central Food Technological Research Institute, Mysore, India under the guidance of **Dr. V. Prakash**, Director, Central Food Technological Research Institute, Mysore during the period May 2005 - 2009.

I further declare that the results of this work have not been previously submitted for any degree or fellowship.

Date: May 2, 2009
Place: Mysore

Bhavani B. S.

CERTIFICATE

I hereby certify that the thesis entitled “**Structure-Function Relationships in Serine Hydroxymethyltransferase**” submitted by **Ms. B. S. Bhavani** for the degree of **Doctor of Philosophy in Biochemistry** to the University of Mysore, Mysore is the result of research work carried out by her in the Department of Protein Chemistry and Technology, Central Food Technological Research Institute, Mysore, India under my guidance and supervision during the period May 2005 - 2009.

I further declare that the results of the work have not been submitted either partially or fully to any other degree or fellowship.

Date: May 2, 2009
Place: Mysore

Dr. V. Prakash
Guide and Supervisor
&
DIRECTOR
Central Food Technological Research Institute
Mysore - 570 020, India

Acknowledgements

*I express my deep sense of gratitude and sincere thanks to **Dr. V. Prakash, Director, Central Food Technological Research Institute, Mysore**, for giving me an opportunity to carry out research in his laboratory. He has been an inspiring mentor who taught me the importance of planning, in the execution of experiments and presentation of scientific data. I will always remember his guidance, support and care extended to me in all aspect during my studies.*

*I am indeed fortunate to have worked with **Prof. H.S. Savithri** and **Prof. N. Appaji Rao**, Department of Biochemistry, Indian Institute of Science, Bangalore. Prof. N. Appaji Rao with his enormous patience in teaching me science, endless zeal for discussions, in depth knowledge to correct even the smallest error and constant encouragement has been a source of inspiration to me. Prof. H.S. Savithri with her cheerful demeanour and care has been instrumental in making me a wholesome person. They have been truly inspirational mentors with sincere and meticulous guidance without which I wouldn't have reached this goal. Their concern for my well being was phenomenal and I will always cherish my association with them.*

*My sincere thanks to **Prof. M.R.N. Murthy**, Molecular Biophysics Unit, IISc, Bangalore, for his wonderful support and valuable suggestions in structural studies of SHMT mutants. All X-ray structures described in the thesis were carried out in collaboration with Prof. M.R.N. Murthy.*

My sincere thanks are due to Dr. Purnima Kaul for her help in carrying out stopped-flow experiments and kind support during my work. I extend my sincere thanks to Dr. A. G. Appu Rao, the Head of the Department, staff members and fellow colleagues in the Department of Protein Chemistry and Technology, CFTRI, Mysore. It was always pleasure to talk to Dr. Jyothi Lakshmi who has been very kind and helpful, thanks are due to her care and the moral support. I thank Dr. K.N. Gurudatt, former head of FSAQCL department, CFTRI, Mysore for his valuable inputs regarding the mechanism of SHMT catalyzed reaction. I thank Prof. Anjali Karande for her support and her cheerful presence will always be remembered. Special thanks to Dr. Nagasuma R Chandra and Prof. N. Srinivasan, IISc, for their help in enzyme docking studies. I would also like to place a record to the authors of some of the manuscripts from where I have borrowed figures for the introduction and to bring out points from discussion in chapters are duly acknowledged in the respective figures.

I acknowledge all the past and present members of Dr. Prakash's, Prof. N. Appaji Rao's, Prof. H.S. Savithri's, Prof M.R.N.Murthy's and Prof. Anjali Karande's laboratory for their support and in creating a congenial work place.

Thanks are due to Dr. V. Rajaram and Ms. Shveta Bisht for their help in determination of the structures of SHMT mutants. Special thanks to Mr. Sagar Chittori for his help in carrying out docking studies.

Friends have been the life line of my stay both in the CFTRI and IISc campus. Rajani, Jimsheena, Poornima, Naveen Kumar, Jyothi, Lisa, Deepa, have been constant companions who have been very helpful. I cherish the happy moments I have had with them. Mere words of thanks would not suffice for their help, support and encouragement. I will always remember the wonderful times I had with them all through my work as research fellow and in life.

Umashankar & his family, Shankar Prakash, Chandrika & little Nomtha deserve a special mention for always being there in my times of need.

I acknowledge with reverence the love and encouragement given to me by my late mother, father and sisters.

My special thanks are due to the Council of Scientific and Industrial Research, New Delhi, India, for providing Senior Research Fellowship for my work.

May 2, 2009
Mysore

Bhavani B. S.

CONTENTS

PARTICULARS	Page No.
<i>LIST OF ABBREVIATIONS</i>	ii
<i>LIST OF FIGURES</i>	vi
<i>LIST OF TABLES</i>	xii
<i>LIST OF SCHEMES</i>	xiv
INTRODUCTION	1
SCOPE AND OBJECTIVES	42
MATERIALS AND METHODS	46
RESULTS AND DISCUSSION	
CHAPTER 1:	62
The role of lysine 226 in the reaction catalyzed by bsSHMT.	
CHAPTER 2:	104
The involvement of glutamate 53 in binding of L-serine and folate, and conversion of bsSHMT from ‘open’ to ‘closed’ form.	
CHAPTER 3:	152
The role of tyrosine residues in cofactor binding and elucidation of mechanism for the tetrahydrofolate-independent cleavage of L- <i>allo</i> threonine.	
CHAPTER 4:	181
The interaction of bsSHMT with inhibitors from extracts of various spices.	
SUMMARY AND CONCLUSIONS	214
REFERENCES	222

LIST OF ABBREVIATIONS

A	absorbance
AAA	aminoxyacetic acid
AAT	aspartate aminotransferase
ADH	alcohol dehydrogenase
α	alpha
ALA	5-aminolevulinate synthase
ALR	alanine racemase
Å	Angstrom
AU	absorbance unit
β	beta
bp	base pair
BSA	bovine serum albumin
bsSHMT	recombinant <i>Bacillus stearothermophilus</i> SHMT
°C	degree Celsius
C ₁	one-carbon fragment
CD	circular dichroism
C _i	Curie
Cpm	counts per minute
Da	Dalton
DADS	diallyl disulfide
DCS	D-cycloserine
DEAE	diethylamino ethane
DGD	dialkylglycine decarboxylase
DHFR	dihydrofolate reductase
Dimedone	5,5'-dimethylcyclohexane-1,3-dione
3D	three-dimensional
DNA	deoxyribonucleic acid
dNTP	deoxyribonucleoside triphosphate
DTT	dithiothreitol
EDTA	ethylenediaminetetraacetic acid
eSHMT	recombinant <i>Escherichia coli</i> SHMT

FPA	family profile analysis
FTHF	5- formyltetrahydrofolate
g	gram
γ	gamma
GABA	γ -aminobutyric acid
Gem-diamine	geminal-diamine
h	hour
HCHO	formaldehyde
hcSHMT	recombinant human liver cytosolic SHMT
HEPES	N-[2-hydroxyethyl]piperazine-N'-[2-ethylenesulfonic acid])
ITPG	isopropyl-1-thio- β -D-galactopyranoside
k_{cat}	catalytic turn over
k_d	dissociation constant
kDa	kilo Dalton
K_m	Michaelis-Menten constant
λ	lambda
λ_{max}	absorption maximum (wavelength)
L	litre
LB	Luria-Bertani medium
μ	micro
M	molar
$M^{-1} \text{ cm}^{-1}$	per molar per centimeter
MA	methoxyamine
mcSHMT	recombinant murine liver cytosolic SHMT
2-ME	2-mercaptoethanol
μg	microgram
ml	milliliter
mm	millimeter
mM	millimolar
min	minute
MPD	2-methyl-2,4-pentanediol
ms	millisecond
NAD	nicotineaminde adenine dinucleotide

NADH	nicotineamide adenine dinucleotide, reduced
n	nano
nm	nanometer
OADS	O-amino-D-serine
OAS	O-acetylserine sulphydrylase
OAT	ornithine aminotransferases
O D	optical density
ODC	ornithine decarboxylase
PAGE	polyacrylamide gel electrophoresis
PCR	polymerase chain reaction
pH	$-\log [H^+]$
PLP	pyridoxal 5'-phosphate
PMP	pyridoxamine 5'-phosphate
PPO	2, 5-diphenyloxazole
QI	quinonoid intermediate
%	percentage
θ	observed ellipticity in degrees
MRW	mean residue weight
rcSHMT	recombinant rabbit liver cytosolic SHMT
rms	root mean square
RT	room temperature ($25 \pm 2^\circ\text{C}$)
SAM	S-adenosyl-L-methionine
SDS	sodium dodecyl sulfate
s	second
scSHMT	recombinant sheep liver cytosolic SHMT
SHMT	serine hydroxymethyltransferase
TATase	tyrosine (aromatic) aminotransferase
TB	terrific broth
TEMED	N,N,N',N'-tetramethylethylenediamine
THF	tetrahydrofolate
Thy S	thymidylate synthase
TPL	tyrosine phenol lyase
TS	tryptophan synthase

TSC	thiosemicarbazide
Tris	tris-(hydroxymethyl)-aminoethane
U	units
UV	ultra-violet
V	volt
Vol	volume
Vs	versus
v/v	volume/volume
w/v	weight/volume
w/w	weight/weight
[3- ¹⁴ C] L-Ser	radiolabelled L- Ser at carbon number 3

Fig I.1	refers to the figures presented in Introduction
Fig 1.1	refers to the figures presented in Chapter 1
Fig 2.1	refers to the figures presented in Chapter 2
Fig 3.1	refers to the figures presented in Chapter 3
Fig 4.1	refers to the figures presented in Chapter 4

Abbreviation for amino acids:

Both three letter and one letter code are used for the abbreviation of amino acids

LIST OF FIGURES (Figure number and Titles)

- Fig I.1: The formation of an external aldimine from internal aldimine via a gem- diamine intermediate.
- Fig I.2: A representation of catalytic diversity among PLP-dependent enzymes.
- Fig I.3: Representative enzyme structures of different fold-type PLP-enzymes.
- Fig I.4: Stereo-chemical explanation for reaction specificity in PLP-enzymes.
- Fig I.5: Steric control of reaction type by dialkylglycine decarboxylase.
- Fig I.6: Schematic representation of the Arg-switch in aminotransferases when both dicarboxylic and aromatic amino acids are used as substrates.
- Fig I.7: Dual substrate specificity can also be achieved by hydrogen bond rearrangement.
- Fig I.8: Conversion of L-Ser to Gly by SHMT.
- Fig I.9: The role of SHMT in metabolism.
- Fig I.10: A schematic representation for enzymes involved in biosynthesis of thymidylate.
- Fig I.11: Structural relationship among aminoxy compounds and amino acid analogues.
- Fig I.12: Structure of bio-active compounds from garlic, turmeric, ginger and chilli.

-
- Fig 1.1: The active site of bsSHMT internal and external aldimine with L-Ser.
- Fig 1.2: SDS-PAGE (12%) analysis of the fractions obtained during the purification of bsSHMT.
- Fig 1.3: SDS-PAGE (12%) analysis of Lys mutants.
- Fig 1.4: Far-UV CD spectra of bsSHMT, K226M and K226Q bsSHMT.
- Fig 1.5: Visible absorption spectra of (a) bsSHMT and (b) K226M bsSHMT before and after sodium cyanoborohydride reduction.
- Fig 1.6: The transamination reaction catalyzed by bsSHMT and K226M bsSHMT.

- Fig 1.7: The reconstitution of apo-enzymes of bsSHMT and Lys mutants with PLP and their interaction with Gly and Gly+THF.
- Fig 1.8: The absorbance changes on the addition of Gly, Gly+THF to bsSHMT (a), K226M (b) and K226Q bsSHMT (c).
- Fig 1.9: Absorbance changes on the addition of Gly, Gly+FTHF to bsSHMT (a), K226M (b) and K226Q bsSHMT (c).
- Fig 1.10: The increase in absorbance for 50s at 495 nm when the bsSHMT was mixed with 10/50 mM Gly in the stopped-flow spectrophotometer.
- Fig 1.11: The increase in absorbance for 200s at 495 nm when bsSHMT was mixed with 10/50 mM Gly in the stopped-flow spectrophotometer.
- Fig 1.12: The decrease in absorbance at 343 nm on mixing bsSHMT with 50 mM Gly in the stopped-flow spectrophotometer.
- Fig 1.13: The increase in absorbance at 425 nm on mixing bsSHMT with Gly in the stopped-flow spectrophotometer.
- Fig 1.14: The stopped-flow scan at 495 nm upon addition of 50 mM Gly to K226M bsSHMT.
- Fig 1.15: The stopped-flow scan at 412/425 nm for the formation of external aldimine upon addition of 50 mM Gly to K226M/K226Q bsSHMT.
- Fig 1.16: The initial increase in absorbance at 495 nm when the bsSHMT (10 mg ml^{-1})-Gly (50 mM) was mixed with THF (70 μM) in stopped-flow spectrophotometer and relative absorbance measured for 50 ms.
- Fig 1.17: The decrease in absorbance at 495 nm on mixing bsSHMT (10 mg ml^{-1})-Gly (50 mM) with THF (70 μM) in stopped-flow spectrophotometer and the reaction was measured for 1 s.
- Fig 1.18: The final increase in absorbance at 495 nm on mixing of bsSHMT (10 mg ml^{-1})-Gly (50 mM) with THF (70 μM) in the stopped-flow spectrophotometer and relative absorbance measured for 100 s.
- Fig 1.19: A graphical representation of the overall reaction on addition of THF to bsSHMT-Gly binary complex, showing initial fast phase and a slow phase.
- Fig 1.20: A graphical comparison of the formation of the quinonoid intermediate upon addition of THF to bsSHMT and Lys mutant Gly binary complexes.
- Fig 1.21: Interaction of MA with bsSHMT and K226M bsSHMT.
- Fig 1.22: The relative absorbance changes of bsSHMT at (a) 425 and (b) 388 nm on addition of MA.

- Fig 1.23: The relative absorbance changes on addition of MA to bsSHMT at (c) 388 and (d) 325 nm.
- Fig 1.24: Interaction of K226M and K226Q bsSHMT with of 10 mM of MA.
- Fig 1.25: The comparison of crystal structures of bsSHMT and K226M bsSHMT.
- Fig 1.26: An overlay of L-Ser external aldimine structures of bsSHMT and K226M bsSHMT.
-
- Fig 2.1: The crystal structure of bsSHMT-Ser and bsSHMT-Gly-FTHF complexes.
- Fig 2.2: SDS-PAGE (12%) analysis of the fractions obtained during the purification of E53Q bsSHMT.
- Fig 2.3: A stereo diagram of E53Q bsSHMT showing active site residues.
- Fig 2.4: A stereo view of electron density maps showing Gly external aldimine in E53Q and bsSHMT.
- Fig 2.5: Absorbance changes on the addition of L-Ser, L-Ser + THF/FTHF to bsSHMT and E53Q bsSHMT.
- Fig 2.6: The visible CD spectrum of bsSHMT and E53Q bsSHMT with L-Ser.
- Fig 2.7: The visible CD spectra of bsSHMT and E53Q bsSHMT with Gly.
- Fig 2.8 (a): A stereo diagram illustrating electron density corresponding to PLP and L-Ser in E53Q bsSHMT-Ser.
- Fig 2.8 (b): A stereo diagram illustrating electron density corresponding to PLP and Gly in E53Q-Gly complex.
- Fig 2.9: The absorbance changes on the addition of Gly, Gly + THF/FTHF to bsSHMT or E53Q bsSHMT.
- Fig 2.10: The time course of disappearance of quinonoid intermediate in E53Q bsSHMT and bsSHMT ternary complexes.
- Fig 2.11: PLP content of bsSHMT and E53Q bsSHMT ternary complexes after dialysis.
- Fig 2.12: A stereo diagram illustrating electron density corresponding to the gem-diamine formed in E53Q bsSHMT in the presence of Gly and FTHF.
- Fig. 2.13: A superposition of residues Y51, E53, Y60 and PLP in E53Q bsSHMT-Gly(FTHF) (yellow) and E53Q bsSHMT-Gly (brown).

- Fig 2.14: A superposition of residues Y51, E53, Y60 and PLP in E53Q bsSHMT-Gly(FTHF)(yellow) and bsSHMT-Gly-FTHF(blue).
- Fig 2.15: Visible CD spectra of bsSHMT-Gly-FTHF and E53Q bsSHMT-Gly(FTHF).
- Fig 2.16: Double reciprocal plots for the formation of quinonoid intermediate before and after dialysis of bsSHMT-Gly-FTHF and E53Q bsSHMT-Gly(FTHF).
- Fig 2.17: The visible CD spectrum of E53Q bsSHMT-Gly-FTHF ternary complex depicting the formation and decomposition of gem-diamine on dialysis.
- Fig 2.18: The visible CD spectrum of E53Q bsSHMT-Gly-FTHF ternary complex dialyzed against buffer D containing Gly (50 mM) for different time intervals.
- Fig 2.19: Reduction of undialyzed E53Q bsSHMT and dialyzed E53Q bsSHMT with NaCNBH₃.
-
- Fig 3.1: Active site geometry of bsSHMT-Ser complex depicting the possible residues involved in catalysis.
- Fig 3.2: SDS-PAGE profile of Y51F, Y61A and Y61F bsSHMT.
- Fig 3.3: An overlay of internal aldimine spectra of bsSHMT, Y51F, Y61F and Y61A bsSHMT.
- Fig 3.4: The reduction of bsSHMT and Y51F bsSHMT by NaCNBH₃.
- Fig 3.5: Interactions of bsSHMT and Tyr mutants with MA.
- Fig 3.6: A superposition of the active sites of bsSHMT (blue) and Y51F bsSHMT (yellow) showing the differences in conformation of residues Y/F51, E53, Y60 and Y61.
- Fig 3.7: Transamination reaction catalyzed by bsSHMT and Tyr mutants.
- Fig 3.8: The spectral changes on addition of L-Ser/Gly and Gly + THF/FTHF to bsSHMT, Y51F, Y61F and Y61A bsSHMT.
- Fig 3.9: The visible CD spectrum of bsSHMT and Tyr mutants and changes on addition of L-Ser and Gly.
- Fig 3.10: A stereo diagram showing an electron density for gem- diamine in Y51F bsSHMT-Gly complex.
- Fig 3.11: A superposition of Y51F bsSHMT (yellow) and bsSHMT (blue) complexes obtained in the presence of L-*allo* Thr.

Fig 3.12: The electron density corresponding to L-*allo* Thr in Y61A bsSHMT.

Fig 4.1: The interaction of bsSHMT and E53Q bsSHMT with MA.

Fig 4.2: The decrease in relative absorbance at 425 nm on addition of MA (2 mM) to E53Q bsSHMT (10 mg ml⁻¹).

Fig 4.3: The increase in relative absorbance at 325 nm on addition of MA (2 mM) to E53Q bsSHMT (10 mg ml⁻¹).

Fig 4.4: The interaction of bsSHMT with AAA.

Fig 4.5: The interaction of E53Q bsSHMT with AAA.

Fig 4.6: The interaction of Y51F, Y61F and Y61A bsSHMT with AAA.

Fig 4.7: The interaction of K226M and K226Q bsSHMT with AAA.

Fig 4.8: The stopped-flow tracings of decrease at 425 nm on addition of AAA (0.5 mM) to bsSHMT (10 mg ml⁻¹).

Fig 4.9: The stopped-flow tracings of increase at 325 nm on addition of AAA (0.5 mM) to bsSHMT (10 mg ml⁻¹).

Fig 4.10: The decrease at 425 nm on addition of AAA (0.5mM) to E53Q bsSHMT (10 mg ml⁻¹).

Fig 4.11: The increase at 388 nm on addition of AAA to E53Q bsSHMT AAA (0.5mM) to E53Q bsSHMT (10 mg ml⁻¹).

Fig 4.12: The decomposition of intermediate absorbing at 388 nm on addition of AAA (0.5mM) to E53Q bsSHMT (10 mg ml⁻¹).

Fig 4.13: The increase at 325 nm on addition of AAA (0.5mM) to E53Q bsSHMT (10 mg ml⁻¹).

Fig 4.14: A Graphical representation for the effect of folate analogues on bsSHMT.

Fig 4.15: A model representation of bsSHMT active site structure docked with L-Ser.

Fig 4.16: (a) An overlay of bsSHMT and docked OADS (b) The active site region of bsSHMT with docked OADS.

Fig 4.17: An overlay of bsSHMT with docked folate analogues.

- Fig 4.18: The binding region of (a) HTS and (b) SPB on bsSHMT.
- Fig 4.19: The effect of essential oils on bsSHMT activity.
- Fig 4.20: The effect of spice extracts on bsSHMT.
- Fig 4.21: An inhibition analysis of bsSHMT activity with garlic extract.
- Fig 4.22: An inhibition analysis of bsSHMT activity by water extract of garlic.
- Fig 4.23: An inhibition analysis of bsSHMT with Alliin, D and L-allyl Gly.
- Fig 4.24: An active site of bsSHMT depicting the docked OADS, S-allyl Cys, Alliin and L-allyl Gly.
-

LIST OF TABLES (Table numbers and Titles)

Table I.1: THF-dependent and – independent reactions catalyzed by SHMT.

Table I.2: Amino acid residues essential for maintaining the structure and function of SHMTs.

Table I.3: List of compounds examined as inhibitors for SHMT.

Table 1.1: A typical purification procedure and activity assay for recombinant bsSHMT.

Table 1.2: Catalytic activity and PLP content of bsSHMT, K226M and K226QbsSHMT.

Table 1.3: The rate for the formation of quinonoid intermediate at 495 nm for bsSHMT-Gly binary complex with varying concentration of Gly and different time points.

Table 1.4: The rate of formation of external aldimine and gem-diamine on addition of Gly to K226M bsSHMT.

Table 1.5: The rate for enhanced formation of quinonoid intermediate on addition of THF to bsSHMT-Gly complex.

Table 2.1: Kinetic constants for bsSHMT and E53Q bsSHMT.

Table 2.2: The apparent T_m (°C) values for bsSHMT and E53Q bsSHMT in the presence and absence of L-Ser and Gly.

Table 2.3: The time course for the disappearance of quinonoid intermediate.

Table 2.4: The rate constants for formation of quinonoid intermediate on addition of Gly, Gly + THF/FTHF to bsSHMT or E53Q bsSHMT.

Table 3.1: Enzymatic activities of bsSHMT and its Tyr mutants.

Table 4.1: Rate contents for bsSHMT and E53Q bsSHMT on interaction with AAA.

Table 4.2: A list of docked folate analogues.

Table 4.3: Table showing binding energy and cluster rank for OADS.

Table 4.4: Table showing binding energy and cluster rank for TSC.

Table 4.5: Table showing binding energy and cluster rank for Alliin.

Table 4.6: The table showing binding energy and cluster rank for L-allyl Gly.

Table 4.7: The table showing binding energy and cluster rank for S-allyl Cys.

LIST OF SCHEMES (Scheme number and Titles)

Scheme 1.1: Schematic representation of the role of Lys 226 in the reaction catalyzed by bsSHMT with L-Ser and Gly.

Scheme 2.1: Formation of L-Ser-external aldimine from internal aldimine via a gem-diamine intermediate.

Scheme 2.2: Retroaldol (shown in red) and direct displacement mechanisms (shown in blue) proposed for SHMT catalysis.

Scheme 2.3: A concerted mechanism which, combines retroaldol and nucleophilic displacement mechanisms.

Scheme 2.4: Probable mechanism for E53Q bsSHMT exhibiting enzyme memory.

Scheme 2.5: Schematic representation of the role of E53Q bsSHMT in SHMT catalyzed reverse reaction with L-Ser. As proposed from the data.

Scheme 2.6: Schematic representation of the role of E53Q bsSHMT in SHMT catalyzed reaction with Gly. As proposed from the data.

Scheme 3.1: Reaction mechanisms proposed for THF-dependent cleavage of L-Ser and THF-independent cleavage of 3-hydroxy amino acids by SHMT.

Scheme 3.2: Proposed mechanism for cleavage of L-*allo* Thr by bsSHMT.

Title of Ph.D. Thesis:

Structure – Function Relationships in Serine Hydroxymethyltransferase

A study of enzymes is central to an understanding of biological function. The binding of substrate(s) to an enzyme and its fit at the active site facilitates a multitude of chemical reactions. The mechanisms of catalysis include general acid-base, covalent and metal ion catalysis. The study of structure-function of enzymes has been central to the elucidation of catalytic mechanism of biochemical reactions. In addition to the factors mentioned above, coenzymes which are vitamin derivatives have provided several new insights into biology.

The versatility of vitamin B6 and the wide distribution of pyridoxal 5'-phosphate (PLP)-dependent enzymes are reflected in the observation that 4% of all catalytic reactions involve this co-enzyme. The availability of biochemical and structural information on more than 140 PLP-enzymes gives a good handle to understand the organization of PLP-enzymes in detail. This information has helped in elucidating the diverse reaction mechanisms of PLP-enzymes. SHMT, one of the PLP-enzymes, the subject of this study belongs to the α -family. It links amino acid and nucleotide metabolism. Serine hydroxymethyltransferase (SHMT) catalyzes THF-dependent hydroxymethyltransfer from L-Ser to tetrahydrofolate (THF) to yield 5, 10-CH₂ THF and Gly. This reaction provides one-carbon fragments for a wide variety of end products in mammalian systems. SHMT being a part of thymidylate cycle, suggested that it could be an alternative target for cancer chemotherapy. SHMT, in addition to L-Ser and Gly inter-conversion, catalyzes THF-independent cleavage of 3-hydroxy amino acids. L-Thr/L-*allo* Thr cleavage by SHMT results in production of acetaldehyde which is a major flavoring compound in production of fermented dairy products. Hence SHMT can be used as a starter culture in the manufacture of dairy products. SHMT can also be used as a biocatalyst in the synthesis of β -hydroxy- α -amino acid derivatives.

The objectives of the present investigation are: biochemical characterization of selected residues involved in THF-dependent and -independent reactions; crystallization of the mutant enzymes with their substrate(s)/inhibitor complexes to understand the role of these residues; probe the retroaldol and direct displacement mechanisms for the THF-dependent L-Ser cleavage; establish the mechanism of THF-independent cleavage of 3-hydroxy amino acids by mutation of specific amino acid residues; and study the interaction of chemical inhibitors and compounds from natural sources to understand the role of SHMT in cancer. With these objectives the present investigation was undertaken and results and conclusions are presented in the form of thesis entitled “***Structure – Function Relationships in Serine Hydroxymethyltransferase***”.

The present study is divided into four chapters:

Chapter 1: The role of lysine226 in the reaction catalyzed by bsSHMT

Lys residue at the active site of PLP-enzymes in addition to anchoring PLP functions as a proton acceptor or a donor in catalysis. It has been proposed that Lys 229 in eSHMT is crucial for product expulsion, which is a rate determining step of catalysis. Lys 226 of bsSHMT was mutated to Met and Gln, overexpressed and the mutant enzymes were purified. The mutant enzymes contained 1 mol of PLP per mol of subunit suggesting that Schiff's base formation with Lys was not essential for PLP binding. K226M and K226Q bsSHMT were inactive for THF-dependent cleavage of L-Ser. However, cleavage of L-*allo* Thr and transamination reaction was not abolished completely. K226M bsSHMT had distinct absorbance maximum at 412 nm and K226Q bsSHMT was similar to that of bsSHMT. The crystal structure of K226M bsSHMT revealed that PLP was bound at the active site in an orientation different (16°) from that of the wild-type enzyme. The absence of reaction intermediate at 388 nm on interaction with methoxyamine (MA) corroborates the suggestion that the active site of K226M bsSHMT was different from that of bsSHMT. Both the Lys mutants were capable of forming an external aldimine; this was also supported by the crystal structure of K226M-Ser/Gly complexes. Spectral studies show the formation of a small amount of quinonoid intermediate on addition of Gly and THF/FTHF to K226M bsSHMT. However, stopped-flow studies suggested enhanced quinonoid intermediate formed on addition of THF was affected drastically. In SHMT, formation of an external

aldimine is accompanied by the change in orientation of PLP by 25°. The orientation of PLP in the external aldimine form (25°) changes to 16° during quinonoid intermediate formation. The quinonoid intermediate is stabilized by interactions of Lys at the active site. In the absence of the -NH₂ group of Lys, the conversion of the external aldimine to product quinonoid intermediate, that is, the change in orientation of PLP from 25° to 16°, may not be possible. This in turn could lead to shifting of equilibrium towards the substrate external aldimine form (L-Ser form).

These results show that Lys 226 is responsible for flipping of PLP from one orientation to another, which is accompanied by C_α-C_β bond cleavage. This flip is important in the THF-mediated enhanced C_α proton abstraction from Gly in the reverse reaction.

Chapter 2: The involvement of glutamate 53 in binding of L-serine and folate, and conversion of bsSHMT from 'open' to 'closed' form

An examination of the crystal structure of bsSHMT binary and ternary complexes suggested that E53 interacts with L-Ser and FTHF. Glu 53 was mutated to Gln and structural and biochemical studies were carried out to examine the role of this residue in catalysis. The mutant enzyme was completely inactive for THF-dependent cleavage of L-Ser, whereas there was a 1.5-fold increase in the rate of THF-independent reaction with *L-allo* Thr. Spectral studies showed that E53Q bsSHMT had absorbance maximum at 425 nm and the addition of L-Ser/Gly resulted in formation of an external aldimine. The crystal structure of E53Q bsSHMT was similar to that of the wild-type enzyme, except for significant changes at Q53, Y60 and Y61. E53Q bsSHMT binary complex with L-Ser or Gly showed that the side chain of L-Ser and carboxyl of Gly were in two conformations in the respective external aldimine structures. The loss in characteristic decrease in molar ellipticity on addition of L-Ser and loss of enhanced thermal stability suggested that E53Q bsSHMT was unable to undergo a conformational change from 'open' to 'closed' form in which THF-dependent reaction occurs. Addition of THF/FTHF to E53Q bsSHMT-Gly complex showed the formation of a quinonoid intermediate. Stopped-flow studies were performed to obtain rate constants for the formation of quinonoid intermediate with mutant and wild-type enzymes. However the quinonoid intermediate formed by the mutant enzyme

was unstable. Dialysis experiments and dissociation constants for FTHF suggested that, the affinity for FTHF to mutant binary complex was lower than bsSHMT. This could be due to loss of interaction of N10 and formyl oxygen of FTHF the enzyme. These results suggested that Glu plays an important role in folate binding.

The crystal structure of the complex obtained on co-crystallization of E53Q bsSHMT with Gly and FTHF revealed that it exists in a gem-diamine form with an orientation of PLP similar to that of wild-type ternary complex. However, electron density for FTHF was not observed. The formation of gem-diamine in the above conditions was supported by circular dichroism measurements of E53Q bsSHMT ternary complex in the visible region. The absence of FTHF in the crystal structure and the formation of quinonoid intermediate suggest that there was an initial binding of FTHF to the binary complex of E53Q bsSHMT leading to an alteration in the orientation of PLP. Subsequently, FTHF falls off from the active site leaving behind the gem-diamine complex.

The differences between the structures of this complex and Gly external aldimine suggest that the changes induced by initial binding of FTHF are retained, even though FTHF was absent in the final structure. These observations indicate that mutant enzyme exhibits a phenomenon known as “enzyme memory”. In this concept, binding of ligands caused conformational changes in the enzyme and even after removal of ligands such imprints of ligand binding were retained by the enzyme. Double reciprocal plots of bsSHMT ternary complex and E53Q bsSHMT-Gly-(FTHF) complex, supports the suggestion that, mutant enzyme exhibits ‘enzyme memory’. There are not many examples of structural evidence for ‘enzyme memory’.

The results obtained from these studies suggest that E53 plays an essential role in THE/FTHF binding and in the proper positioning of C_β of L-Ser for direct attack by N5 of THF. It does not have an important role in THF-independent reactions.

Chapter 3: The role of tyrosine residues in cofactor binding and elucidation of mechanism for the tetrahydrofolate-independent cleavage of L-allo threonine

Tyr residues play multiple functions in enzyme catalysis. The crystal structure of bsSHMT showed that hydroxyl group of Y51 interacted with the phosphate group of PLP. Binary complex of bsSHMT-Ser showed change in conformation in Y61 on binding of L-Ser. The new conformation Y61 is close to C_β of the bound ligand, L-Ser. The active site Tyr's was mutated to Y51F, Y61F and Y61A bsSHMT to understand their role in bsSHMT catalysis. Mutation of these residues resulted in a complete loss of THF-dependent and -independent activities. The PLP content of Y51F and Y61F bsSHMT as isolated was 0.2 mol/mol and 0.6 mol/mol of subunit, respectively, compared to 1 mol/mol of subunit in bsSHMT. The mutant enzyme could be completely reconstituted with PLP. However, there was an alteration in the λ_{\max} value of the internal aldimine (396 nm) in the case of Y51F bsSHMT. A decrease in the rate of reduction with NaCNBH₃ and a loss of the intermediate in the interaction with MA suggests that the active site environment is altered in the case of Y51F bsSHMT due to mutation. The mutation of Y51 to F strongly affects the binding of PLP, possibly as a consequence of a change in the orientation of the phenyl ring (75°) in Y51F bsSHMT structure. The results obtained for Y61F were also similar to that of Y51F bsSHMT.

Y61A bsSHMT, as isolated had 1mol/mol of subunit and a absorption maximum of 425 nm similar to bsSHMT. In addition, Y61A bsSHMT was able to form an external aldimine; this change was supported by enhanced thermal stability of the mutant enzyme on addition of L-Ser. However, the formation of the quinonoid intermediate was hindered. An examination of the active site geometry of bsSHMT and Y51F and Y61A mutants show that Y51 and Y61 are not suitably placed for the removal of the proton from the hydroxyl group of L-*allo* Thr. In bsSHMT, the hydroxyl group of Y51 is at a distance of 3.6 Å and 3.8 Å from C_α of Gly and Ser, respectively. Of the two residues, Y51 is unlikely to be involved in proton abstraction from C_α of the bound ligand due to its longer distance and improper geometry. In contrast, the OH of Y61 is at a distance of 3.3 Å and 3.2 Å from C_α of Gly and Ser, respectively. In Gly, L-Ser and L-*allo* Thr complexes of Y51F bsSHMT, the OH of

Y61 and C α of bound ligand are at distances 4.97, 4.39 and 4.39 Å, respectively. Y61 therefore may be involved in C α proton abstraction in the THF-independent reaction.

This might explain the loss of L-*allo* Thr cleavage activity of Y51F bsSHMT. It could therefore, be concluded that Y51 is important for PLP binding and proper positioning of Y61, while Y61 could be involved in the abstraction of the proton from C α carbon of L-*allo* Thr. Based on these observations, a possible mechanism for SHMT catalyzed cleavage of L-*allo* Thr is suggested.

Chapter 4: The interaction of bsSHMT with specific inhibitors from extracts of various spices

The pivotal role of SHMT in the interconversion of folate coenzymes and its altered kinetic properties in neoplastic tissues suggested that it could be a potential target for cancer chemotherapy. This chapter deals with understanding the interaction of aminoxy compounds with K226M, K226Q, E53Q, Y51F, Y61F and Y61A bsSHMT. Methoxyamine (MA) and aminoxyacetic acid (AAA) interacted with the mutant proteins in different manner. K226M, K226Q bsSHMT did not react with MA and E53Q, Y51F, Y61A and Y61F bsSHMT failed to form 388 nm intermediate on addition of MA. These results suggest that any change at the active site environment or PLP orientation in bsSHMT could lead to the loss of intermediate formation on interaction with MA.

Lys mutants were able to interact with AAA, however the interaction rate was slower compared to bsSHMT suggesting that AAA was a more reactive compared to MA. The absence of Schiff's base and a change in the orientation of PLP at the active site of K226M and K226Q bsSHMTs probably results in poor binding of AAA at the active site. Y51F, Y61F and Y61A bsSHMT showed a similar interaction pattern as that of bsSHMT. Only E53Q bsSHMT showed the formation of an intermediate absorbing at 388 nm on addition of AAA. Stopped-flow studies suggested a drastic decrease in the rate at which AAA interacts with E53Q bsSHMT, when compared to bsSHMT. It is possible that Glu 53 may be the crucial residue involved in binding of AAA as well as in enhancing the rate of the reaction.

A fruitful approach of identifying compounds which have anti-carcinogenic effect is to carry out homology modeling and docking of compounds available in several chemical libraries. Homology modeling and docking of commercially available folate analogues were performed. Docking of folate analogues resulted in identification of 14 best compounds of these four water soluble compounds were examined for their ability to inhibit bsSHMT. Activity studies suggested that folate analogues failed to inhibit bsSHMT. In addition to synthetic compounds, naturally occurring compounds from spices that can potentially work as anti-cancer agents were also analyzed for bsSHMT inhibition. The effect of spices such as garlic, ginger, chilli, turmeric extracts was examined. Among all spices, heat-treated and lyophilized garlic extract showed 91% inhibition of bsSHMT. D and L-allyl Gly analogues of substrate L-Ser and S-allyl Cys (probable inhibitor form garlic extract) D and L-allyl Gly, Alliin did not inhibit bsSHMT activity.

Docking studies with S-allyl Cys, D and L-allyl Gly and alliin suggest that alliin, L-allyl Gly and S-allyl Cys bind at the active site of bsSHMT with different orientations. However, alliin and L-allyl Gly bind in similar orientation/position which is different from that of OADS. Binding of S-allyl Cys was almost similar to that of OADS. These results suggest that S-allyl Cys could be a potential inhibitor. Chemical synthesis of S-allyl Cys and further activity measurement has to be carried out to demonstrate the inhibition. These results emphasize the importance of examining the naturally occurring and synthetic compounds as possible chemotherapeutic agents.

The results presented in this study bring in the importance of correlating structural information with catalytic function. The mutation of Lys 226 of bsSHMT demonstrated its role in facilitating the change in orientation of PLP during catalysis. Glu 53 on interaction with L-Ser positions the C_{α} - C_{β} bond for attack by N5 of THF, a crucial step in L-Ser cleavage. The loss of efficient binding of FTHF to E53Q-Gly binary complex up on Glu 53 mutation results in the enzyme exhibiting a phenomenon called 'enzyme memory'. Tyr 51 is involved in cofactor binding. Tyr 61 plays an important role in C_{α} proton abstraction leading to THF-independent cleavage of 3-hydroxy amino acids. These observations prompted proposal of a new mechanism for aldol cleavage of 3-hydroxy amino acids. Both

commercially available and naturally occurring bioactive compounds from spices that can serve as anti-cancer agents were analyzed for bsSHMT inhibition. Garlic extract showed the maximum inhibition suggesting the importance of the naturally occurring compounds as possible and potential chemotherapeutic agents against cancer.

The summary and conclusions in the thesis briefly highlights the salient features of the present investigation. The literature cited in the complete text is arranged in alphabetical order under reference section, which gives all the relevant details including title, journal year, volume and pagination.

The above investigation is comprehensively documented in the form of a thesis for the award of Ph. D degree and being submitted in the subject area of Biochemistry to the University of Mysore, Mysore, India

Bhavani B. S.
(Candidate)

Dr. V. Prakash
Guide and Supervisor
and
DIRECTOR
Central Food Technological Research Institute
Mysore – 570020, India

Place: Mysore
Date

INTRODUCTION

Enzymes are biological catalysts which accelerate the rate of bio-chemical reactions. The substrates are bound to specific binding sites on the enzyme through specific interactions with the amino acid residues of the enzyme. The spatial geometry required for the interaction(s) between the substrate and the enzyme makes each enzyme selective for its substrates and ensures that only specific products are formed. Although enzymes may be modified during their participation in the reaction sequence, they return to their original form at the end of the catalytic cycle. In addition to increasing the speed of reactions, enzymes provide a means for regulating the rate of metabolic pathways by controlling key steps by degradation, interaction with metabolites and inhibitors.

The active site of an enzyme is formed by one or more regions of the polypeptide chain. Within the active site, cofactors and functional groups from the polypeptide chain participate in transforming the bound substrate molecule(s) into product(s). The proximity of the bound substrate molecules and their precise orientation towards each other contribute to the catalytic efficiency of the enzyme. The specificity of enzymes towards their substrate(s) arises from the three-dimensional arrangement of specific amino acid residues in the enzyme that form binding sites for the substrate(s) and activate them during the course of the reaction.

The “lock-and-key” and the “induced-fit” models for substrate binding describe two aspects of the binding interaction between the enzyme and substrate(s). In the lock and key model, the substrate binding site contains amino acid residues organized in a three-dimensional complementary arrangement that “recognizes” the substrate and binds it through multiple hydrophobic, electrostatic interactions, and hydrogen bonds. The amino acid residues that bind the substrate can come from different parts of the linear amino acid sequence of the enzyme. In this model the enzyme and the substrate are assumed to be conformationally rigid as in a lock and key. In the induced-fit model when the substrate(s) binds to the enzyme, it undergoes a conformational change (“induced-fit”) that repositions the side chains of the amino acid residues at the active site and increases the number of binding interactions. Similarly the enzyme undergoes subtle conformational change upon binding to the substrate. In induced fit model the substrate binding site is not a rigid “lock” but rather a dynamic surface created by the flexible overall three-dimensional structure

of the enzyme. The conformational change induced by substrate binding is usually to reposition the functional groups in the active site. This promotes the reaction and improves the binding of a co-substrate, or activates an adjacent subunit through cooperatively (Koshland, 1970).

Mechanisms of enzyme catalysis

General acid-base catalysis

Catalysis of this type that uses only the H^+ or OH^- ions of water is referred as general acid-base catalysis. In the active site of an enzyme, a number of amino acid side chains can similarly act as proton donors and acceptors. These groups can be precisely positioned in an enzyme active site to allow proton transfers, providing rate enhancements of the order of 10^2 to 10^5 fold. This type of increased catalysis occurs in the vast majority of enzymes. In fact, proton transfers are the most common features of biochemical reactions.

Covalent catalysis

The process of covalent catalysis involves the formation of a covalent bond between the enzyme and one or more substrates. The modified enzyme then becomes a reactant. Covalent catalysis introduces a new reaction pathway that is energetically more favourable and therefore faster than the reaction pathway in homogeneous solution. Covalent catalysis is particularly common among enzymes that catalyze group transfer reactions. Residues on the enzyme that participate in covalent catalysis generally are Cys or Ser and occasionally His. The proteolytic enzyme, chymotrypsin is an excellent example of this mechanism.

Metal ion catalysis

Metal ions play an important role in catalysis. They serve as an electrophilic center, stabilizing negative charge on reaction intermediates. Alternatively, the metal ion may generate a nucleophile by increasing the acidic nature of a nearby molecule. The metal ion may bind to substrate(s), increasing their affinity to the enzyme as well as enhance specificity. In addition to this function in catalysis, metal ions bind to the enzyme and enhance its catalytic power by several orders of folds.

In addition to these mechanisms, determination of three dimensional structures of enzymes complexed with substrate(s) and inhibitors helps in understanding the mode of enzyme function or action. The role of amino acids, changes in the domain movements and the conformational changes at the active site of an enzyme are clear from in X-ray structures of enzymes and their complexes. Therefore, the relationship between protein structure and function is one of the foremost challenges in biology. In the case of enzymes, the study of mechanistically diverse super-families has provided valuable information on structure-function relationships which is useful in areas such as enzyme engineering, drug design, signal transduction, etc., in addition to catalysis.

Structure-function of PLP-dependent enzymes

A number of the enzymes require an additional organic or inorganic substance for their catalytic activity. Several vitamin derivatives function as coenzymes, and one such is pyridoxine or vitamin B6. These vitamin derivatives are often converted to coenzymes by phosphorylation and other modifications. In the case of B6-enzymes, pyridoxal 5'-phosphate (PLP) or pyridoxamine 5'-phosphate (PMP) is the cofactor involved in enzyme catalysis. These aspects have been extensively reviewed (Snell, 1981).

PLP-dependent enzymes have been the subject of extensive research for the past fifty years. The main theme of this research work is to understand the structure-function relationship, versatility in the reactions catalyzed and elucidation of the reaction mechanisms. In addition, a few of the PLP-dependent enzymes have been drug targets due to their crucial role in various metabolic pathways. These enzymes are involved not only in the synthesis, inter-conversion and degradation of amino acids, but also in the replenishment of one-carbon units, synthesis and degradation of biogenic amines (Eliot and Kirsch, 2004). To date, more than 140 PLP-enzymes have been identified and more than 40 crystal structures of these enzymes and their binary and ternary complexes with different substrates, substrate analogues and inhibitors are available in the protein data base (<http://www.rcsb.org>).

In PLP-enzymes, the cofactor forms a Schiff's base with ϵ -amino group of Lys which is referred to as an internal aldimine. Internal aldimine is the resting enzyme form (Fig I.1) and has a broad absorption maximum between 410-430 nm, depending on the type of enzyme and its source. The incoming amino acid substrate displaces the active site Lys to form a new covalent bond between PLP and α -amino group of the substrate, which is referred as an external aldimine. Formation of an external aldimine in PLP-dependent enzymes proceeds through another intermediate called geminal diamine (gem-diamine) which absorbs at 343 nm. Only in few cases, this intermediate has been spectrally observed. In gem-diamine, both ϵ - amino group of active site Lys and the α -amino group of the substrate are linked to PLP (Fig I.1). Both internal and external aldimine have almost overlapping λ_{\max} between 410-430 nm.

The external aldimine is a common central intermediate in all PLP-catalyzed reactions. Divergence in reactions occurs from this intermediate. Reaction specificity and versatility depends on substrate bond to be cleaved. This also determines the type of reaction. The enzymatic reactions at C_{α} position include transamination, decarboxylation, racemization, elimination and replacement of an electrophilic R group. Cleavage at β and γ position includes elimination or replacement of various functional groups in the reactions (Fig I.2) (Toney, 2005).

Classification of PLP-dependent enzymes

The classification of PLP-enzymes was based on the carbon atom involved in covalency changes as well as on the bond to be cleaved during catalysis. The three major groups identified were α , β and γ family depending on the carbon atom of the amino acid involved in the reaction. Aspartate aminotransferase (AAT) represents the α family, tryptophan synthase (TS) is a type member of the β family and alanine racemase (ALR) represents the γ family. Serine hydroxymethyltransferase (SHMT), the enzyme of interest in this study belongs to the α family. It was the understanding from the earlier work that the classification of PLP-enzymes would correlate with the type of reaction that they are involved with.

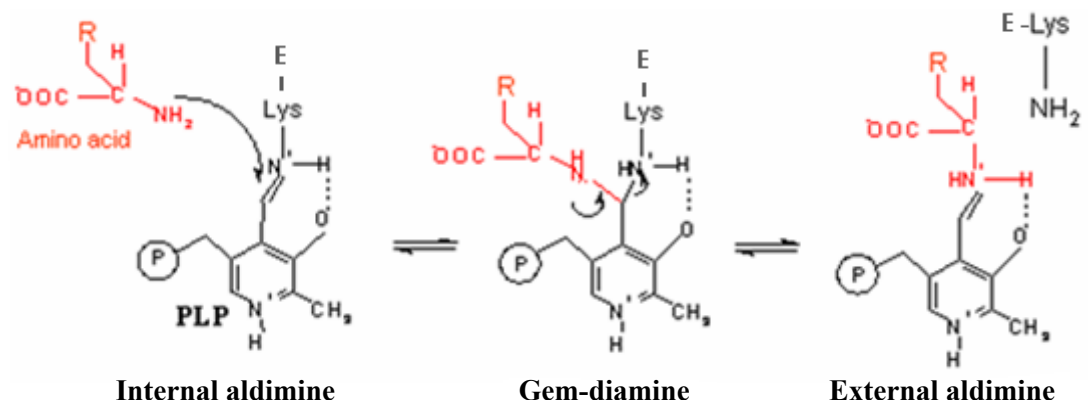


Fig I.1: The formation of an external aldimine from internal aldimine via a gem-diamine intermediate.

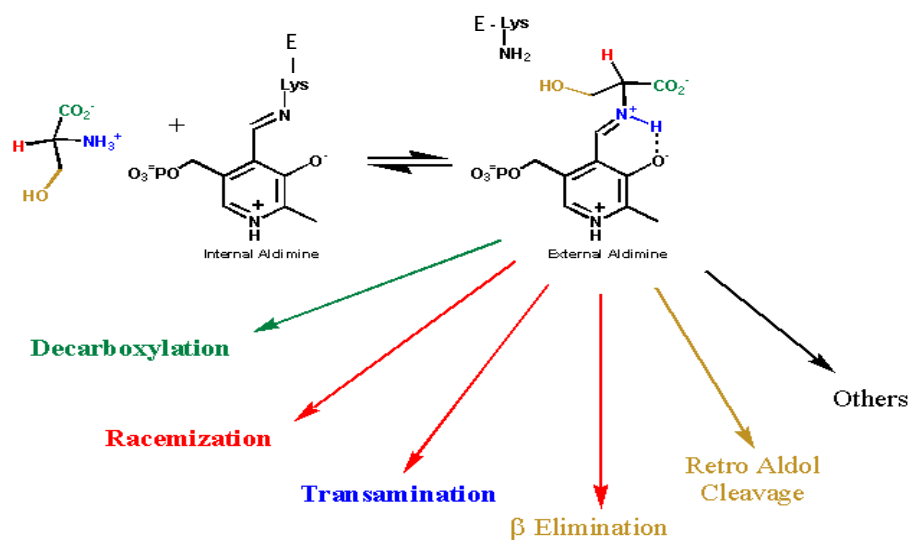


Fig I.2: A representation of catalytic diversity among PLP-dependent enzymes. (Reproduced from Toney, 2005)

It was found later that each of the major structural classes contain representatives of multiple reaction types. The availability of the three-dimensional (3-D) structures of several PLP-enzymes and the evolutionary relationships among PLP-enzymes has become reasonably clear now. Despite the low level of sequence similarity, members of a particular fold strongly resemble each other in their 3-D structures.

Mehta and Christen (2000) re-classified all PLP-dependent enzymes based on the family profile analysis (FPA), sequence similarity and structural folds. The availability of 3-D structures and sequences in the data base gave inputs into the new classification. According to this classification all PLP-dependent enzymes fall into five types of folds (Mehta and Christen, 2000). A few salient features of these fold types are presented below.

Fold Type I: A majority of known structures and the best characterized PLP-enzymes belong to fold type I. These enzymes function as homodimers or higher oligomers consisting of two active sites per dimer. The active site lies at the interface of the dimers and residues from both the dimers contribute to catalysis as well as maintaining the oligomeric status of the enzyme. One of the best studied among fold type I enzymes, is AAT. Each monomer comprises of a large domain, a small domain and an amino terminal segment. Greatest similarity in folding is seen in the large domain, which is made up of eight α - helices packed around a seven-strand β -sheet. All the strands of this sheet run parallel except for one. Residues involved in coenzyme binding are mostly from carboxy terminal ends of these β -sheets. The small domains are also similar to each other in their basic architecture, being α/β with a core of three or four antiparallel β -strands. Only two residues are conserved throughout the α -family, they are Lys that forms the Schiff's base with PLP and Asp that interacts with the pyridinium N of PLP.

Fold Type II: The enzymes belonging to fold type II mainly catalyze β -elimination reactions. TS is a type member of fold type II enzymes. TS is an $\alpha_2\beta_2$ tetramer, in which β is the PLP-binding subunit and α is a regulatory subunit (Hyde *et al.*, 1988). TS active sites which catalyze the two parts of the reactions are 2.5 Å apart. The

most striking feature of the structure is a tunnel which connects the two active sites and channels the intermediate form α to β subunits (Mehta and Christen, 2000; Miles, 1991). Most of the enzymes belonging to this fold type are structurally organized as $\alpha_2\beta_2$ subunits. The active site in fold type II enzymes lies in a cleft formed between C-terminal ends of two β -sheets. The Lys residue to which PLP is bound is located at the beginning of a helix in the N-terminal domain. PLP is bound in the same orientation as in the fold type I family. Unlike fold type I family of enzymes, in this family PLP is coordinated by residues from only one subunit, though the functional form is a homodimer or higher order oligomer. The pyridine nitrogen of this family is coordinated by a L-Ser residue. Members of this family, like threonine synthase and cystathionine β -synthase, have additional regulatory domains. Threonine synthase and cystathionine β -synthase are allosterically regulated by S-adenosyl-L-methionine (SAM) (Finkelstein *et al.*, 1975), Ile and Val, respectively (Madison and Thompson, 1976).

Fold Type III: ALR and a subset of amino acid decarboxylases represent this family, which is characterized by $(\beta/\alpha)_8$ barrel. The unique feature of this family is that a similar type of fold is also seen in non-PLP-dependent enzymes (Christen and Mehta, 2001). PLP forms Schiff's base with active site Lys, which lies in the C-terminal end of the first strand of $(\beta/\alpha)_8$ barrel. Unlike in the other fold types (I and II), the residue coordinating with pyridinium N of PLP is not conserved in this fold type. In ALR pyridinium N of PLP interacts with Arg and in ornithine decarboxylase (ODC), it interacts with Glu, suggesting that the nitrogen is protonated in the later enzyme.

Fold Type IV: This group is also called as D-amino acid aminotransferase family. Enzymes belonging to fold IV are similar to fold types I and II. These enzymes are also functional homodimers and the catalytic region of each monomer is composed of a small and large domains. The cofactor is bound in a site that is a near mirror image of the fold type I and II binding sites, so that the *re* phase is exposed to solvent rather than the *si* phase (Sugio *et al.*, 1995). Branched chain amino acid aminotransferase and 4-amino-4-deoxychorisimate lyase belong to this fold type. A representative crystal structure of the enzymes belonging to these four fold types are shown in Fig I.3.

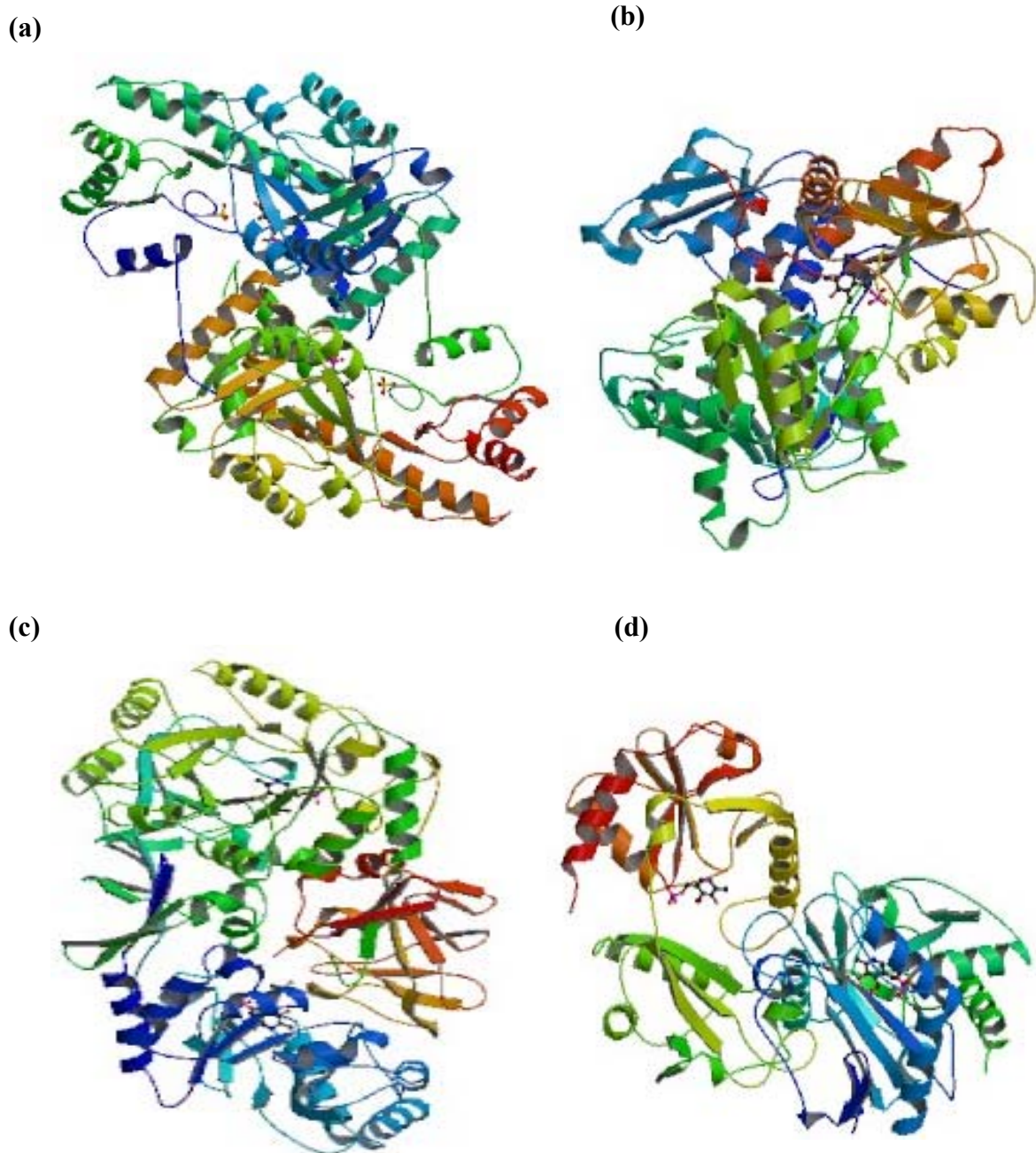


Fig I.3: Representative enzyme structures of different fold-type PLP-enzymes.

(a) *E. coli* AAT [fold type I] (Jager *et al.*, 1994)

(b) *Arabidopsis thaliana* O-acetylserine sulfhydrylase (OAS) [fold type II] (Burkhard *et al.*, 1998)

(c) *Bacillus stearothermophilus* ALR [fold type III] (Shaw *et al.*, 1997)

(d) Thermophilic *Bacillus sp.* D-amino acid aminotransferase [fold type IV] (Sugio *et al.*, 1995)

Fold Type V: This is also referred as glycogen phosphorylase family. These enzymes are mechanistically distinct from other known fold types, in that they utilize the phosphate group of PLP for catalyses (Mehta and Christen, 2000).

Thus, it can be seen from the survey of literature presented, that there is considerable unity in diversity in the organization and function of PLP- dependent enzymes.

Basis for the catalytic diversity among PLP-dependent enzymes

Although PLP-enzymes catalyze a variety of apparently different reactions, Dunathan (1966) proposed an elegant hypothesis to explain this diversity. The central feature of this proposal is that, the bond to be broken will align perpendicularly with the pyridine ring of the cofactor. The cofactor functions to stabilize negative charge developed at C_{α} in the transition state (Dunathan, 1966) (Fig I.4). The stabilization of C_{α} -anion is facilitated by delocalization of the negative charge through π bond system of the cofactor. For this reason, PLP is often described as an “electron sink”.

The control of substrate orientation enables the enzyme to distinguish between different types of reactions. This hypothesis ensures that the carbanion is stabilized by conjugation with an extended π system. This postulation was supported, when the crystal structure of AAT complexed with its substrate(s) was solved (Ford *et al.*, 1980). A completely formed carbanion in the reaction is referred to as a quinonoid intermediate. This intermediate shows an absorbance maximum at 495 nm. The features of the Dunathan hypothesis are explained with a few examples.

Transamination

Transamination is the main reaction catalyzed by AAT. In addition to this reaction, the enzyme also catalyzes recemization. This is achieved by closure of the enzyme around the substrate, so that water molecules do not gain access to the quinonoid intermediate to protonate it from the *re* phase (Kochhar and Christen, 1992). In addition to this, there are no acidic amino acid residues at the active site to donate a proton to the *re* phase of the intermediate. This pathway leads to transamination rather than recemization reaction.

Recemization

ALR catalyzes the interconversion of L- and D-Ala (Sun and Toney, 1999). ALR acts on substrates incapable of undergoing an elimination reaction. Therefore, the major side reaction that must be limited is transamination. A major factor facilitating this transamination reaction is an Asp residue that interacts with pyridinium N in all AAT and other fold type I enzymes, thereby maintaining protonation of PLP. The corresponding residue is an Arg in the bacterial ALR, which is expected to maintain the cofactor in the unprotonated form. The lack of a proton at this position would greatly diminish the electron withdrawing properties of PLP. However, these structural insights can not be generally applied to all PLP-dependent racemases because one of the alanine racemases belonging to fold type I has an Asp residue that interacts with the pyridinium N (Paiardini *et al.*, 2003).

Dialkylglycine decarboxylase (DGD)

DGD is both an aminotransferase as well as a decarboxylase. A complete catalytic cycle involves decarboxylation and transamination of dialkylglycine to generate a ketone product and PMP-form of the enzyme. This is followed by reaction with pyruvate in a typical transamination to generate Ala and to restore the PLP-form of the enzyme. Structural and mechanistic studies have demonstrated that the decarboxylation of the dialkyl amino acids is forced by large side chains, which are not accommodated in the same site as the methyl side chain of Ala. Instead they occupy the same position as the alanine carboxylate. This reorientation results in the scissile bond positioning itself between C_α and the carboxylate rather than that between C_α and the proton (Sun *et al.*, 1998). Thus decarboxylation is preferred over deprotonation in the reaction catalyzed by DGD (Fig I.5).

It is clear from the above discussion that interaction between substrate, cofactor and enzyme residues lead to proper positioning of the bond to be cleaved in PLP-enzymes catalyzing different types of reactions.

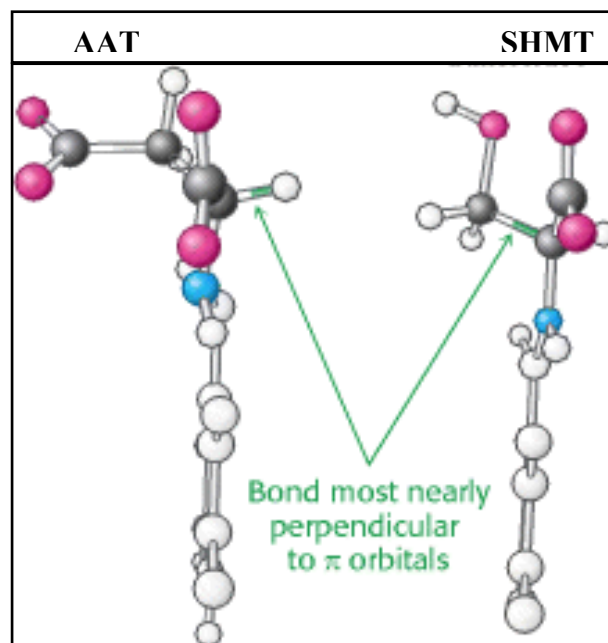


Fig I.4: Stereo-chemical explanation for reaction specificity in PLP-enzymes.
 In AAT, the C_{α} -H bond is nearly perpendicular to the p-orbital system and is cleaved. In SHMT, a small rotation about the N- C_{α} bond places the C_{α} - C_{β} bond perpendicular to the π system, favouring its cleavage.

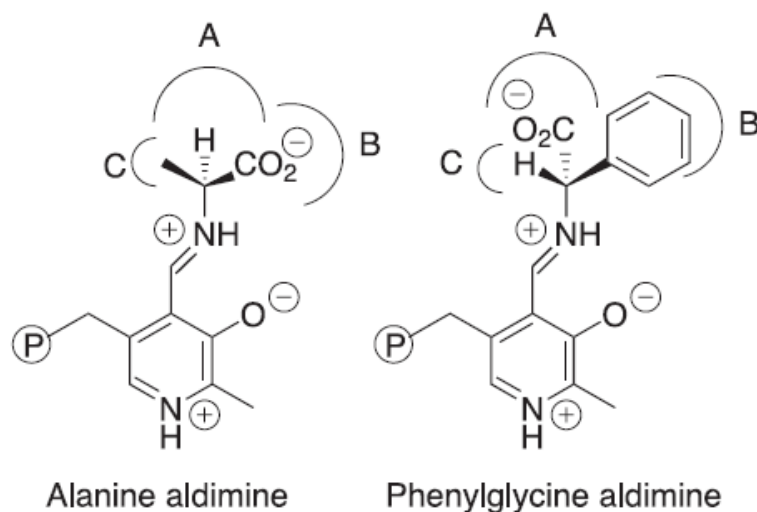


Fig I.5: Steric control of reaction type by dialkylglycine decarboxylase.
 (reproduced from Sun *et al.*, 1998).

The three substituents on C_{α} occupy distinct binding sites, labeled A, B, and C. While A and B sites are tolerant to accommodate carboxylates and hydrogen or large alkyl groups, respectively, the C site can only accommodate small alkyl groups. Amino acid substrates with small side chains, such as alanine, bind preferably with their carboxylate moieties in the B site, placing the C_{α} proton in the reactive A site. Substrates with a large side chain (such as the phenylglycine), however, bind with that group in the B site, forcing the carboxylate into the reactive A site. As a consequence substrate fit at the active site, enzyme can differentiate between decarboxylation and deprotonation reactions.

Determinants of substrate specificity

In addition to the criteria underlying reaction specificity presented in the previous section, PLP-enzymes, in some instances show wide substrate specificity. Most of the PLP-dependent enzymes can accommodate two different substrates for catalysis. A few enzymes have different binding pockets for different substrates, however there are enzymes which bind to two different substrates at the same active site as well. It is well known that, binding of a substrate to the enzyme pocket, induces a conformational change in the enzyme and the residues interacting with substrates may confer substrate specificity. Two examples of this phenomenon are conversion of the enzyme from an 'open' to 'closed' form and the Arg switch observed in PLP-enzymes.

Transitions from 'open' to 'closed' form of PLP-enzymes

Substrate-induced conformational change in PLP-enzymes is substantiated in the case of AAT (Picot *et al.*, 1991) by experiments that include X-ray crystallography and other biophysical and biochemical methods. Both cytoplasmic and mitochondrial isoenzymes of AAT exist in one of the two conformations 'open' and 'closed' form. In the absence of amino acid substrate the enzyme active site is 'open', whereas in the presence of substrate the enzyme is in the 'closed' form. In this form there is no access of solvent into the active site. The differences in the two conformations have been described in detail, the requirement for this conformational change is to increase substrate and reaction specificity to the high levels observed in this enzyme. AAT has full catalytic activity only when it is in the closed conformation produced by binding of the substrate.

Another example of a change in the conformation on addition of substrate is SHMT, which exhibits a broad range of reaction and substrate specificity. SHMT, from several sources exists in equilibrium between 'open' and 'closed' forms. Amino acid substrates enter and leave the active site in the open form. Unlike in the case of AAT (Picot *et al.*, 1991), this conformational change has not been obvious in crystal structure of SHMT (Trivedi *et al.*, 2002). However, enhancement of thermal stability is a characteristic feature of the SHMT-Ser binary complexes. This change has been ascribed to the conversion of the enzyme from an 'open to a closed' form and this

hypothesis has been supported by peptide bond exchange studies, thermal denaturation and CD studies (Schirch *et al.*, 1991).

Arg switches and hydrogen bond networks

In addition to changes from ‘open’ to ‘closed’ conformation, Arg switches and hydrogen bond networks play an important role in governing substrate specificity. The first example of Arg switch was observed in an engineered enzyme that was constructed by introducing six mutations into the primary structure of AAT (Onuffer and Kirsch, 1995). These changes resulted in a substantial increase in activity towards aromatic substrates. The subsequent determination of the structure of the mutant enzyme showed that the large aromatic substrates are accommodated by a movement of Arg 292 out of the active site (Malashkevich *et al.*, 1995b) (Fig I.6).

However, Arg switches are not unique to engineered enzymes. A well-characterized Fold type I enzyme - tyrosine (aromatic) aminotransferase (TATase) has a natural specificity for the aromatic amino acids Tyr, Phe, and Trp, as well as for the dicarboxylic amino acids, Asp and Glu. A number of structures are available of the *Paracoccus denitrificans* TATase that clearly demonstrates the Arg switch (Okamoto *et al.*, 1998 ; Okamoto *et al.*, 1999). Crystallographic and modeling studies suggest γ -aminobutyric acid (GABA) (Toney *et al.*, 1995; Storici *et al.*, 1999a) and ornithine aminotransferases (OAT) (Storici *et al.*, 1999b), adopt a similar strategy. These enzymes react with both ω -amino acid substrates and the common substrate, Glu. AAT and TATase, bind the dicarboxylic acid substrate via two conserved Arg residues. The carboxylate of the ω -amino acid and GABA, occupies the same position as the γ -carboxylate of Glu. The second Arg (equivalent to Arg 386 of AAT) moves to interact with a conserved Glu near the active site.

Sequence alignments studies indicated that, a sub-group of aminotransferases (designated I γ) lack an equivalent Arg 292 (Jensen and Gu, 1996). The only structure available for a TATase of this group is that of the unliganded *Pyrococcus horikoshii* enzyme (Fig I.7) (Matsui *et al.*, 2000). Modeling of the substrates in the active site suggests that this enzyme binds Glu via an extended hydrogen-bonding network,

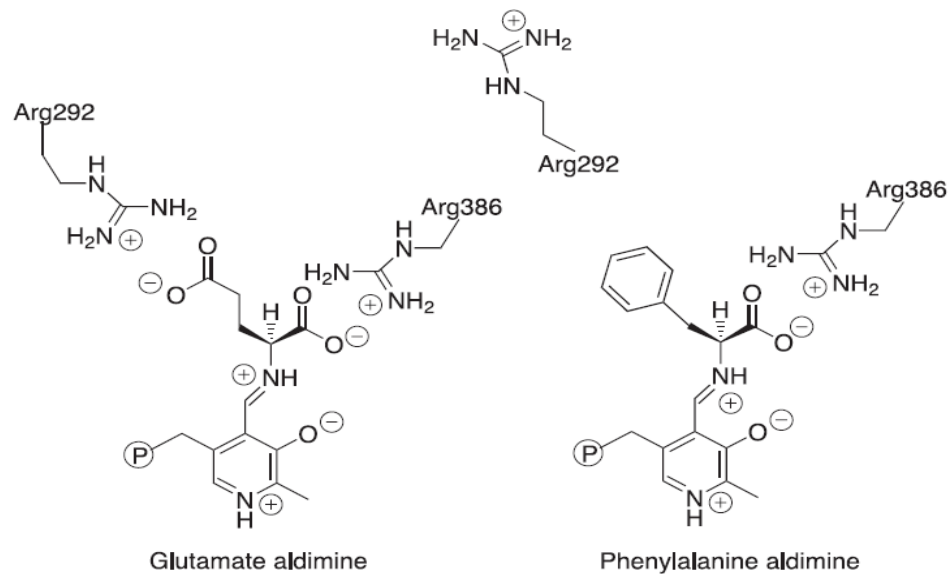


Fig I.6: Schematic representation of the Arg-switch in aminotransferases when both dicarboxylic and aromatic amino acids are used as substrates. (reproduced from Malashkevich *et al.*, 1995b)

The γ -carboxylate of glutamate (left) interacts with Arg 292. This residue reorients itself to point away from the active site when aromatic substrates bind (right). This movement allows the enzyme to accept both types of substrates.

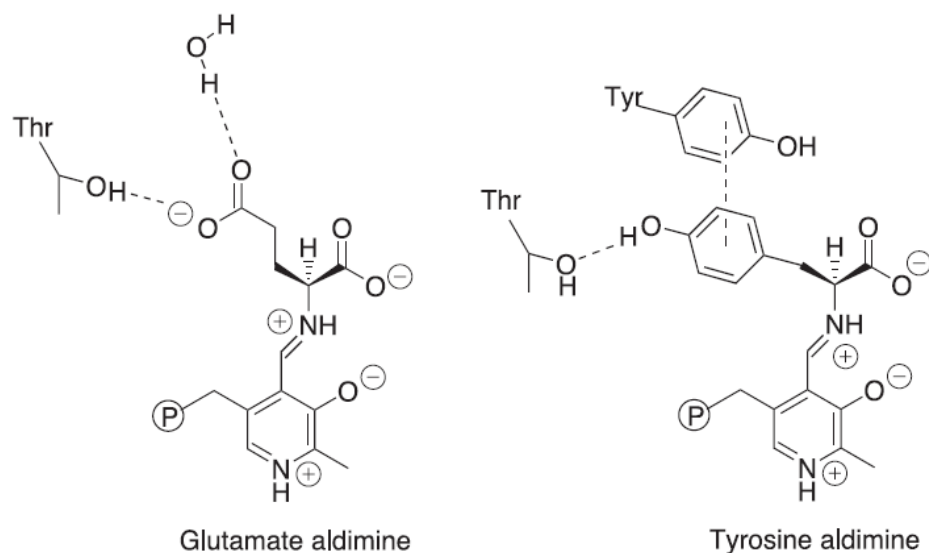


Fig I.7: Dual substrate specificity can also be achieved by hydrogen bond rearrangement (reproduced from Matsui *et al.*, 2000 and Ura *et al.*, 2001)

P. horikoshii TATase binds the γ -carboxylate of Glu via a hydrogen bond network rather than an Arg residue. Direct interactions are made with a Thr residue and a tightly bound water molecule. Modeling of bound Tyr suggests that the hydrogen bond network is rearranged so that the aromatic ring stacks against a nearby tyrosine residue. In addition it makes a hydrogen bond with the same Thr residue that is involved in Glu binding.

which has been observed in the AAT from this same organism (Ura *et al.*, 2001). The absence of a positively charged residue in this TATase makes it much easier to accommodate the uncharged substrates by simple rearrangement of the hydrogen bond network (Fig I.7). Moreover, absence of the flexible Arg side chain allows this enzyme to distinguish between Glu and Asp. Hence, a number of diverse strategies are employed by different enzymes to achieve the common objective of ensuring high degree of substrate specificity and preventing wasteful side reactions.

Change in the reaction specificity

Many PLP-dependent enzymes exhibit change in reaction specificity on site-specific mutations of active site residues (Henderson *et al.*, 1991; Graber *et al.*, 1995; Vacca *et al.*, 1995; Vacca *et al.*, 1997; Graber *et al.*, 1999). Graber *et al* showed that the reaction specificity of AAT could be altered to catalyze the β -decarboxylase reaction. This was achieved by converting the Tyr 225 to Arg and coupling it to another mutant, R386A. Mutation of the active site Arg 386 to Lys altered the reaction and substrate specificity of AAT (Vacca *et al.*, 1997).

Mutation of His 230 of sheep liver cytosolic SHMT (scSHMT) to Tyr resulted in an induction of NADH oxidation ability. H230Y mutant was found to catalyze oxidation of NADH in an enzyme concentration-dependent manner, instead of utilizing L-Asp as a substrate (Talwar *et al.*, 2000b). The NADH oxidation could be linked to oxygen consumption or reduction of nitrobluetetrazolium. The reaction was inhibited by radical scavengers like superoxide dismutase and D-mannitol. This oxidation was not observed with either the wild-type SHMT or other in histidine mutants (H230A, H230F and H230N).

These observations also points out to the potential of engineering PLP-enzymes for many industrial purposes for the production of unique industrial end products, especially amino acid derivatives.

Serine hydroxymethyltransferase

This thesis describes the investigations on the structure-function relationships of SHMT and its potential as a target for cancer chemotherapy. It is therefore appropriate to discuss these aspects in detail in this section.

SHMT, belongs to the α -family (Fold type I) of PLP-enzymes (Mehta and Christen, 2000). It catalyzes the reversible interconversion of L-Ser and THF to Gly and 5, 10-methylene THF (Fig I.8). The reversible conversion of L-Ser to Gly proceeds via several intermediates with distinct absorbance maxima. This has aided in elucidating the reaction mechanism. In addition to catalyzing THF-dependent cleavage of L-Ser, SHMT also catalyzes the THF-independent cleavage of L-*allo*Thr, transamination, decarboxylation and racemization reactions. Table I.1 summarizes the various reactions catalyzed by SHMT (Malkin and Greenberg, 1964; Chen and Schirch, 1973; Ulevitch and Kallen, 1977a).

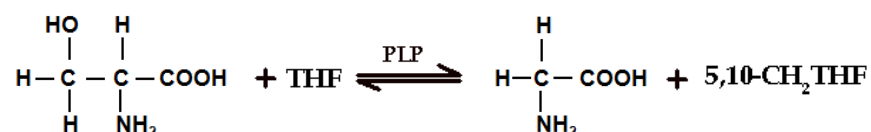


Fig I.8: Conversion of L-Ser to Gly by SHMT.

Table I.1: THF-dependent and – independent reactions catalyzed by SHMT

Substrates	Products
THF-dependent reactions	
L-Ser + tetrahydrofolate (THF)	Gly + 5, 10-CH ₂ THF
α -Methyl-L-Ser + THF	D-Ala + 5, 10-CH ₂ THF
THF-independent reactions	
L- <i>allo</i> Thr	Gly + acetaldehyde
L- Thr	Gly + acetaldehyde
D-Ala + PLP	pyruvate + ammonia + PMP
L-Ala + PLP	pyruvate + ammonia + PMP
L-Ala	D-Ala
L- <i>erythro</i> β -Phenyl Ser	Gly + benzaldehyde
L- <i>threo</i> β -Phenyl Ser	Gly + benzaldehyde

Importance of SHMT

SHMT is a key enzyme linking carbohydrate, amino acid and nucleic acid metabolism, highlighting the importance of its substrate, L-Ser in the metabolic pathway (Fig I.9). The reaction that is relevant to the subject matter of this thesis is its role in the interconversion of folate coenzymes. SHMT catalyzes the formation of 5, 10-methylene THF which, serves as a key intermediate in the biosynthesis of methionine, thymidylate, purines, formyl t-RNA and a variety of other end products that require one-carbon fragments for their synthesis (Kumar *et al.*, 1976; Snell, 1984, 1985; Matthews and Drummond, 1990; Appaji Rao *et al.*, 2000). For these reasons this enzyme has attracted considerable attention and has been isolated from a variety of sources ranging from microorganisms to mammalian system.

SHMT has been isolated and characterized from various sources from human liver (hc) (Renwick *et al.*, 1998) to *E. coli* (e), (Scarsdale *et al.*, 2000). SHMT, from prokaryotes is a dimer, while that from eukaryotic organisms is a tetramer (dimer of tight dimers). Only in the case of *Trypanosoma cruzi* SHMT exists as a monomer (Capelluto *et al.*, 2000). In addition, SHMT has been isolated and characterized from rabbit liver (rc) (Scarsdale *et al.*, 1999), murine (mc) (Szebenyi *et al.*, 2000) and *B. stearotherophilus* (bs) (Trivedi *et al.*, 2002), *Plasmodium falciparum* (Franca *et al.*, 2005), *Methanococcus jannaschii* (Angelaccio *et al.*, 2003), *Mycobacterium tuberculosis* (Chaturvedi and Bhakuni, 2003), *Streptococcus thermophilus* (Vidal *et al.*, 2005), zebrafish cytosolic SHMT (Chang *et al.*, 2007), *Trichomonas vaginalis* (Mukherjee *et al.*, 2006), *Leishmania donovani* SHMT (Vatsyayan and Roy, 2007), *Mycobacterium leprae* (Sharma and Bhakuni, 2007) and *Plasmodium vivax* (Leartsakulpanich *et al.*, 2008).

In the recent years, the focus of the studies on SHMT's has been to understand the structure of these enzymes and their complexes with substrates and inhibitors. These structures have enabled probing the residues involved in catalysis and the mechanisms of the physiological and side reactions. The effort at identifying the active site residues and their role in catalysis is described in the next section.

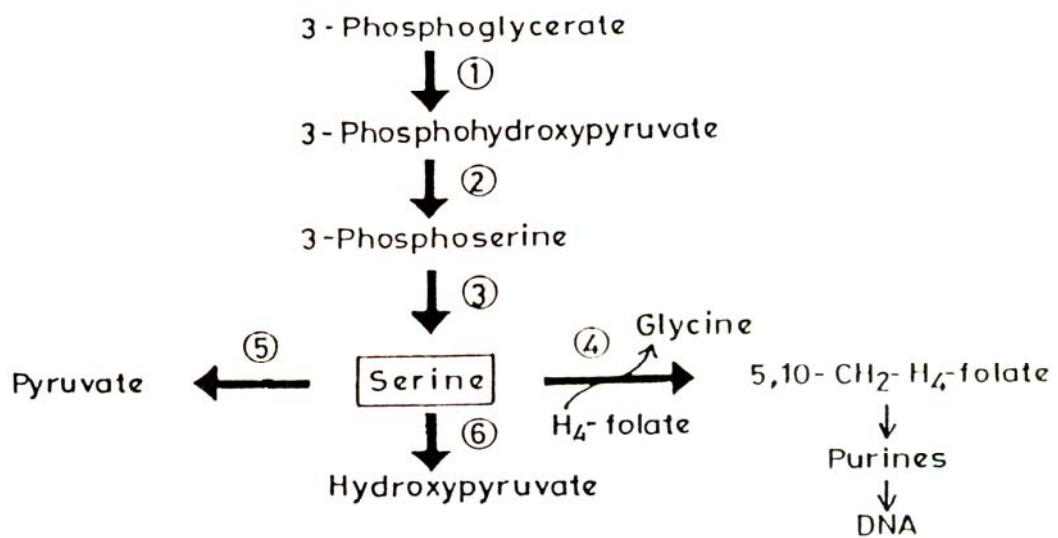


Fig I.9: The role of SHMT in metabolism.

The enzymes involved in conversion of metabolites in the above pathway are represented below

- ① 3 - Phosphoglycerate dehydrogenase
- ② Phosphoserine aminotransferase
- ③ Phosphoserine phosphatase
- ④ SHMT
- ⑤ Serine dehydratase
- ⑥ Serine aminotrasferase

Active site residues of SHMT

The role of the active site residues has been greatly facilitated by the availability of the crystal structure of SHMT and its complexes with substrate(s) from human liver (hc) (Renwick *et al.*, 1998), rabbit liver (rc) (Scarsdale *et al.*, 1999), *E. coli* (e), (Scarsdale *et al.*, 2000) murine (mc) (Szebenyi *et al.*, 2000) and *B. stearothersophilus* (bs) (Trivedi *et al.*, 2002) in the protein data base. The availability of the sequences of this enzyme from several sources and their analysis has enabled a detailed investigation on the amino acids essential for catalysis and subunit assembly. The roles of some of these residues were established through biochemical, kinetic and spectroscopic methods are listed in Table I.2.

It is evident from the Table I.2 that SHMT has several crucial residues at the active site which participate in catalysis. The active site residues in this enzyme have attracted the attention ever since its discovery. The present investigation deals with the elucidation of the role of Lys, Glu, and Tyr residues in the reaction catalyzed by bsSHMT. The function of these residues in other SHMTs is discussed briefly in the following section.

Lys 229 of eSHMT

It was suggested that K229 of eSHMT, in addition to anchoring PLP plays an important role in proton abstraction and product release during catalysis. To evaluate the proposal, active site Lys 229 of eSHMT was mutated to Gln, Arg, and His. Substitution of Lys 229 with Arg and His resulted in an enzyme containing a low amount of PLP as the aldehyde. The addition of L-Ser or Gly converted some of the bound PLP to the external aldimine. However, on removal of L-Ser the external aldimine is converted back to the aldehyde. This observation suggested that the low affinity for binding of L-Ser to the mutant enzymes (Schirch *et al.*, 1993a). Among all the mutants, only the K229Q eSHMT was similar to wild-type enzyme in its ability to bind to PLP. K229Q eSHMT was purified as a mixture of external aldimines of the two amino acid substrates Gly and L-Ser. K229Q eSHMT was able to catalyze the transamination of D-Ala at 40% of the rate of the wild-type SHMT. K229Q-Gly was converted to K229Q-Ser complex when 5, 10-CH₂ THF was added,

Table I.2: Amino acid residues essential for maintaining the structure and function of SHMT's.

Source	Residues	Possible roles	References cited
scSHMT	Y73	PLP binding	(Jala, 2002)
	E74	'Open' to 'closed' form	(Jala <i>et al.</i> , 2000)
	R80	Inter-subunit interaction	(Jala, 2002)
	Y82	Stabilizing quinonoid intermediate	(Jala <i>et al.</i> , 2000)
	D89	Inter subunit interaction	(Jala, 2002)
	R89	Enzyme folding	(Jala, 2002)
	W110	Maintenance of oligomeric structure	(Jala, 2002)
	H134	Inter-subunit interaction	(Jagath <i>et al.</i> , 1997b)
	H147	Cofactor binding/stacking interaction	(Jagath <i>et al.</i> , 1997b)
	H150	Proton abstraction	(Jagath <i>et al.</i> , 1997b)
	D227	PLP interaction	(Jala, 2002)
	H230	Enhance proton abstraction	(Talwar <i>et al.</i> , 2000a)
	K256	PLP binding/maintain oligomeric structure	(Talwar <i>et al.</i> , 1997)
	R262	Distal interactions with PLP	(Jala <i>et al.</i> , 2003a)
	P297	Imparting substrate specificity	(Talwar <i>et al.</i> , 2000c)
H304	Inter-subunit interaction	(Jala, 2002)	
H356	Charge relay	(Jala, 2002)	
R401	Substrate binding	(Jagath <i>et al.</i> , 1997a)	
eSHMT	K229	Schiff's base with PLP and product expulsion	(Schirch <i>et al.</i> , 1993a)
	Y65	L-Ser binding ('Open' to 'closed' conversion)	(Contestabile <i>et al.</i> , 2000)
	R363	L-Ser binding	(Fratte <i>et al.</i> , 1994)
	H228	Stereo specificity	(Stover <i>et al.</i> , 1992)
	P257	Maintaining structure and function and folding	(Fu <i>et al.</i> , 2003)
	P258	Maintaining structure and function and folding	(Fu <i>et al.</i> , 2003)
P264	Maintaining structure and function and folding	(Fu <i>et al.</i> , 2003)	
rcSHMT	E75	L-Ser hydroxyl proton abstraction	(Szebenyi <i>et al.</i> , 2004)

suggesting that the enzyme was capable of catalyzing the reaction. However, the rate for this reaction could not be measured because of the low k_{cat} value. It was also demonstrated that K229Q eSHMT catalyzes the conversion of the bound L-Ser to Gly in the presence of THF to form 5, 10 -CH₂ THF at 2% of k_{cat} value of the wild-type enzyme. These observations suggested that the enzyme was capable of a single turn over (Schirch *et al.*, 1993a). Based on these results, it was suggested that, the Lys 229 plays a critical role in expelling the product by converting the external aldimine to an internal aldimine. These authors have showed that, in the absence of Lys 229, ammonia can also catalyze the same function, at a much slower rate (Schirch *et al.*, 1993a).

Lys 256 of scSHMT

The corresponding residue in scSHMT, Lys 256 was mutated to Gln and Arg. On mutation, the tetrameric enzyme was converted to a dimer, failed to bind PLP and was catalytically inactive (Talwar *et al.*, 1997). All the above studies suggested that Lys 256 plays an important role in binding PLP and maintaining the tetrameric structure of the enzyme (Talwar *et al.*, 1997). It can be suggested that an examination of the Lys mutants suggested that this residue has a different function in the dimeric and tetrameric forms of the enzyme.

Glu 74 of scSHMT

The retroaldol mechanism suggested for SHMT catalysis involves a proton abstraction from the hydroxymethyl group of L-Ser by an active site residue. Glu is a highly conserved residue in SHMT which prompted an examination of its role in SHMT catalysis. E74 scSHMT was mutated to Gln in scSHMT. THF-dependent cleavage of L-Ser was decreased by 300-fold when compared to wild-type. However, THF-independent cleavage of L-*allo* Thr and D-Ala were unaffected (Jala *et al.*, 2000). Thermal melting studies suggested that, on addition of L-Ser or Gly to mutant enzyme, it failed to show any change in the T_m . Addition of Gly and THF to mutant enzyme resulted in formation of the quinonoid intermediate absorbing at 495 nm. All the above results suggested that, E74 was not involved in proton abstraction, but is involved in conversion of enzyme from 'open' to 'closed' form, which is necessary for the physiological reaction to occur (Jala *et al.*, 2000).

Glu 75 of rcSHMT

The corresponding residue of E74 scSHMT in rcSHMT, (E75) was mutated to Gln and Lue. THF-dependent cleavage of L-Ser was completely abolished in the case of E75L mutant and a 500 fold decrease in the case of E75Q rcSHMT. It has been reported that the k_{cat} value for THF-independent cleavage of L-Ser was 0.13 and 0.34 min^{-1} for E75Q and E75L scSHMT, when compared to wild-type. L-*allo* Thr cleavage was enhanced by 110 and 430% for E75L and E75Q rcSHMT compared to wild-type respectively (Szebenyi *et al.*, 2004). Spectral studies suggested the formation of quinonoid intermediate at 495 nm on addition of L-Ser to both the mutants but were not seen in the wild-type. Rate of formation of quinonoid intermediate for E75Q was 460 and 11 min^{-1} and 64 and 23 min^{-1} for E75L rcSHMT. Based on the above results, it was concluded that formaldehyde release was rate limiting step in the reaction and E75 plays a role as an acid in cleavage of L-Ser by SHMT. Crystal structures of mutants with L-Ser and Gly were solved, however the structures were of low resolution and density for L-Ser or Gly was not clear in the respective binary complexes (Szebenyi *et al.*, 2004).

Tyr 65 of eSHMT

Tyr residues have been postulated to be involved in proton abstraction and cofactor binding. Tyr 65 of eSHMT was mutated to Phe to evaluate the role of this residue in eSHMT catalysis. On mutation of Y65, THF-dependent cleavage of L-Ser was decreased by 400 fold. Proton exchange studies with the mutant enzyme showed a 370-fold decrease compared to wild-type enzyme. THF-independent cleavage of L-*allo* Thr was completely abolished. Transamination reaction with D- and L-Ala was increased by 4-fold. The rate of hydrolysis of 5, 10-methenyl THF was comparable with wild-type enzyme (Contestabile *et al.*, 2000). Affinity for L-Ser and Gly were greatly altered in the mutant enzyme. A comparative analysis of rabbit and *E. coli* SHMT structures supports the 'open' to 'closed' conformational change that takes place when substrate amino acids bind. The carboxyl group of substrate Gly and the Arg 363 guanidinium group form an ion pair with two H-bonds (2.7 and 2.8 Å, respectively) in the ternary complex of *E. coli* SHMT, consistent with a critical role for this interaction in inducing the conformational change. It was concluded that in the closing of the active site the carboxyl group of substrate Gly moves to make close contact with the side chains of Arg 363 and Tyr 65. In addition to Tyr 65 and Arg

363, both Ser 35 and His 203 are also within H-bonding distance to the carboxyl group of Gly in the closed ternary complex (Contestabile *et al.*, 2000). Activity and affinity studies of the Y65F eSHMT suggest that Tyr 65 is not the catalytic base but that it may play a critical role in the ‘open’ to ‘closed’ conformational change that takes place on substrate binding.

Tyr 82 of scSHMT

Tyr 82 corresponding to Tyr 65 of eSHMT was mutated to Phe in scSHMT. Mutation resulted in 95% loss in activity with L-Ser and addition of Gly and THF did not yield the quinonoid intermediate. However, a small amount of proton exchange was observed. Y82F scSHMT could be converted to the ‘closed form’ in the presence of L-Ser as indicated by enhanced thermal stability (Jala *et al.*, 2000). Attempts to measure the formation of formaldehyde by complexing it with dimedone in the absence of THF showed that this mutant was not capable of forming formaldehyde rapidly. The mutation did not affect either PLP binding nor external aldimine formation. These observations suggested that Y82 was not involved in the formation of hemiacetal intermediate, but could be involved in stabilizing the quinonoid intermediate (Jala *et al.*, 2000).

Role of conserved residues in other PLP-dependent enzymes

It is of interest to discuss the role of above mentioned residues in other PLP-dependent enzymes in addition to SHMT. A combination of biochemical and structural studies on site-specific mutants of PLP-enzymes unravels the role of active site residues. These studies help in elucidation of the mechanism of catalysis.

Fold type I

Lys residues in PLP-enzymes, in addition to anchoring PLP as an internal aldimine, can function as a proton acceptor and donor, positioning the substrate and product release during catalysis. Mutational studies in combination with X-ray diffraction have provided valuable information on the function of these residues in catalysis. In this section role of active site Lys and Tyr of AAT, ODC and ALA are discussed in brief.

Lys 258 of AAT

AAT belongs to fold type I of PLP-enzymes and Lys 258 was proposed to anchor PLP and be involved in proton abstraction. Lys 258 of AAT was changed to Ala, Arg and His (Malcom and Kirsch, 1985; Ziak *et al.*, 1990; Toney and Kirsch, 1991a; Toney and Kirsch, 1993; Malashkevich *et al.*, 1995a). All the mutants were able to bind PLP even in the absence of Lys, suggesting that the enzyme can bind PLP by other interactions at the active site. Mutation of K258A AAT resulted in 10^6 - 10^8 times decrease in activity compared to wild-type AAT (Toney and Kirsch, 1993). K258R AAT was also virtually inactive but formed a quinonoid intermediate that was stable over several minutes suggesting that the reaction was blocked beyond this step by the mutation (Toney and Kirsch, 1991a). Mutation of K258 to H gave an enzyme 10^3 times slower in the overall reaction with L-Glu and 2-oxaloacetate and 10^6 times slower with 2-oxoglutarate. The three-dimensional structure of this mutant showed that N ϵ 2 of the imidazole ring to be 4 Å away from C $_{\alpha}$ or C-4' of the PLP-substrate adduct and thus too far to act directly as an acid-base catalyst (Ziak *et al.*, 1993; Malashkevich *et al.*, 1995a). The residual activity was probably due to a water molecule which was present in the 'closed' active site. Replacement of K258 by γ -thialysine, which is less basic than lysine, reduced k_{cat} approximately 10-fold and the proton abstraction was rate limiting (Gloss and Kirsch, 1995).

In addition to Lys, Tyr at the active site is postulated to be involved in proton abstraction in several PLP-enzymes and is a part of a charge relay system in some cases. In this section Tyr site specific mutants of AAT and 5-aminolevulinate synthase (ALA) are discussed in brief.

Tyr 225 of AAT

Tyr 225 is positioned within H-bonding distance of O-3' of PLP in AAT. Mutation of this residue to F resulted in a marked decrease in the k_{cat} value. The spectroscopic evidence indicated that the co-enzyme could still bind to the mutant enzyme as a Schiff's base (Golberg *et al.*, 1993), although with decreased affinity. An important consequence of the mutation was the lowering of the pK $_a$ of the internal aldimine. As a consequence, the k_{cat} was decreased by 450-fold compared to the wild-type enzyme. The K_m values for L-Asp and dissociation constant for α -methyl-

DL-Asp are 20 and 37 fold lower, respectively, than the wild type. An increased affinity for the substrate in the case of mutant enzyme was observed. These results were interpreted in terms of competition between the Tyr 225 –OH group and the substrate or the quasi-substrate amino group for the coenzyme (Golberg *et al.*, 1993). The rates of β -elimination reactions were not affected in this mutant suggesting Tyr 225 may not play a crucial role in proton abstraction. In conclusion, Tyr 225 stabilizes the reactive unprotonated form of the internal aldimine at physiological pH values. The mutation studies also reveal that the intrinsic free energy for binding of substrate is greater than that for the mutant enzyme alone. The excess energy is utilized to increase the rate of the subsequent reactions (Golberg *et al.*, 1993).

Tyr 70 of AAT

In addition to Y225, the role of Y70 in AAT catalysis was analyzed. Y70 makes hydrogen bonds to 5'-phosphate of the PLP and to the ϵ - amino of K258 in the aldimine and ketimine intermediates. The mutation of this residue to H (Pan *et al.*, 1994) or F (Toney and Kirsch, 1987; Inoue *et al.*, 1991) results in a partial loss of catalytic activity suggesting that it's contribution to PLP binding is probably the reason why this residue is conserved in all AAT.

Tyr 121 of 5-aminolevulinatase synthase (ALA)

Tyr 121 is a conserved residue in all known sequences of ALA, it corresponds to Tyr 70 of *E. coli* AAT, which has been shown to interact with the cofactor and prevent the dissociation of the cofactor from the enzyme. This residue was substituted by F and H (Tan *et al.*, 1998). The Y121F mutant retained 36% of the wild-type activity and the K_m value for substrate Gly increased 34-fold, while the activity of the Y121H mutant was decreased to 5% of the wild-type activity and the K_m value for Gly increased fivefold. Y121F, and Y121H, respectively. The UV-visible absorbance and CD spectra of Y121F and Y121H mutants were similar to those of the wild-type with the exception of an absorption maximum shift (420 to 395 nm) for the Y121F mutant in the visible region of the spectrum, suggesting that the cofactor binds the Y121F mutant enzyme in a more unrestrained manner. Y121F and Y121H mutant enzymes also exhibited lower affinity than the wild-type for the cofactor, reflected in the k_d values for PLP (Tan *et al.*, 1998). Further, Y121F and

Y121H were less thermostable than the wild-type. These findings indicate that Tyr 121 plays a critical role in cofactor binding of murine erythroid ALA (Tan *et al.*, 1998).

Fold type II

TS represent fold type II family, and the role of active site residues like Lys and Glu are discussed in brief. In addition studies on Lys mutants of cystathionine β -synthase is also presented.

Lys 87 of TS

TS catalyzes synthesis of L-Trp and D-glyceraldehyde 3-phosphate from indole-3-glycerol phosphahate and L-Ser and belongs to fold type II. Replacement of this residue by Thr does not prevent PLP binding. K87T was able to form an external aldimine with L-Ser very slowly. On addition of β -chloro-alanine, L-Trp and D-Trp significant spectral changes were observed. The K87T could catalyze β -elimination of β -chloro-alanine and L-Ser very slowly leading to the formation of aminoacrylate (Lu *et al.*, 1993). The gel filtration experiments showed that, external aldimine formed with Ser and Trp were stable for a concidrable period of time. From the above studies it was concluded that, K87 is an essential catalytic residue in β -elimination and β -replacement reactions and serves important roles in transimination and product release step of catalysis (Lu *et al.*, 1993).

Lys 119 of cystathionine β -synthase

ϵ -Amino group of Lys 119 of cystathionine β -synthase forms Schiff's base with PLP, resulting in the formation of internal aldimine. This residue has been proposed to be involved in proton abstraction step of catalysis. Hence, Lys 119 was mutated to Ala. Mutation resulted in 10^3 -fold decreased activity, which increased approximately 2-fold in the presence of an exogenous base, ethylamine. Mutant enzyme was able to form external aldimine in presence of L-Ser or cystathionine, this was supported by spectral shift from 412 to 420 nm. However, an aminoacrylate intermediate was not formed at detectable levels. These results suggest a role for K119 as a general base in the reaction catalyzed by human cystathionine β -synthase (Evande *et al.*, 2004).

Glu 109 of TS

In addition to Lys, Glu is another residue which is highly conserved among most of the PLP-enzymes. This residue has been postulated to be involved in proton abstraction or in substrate binding. Glu 109 has been identified on the basis of X-ray structure as the residue potentially responsible for inducing the nucleophilicity of the indole group by proton abstraction from N-1. This proposal is supported by mutation of E109 to D (Dunn *et al.*, 1990). The steady-state rate of the β -reaction was reduced 27-fold and accumulation of the quinonoid chromophore was no longer detectable. These results suggest that mutation of E109 to D affected quinonoid intermediate generation, suggesting that formation of a covalent bond between indole and aminoacrylate could be a rate limiting step (Dunn *et al.*, 1990).

Fold type III

ALR is a type member of fold type III, the role of active site Lys 39 and Tyr 265 and R219 is described in brief in the following section.

Lys 39 of ALR

ALR catalyzes racemization reaction of D-Ala to L-Ala. The active site Lys 39 which anchors PLP was mutated to Ala. The mutant enzyme was inherently inactive, but gained activity to the extent of 0.1% of the wild-type enzyme, upon addition of 0.2 M methylamine. The amine-assisted activity of the mutant enzyme depended on the pK_a values and molecular volumes of the alkylamines used (Watanabe *et al.*, 1999a). A strong kinetic isotope effect was observed when α -deuterated D-Ala was used as a substrate in the methylamine-assisted reaction. In contrast, only L-enantiomer of Ala showed a solvent isotope effect in deuterium oxide in the methylamine-assisted reaction. These results suggest that methylamine serves as a base not only to abstract the α -hydrogen from D-Ala but also to transfer a proton from water to the α -position of the deprotonated intermediate to form D-Ala. Lys 39 of the wild-type enzyme probably acts as the catalyst base specific to the D-enantiomer of Ala (Watanabe *et al.*, 1999a).

Lys 69 of ODC

The ϵ - amino group of Lys 69 of ODC forms Schiff's base with PLP resulting in the formation of internal aldimine. It was of interest to envisage the role of Lys 69 in addition to anchoring PLP hence, Lys 69 of ODC was replaced to Arg and Ala. Analysis of K69A ODC demonstrated that the mutant enzyme was co-purified with amines (e.g. putrescine) and these amines were tightly bound at the active site through a Schiff base with PLP. In the case of K69R ODC, spectral studies showed that PLP is probably bound to this mutant enzyme in the aldehyde form. The pre-steady-state kinetic analysis of K69R ODC with L-Orn and putrescine demonstrated that the rates of both product release and the decarboxylation steps were decreased by 10,000 fold. Further, the rates of Schiff base formation between K69R ODC and either substrate or product were decreased by at least 1000 fold (Osterman *et al.*, 1999). Product release remains as a dominant rate-limiting step in the reaction. The effect of mutating Lys 69 on the decarboxylation step suggests that Lys 69 may play a role in the proper positioning of the α -carboxylate for efficient decarboxylation. K69R ODC binds diamines and amino acids with higher affinity than the wild-type enzyme; however, Lys 69 does not mediate substrate specificity. Wild-type and K69R ODC have similar ligand specificity. All these studies suggest that, Lys 69 plays a role in the positioning of the COO^- group for efficient catalysis. This helps in confining catalytic competency to only the biological amino acid, L-Orn (Osterman *et al.*, 1999).

Tyr 265 of ALR

Tyr 265 was postulated to be involved in proton abstraction in combination with Lys of ALR. Hence, Tyr 265 of ALR was mutated to Ala, Ser and Phe. The Y265A mutant was a poor catalyst for alanine racemization, like Y265S and Y265F. However, Y265A and Y266S catalyzed transamination with D-Ala much more rapidly than the wild-type enzyme, and the bound coenzyme, PLP, was converted to PMP (Watanabe *et al.*, 1999 b). The rate of transamination catalyzed by Y265F was about 9% of that by the wild-type enzyme. However, Y265A, Y265S, and Y265F were similar in that L-Ala was inert as a substrate in transamination. The apo-form of the wild-type enzyme catalyzes the abstraction of tritium non-specifically from both (4'S)- and (4R)-[4'- ^3H]PMP in the presence of pyruvate (Watanabe *et al.*, 1999b).

In contrast, apo-Y265A abstracts tritium virtually from only the *R*-isomer. This indicates that the side-chain of Y265 abstracts the C_α-hydrogen of L-Ala and transfers it to the *pro-S* position at C-4' of PMP. Y265 is the counterpart residue to K39 that transfers the α-hydrogen of D-Ala to the *pro-R* position of PMP. In conclusion, Y265 of ALR serves as the base specific to L-Ala (Watanabe *et al.*, 1999a).

In addition to mutational studies on Tyr residues, studies on Arg 219 mutants (R219K, R219A, and R219E) support the two-base mechanism involving Y265 and K39. R219 and Y265 are connected through H166 via hydrogen bonds. The R219 mutants exhibit increased primary isotope effects but unchanged solvent isotope effects in the L → D direction and increased solvent isotope effects but unchanged primary isotope effects in the D → L direction compared to wild-type (Sun and Toney, 1999). These results support a two-base racemization mechanism involving Y265 and K39. They additionally suggest that Y265 is selectively perturbed by R219 mutations through the H166 hydrogen-bond network. The group responsible for this ionization is likely to be the phenolic hydroxyl of Y265, whose pK_a is electrostatically perturbed in the wild-type by the H166-mediated interaction with R219. Accumulation of an absorbance band at 510 nm, indicative of a quinonoid intermediate, only in the D → L direction with R219E provides additional evidence for a two-base mechanism involving Y265 and K39 (Sun and Toney, 1999).

It is evident from the discussion presented above that fold type I, II and III enzymes Lys, Tyr, and Glu residues play a crucial role in catalysis, although there are subtle differences in their functions.

SHMT as a drug target

The search for targets and molecules that can interact with them has been a long time goal of the drug discovery research. Historically enzymes have been a favorite drug target and some of these chemicals are now in clinical use. Several PLP-enzymes have been studied as possible targets for various disease conditions (Amadasi *et al.*, 2007). SHMT is not only a PLP-dependent enzyme but also involved in folate metabolism. Two enzymes of this pathway namely dihydrofolate

reductase (DHFR) and thymidylate synthase are still effective targets in cancer chemotherapy. The relationships between SHMT and these two enzymes are shown in Fig I.10. It is clear from the Fig I.10 that the three enzymes SHMT, DHFR and thymidylate synthase are essential for the synthesis of thymidylate, a unique metabolite required for DNA biosynthesis and is not obtained by the salvage pathway. Methotrexate, one of the earliest anticancer compounds, targets DHFR and has been in clinical use for more than 50 years (Huennekens, 1994). The 5-Fluorouracil and tumodex are clinically established inhibitors of thymidylate synthase (Rustum *et al.*, 1997). In addition, these inhibitors are also used as antibacterial and antiprotozoal agents (Hartman, 1993; Then, 1993). Drug resistance is a common problem in chemotherapy (Volm, 1998). Therefore there is a continued search for novel drug targets and SHMT as a part of thymidylate synthase cycle has been preferred as a possible target (Fig I.10). It has been shown that SHMT levels were increased by 5 to 10 fold in most of the cancer cells (Bertino *et al.*, 1963; Thorndike *et al.*, 1979). The increased SHMT activity along with enhanced DNA synthesis in neoplastic tissues has suggested that SHMT might be a target for cancer chemotherapy (Rao *et al.*, 2000).

Two common approaches for inactivating a target have been the use of chemicals and biologicals. The chemical compounds that have been examined for inhibiting SHMT activity has been either amino acid or folate analogues. The early attempts of identifying folate analogues (mostly DHFR inhibitors) were unsuccessful (Baskaran, 1989), except for couple of triazine derivative containing a sulphonyl fluoride group and FTHF (Snell and Riches, 1989).

The amino acid derivatives appeared to be more promising as inhibitors. Table I.3 lists a few important compounds examined as inhibitors for SHMT. D-cycloserine (DCS), an analogue of L-Ser, was not a good inhibitor of SHMT *in vitro*. DCS was found to inactivate selectively SHMT in mouse liver extract (Bukin Iu and Sergeev, 1968) and in sheep liver extract (Manohar *et al.*, 1984).

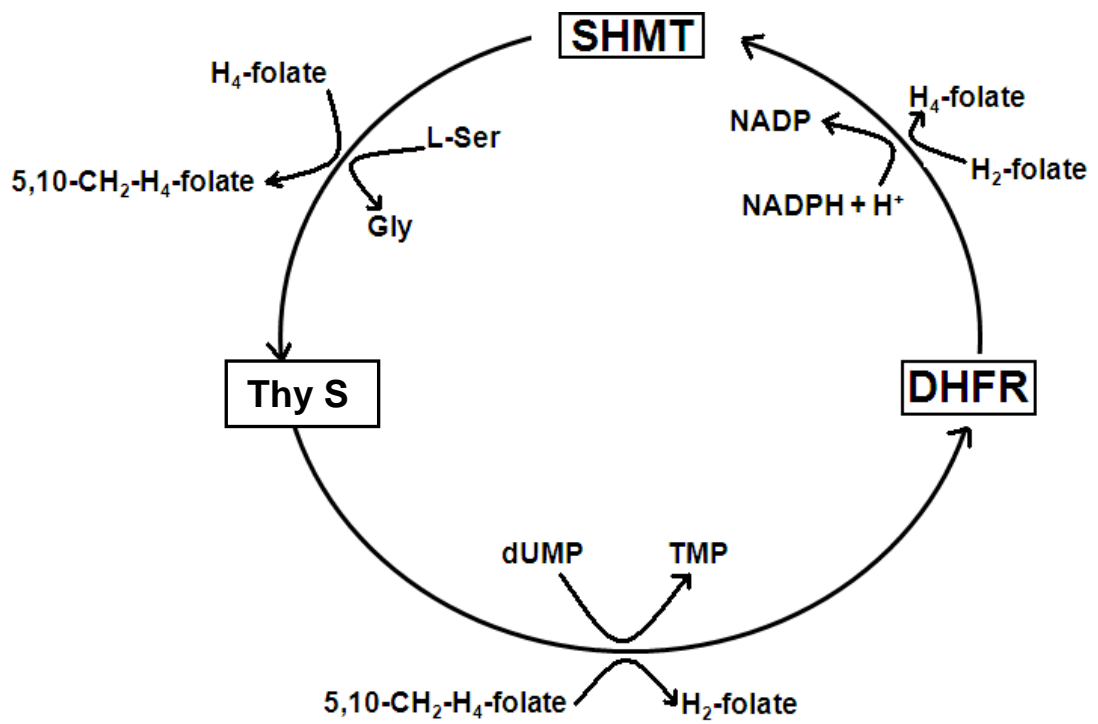
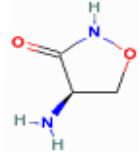
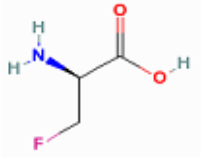
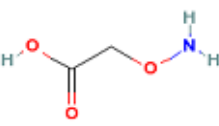
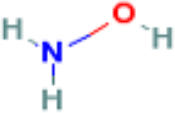
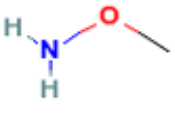
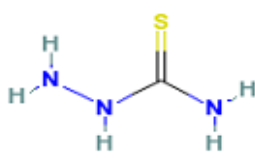
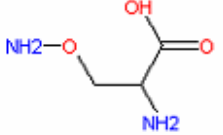
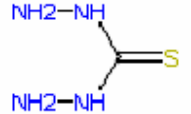


Fig L.10: A schematic representation for enzymes involved in biosynthesis of thymidylate.

Table I.3: List of compounds examined as inhibitors for SHMT.

No.	Compound	Structure	K_i	References cited
1	D-Cycloserine		0.7 mM	(Wang <i>et al.</i> , 1981)
2	3-Fluoro-D-Alanine		56 mM	(Wang <i>et al.</i> , 1981)
3	Aminooxyacetic acid		2 μ M	(Baskaran, 1989; Baskaran <i>et al.</i> , 1989b)
4	Hydroxylamine		2 μ M	(Baskaran, 1989)
5	Methoxyamine		25 μ M	(Acharya <i>et al.</i> , 1991; Acharya <i>et al.</i> , 1992)
6	Thiosemicarbazide		50 μ M	(Acharya <i>et al.</i> , 1992; Acharya and Rao, 1992)
7	O-Amino-D-Serine		1.8 μ M	(Baskaran, 1989; Baskaran <i>et al.</i> , 1989a)
8	Thiocarbohydrazide		3 μ M	(Acharya <i>et al.</i> , 1992)

It is also well known that DCS inhibits other PLP-dependent enzymes like alanine aminotransferase and AAT (Christen and Metzler, 1985). O-Amino-D-Ser (OADS), a hydrolytic product of DCS, and an aminoxy analogue of L-Ser was a very potent inhibitor of SHMT with a K_i of 1.8 μM (Baskaran *et al.*, 1989a). The unique feature of interaction of this inhibitor with SHMT was the generation of a characteristic intermediate (Baskaran *et al.*, 1989a).

In addition to OADS, methoxyamine (MA) and aminoxyacetic acid (AAA) which are derivatives of hydroxylamine (HA) have been extensively used in the study of inhibition mechanism of SHMT (Baskaran, 1989; Acharya, 1992; Jagath, 1997). HA is a strong nucleophile which disrupts the PLP-Schiff's base at the active site. MA is a smallest substituted derivative of hydroxylamine. It has been shown that, MA is the reversible non-competitive inhibitor of scSHMT with a K_i of 25 μM (Acharya *et al.*, 1991). MA interacts with SHMT forming an intermediate absorbing at 388 nm. It was proposed that this intermediate was PLP and is slowly converted to the final oxime product absorbing at 325 nm. The reaction of AAA with the Schiff base of the enzyme resulted in the formation of PLP and was biphasic with rate constants of 191 and 19 s^{-1} . The formation of the PLP-AAA oxime measured by decrease in absorbance at 388 nm on interaction of AAA with the enzyme had a rate constant of 5.2 $\text{M}^{-1} \text{s}^{-1}$ (Baskaran *et al.*, 1989b). The reaction of DCS with the enzyme was much slower than the aminoxy compounds.

These results indicate that aminoxy compounds which are structural analogues of L-Ser (OADS and AAA) form PLP as an intermediate prior to the generation of the oxime. A detailed kinetic analysis of MA interaction with SHMT revealed that it was a poor inhibitor when compared to AAA and OADS. This lead to the conclusion that, the presence of a α -carboxyl and amino group in a compound is necessary for effective inhibition. The structural relationships of the aminoxy compounds and amino acid analogues are given in Fig I.11 to highlight their relationships.

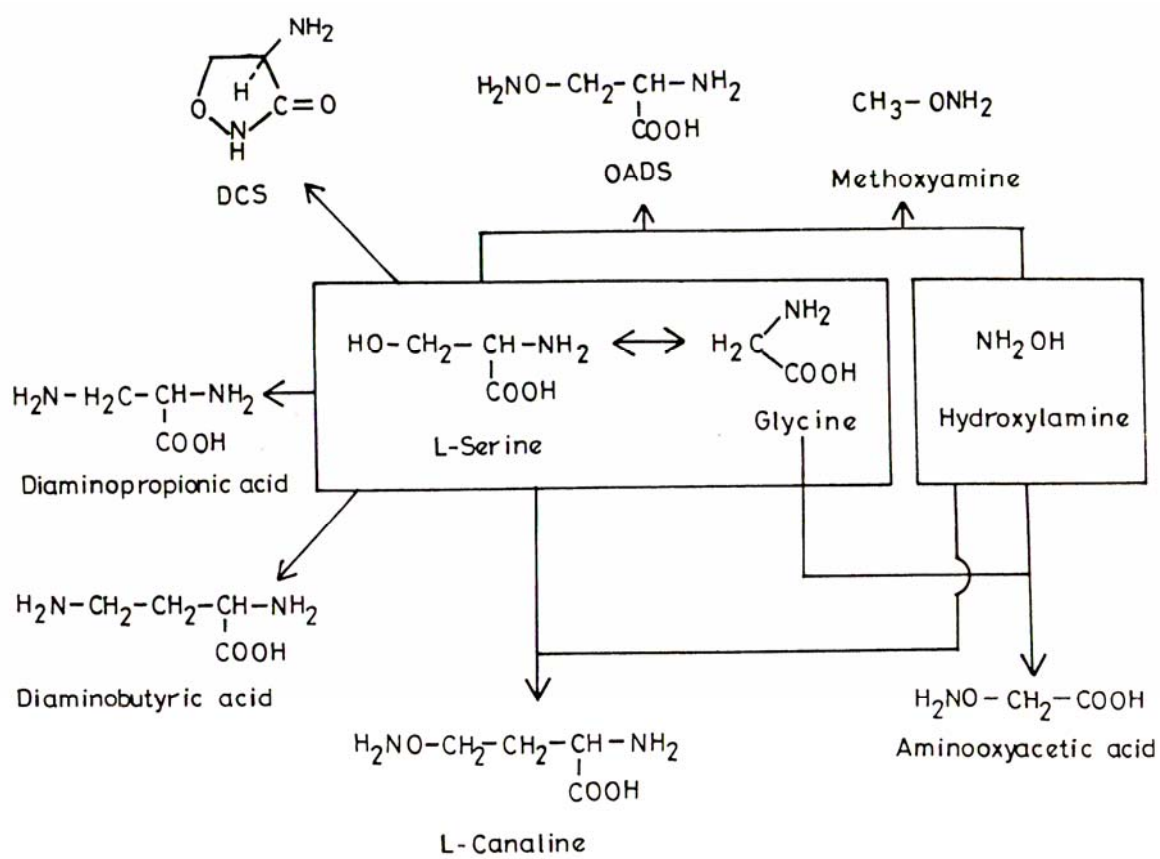


Fig I.11: Structural relationship among aminoxy compounds and amino acid analogues.

Earlier reports also suggested that the plant amino acid, mimosine, inhibits DNA replication in mammalian cells by targeting SHMT (Oppenheim *et al.*, 2000). Thiosemicarbazide (TSC) is a well studied inhibitor of PLP-dependent enzymes (Kolsterman, 1986). It is another well studied inhibitor of SHMT (Acharya and Rao, 1992). TSC shows a slow tight binding inhibition with SHMT. Interaction with TSC generated a novel quinonoid intermediate which was not seen earlier in other PLP-enzymes. The intermediate could not be removed by dialysis. This intermediate was slowly converted to the final product with a rate constant of $4 \times 10^{-5} \text{ s}^{-1}$ (Acharya and Rao, 1992). Studies with TSC suggest that, TSC locks up the enzyme in an inactive form for a long period. This inhibitor was specific for SHMT, as other PLP-dependent enzymes were unaffected. Further, kinetic studies with substituted derivatives of TSC showed that proton abstraction from N2 atom was an important step in the interaction. In addition to TSC, 4-chloro-L-Thr was shown to be a mechanism based inhibitor of SHMT (Webb and Matthews, 1995).

Although, SHMT can be an alternative target of cancer, as described above, the following points need to be kept in mind in evaluating its potential. (i) As a number of PLP-dependent enzymes exhibit catalytic diversity, it may be difficult to attain a high degree of specificity, (ii) since SHMT exists in two isoforms, cytosolic and mitochondrial form, designing new inhibitor would need to be more specific, (iii) A balance between the positive and negative side effects of drug should be considered, (iv) targeting a particular cancerous organ/tissue or cell for delivering the drug leaving normal tissue unaffected.

Naturally occurring compounds as potential bioactive molecules

Much before using synthetic compounds as drugs, and the advent of modern medicine, medicinal herbs have been used in primary health care in many centuries. Over the past 20 years, extensive research has been undertaken to explore the benefits of vegetables, fruits and spices. Several epidemiological studies have shown that a diet rich in plant foods may reduce the development of certain chronic diseases. Studies suggest that a most of the spices contain anti-oxidants and other chemicals of medicinal value. Two examples relevant to cancer therapy are

vincristine and vinblastine (Nelson, 1982; Tsuruo *et al.*, 1983; William *et al.*, 1994). A wide variety of phenolic substances derived from spices possess potent anti-oxidant, anti-inflammatory, anti-microbial and a few of them have anti-carcinogenic activities also (Young-Joon, 2002). Some examples of anti-oxidative and anti-inflammatory spice ingredients with chemopreventive potential are curcumin, gingerol, alliin, allyl thiosulfates and capsaicin. Since pro-inflammatory and pro-oxidant states are closely linked to tumor promotion, substances with potent anti-inflammatory and/or anti-oxidant activities are anticipated to exert chemopreventive effects on carcinogenesis. Curcumin, a yellow pigment present in the rhizome of turmeric, the oleoresin from rhizomes of ginger contains gingerol (1-[4'-hydroxy-3'-methoxyphenyl]-5-hydroxy-3-decanone) and the principal pungent substance capsaicin (trans-8-methyl-N-vanillyl-6-nonenamide) in chilli exhibit a wide array of pharmacological and physiological activities (Young-Joon, 2002) (Fig I.10).

The effects of curcumin, gingerol and capsaicin appear to be associated with their anti-oxidant and/or anti-inflammatory activities. One of the most important targets of these chemo-preventive spice ingredients involves NF-kB that regulates expression of a whole variety of genes, including cyclooxygenase-2 (COX-2) responsible for inflammation and malignant transformation. The inhibition of NF-kB activation by curcumin, gingerol and capsaicin is thought to be mediated through multiple mechanisms, one of which involves the mitogen-activated protein (MAP)-kinase cascades (Young-Joon, 2002). In addition to turmeric, ginger and chilli, garlic is known to have anti-carcinogenic activity. Since garlic extract has been used in the present study, structures of a few bio-active compounds present in garlic extract are already shown in Fig I.10.

Garlic and Cancer

Garlic is universally used as a flavoring agent in foods and in traditional medicine. The beneficial effects of garlic consumption in treating a wide variety of human diseases and disorders have been recorded and passed down in many civilizations. The genus *Allium* comprises over 600 species, which include *Allium cepa* (onion), *Allium porrum* (leek), *Allium sativum* and *Allium schoenoprasum* (chives). The genus *Allium* belongs to the Alliaceae family (Rahman, 2003). Garlic

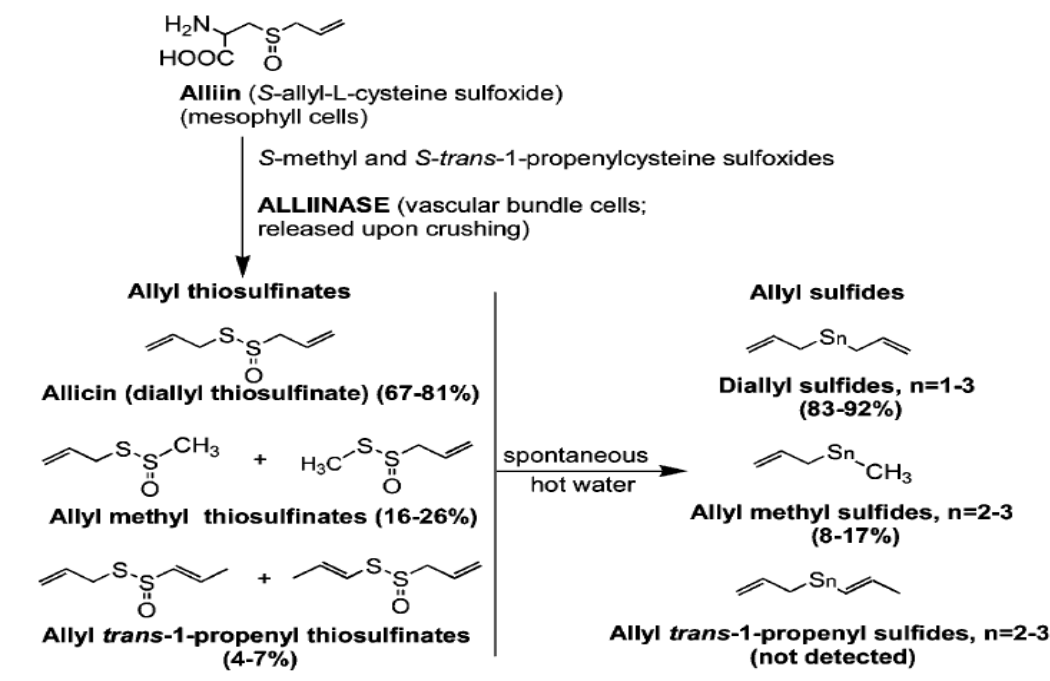
contains unique organo-sulfur compounds, which confers characteristic flavour and odour and contributes to its potent biological activity.

Large numbers of investigations on active principles from garlic have focused attention on the sulfur compounds (Fig I.12). Amongst these, nearly 85% comprise of alliin and two γ -glutamylpeptides. Alliin is considered as the parent substance of the therapeutically active sulfur components of garlic. When garlic is crushed, cut or chewed, alliin is exposed to alliinase and the thiosulfinate, allicin is formed (Larry and Christopher, 2005). Allicin is a reactive intermediate species that can be transformed into a variety of compounds depending on environmental conditions and extraction methods and is also thought to be responsible for the odor of fresh cut or crushed garlic. Besides the organosulfur compounds (Fig I.12), garlic also contains carbohydrates (fructans), enzymes (alliinase, catalase), proteins, free amino acids, lipids, polyphenols and phytosterols (Larry and Christopher, 2005).

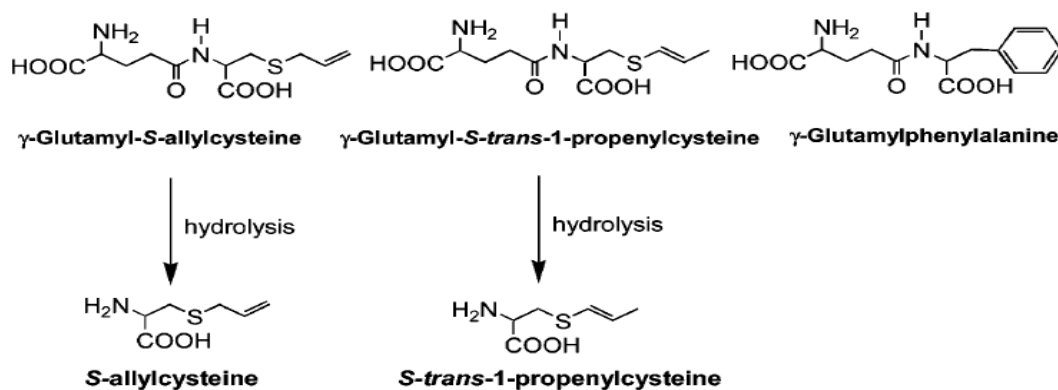
Earlier studies have reported that, garlic has anti-oxidants, anti inflammatory, anti-microbial and anti-carcinogenic activities (Rahman, 2003). Many studies have reported the anti-cancer effects of garlic. For example, diallyl disulfide (DADS) is an oil-soluble organosulfur compound found in garlic and is reported to have anti-cancer properties against both hormone-dependent and -independent breast cancers and may harmonize with polyunsaturated fatty acids which are known as modulators of breast cancer cell growth (Nakagawa *et al.*, 2001). In support of this, other studies indicate that derivatives of garlic can inhibit proliferation of a human prostate cancer cell lines and a human breast cancer cell line (Pinto and Rivlin, 2001). Garlic also inhibits the proliferation of human colon; lung and skin cancer cells and induces apoptosis of human colon tumour cells by increasing intracellular calcium concentrations (Sundaram and Milner, 1996 a, b).

Recently γ -glutamyl-Se-methylselenocysteine from garlic has been shown to be a cancer chemo-preventative agent (Dong *et al.*, 2001). The use of herbal medicines plays a significant factor in modern health care. However, mechanisms of action of herbs and phytochemicals need to be established in *vitro* and in *vivo*. At the moment the studies have been conducted using fresh garlic and a host of different

Compounds derived from garlic



γ-Glutamyl dipeptides



Components derived from turmeric, ginger and chilli

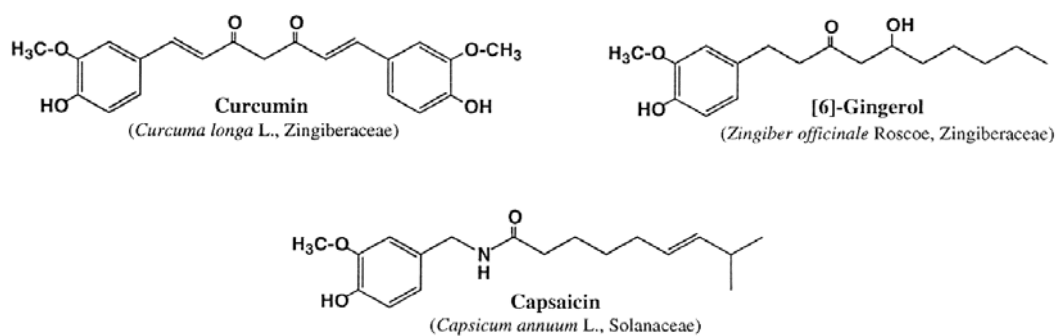


Fig I.12: Structure of bio-active compounds from garlic, turmeric, ginger and chilli.

garlic preparations but few studies have been carried out with isolated compounds. In addition to using the substrate analogues of L-Ser or Gly as inhibitors, several compounds can be isolated for spices and inhibition studies performed to elucidate their potential as anti-cancer agents. Since the chemical structure these compounds are available, further chemical modifications can be carried out to obtain a better inhibitor for SHMT.

Additional attributes of SHMT molecule

In addition to SHMT being a target for cancer chemotherapy, recent reports suggest that, SHMT can be used as starter culture in yogurt preparation and as a biocatalyst. In yogurt, the typical flavor is caused by lactic acid, which imparts an acidic and refreshing taste, and a mixture of various carbonyl compounds like acetone, diacetyl, and acetaldehyde, which is considered as the major flavoring component (Chaves *et al.*, 2002). SHMT catalyzes interconversion of L-Thr or L-*allo* Thr to Gly and acetaldehyde. This reaction can be exploited, by supplementation of the growth medium with L-Thr and by using a strain which consists of stable SHMT as a starter culture. This helps in controlled and improved acetaldehyde production in fermented (dairy) products (Chaves *et al.*, 2002).

β -Hydroxy- α -amino acids are an important class of natural products with biological activity both on their own and as constituents in many naturally occurring complex compounds, such as antibiotics and immunosuppressants (Saeed and Young, 1992; Yadav *et al.*, 1995). There are two preliminary reports on SHMT being used as biocatalyst in literature. It is shown that, SHMT was capable of reacting with synthetic aldehydes for the production of β -hydroxy- α -amino acids with moderate stereospecificity. A kinetically controlled reaction with SHMT has been used for the synthesis of hydroxythreonine derivatives, yielding γ -benzyloxy-L-*allo* Thr and γ -benzyl-oxymethyl-L-*allo* Thr with high diastereoselectivity (Vidal *et al.*, 2005; Gutierrez *et al.*, 2008). SHMT, from *Streptococcus thermophilus* was used as stereocomplementary biocatalysts for the aldol addition to Gly and N-Cbz amino aldehydes (Cbz-benzyloxycarbonyl) and benzyloxyacetaldehyde. By manipulating reaction parameters, such as temperature, Gly concentration, and reaction media, SHMT yielded exclusively L-*erythro* diastereomers in 34-60 % conversion. Further

SHMT has high synthetic activity with negligible retroaldol activity on L-Thr at 4° C. The *L-erythro* isomer was kinetically favored and the reactions were virtually irreversible and highly stereoselective. It was also found that treatment of the prepared N-Cbz-gamma-amino-beta-hydroxy-alpha-amino acid derivatives with potassium hydroxide (1 M) resulted in the spontaneous formation of 2-oxazolidinone derivatives of the beta-hydroxyl and gamma-amino groups in quantitative yield. This reaction might be useful for further chemical manipulations of the products (Gutierrez *et al.*, 2008)

It is evident from the above literature survey that there are several ambiguities to be resolved in the structural and functional aspects of SHMT. The determination of 3-D structures of site specific mutants of bsSHMT and their complexes with substrate(s) and inhibitor(s) may help in resolving these ambiguities. It was expected that these studies would clarify questions on the role of specific amino acid residues in the reaction mechanism of SHMT. In addition to characterization of site specific mutants, an attempt was also made to screen the potential bioactives using such molecules from selected spices for the identification of possible compounds with anti-cancer activity.

SCOPE AND OBJECTIVES

Serine hydroxymethyltransferase (SHMT), a PLP-dependent enzyme catalyzes the reversible conversion of L-Ser and THF to Gly and 5, 10 CH₂ THF and THF-independent cleavage of 3-hydroxy amino acids. SHMT, a key enzyme in the biosynthesis of amino acids and nucleotides, is a target for cancer chemotherapy. The available biochemical and structural data on SHMT from different sources ranging from *E. coli* to human has enabled the identification and critical examination of the roles of active site residues in different steps of the reaction catalyzed by the enzyme. However, the exact roles of these residues in the reaction mechanisms are less understood. Determination of the structures of mutant SHMTs with bound substrate(s)/inhibitors, biophysical and kinetic studies would be critical to understand the mechanistic details of the reaction.

The objectives of the present investigation are: mutation of selected amino acid residues in the active site of bsSHMT that could be involved in THF-dependent and -independent reactions, biochemical characterization of the mutant enzymes and crystallization of the mutant enzymes with their substrate(s)/inhibitor complexes to understand the role of these residues. Establish the mechanism of THF-independent cleavage of 3-hydroxy amino acids and study the interaction of chemical inhibitors and compounds from natural sources to understand the role of SHMT in cancer. This thesis consists of the following chapters including results and discussion in each chapter.

Specific objectives of the present study are:

CHAPTER 1: The role of lysine 226 in the reaction catalyzed by bsSHMT

Lys residue at the active site of PLP-enzymes, in addition to anchoring the cofactor, it functions as a proton acceptor or a donor and confers reaction specificity to the PLP-enzymes. It has also been proposed that Lys 229 in eSHMT is crucial for product expulsion in the rate determining step of catalysis. However, in other PLP-dependent enzymes, the corresponding residue has been implicated in proton abstraction step of catalysis. In the present investigation, Lys 226 of bsSHMT is

mutated to Met and Gln by site-directed mutagenesis (PCR-based sense and antisense primer method). After confirming the mutations by DNA sequencing and ensuring that there are no mutations elsewhere in the molecule, the mutant clones are overexpressed in *E.coli*. The mutant proteins are purified by procedures already established for the bsSHMT. Attempts are made to co-crystallize the mutant proteins and with their substrate(s)/inhibitor(s) complexes. The biophysical and biochemical properties of Lys mutants will be examined. The results are evaluated for establishing the role of the Lys residue in catalysis.

CHAPTER 2: The involvement of glutamate 53 in binding of L-serine and folate, and conversion of bsSHMT from 'open' to 'closed' form

The retroaldol mechanism for the THF-dependent reaction of L-Ser requires a well positioned residue in the active site that could abstract a proton from hydroxymethyl group of L-Ser. It has been suggested, that a Glu residue at the active site can carry out this function. The crystal structure of the binary and ternary complex of bsSHMT suggests that Glu 53 interacts with the hydroxymethyl group of L-Ser and N5 and formyl oxygen of FTHF. In order to examine the role of this residue, Glu 53 is mutated to Gln and the mutant enzyme are characterized and attempts are made to co-crystallize it with substrate(s)/inhibitor(s) complexes by a procedure standardized earlier for bsSHMT.

CHAPTER 3: The role of tyrosine residues in cofactor binding and elucidation of mechanism for the tetrahydrofolate-independent cleavage of L-allo threonine

In addition to L-Ser and Gly interconversion, SHMT also catalyzes the THF-independent cleavage of 3-hydroxy amino acids and transamination. Although extensive studies have been carried out on the mechanism of THF-dependent reaction of SHMT, not much is known about the mechanism of THF-independent cleavage of 3-hydroxy amino acids. Studies with the mutant enzymes of SHMTs suggest that the THF-dependent and THF-independent reactions might be proceeding by different mechanisms. It is possible that the cleavage occurs by a mechanism different from the classical retroaldol cleavage. Y51 and Y61 will be mutated to F, F/A and Y61A and the structural and functional studies are carried out to examine the role of Tyr residues in bsSHMT catalysis.

CHAPTER 4: *Interaction of bsSHMT with specific inhibitors from extracts of various spices*

This study would help in monitor interaction of aminoxy compounds with bsSHMT and its mutants to study their differences in the interactions. The pivotal role of SHMT in the interconversion of folate coenzymes and its altered kinetic properties in neoplastic tissues suggested that it could be a potential target for cancer chemotherapy. In addition to known inhibitors, the effect of spices extracts, such as garlic, turmeric, chilli and ginger is examined to indentify selected bio-active compounds with possible therapeutic functions. Complementing these efforts, homology modeling and bioinformatic approaches would be employed to look for compounds that could inhibit SHMT activity.

MATERIALS AND METHODS

Materials

Acrylamide (A 3553), D-Ala (A 7377), alcohol dehydrogenase (ADH) (A 3263), L-*allo* Thr (210269), aminooxyacetic acid (AAA) (A 4508), ampicillin (A 0166), bovine serum albumin (BSA) (A 7030), bromophenol blue (B 5525), Coomassie Brilliant Blue (B 8647), chloramphenicol (C 3175), DL-dithiothreitol (DTT) (D 0632), 2,5-diphenyloxazole (PPO) (D 4630), diethylaminoethyl-(DEAE)-cellulose(D6418), 5,5-dimethyl-1,3-cyclohexanedione (dimedone) (D 153303), Dialysis tubing (D 2272), ethylenediaminetetraacetic acid (EDTA) (E 5134), folic acid (F 7876), Glycine (G 6201), isopropyl-1-thio- β -D-galactopyranoside (IPTG) (I 5502), methoxyamine (MA) (226904), 2-mercaptoethanol (2-ME) (M 7522), N,N'-methylene-bis-acrylamide (01704), NADH (N 6660), pyridoxal 5'-phosphate (PLP) (P 3657), 2-methyl 2,4-pentanediol (MPD) (68336), L-Ser (S 1315), sodium dodecyl sulfate (SDS) (L 3771), trichloroacetic acid (TCA) (T 0199), N,N,N',N'-tetramethylenediamine (TEMED) (T 9281), Tris-(hydroxymethyl) aminomethane (Tris-base) (154563) The above chemicals were obtained from Sigma Chemicals Co. St. Louis, MO, USA. L-[3-¹⁴C] Ser (55m Ci/mmol) was obtained from Amersham Pharmacia Biotech, Bucks, UK. Deep Vent polymerase and DpnI restriction enzyme purchased from New England Biolabs, Inc., Beverly, MA, USA. The oligonucleotide primers were custom synthesized by Bangalore Genei Pvt. Ltd., Bangalore or Microsynth, Balgach, Switzerland. Centricon filters were from Amicon Inc., Beverly, MA, USA. All other biochemicals used in this study were analytical grade and of the highest purity available.

Methods

Preparation of THF

THF was prepared by hydrogenation of folic acid using platinum oxide as a catalyst (Hatefi *et al.*, 1959). A suspension of platinum oxide (10 mg/ml) in glacial acetic acid was taken in a hydrogenation vessel and reduced with hydrogen gas at a pressure of 30 lbs/sq inch for 6 h using a *Parr* hydrogenation apparatus. Folic acid (10 mg ml⁻¹) was added in glacial acetic acid (100 ml) and the hydrogenation was continued for 12 h. During the course of hydrogenation, the yellow colored folic acid solution changed to a nearly colorless solution of THF. After the completion of the reaction, the contents of the hydrogenation vessel were filtered through a sintered

glass funnel attached to a round bottom flask immersed in liquid nitrogen and immediately lyophilized. The white powder, thus obtained, was dissolved in 0.4 M potassium phosphate buffer, pH 7.4, containing 1.8 mM DTT and stored at -70°C in small aliquots under liquid nitrogen. The concentration of the THF was estimated by measuring the absorbance at 297 nm. A molar extinction coefficient value of $28 \times 10^3 \text{ M}^{-1}\text{cm}^{-1}$ was used to calculate the concentration of THF (Huennekens *et al.*, 1963).

Preparation of L-[3-¹⁴C]-Ser for enzyme assay

A stock solution of L-Ser was prepared by dissolving L-Ser (37.84 mg) in water and 1 ml of radioactive L-Ser (50 mCi/mmol), was added and the volume made up to 10 ml. The final concentration of L-Ser was 36 mM. To determine the specific counts, 10 µl of this solution was spotted on a GF/C disk and dried (Jagath, 1997). The disk was placed in 6 ml of scintillation fluid (0.6 % w/v PPO in toluene) and the radioactivity was measured using a LKB Rackbeta 1209 Liquid Scintillation Counter.

Bacterial strains and growth conditions

Escherchia coli strain DH5α (BRL) was used for subcloning. The BL21 (DE3) pLysS (Studier and Moffatt, 1986) strain was used for bacterial expression of pRSH (*Bacillus stearothermophilus* (bs)SHMT gene cloned and overexpressed in pRSET C vector) and mutant constructs were similarly overexpressed. Luria–Bertani (LB) medium or terrific broth (TB) with 50 µg ml⁻¹ of ampicillin was used for growing *E. coli* cells harboring the plasmids (Sambrook and Russell, 2001).

Site-directed mutagenesis

Mutants were constructed by a PCR-based sense-antisense primer method (Weiner *et al.*, 1994) using appropriate primers and Deep Vent polymerase. bsSHMT gene cloned in pRSET C vector was used as a template for the construction of mutants. The smaller size (2.9 kb) of pRSET C enabled easy generation of mutants directly in this expression vector. The PCR conditions used to polymerize the complete vector were as follows. The wild type template (pRSH) (80 ng) obtained as described earlier (Jala *et al.*, 2002). Sense and antisense primers (50 pmol) were added to PCR tubes containing 0.4 mM dNTPS, 1mM MgSO₄, 2.5 U of The amplification reaction was carried out in a Perkin-Elmer PCR machine using the

following cycling conditions: denaturation of the template at 95°C for 4 min followed by 20 cycles at 94°C for 45 S (denaturation), 52°C for 1 min (annealing) and 72°C for 5 min (extension). The reaction was continued for 20 min at 72°C to complete the extension. Sense and antisense primers were used on pRSH template to construct site-directed mutants. The PCR amplified mixture was treated with *DpnI* (10 units) at 37°C for 1 h to digest the methylated DNA (template DNA) and transformed into DH5 α - competent cells (Alexander, 1987) The presence of the mutations were confirmed by sequencing the plasmid (Sanger *et al.*, 1977) DNA by using SequenaseTM version 2.0 sequencing kit or by using automated DNA sequencer. All sequencing data were obtained from commercial sources.

Primers used for mutational studies

Underlined nucleotides indicate the changes introduced to achieve the mutation of the desired residues.

K226Q sense: 5'GACGACGCATACAACG TTGCGC 3'

K226Q antisense: 5'GCACAACGTTTGAT TGCGTCGTC 3'

K226M sense: 5'GACGACGCATATGACGTTGCGC 3'

K226M antisense: 5'GCGCAACGTCCATATGCGTCGT 3'

E53Q sense: 5'CAAATACGCGCAAGGCTATCCG3'

E53Q antisense: 5'CGGATAGCCTTGCGCGTATTTG 3'

Y51F sense: 5'GACGAACAAATTCGCGGAAGG 3'

Y51F antisense: 5'CCTTCCGCGAATTTGTTGTCGTC 3'

Y61F sense: 5'GCCGCTATTTTGGCGGCTGC3'

Y61F antisense: 5'GCAGCCGCCAAAATAGCGGCG 3'

Y61A sense: 5'CGCCGCTATGCTGGCGGCTGC 3'

Y61A antisense: 5'GCAGCCGCCAGCATAGCGGCG 3'

Preparation of competent E. coli cells

Competent *E. coli* cells were prepared according to the method described earlier (Alexander, 1987). The bacterial strain was streaked on Luria-Bertani (LB) broth-agar plate with chloramphenicol (for *E. coli* BL 21 (DE3) pLys S strain) or without antibiotics (for *E. coli* DH5 α strain) and incubated at 37°C for 12 h. A single colony was inoculated into 2.5 ml of 2X LB medium (2 g tryptone, 1 g yeast extract

and 0.1 g NaCl per 100 ml) and grown at 30°C for 16 h. The cells (1%) were inoculated into 450 ml terrific broth (trypton 6g, yeast extract 12g, glycerol 2 ml, potassium salt 50 ml in 2 L culture conical flasks, 500 ml each) and grown at 30°C till A_{600} reached 0.4-0.5 (~3 to 4 h). The *E. coli* cells were chilled in ice for 1-2 h and harvested by centrifugation at 4000xg for 15 min at 4°C. The cell pellet was resuspended in a small volume of ice-cold acid-salt buffer (100 mM CaCl_2 , 70 mM MnCl_2 and 40 mM sodium acetate, pH 5.2-5.5), the cell suspension was made up to 0.5 volume of *E. coli* culture and incubated on ice for 45 min. The cells were centrifuged at 4000xg for 15 min at 4°C. The cell pellet was resuspended in 0.5 ml of ice-cold acid-salt buffer; the volume was made up to 4.5 ml by addition of acid-salt buffer and cold 80% glycerol. The final volume of cell suspension was 1/20th of the volume of bacterial cultures, i.e. *E. coli* cells from 90 ml culture medium were suspended in 4.5 ml of ice-cold acid-salt buffer containing 15% glycerol. Aliquots of 0.2, 0.4 and 0.6 ml were stored at -70°C.

The plasmid to be transformed (1-10 ng) was added to 50 μl of competent cells and mixed gently and kept on an ice-bath for 45 min. After incubation, the cells were given a heat-shock at 37°C for 5 min. To this transformed *E. coli* cell suspension, 450 μl of 2X LB medium was added and kept at 37 °C for 1.5 h to allow *E. coli* cells to express the antibiotic-resistant gene (β -lactamase in the case of ampicillin). The transformed *E. coli* cells were plated on an appropriate LB-agar plates (1.5%) containing antibiotic (ampicillin) and incubated at 37°C for 12-14 h. Isolation of plasmid DNA was carried out by alkaline lysis method as described earlier (Studier and Moffatt, 1986). The purity of the DNA sample was assessed by measuring the A_{260}/A_{280} ratio. For pure DNA preparations the ratio was 1.8. Quantitative estimates of DNA were obtained directly from absorbance at 260 nm (1 O.D. = 50 $\mu\text{g ml}^{-1}$ for dsDNA or 33 $\mu\text{g ml}^{-1}$ for single-stranded oligonucleotides without any correction for scattering).

DNA sequencing

Double stranded DNA was sequenced as described by Sanger's dideoxy DNA sequencing method (Sanger *et al.*, 1977) with Sequenase TM version 2.0 DNA

sequencing kit using [α - 32 P] dATP. Double stranded plasmid DNA (5-7 μ g, RNA-free) was alkali denatured before carrying out the sequencing reaction. Some of the plasmid DNAs was sequenced using automated DNA sequencer at the DNA sequencing facility available at the Department of Biochemistry, Indian Institute of Science, Bangalore, India.

Overexpression of bsSHMT and mutant clones

The wild-type and mutant clones were transformed into BL21 (DE3) pLysS strain of *E. coli*. The cells harboring the plasmids were grown overnight in LB medium containing 50 μ g/ml ampicillin at 37°C. LB (25 ml) media were inoculated with the overnight culture (1 %) *E. coli* cells and induced with 0.3 mM IPTG after the absorbance (A_{600}) reached a value of 0.5. The cells were grown for an additional 3 h and harvested. The cells were resuspended in 2 ml of buffer A (50 mM potassium phosphate buffer, pH 7.4, 2 mM EDTA and 5 mM 2-ME, 100 μ M PLP). An equal volume of 2X SDS-polyacrylamide gel electrophoresis (PAGE) loading buffer was added to 20 μ l of resuspended cells and saved for analysis of total proteins. The remaining cells were sonicated for 10 min and the insoluble fraction was resuspended in 2 ml of water. The total, soluble and insoluble fractions were analyzed by SDS (10% w/v) PAGE (Laemmli, 1970).

Purification of bsSHMT

Purification of the wild-type (bsSHMT) and all the mutant enzymes were carried out according to the procedure described earlier (Jala *et al.*, 2002). The plasmid harboring the construct of interest was transformed into BL21 (DE3) pLysS strain of *E. coli*. A single colony was inoculated into 25 ml LB medium containing 50 μ g/ml ampicillin and grown overnight at 37°C, and 4 % (20 ml) of this overnight culture was inoculated into 500 ml of terrific broth containing 50 μ g/ml ampicillin. After 3 - 4 h of growth, the cells were induced with 0.3 mM IPTG. (SHMT gene in pRSET C vector was expressed well and the cells were grown and induced at 30°C). The cells were harvested 4 h after induction and resuspended in 60 ml of buffer A. The cell suspension was sonicated until it was optically clear. The lysate was centrifuged at 15,000xg for 30 min. The supernatant was subjected to 0-65% ammonium sulfate fractionation and the pellet obtained was resuspended in 10-15 ml

of buffer B (20 mM phosphate buffer, pH 6.4, containing 1 mM EDTA, 1 mM 2-ME and 50 μ M PLP) and dialyzed against the same buffer with two changes. The dialyzed sample was loaded on to a DEAE-cellulose column (2 \times 15 cm) previously equilibrated with buffer B. The column was washed with 500 ml of buffer B and the bound protein was eluted with 50 ml of buffer C (200 mM potassium phosphate, pH 6.4, containing 1mM EDTA, 1mM 2-ME, 50 μ M PLP). The eluted protein was precipitated at 65% ammonium sulfate saturation, and the pellet was re-suspended in 50 mM potassium phosphate buffer, pH 7.4, containing 1 mM EDTA, 1 mM 2-ME (50 mM potassium phosphate, pH 7.4, containing 1mM EDTA, 1mM 2-ME) and dialyzed against the same buffer (2 L, with two changes) for 24 h.

Protein estimation

a) Lowry's method:

Protein was estimated by Lowry's procedure using bovine serum albumin as the standard (Lowry *et al.*, 1951). The reaction mixture consists of the following reagents, solution A; 2% Na₂CO₃ in 0.1N NaOH; solution B: 0.1ml of 5.5% CuSO₄.5H₂O in 1% of 1.35% sodium potassium tartarate; solution C: Mix 50 ml of solution A with 1 ml of solution B. solution D: Diluted Folin's reagent (Commercially available reagent consists of sodium tungstate and sodium molybdate in phosphoric acid). To a sample of 10 to 100 μ g of protein in 1 ml, 1 ml of solution C is added. Mixed well and allowed to stand for 10 min in the dark. Solution D (100 μ l) was added, mixed rapidly and allowed to stand for 20 min in the dark. The absorbance of the solution was recorded at 660 nm and concentration of protein was determined using BSA standard curve.

b) By absorbance at 280 nm:

The amount of protein in the sample was estimated by using the standard value, is 1 mg of BSA and has an absorbance of 1 at 280 nm. The concentration of bsSHMT and its mutants was determined spectrophotometrically using Shimadzu 1601 UV-Vis double beam spectrophotometer (Layne, 1957; Alastair and Learmonth, 2002)

Sodium dodecyl sulfate polyacrylamide gel electrophoresis (SDS-PAGE)

The bsSHMT fractions were subjected to SDS-PAGE as described below. SDS-PAGE (12%) was carried out by the protocol using a discontinuous buffer system (Laemmli, 1970). The polyacrylamide gels containing 0.1% SDS were cast in a 1.5 mm slab gel apparatus locally fabricated. The electrophoresis was performed at 100 V in 0.025M Tris-0.2M Gly buffer, pH 8.3, containing 0.1% SDS. The protein (20-40 µg) was mixed with the sample buffer pH 6.8, containing 5% (v/v) 2-ME, 10% (v/v) glycerol, 2% (w/v) SDS and 0.1% bromophenol blue. The samples were heated in a boiling water bath (98°C) for 3 min and subjected to electrophoresis. The standard SDS-PAGE molecular weight (M_r) markers (β -galactosidase 166 kDa; bovine serum albumin 66.2 kDa; ovalbumin 45 kDa; lactate dehydrogenase 35 kDa; restriction endonuclease Bsp981 25 kDa; β -lactoglobulin 18.4 kDa; lysozyme 14.4 kDa) were also similarly denatured and electrophoresed. The gels were stained with 0.1% Coomassie Brilliant Blue R-250 prepared in 40% methanol, 10% acetic acid and then destained in 10% acetic acid, 10% isopropanol, 10% methanol to visualize the protein bands.

Preparation of dialysis membranes

The 25 mm flat dialysis membrane of 10000-12000 Da and 30000-50000 Da molecular weight cut-off were washed with distilled water thoroughly. The membrane was treated further with 0.2% sodium bicarbonate and 0.2% EDTA and boiled for 30 mins. The treated dialysis bags were rinsed thoroughly and boiled thrice in double distilled water before using for different experiments.

Enzyme assays

THF-dependent cleavage of L-Ser

The hydroxymethyltransferase activity was monitored using the procedure described earlier (Taylor and Weissbach, 1965). The buffer used for the assay was 0.4 M potassium phosphate, pH 7.4, containing 1 mM EDTA, 1 mM DTT and 50 µM PLP. The enzyme (1 µg) was preincubated with 3.6 mM [$3\text{-}^{14}\text{C}$] L-Ser for 5 min at 37°C and the reaction was started by the addition of 1.8 mM THF. It was continued

for a further 15 min and then stopped by addition of 100 μ l of dimedone (0.4 M in 50 % alcohol). The reaction mixture was heated in a boiling water-bath for 5 min and then allowed to cool. The $H^{14}CHO$ -dimedone adduct was extracted into 3 ml of toluene and 1 ml of this extract was added to the scintillation fluid and the radioactivity measured in a Rackbeta Liquid Scintillation Counter. One unit of enzyme activity was defined as the amount of enzyme required to catalyze the formation of 1 μ mol of HCHO /min at 37°C. Specific activity was expressed as units/mg protein.

THF-independent cleavage of L-allo Thr

Cleavage of L-allo Thr to yield Gly and acetaldehyde was monitored in a coupled assay with alcohol dehydrogenase (ADH). NADH oxidized was estimated at 340 nm as a function of time, using a Shimadzu UV 160A spectrophotometer. The enzyme concentration used for the study was 50 μ g for bsSHMT and 50-500 μ g for the mutant proteins. The reaction was monitored as described elsewhere (Malkin and Greenberg, 1964). The reaction was started by adding bsSHMT or its mutant forms to one ml of reaction mixture containing ADH (100 μ g), NADH (250 μ M) and L-allo Thr (0-10 mM). The reaction was monitored at 37°C for 10 min by measuring absorbance at 340 nm in a continuous manner as described earlier (Malkin and Greenberg, 1964). The amount of product formed was measured by correlating it to the amount of NADH oxidized using the molar extinction coefficient of 6220 $M^{-1}cm^{-1}$ for NADH (Ciotti and Kaplan, 1957). The change in absorbance at 340 nm per min was measured at various substrate concentrations and a double reciprocal plot of $\Delta A_{340}/min$ vs substrate concentration was used to obtain the kinetic parameters, K_m and V_{max} .

Transaminase activity

SHMT catalyzes the transamination of D-Ala to pyruvate and the enzyme-bound PLP is converted to pyridoxamine 5'-phosphate (PMP). The rate of the reaction was monitored by the procedure as described earlier (Schirch and Jenkins, 1964b). The enzyme (1 mg ml^{-1}) was incubated with 200 mM of D-Ala in 50 mM potassium phosphate buffer, pH 7.4, containing 1 mM EDTA, 1 mM 2-ME at 37°C and the reaction was monitored by taking the spectra at different time intervals. The

decrease in absorbance value at 425 nm due to the disappearance of bound PLP or by the increase in absorbance value at 325 nm due to the formation of PMP was taken for the calculation of pseudo first order rate constant (Schirch and Jenkins, 1964b). The pseudo first order rate constants were calculated by plotting $\ln \Delta A / \Delta A_t$ Vs time where ΔA = change in absorbance at time 't' and ΔA_t = maximum change in absorbance observed.

Preparation of bsSHMT or mutant apo-enzymes

Apo-enzymes were prepared as described earlier, with minor modifications (Schirch and Jenkins, 1964b; Schirch *et al.*, 1991). D-Ala (100 mM) was added to the holo-enzyme in 50 mM potassium phosphate buffer pH 7.4 containing 1 mM 2-ME, 1 mM EDTA, and incubated at 37°C for 2 h to 12 h depending on the role of the reaction with mutant protein(s). Pyruvate and PMP formed due to transamination, was removed by dialysis against in 50 mM potassium phosphate buffer, pH 7.4, containing 1 mM EDTA, 1 mM 2-ME not containing PLP at 4°C for 12 h. This procedure gave an apo-enzyme which is devoid of any absorbance at 425 nm. Reconstitution of apo-enzyme was carried out by addition of PLP (50-500 μ M) to the apo-enzymes in 50 mM potassium phosphate buffer, pH 7.4, containing 1 mM EDTA, 1 mM 2-ME, incubating for 45 min at 4°C and dialyzing overnight against the same buffer not containing PLP with 2 changes (1 L).

Spectroscopic methods

Absorption spectroscopy

The absorption spectra of the enzyme(s) were recorded in a Shimadzu UV-160A spectrophotometer or Jasco-V-230 UV-VIS spectrophotometer. All the spectra were recorded in the range of 300-550 nm. Absorbance measurements and spectral studies were recorded at $25 \pm 2^\circ\text{C}$ using respective buffers as a blank.

Circular dichroism (CD) measurements

Far-UV CD

Far-UV CD spectral measurements were made in a Jasco J-500A spectropolarimeter. The spectra were recorded at $25 \pm 2^\circ\text{C}$ in 50 mM potassium

phosphate buffer, pH 7.4, containing 1 mM EDTA, 1 mM 2-ME from 250 nm to 195 nm using a protein concentration of 0.1- 0.2 mg ml⁻¹ of bsSHMT and its mutants. Spectropolarimeter was fitted with a xenon arc lamp, the far-UV measurements from 200-250 nm with 1mm path length. The instrument was calibrated with aqueous solution of d-camphor sulphonic acid. Dry nitrogen gas was purged continuously into the instrument before and during the measurements. The rotations were converted to molar ellipticity values by using a mean residue 115 for the proteins and also using molecular weight. The molar ellipticity values were evaluated at 1nm intervals using the equation (Alder *et al.*, 1973).

$$[\theta]_{\text{MRW}} = \frac{[\theta]_{\text{obs}} \times \text{MRW}}{10 \times d \times c} \dots\dots\dots (1)$$

where $[\theta]_{\text{obs}}$ is the observed ellipticity (deg), d is the path length of the cell used (cm), C is the protein concentration (g/ml) and MRW is the mean residue weight of the protein. The secondary structural analysis was performed according to the built in computer program of the instrument (Yang *et al.*, 1986).

Circular dichroism measurements in the visible region

Visible CD spectral measurements were made in a Jasco J-500A spectropolarimeter using a cuvette of 10 mm path length. The spectra were recorded at 25 ± 2°C in 50 mM potassium phosphate buffer, pH 7.4, containing 1 mM EDTA, 1 mM 2-ME (Millipore filtered) from 300 nm to 550 nm using protein at a concentration of 1 mg ml⁻¹ SHMT. The data was plotted as θ_{MRW} using subunit M_r of 45,000 Da for bsSHMT and also for the site-specific mutants.

Stopped-flow spectrophotometry

The pre-steady state kinetics of the reactions of the wild-type and the mutant enzymes were monitored using a SX.18MV-R stopped-flow spectrophotometer using cells with a path-length of 2 mm and a pressure of 125 psi was used for mixing (8 bar, compressed nitrogen). The dead time of the instrument was 10 ms. All experiments were performed in 50 mM potassium-phosphate, (pH 7.4), containing

1 mM EDTA and 1 mM 2-ME. Single wavelength stopped-flow kinetic measurements were performed at 25°C maintained by a chain of circulating water-baths. The components were mixed using two syringes, one containing the enzyme (10 mg ml⁻¹) and the other containing the ligand. The contents were mixed and the reaction was initiated automatically. Single wavelength data were collected using different time regimes. For each data set, at least 1000 data points were collected. All experiments were repeated for a minimum of three times (Baskaran *et al.*, 1989b; Acharya *et al.*, 1991) and the data were analyzed using the SX.18MV-R v4.42 software program supplied by the manufactures.

Thermal denaturation studies

The thermal denaturation of bsSHMT and the site-specific mutants were carried out in the absence and presence of ligands, such as L-Ser and Gly, by measuring the absorbance changes at 287 nm using a Jasco V-530 UV-VIS spectrophotometer. A clear protein solution (300 µg ml⁻¹) was prepared in 50 mM potassium phosphate buffer, pH 7.4, containing 1 mM EDTA, 1 mM 2-ME. The protein (300 µl), with or without the ligand, was taken, with appropriate blanks, in thermal quartz cuvettes and equilibrated at 30°C to obtain the baseline. The samples were heated from 30°C to 80°C at the rate of 1°C/min using a thermal control unit. The absorbance change in each case was monitored at 287 nm and the values were averaged from two independent experiments. The first derivative of the denaturation profile was used to evaluate the apparent transition temperatures (T_m) using the software supplied along with the instrument. The results were analyzed according to the following formula, (White and Olsen, 1987) in which the fraction of the protein in the denatured state (F_D) is given by :

$$F_D = A_T - A_N / A_D - A_N \dots\dots\dots (2)$$

where A_N is the absorbance of the protein sample at 30°C, A_D is the absorbance of the sample at 80°C and A_T is the absorbance of the protein sample at different temperatures between 30°C and 80°C. The apparent T_m was defined as the temperature at which the value of F_D was 0.5.

Estimation of PLP at the active site

The purified enzymes (1 mg ml^{-1}) were incubated in 0.1 N NaOH for 5 min and the absorption spectra were recorded in the range of 300-550 nm. The PLP content was determined by assuming the molar absorption coefficient of PLP to be $6600 \text{ M}^{-1} \text{ cm}^{-1}$ at 388 nm (Peterson and Sober, 1954).

Reduction of bsSHMT and its mutants with sodium cyanoborohydride

The spectra of wild-type and mutant enzymes (1 mg ml^{-1}) were recorded. After addition of 1 mM NaCNBH_3 , the spectra were recorded at 0, 5 and 30 min respectively (David *et al.*, 1986). The PLP Schiff's base is reduced to a covalently linked secondary amine. This reaction can be conveniently monitored by a change in absorbance maxima from 430 to 325 nm.

Steady-state kinetic studies on the stability of quinonoid intermediate

The addition of FTHF to SHMT-Gly complex results in the formation of quinonoid complexes which absorb at 500 nm. In order to monitor the steady-state kinetics of the reaction and the consequences of the mutation on the reaction, steady-state kinetic experiments were performed. Double reciprocal plots for the formation of quinonoid intermediate on addition of Gly and FTHF before and after dialysis of bsSHMT and its mutants was determined by recording increase in absorbance at 500 nm in a UV-Vis Spectrophotometer (Katz and Westley, 1979) The enzyme (1 mg ml^{-1}) was incubated with 10 mM Gly and different concentrations of FTHF ($0\text{--}400 \text{ }\mu\text{M}$) for 1 min and absorbance was measured at 500 nm. The reciprocal of A_{500} was plotted versus the corresponding reciprocal of FTHF concentration.

Determination of dissociation (k_d) constants

The k_d of FTHF for wild-type and mutant binary complex was determined from double reciprocal plots of the change in A_{500} versus FTHF concentration ($2\text{--}40 \text{ }\mu\text{M}$) at different fixed concentrations of Gly ($2\text{--}10 \text{ mM}$). A replot of the y-intercept versus concentration of Gly gave the k_d values for FTHF. Both wild-type and mutants (1 mg ml^{-1}) were used for determining the dissociation constants (Schirch and Ropp, 1967; Stover and Schirch, 1991).

Preparation of garlic extract

80 g of fresh garlic was crushed in pestle and mortar with 30 ml of distilled water and suspended in 80 ml of distilled water. The entire garlic extract was boiled in a water bath for 20 min and filtered using Whatman no 1 filter paper. The flow through was re-boiled and filtered using Amicon filters. The filtrate was centrifuged at 12000 rpm for 20 min at 4°C and the supernatant was lyophilized. The Lyophilized powder was dissolved in 2 ml of water. Further the extract was used for inhibition analysis of bsSHMT.

Crystallization, data collection, processing, structure determination and model building

Crystallization

Crystallization was done by hanging drop vapor diffusion method. In this method a droplet of sample (enzyme) usually 3 μ l is mixed with the reagent of equal volume and placed on a siliconized glass cover slide. The glass cover slide is kept inverted over the reservoir containing the same reagent (0.4-0.5 ml) of higher concentration and sealed air tight using grease. Due to the difference in the concentration of the reagent in the droplet and reservoir, water is pulled from the droplet in a vapor phase such that equilibrium is attained. In this process, the enzyme in the droplet is also concentrated increasing its relative supersaturation in the drop. The advantage of using hanging drop vapor diffusion method is that a large number of conditions can be screened with relatively small amount of enzyme. However, it took a little longer time to set up the crystallization.

Crystals of bsSHMT and its mutants were grown under the same conditions as described for the wild-type enzyme (Trivedi *et al.*, 2002). In brief, after the final ammonium sulfate precipitation, the enzyme was dissolved in 100 mM HEPES pH 7.5 with 0.2 mM EDTA and 5 mM 2-ME and washed with 200 ml of the same buffer by repeated dilution followed by concentration using Amicon centricon filters. Crystals were obtained by mixing 4 μ l of protein solution (18 mg ml⁻¹) with 4 μ l of reservoir solution containing 100 mM HEPES buffer, pH 7.5, 0.2 mM EDTA, 5 mM

2-ME, and 50% 2-methyl-2,4-pentanediol (MPD). Crystals for binary complex of bsSHMT and its mutant's with L-Ser, Gly, L-*allo* Thr and Gly-FTHF were grown under the same condition, except that the reservoir solution contained 20 mM L-Ser/Gly/L-*allo* Thr/Gly-FTHF. Crystals of K226Q complex with Gly were obtained under the same conditions, except that the reservoir solution contained 20 mM Gly and 100 μ M PLP.

X-ray diffraction data collection and processing

For data collection, crystals were soaked in the mother liquor for a few seconds and flash-frozen in a stream of nitrogen at 100 K for collecting data. X-ray diffraction data were collected using a Rigaku RU-200 rotating-anode X-ray generator (Cu-K α radiation) equipped with a MAR research imaging-plate detector system. *DENZO* and *SCALEPACK* of HKL suite were used for indexing, integration, data reduction and scaling (Otwinowsky and Minor, 1997).

Structure determination and model building

The mutant crystals were isomorphous compared to those of wild-type bsSHMT. Therefore, the bsSHMT crystal structure (1KKJ) (Trivedi *et al.*, 2002) was used as the initial model for the refinement of structures of the mutant internal aldimine. Before initiating the refinement, PLP and water molecules were removed from the model. The model was then subjected to rigid body refinement followed by restrained refinement using the program REFMAC5 (Murshudov *et al.*, 1997) of CCP4 suite of programs (CCP4, 1994). Five percent of unique reflections were used to monitor the progress of refinement by R_{free} . Visualization of the electron density map and model fitting were done using the program COOT (Emsley and Cowtan, 2004). Structure was validated using PROCHECK (Laskowski, 1993). For the complexes of bsSHMT mutants with Gly, L-Ser and L-*allo* Thr, bsSHMT-Gly external aldimine crystal structure (1KL1) was used as the initial model.

RESULTS AND DISCUSSION

Chapter 1

The role of lysine 226 in the reaction
catalyzed by bsSHMT

It has been well documented that, in all PLP-dependent enzymes, the coenzyme forms a Schiff's base with ϵ -amino group of an active site Lys residue, which is termed as 'internal aldimine' (Fig I.1) (Dunathan, 1966; Christen *et al.*, 1996; Denessiouk *et al.*, 1999; Mehta and Christen, 2000; Christen and Mehta, 2001). The active site Lys is one of the highly conserved amino acid residues in all PLP-dependent enzymes. Nucleophilic attack by the amino group of the incoming amino acid substrate, on the ϵ -amino group of Lys, results in the formation of an 'external aldimine', i.e. a Schiff base between the amino group of the substrate and the aldehyde group of the cofactor. This reaction proceeds through the formation of gem-dimaine, in which both the amino acid substrate and PLP are linked to the enzyme active site Lys (Fig I.1). This is an obligate intermediate in all PLP-catalyzed reactions (Dunathan, 1966). Lys residue which is involved in PLP binding has been postulated to serve one or more roles in the enzymatic reactions, namely in cofactor binding as a Schiff's base, formation of enzyme-substrate intermediates (Schirch and Mason, 1963; Schirch, 1982; Toney and Kirsch, 1991a), in α -proton abstraction (Ziak *et al.*, 1990); in maintain oligomeric status (Talwar *et al.*, 1997); or facilitate product release (Schirch *et al.*, 1993a). The role of K258 residue in AAT has been confirmed as C_{α} proton abstractor by elucidation of three dimensional structure of AAT and its mutants (Ziak *et al.*, 1993; Malashkevich *et al.*, 1995a). Based on the spectral and kinetic studies on K229Q eSHMT, it was proposed that Lys is involved in product expulsion (Schirch *et al.*, 1993a). However, this proposal was made in the absence of the crystal structure of Lys mutants and its substrate complexes (Schirch *et al.*, 1993a). The structure of bsSHMT, its binary complex and ternary complexes were determined earlier (Trivedi *et al.*, 2002).

The active site of bsSHMT internal and external aldimine with L-Ser is shown in Fig 1.1 (Trivedi *et al.*, 2002). It was of interest to examine the role of K226 in bsSHMT by mutation of this residue. The biochemical characterization and the crystal structure of mutant SHMTs (K226M and K226Q bsSHMT) are described in this chapter. Crystal structures of Lys mutants and their complexes with L-Ser and Gly are reported for the first time.

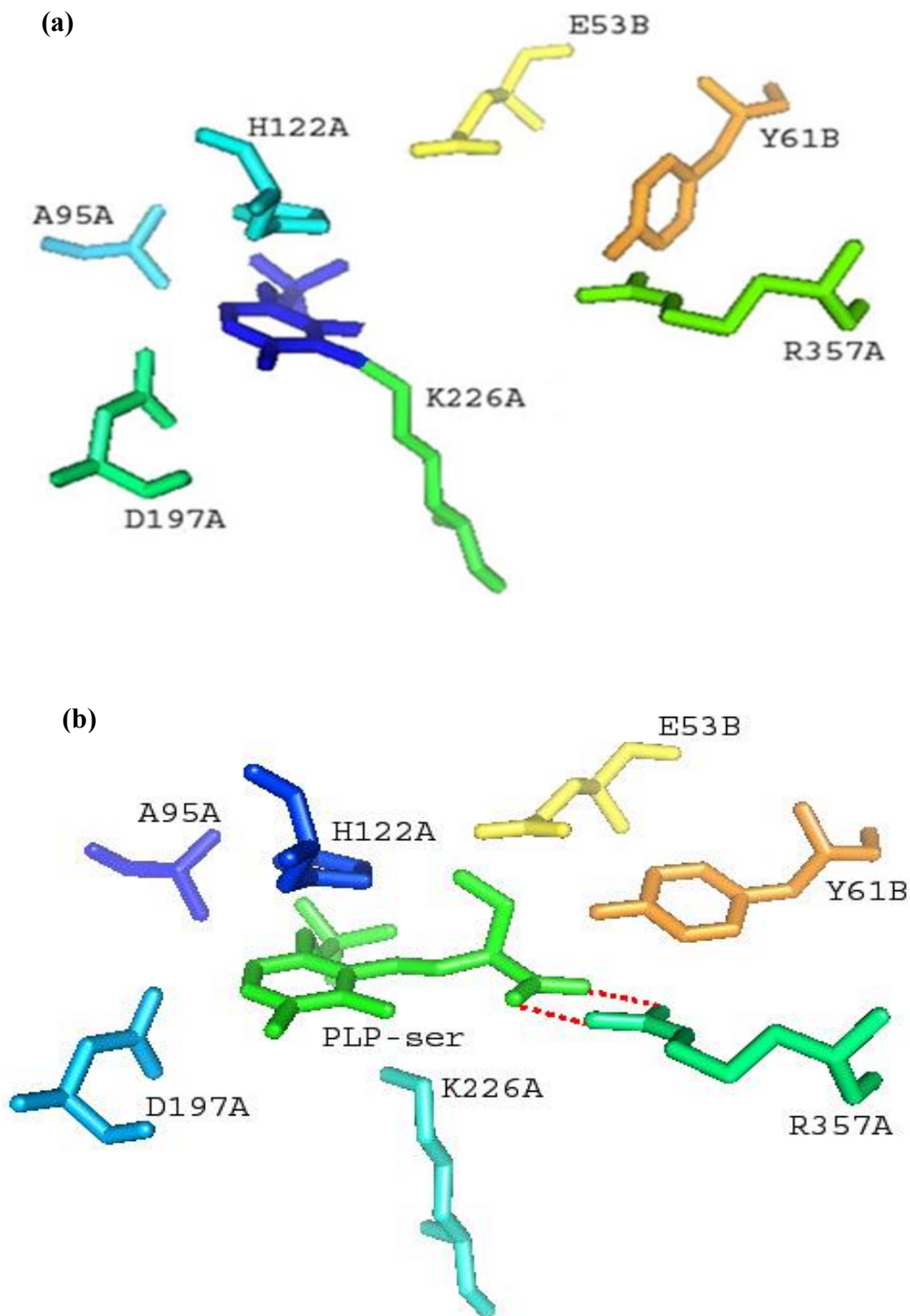


Fig 1.1: The active site of bsSHMT internal and external aldimine with L-Ser.
(a) Internal aldimine showing Schiff's base between bound PLP (Blue) and Lys 226 (Light green). Other active site residues are also shown in the figure (Trivedi *et al.*, 2002).
(b) External aldimine showing Schiff's base between PLP and L-Ser (Green). The carboxylate of L-Ser is interacting with Arg 357 (Trivedi *et al.*, 2002).

Results

Overexpression and purification of bsSHMT

Overexpression and purification of bsSHMT was carried out as described in methods. The SDS-PAGE of the fractions obtained during the purification of bsSHMT is shown in Fig 1.2. It can be seen that the enzyme gives a single band on SDS-PAGE and by comparison with the markers electrophoresed similarly gives a subunit molecular weight of 45 kDa. Earlier studies have shown that the native enzyme was a dimer with a molecular weight of 90 kDa (Jala *et al.*, 2002).

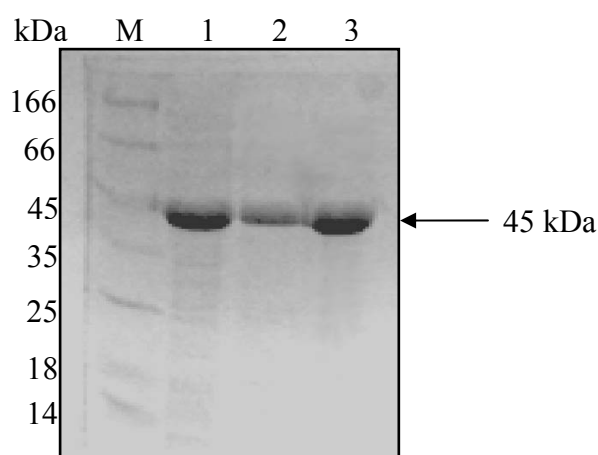


Fig 1.2: SDS-PAGE (12%) analysis of the fractions obtained during the purification of bsSHMT.

Lane 1: bsSHMT crude extract (Total cell lysate or soluble fraction); Lane 2: bsSHMT DEAE-cellulose eluted fraction; Lane 3: bsSHMT. M: markers in kDa (β -galactosidase 166; bovine serum albumin 66.2; ovalbumin 45; lactate dehydrogenase 35; restriction endonuclease Bsp981 25; β -lactoglobulin 18.4; lysozyme 14.4)

Activity measurements of bsSHMT

Table 1.1: A typical purification procedure and activity assay for recombinant bsSHMT

Enzyme	Total protein (mg)	Sp. Activity ^a	Fold Purification
Crude preparation	2400	1.8	1.0
Dialysate	1122	2.7	1.5
DEAE-Cellulose fraction	70	4.0	2.2
Final pooled fraction	53	5.3	3.0

a. expressed as μmol of HCHO/min/mg protein

Site-directed mutagenesis, over expression and purification of Lys mutants

As the objective of this investigation was to examine the role of Lys residues in SHMT catalyzed reaction, K226M and K226Q bsSHMT mutants were generated and overexpressed as described in methods. The overexpressed mutant proteins were purified according to the procedure described in methods section. Mutation was confirmed by DNA sequencing. The purified proteins were subjected to SDS-PAGE as described for bsSHMT. Fig 1.3 shows SDS-PAGE profile of Lys mutants. It can be seen from the Fig that the mutation has not affected the mobility of these enzymes and is appearing at the same position as that of wild-type.

Biophysical and biochemical characterization of Lys mutants

Biophysical:

The far UV CD spectra of bsSHMT, K226M and K226Q bsSHMT were recorded in 50 mM potassium phosphate buffer, pH 7.4, containing 1 mM EDTA, 1 mM 2-ME as described in methods section. Spectra were recorded in the range of 190-260 nm using 0.1 – 0.2 mg ml⁻¹ protein. The far-UV CD spectra of K226M and K226Q bsSHMT were similar to bsSHMT with troughs at 208 to 225 nm ranges suggesting that both the mutants had considerable amount of secondary structure like bsSHMT (Fig 1.4). These results demonstrate that there were no gross conformational changes in the enzyme upon site-specific mutation of Lys 226.

Biochemical:

PLP content and catalytic activity of bsSHMT and Lys mutants

As Lys residue anchors PLP, its mutation could affect PLP content, it was necessary to estimate PLP content of the Lys mutants and restore it to near normal values before carrying out biochemical characterization of these mutants. The amount of PLP in bsSHMT, K226M and K226Q bsSHMT was estimated by treating the enzyme (1 mg ml⁻¹) with 0.1 N NaOH for 5 min at 25 ± 2°C.

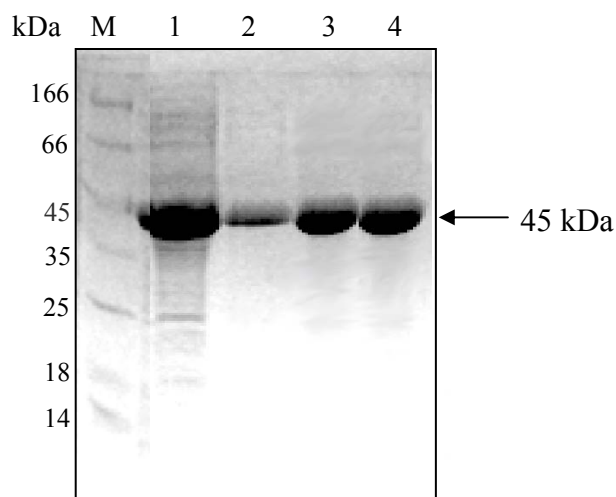


Fig 1.3: SDS-PAGE (12%) analysis of Lys mutants.

M: markers in kDa (β -galactosidase 166; bovine serum albumin 66.2; ovalbumin 45; lactate dehydrogenase 35; restriction endonuclease Bsp981 25; β -lactoglobulin 18.4; lysozyme 14.4); Lane 1: K226M bsSHMT crude extract (Total cell lysate or soluble fraction); Lane 2: K226M bsSHMT DEAE-cellulose eluted fraction; Lane 3: purified K226M bsSHMT; Lane 4: purified K226Q bsSHMT.

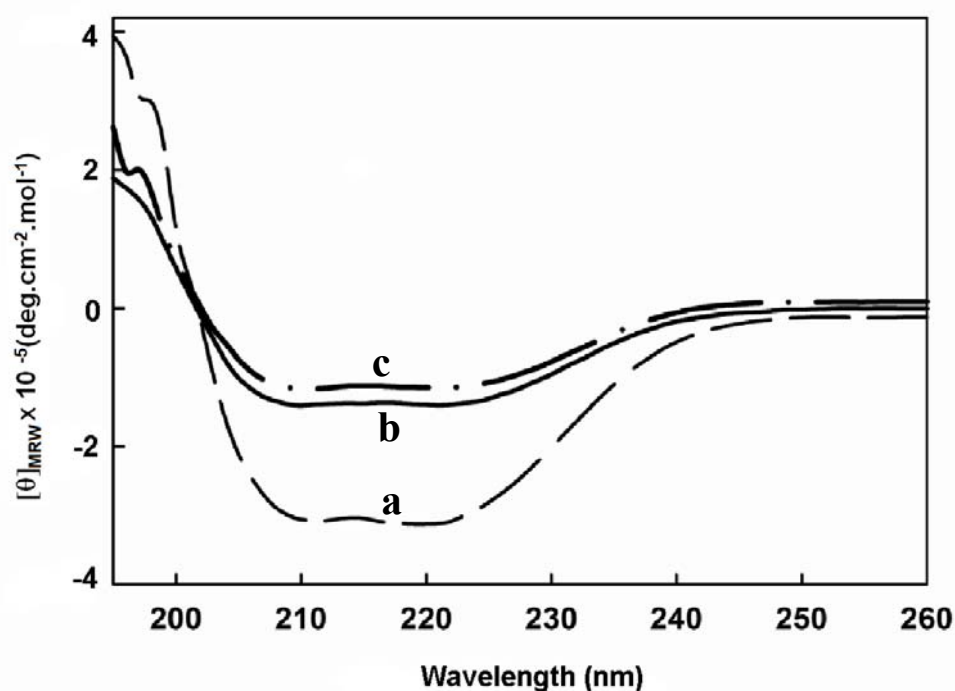


Fig 1.4: Far-UV CD spectra of bsSHMT, K226M and K226Q bsSHMT.

The spectra were recorded from 195-260 nm in Jasco J-500A spectropolarimeter. The protein concentration used was 0.2 mg ml^{-1} in 50 mM potassium phosphate buffer, pH 7.4, containing 1 mM EDTA, 1 mM 2-ME. (a) bsSHMT; (b) K226M bsSHMT and (c) K226Q bsSHMT.

The absorbance of bsSHMT and mutants were recorded in the range of 300-500 nm. Amount of PLP was monitored by measuring absorbance at 388 nm. The PLP content of K226M bsSHMT was 1 mol of PLP/mol of subunit, similar to that of bsSHMT (Table 1.1), whereas K226Q bsSHMT, as isolated, contained 0.5 mol of PLP/mol of subunit. PLP content of this mutant was restored to 1 mol of PLP/mol of subunit on addition of 100 μ M of PLP. The solution was incubated for 45 min at 4 °C and dialysed for 24 h against buffer not containing PLP (50 mM potassium phosphate buffer, pH 7.4, 1 mM EDTA, 1 mM 2-ME). This restored the PLP content to 1 mol of PLP/mol of subunit (Table 1.1). These observations suggest that PLP may not be as tightly bound in K226Q bsSHMT compared to K226M bsSHMT. Both, K226M and K226Q bsSHMT preparations containing 1 mol of PLP/mol of subunit were used throughout these studies.

Catalytic properties of bsSHMT, K226M and K226Q bsSHMT

Hydroxymethyltransferase reaction

The THF-dependent cleavage of L-Ser by bsSHMT, K226M and K226Q bsSHMT was carried out as described in methods section. The activity assay of bsSHMT was carried out using 1 μ g and the mutant enzyme activity was measured using varying concentrations (0.001-1mg). The specific activity of bsSHMT was 5.2 U/mg, whereas K226M and K226Q bsSHMT, as isolated, had 0.023 U/mg, and 0.021 U/mg, respectively. As both the mutant clones were overexpressed in *E. coli* strain (BL21 pLys S) containing GlyA gene (responsible for SHMT expression), it was necessary to establish that the small amount of activity seen at high protein concentration used in the assay was due to contaminating eSHMT.

In bsSHMT, PLP is linked as an internal aldimine, which can be reduced by borohydride. Lys mutants do not contain the Lys residue to form internal aldimine Schiff's base with PLP and cannot be reduced. This difference provides a method for distinguishing the mutant enzyme from the wild-type enzyme. The bsSHMT, K226M and K226Q bsSHMT (2 mg ml⁻¹) were treated with 0.4 mM sodiumcyanoborohydride (NaCNBH₃) (Schirch *et al.*, 1993a) incubated for 30 min at 37°C, and dialyzed overnight against 50 mM potassium phosphate buffer, pH 7.4, containing 1 mM EDTA, 1 mM 2-ME. This treatment reduces the enzyme Schiff's base to

secondary amine (Table 1.2 and Fig 1.5). The bsSHMT lost all its activity, and the mutant enzymes also lost the residual activity on treatment with NaCNBH₃. These observations suggest that the residual activity could be due to eSHMT, indicating that this activity may be due to the very small amount of constitutively expressed eSHMT. An insignificant unit of activity was observed even at the 10,000- fold excess of the mutant enzyme protein (1 mg for mutant, 1 µg for wild-type).

Aldol cleavage and transamination reaction catalyzed by bsSHMT, K226M and K226Q bsSHMT

In addition to the physiological reaction, SHMT catalyzes the THF-independent retroaldol cleavage of L-*allo* Thr yielding Gly and acetaldehyde as products. For retroaldol cleavage different enzyme concentrations (50-200 µg) were used and a similar procedure was used as described in methods section. K226M and K226Q bsSHMT had only 8% of THF-independent cleavage of L-*allo* Thr compared to that of bsSHMT (100%) (Table 1.2).

SHMT also catalyzes transamination of D-Ala to yield, PMP and pyruvate as products. Transamination reaction catalyzed by bsSHMT and K226M bsSHMT with D-Ala was examined by monitoring changes in the enzyme spectrum at 425 nm on addition of 100 mM D-Ala. The reaction resulted in a time-dependent decrease in absorbance at 425 nm and a concomitant increase at 325 nm due to the formation of PMP. The changes in absorbance values at 425 or 325 nm were used to calculate pseudo-first-order rate constants for both bsSHMT and lysine mutants.

The rate constants for transamination reaction with D-Ala for K226M and K226Q bsSHMT were 0.021 and 0.015 s⁻¹, respectively, compared to 0.04 s⁻¹ for the wild-type enzyme (Table 1.2). These results suggest that mutation had no effect the THF-independent activity. On the other hand, the THF-dependent physiological reaction is curtailed significantly. Both retroaldol cleavage of L-*allo* Thr and transamination reaction was monitored as described in methods section.

Table 1.2: Catalytic activity and PLP content of bsSHMT, K226M and K226QbsSHMT.

Enzyme	Specific activity ($\mu\text{mol}/\text{min}/\text{mg}$)			Pseudo first order rate (s^{-1}) ^c	PLP content ^d (mol/mol)
	Before reduction ^a	After reduction ^b			
		L-Ser	L- <i>allo</i> Thr		
bsSHMT	5.2	0	64×10^{-2}	4×10^{-2}	1
K226M	2.3×10^{-2}	0	50×10^{-2}	2.1×10^{-2}	1
K226Q	2.1×10^{-2}	0	40×10^{-2}	1.5×10^{-2}	1

a. Specific activity with L-Ser as substrate before reduction - μmol of HCHO/min/mg protein.

b. Specific activity in presence of L-Ser and L-*allo* Thr as substrate after reduction of enzymes with NaCNBH₃

c. Transamination reaction with D-Ala

d. PLP content calculated per mol of subunit assuming a value ϵ of $6600 \text{ cm}^{-1} \text{ M}^{-1}$ at 388nm.

Sodium cyanoborohydride reduction of bsSHMT and Lys mutants

Reduction of the PLP-Schiff's base on addition of sodium cyanoborohydride can be monitored by spectral changes. Spectrum of bsSHMT and K226M bsSHMT was recorded in the range of 300-500 nm in 50 mM potassium phosphate buffer, pH 7.4, containing 1 mM EDTA, and 1 mM 2-ME. The bsSHMT and K226M bsSHMT had a λ_{\max} of 425 and 412 nm respectively (Fig 1.5). It is pertinent to mention that internal aldimine for PLP-enzymes have λ_{\max} values in the range of 400-430 nm. It was therefore of interest to examine PLP interaction at the active site of mutant.

Addition of 0.4 mM NaCNBH₃ results in reduction of Schiff's base to secondary amine in the case of bsSHMT (Fig 1.5a) and only a small decrease in absorbance at 412 nm was observed in the case of K226M bsSHMT (Fig 1.5b) which could be due to contaminating eSHMT. An overnight dialysis of NaCNBH₃ treated bsSHMT in 50 mM potassium phosphate buffer, pH 7.4, containing 1 mM EDTA, 1 mM 2-ME, showed a new absorbance peak at 330 nm, suggesting the formation of secondary amine (Fig 1.5a). However K226M bsSHMT did not show any further decrease at 412 nm after overnight dialysis. These results suggested that 412 nm peak was probably not a Schiff's base.

Preparation of apo-enzyme and reconstitution with PLP

Transamination reaction has been extensively used to study the reversible binding of PLP at the active site (Schirch and Jenkins, 1964a). In wild-type enzyme, PLP could be removed in 1 h upon reaction with D-Ala (Fig 1.6a), in case of K226M bsSHMT, overnight (12 h) incubation was required to remove the bound PLP (Fig 1.6a). Reconstitution of apo-enzyme was carried out by addition of 50 μ M PLP to the apo-enzymes, which resulted in regain of absorbance at 412 nm for the mutant enzyme and 425 nm for apo-bsSHMT (Fig 1.6 a, b). Addition of 50 mM Gly to reconstituted apo-enzyme of bsSHMT showed a decrease at 425 nm and a small peak at 495 nm, suggesting formation of an external aldimine and quinonoid intermediate, respectively (Fig 1.7a). Addition of 50 mM Gly to the reconstituted apo-enzyme of the K226M bsSHMT resulted in a shift in the absorbance maximum from 412 to 425 nm (Fig 1.7 b). The addition of PLP restored the activity of apo-bsSHMT to its normal value (5 units) and the Lys mutants were inactive.

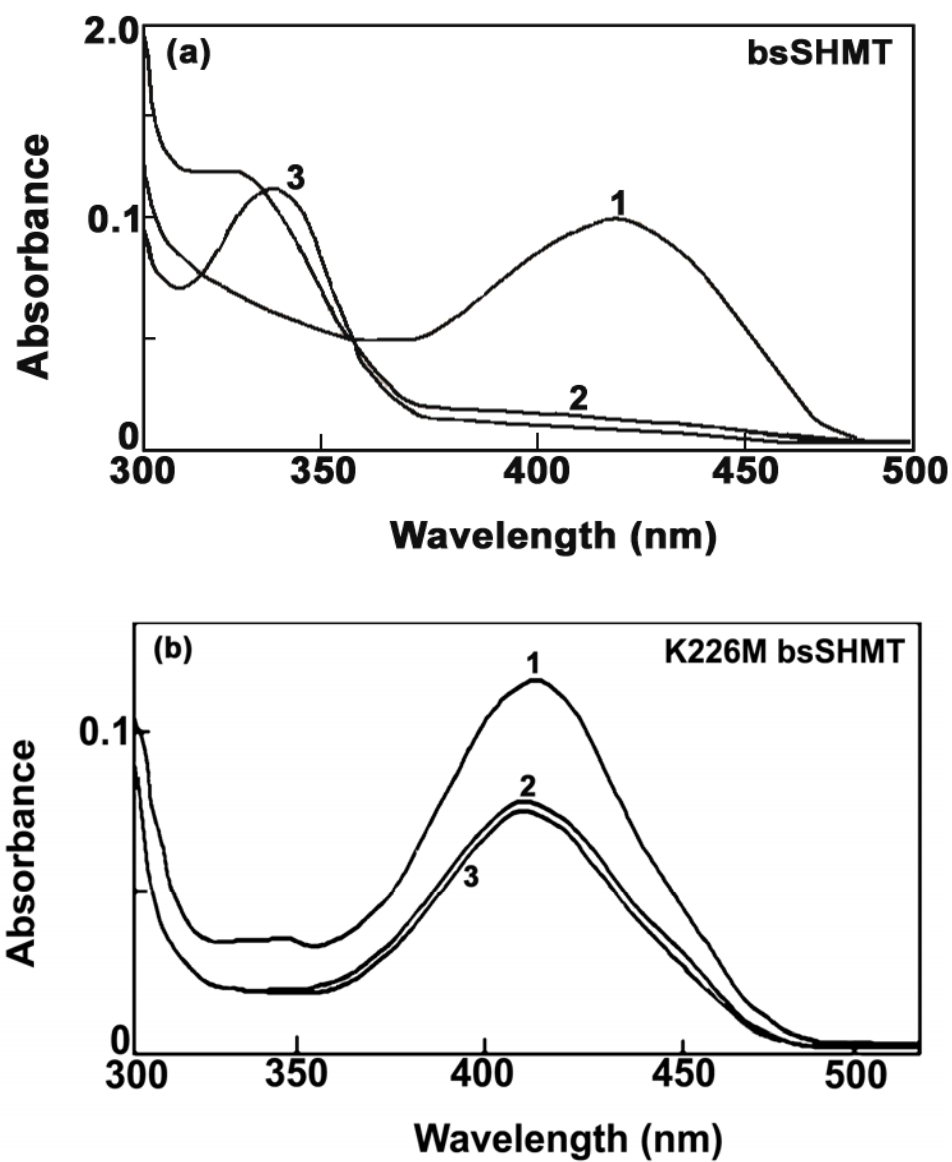


Fig 1.5: Visible absorption spectra of (a) bsSHMT and (b) K226M bsSHMT before and after sodium cyanoborohydride reduction.

Curve 1: Spectrum of bsSHMT or K226M bsSHMT.

Curve 2: in presence of 0.4 mM NaCNBH₃ after 5 min incubation.

Curve 3: after overnight dialysis in 50 mM potassium phosphate buffer, pH 7.4, containing 1 mM EDTA, and 1 mM 2-ME.

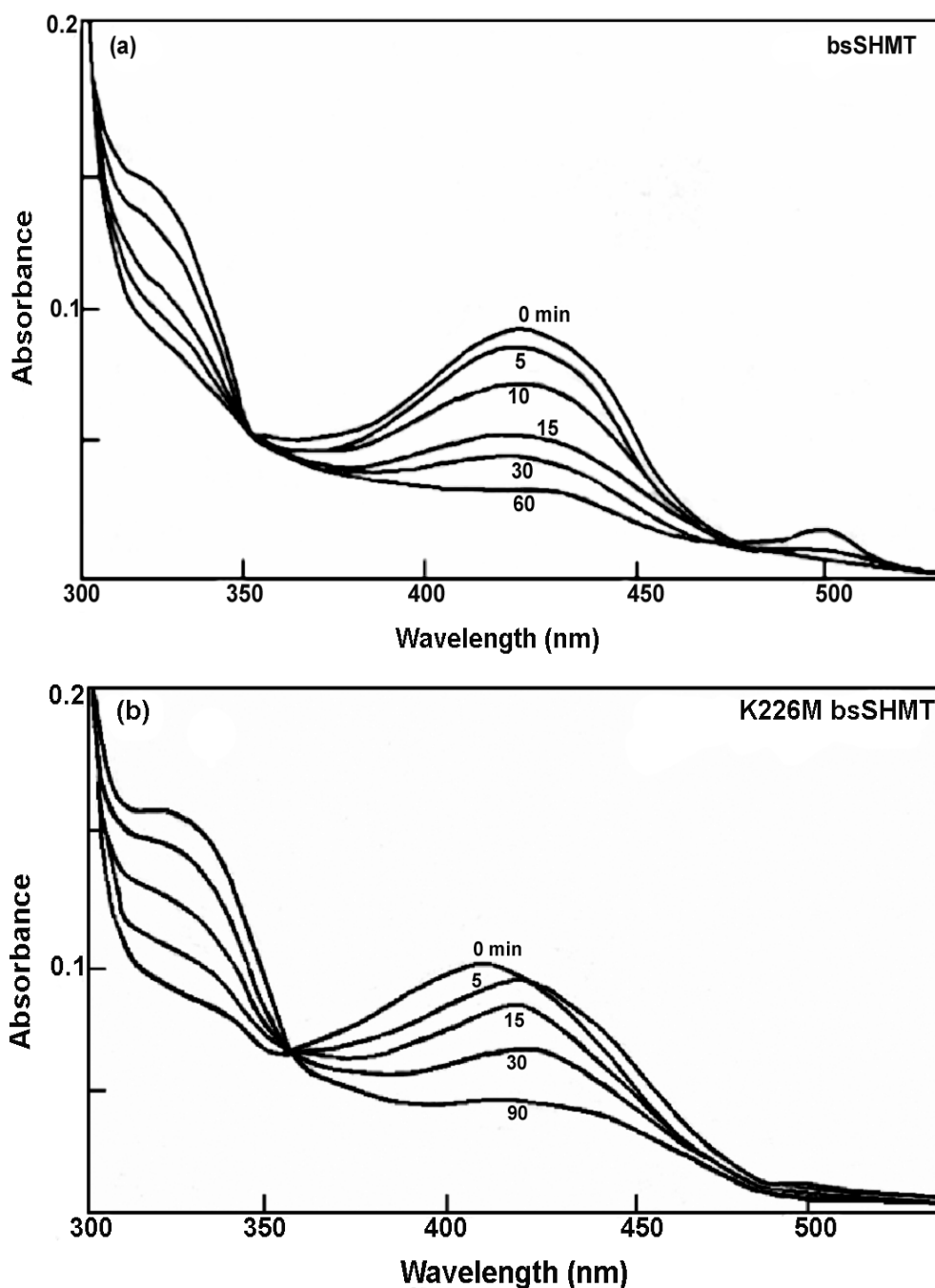


Fig 1.6: The transamination reaction catalyzed by bsSHMT and K226M bsSHMT.

D-Ala (100 mM) was added to bsSHMT (a) or K226M bsSHMT (b) both the enzyme at 1 mg ml⁻¹ and spectra were recorded at 37°C in 50 mM potassium phosphate buffer, pH 7.4, containing 1 mM EDTA, 1 mM 2-ME at the different time interval. The isobestic point is seen at 350 nm for bsSHMT and at 355 nm for K226M bsSHMT.

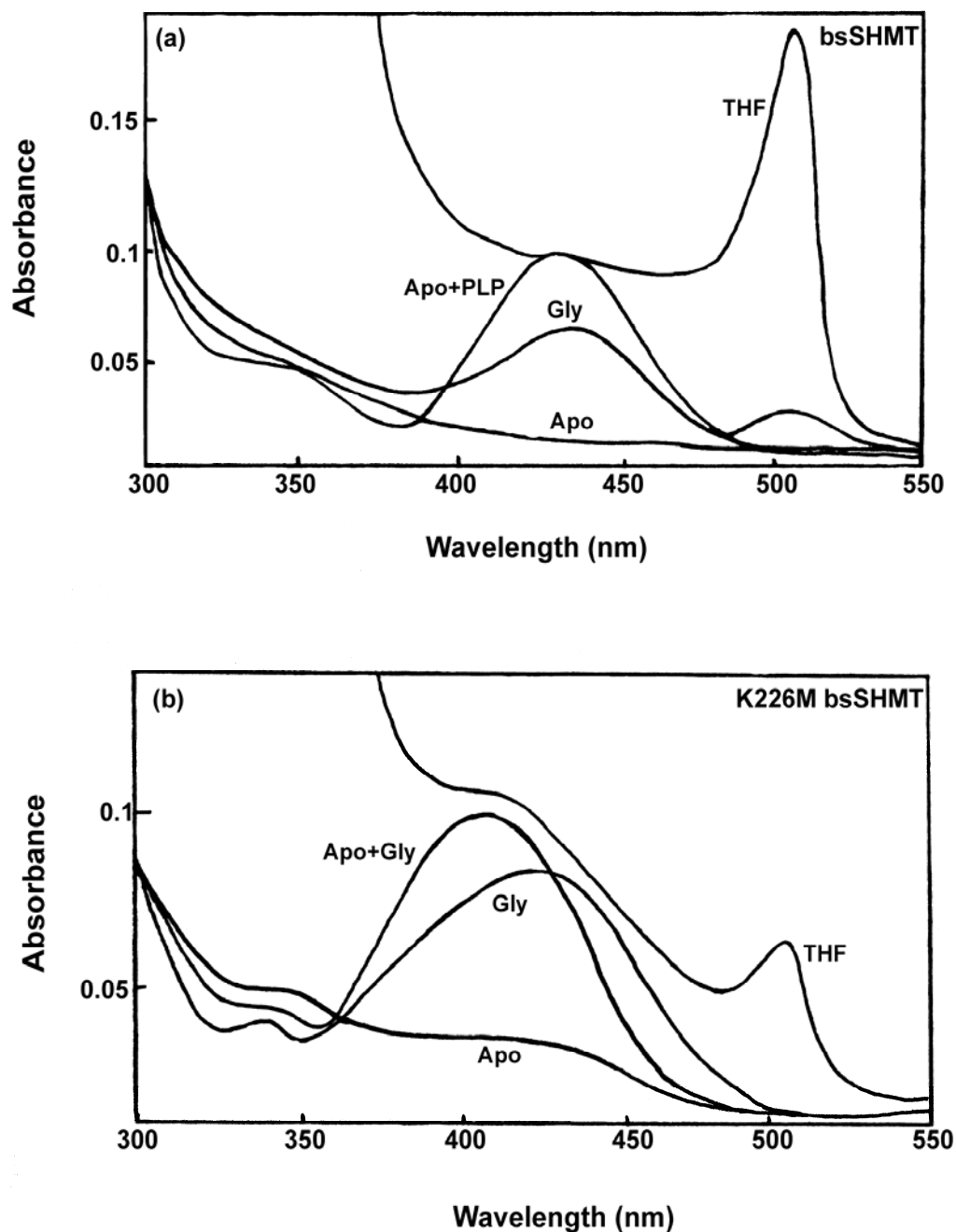


Fig 1.7: The reconstitution of apo-enzymes of bsSHMT and Lys mutants with PLP and their interaction with Gly and Gly+THF.

Apo-enzymes were obtained by transamination reaction with D-Ala (100 mM) in 50 mM potassium phosphate buffer, pH 7.4, containing 1 mM EDTA, 1 mM 2-ME using 1 mg ml^{-1} of bsSHMT and Lys mutants. The reconstitution of apo-enzymes was carried out with PLP (50 μM). Further, 50 mM Gly + THF (1.8 mM) was added to both reconstituted bsSHMT and K226M bsSHMT.

The reconstituted bsSHMT-Gly binary complex formed the quinonoid intermediate absorbing at 495 nm upon addition of THF. The reconstituted K226M bsSHMT-Gly binary complex showed shift in λ_{\max} from 412 to 425 nm. Further, on addition of THF a small amount of quinonoid intermediate was formed (Fig 1.7 b). These results suggest that the mutation of the Lys residue did not affect the reversible binding of PLP to the enzyme, although the internal aldimine was not formed as evidenced by the inability of NaCNH₃ to reduce the mutant enzyme. This suggestion was probed further by examining the spectral properties and 3D-structure of the mutant enzymes and their substrate complexes.

Formation of quinonoid intermediate on addition of Gly and THF to K226M and K226Q bsSHMT

In order to examine the role of Lys in proton abstraction step in the reaction catalyzed by SHMT, spectral studies were carried out. Spectrum of bsSHMT, K226M and K226Q bsSHMT (1 mg ml⁻¹) in 50 mM potassium phosphate buffer, pH 7.4, containing 1 mM EDTA, 1 mM 2-ME were recorded in the range of 300-550 nm. bsSHMT showed a λ_{\max} at 425 nm (Fig 1.8 a). K226M bsSHMT showed an absorbance maximum at 412 nm (Fig 1.8 b) While the K226Q bsSHMT had λ_{\max} at 425 nm similar to that of bsSHMT (Fig 1.8 c). Addition of Gly to bsSHMT resulted in a small increase in absorbance at 495 nm (Fig 1.8 a), indicating the formation of a quinonoid intermediate, which was not seen in the mutants. Addition of Gly to K226M resulted in a shift in the absorbance maximum from 412 to 425 nm, suggesting that PLP at the active site has the ability to react with the substrate and form an external aldimine complex (Fig 1.8 b). However K226Q bsSHMT showed a small decrease at 425 nm but no shift in absorbance on addition of Gly 50 mM. Absence of a 495 nm peak was evident from the spectra of the mutants, suggesting they failed to form a quinonoid intermediate (Fig 1.8 b,c) on addition of Gly.

Addition of THF (1.8 mM) to K226M and K226Q bsSHMT binary complex resulted in the appearance of a very small peak (0.0567 AU) at 495 nm (Fig 1.8 b,c). However, addition of THF (1.8 mM) to bsSHMT resulted in a large increase in the absorbance at 495 nm (0.234 AU) (Fig 1.8 a).

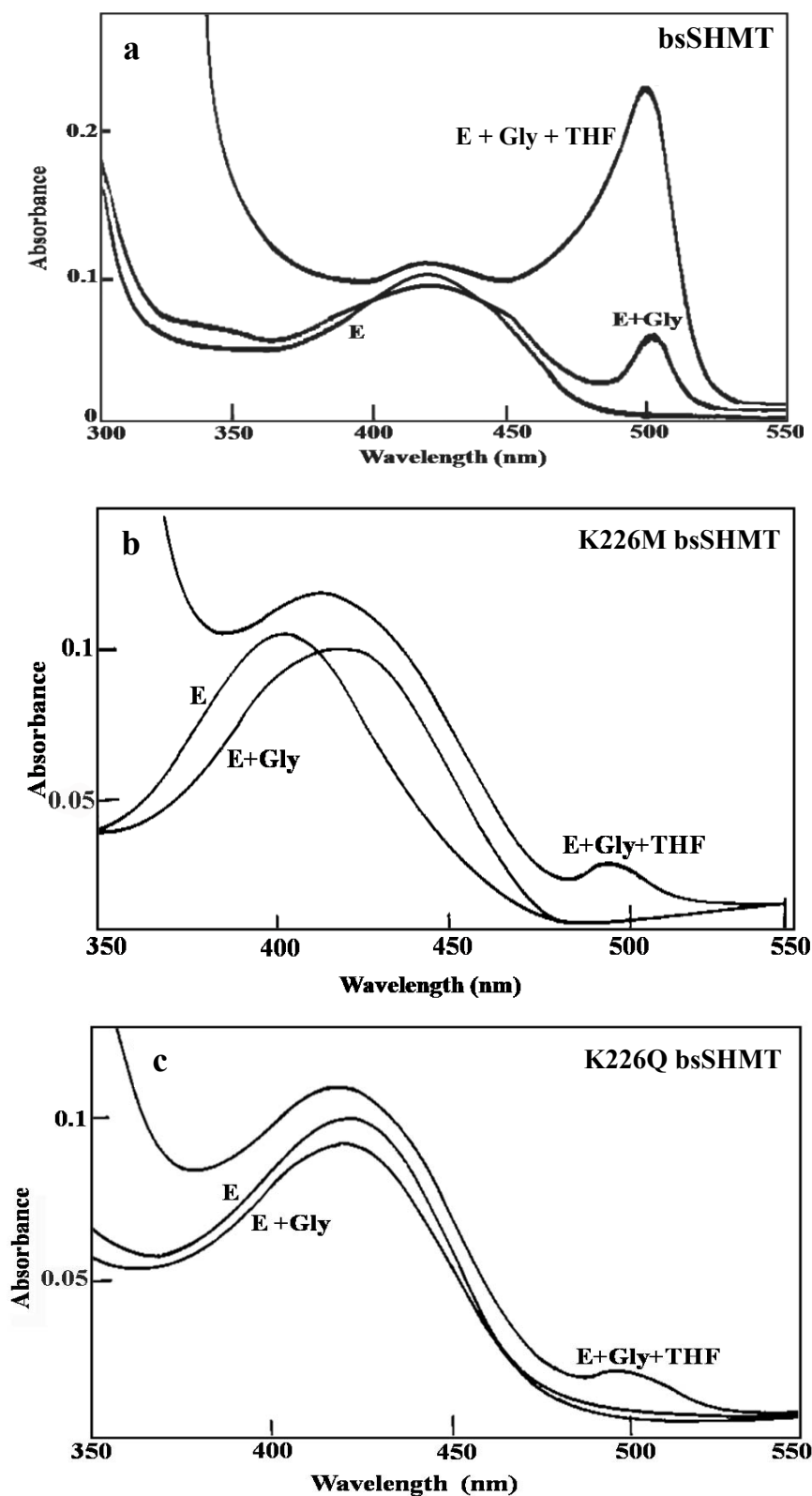


Fig 1.8: The absorbance changes on the addition of Gly, Gly+THF to bsSHMT (a), K226M (b) and K226Q bsSHMT (c).

Curve E: bsSHMT or K226M or K226Q bsSHMT.

Curve E + Gly: bsSHMT and Lys mutants in presence of 50 mM Gly.

Curve E+Gly+THF: bsSHMT and Lys mutant binary complexes in presence of 1.8 mM THF.

An analogue of THF, FTTHF which reacts with the enzyme generates a quinonoid intermediate during SHMT reaction with Gly (Stover and Schirch, 1991). It can be seen from Fig 1.9 that the bsSHMT, upon interaction with Gly and FTTHF (1 mM), yielded the characteristic quinonoid intermediate with a maximum absorbance at 500 nm (Fig 1.9 a). Both K226M and K226Q bsSHMT showed a minor increase at 500 nm (Fig 1.9 b, c).

Rapid reaction studies of bsSHMT and Lys mutants:

Rate of formation of quinonoid intermediate

It is evident from the Fig 1.8 (a) that on addition of Gly to bsSHMT, results in the formation of quinonoid intermediate (QI) (24 % of that seen when Gly and THF were added-100%) at 495 nm. This formation occurs rapidly and maximum absorbance was attained after 15 min. Hence it was of interest to measure the rate of formation of quinonoid intermediate. In addition to the formation of QI at 495 nm, at 425 nm a decrease of 1% of the absorbance of the native enzyme was observed, this could be due to the external aldimine formation via gem-diamine. Studies on scSHMT showed the formation of gem-diamine (λ_{\max} at 343 nm) on addition of Gly. However in the case of bsSHMT gem-diamine was not observed at 343 nm. It was hypothesized that the formation and dissociation of gem-diamine from internal aldimine to external aldimine was fast in the case of bsSHMT and hence gem-diamine peak was not observed. Since both the reactions occur very fast, it was of interest to monitor the rates and changes at 425, 343 and 495 nm. Unlike bsSHMT, K226M bsSHMT showed a λ_{\max} at 412 nm (Fig 1.8 b).

The addition of Gly (50 mM) resulted in a shift in λ_{\max} at 425 nm. This was an interesting observation, which may help in monitoring the rate of formation of external aldimine in the mutant K226M bsSHMT. In bsSHMT both internal and external aldimine absorb at 425 nm and the absorbance change on addition of Gly to bsSHMT is minimal (Fig 1.9 a). It is difficult to monitor the changes at 425 nm in the case of bsSHMT. K226Q bsSHMT was similar to bsSHMT with a λ_{\max} at 425 nm and addition of Gly showed a similar decrease in λ_{\max} at 425 nm. Unlike bsSHMT, both the Lys mutants did not show any peak at 495 nm on addition of Gly (Fig 1.8 b, c).

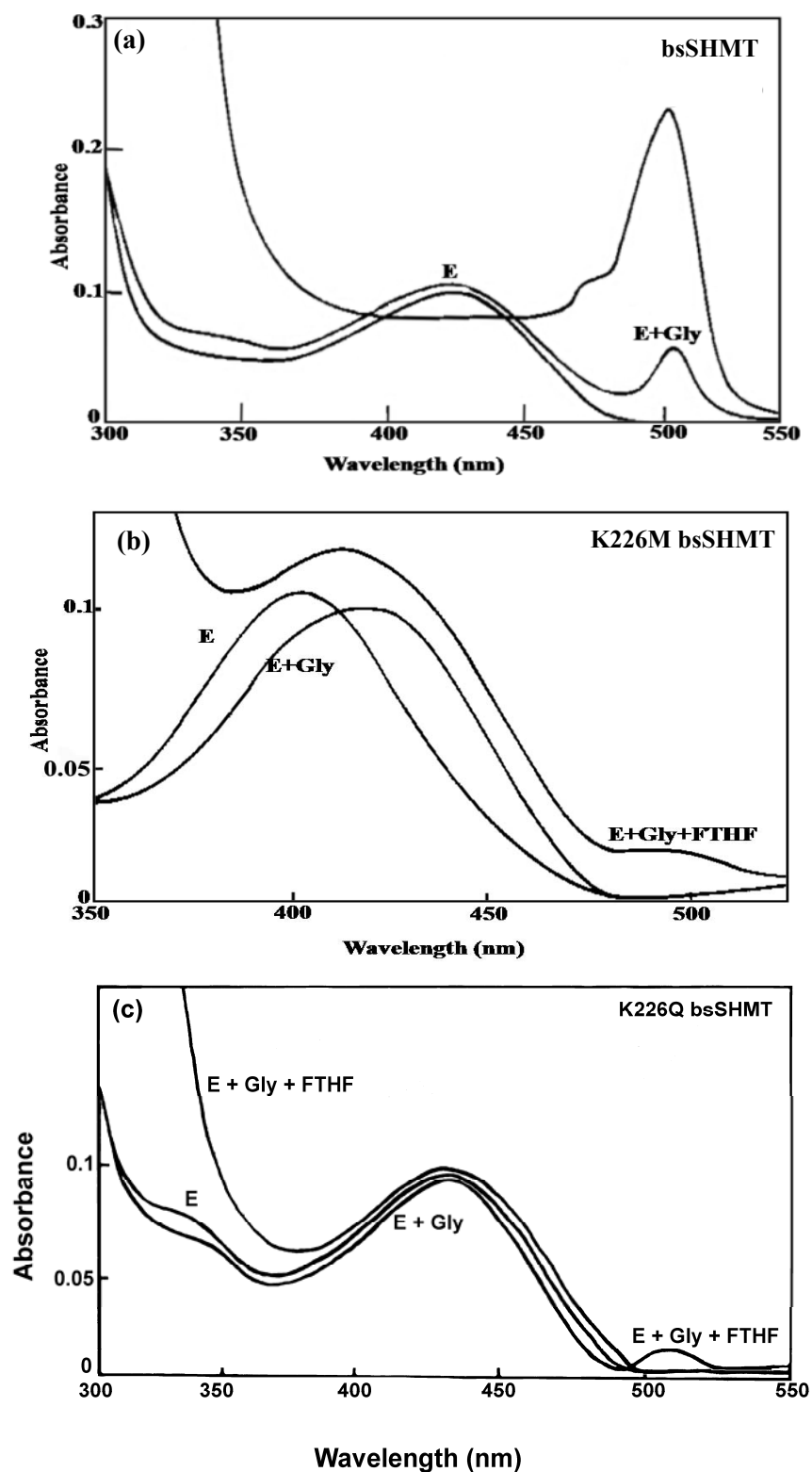


Fig 1.9: Absorbance changes on the addition of Gly, Gly+FTfH to bsSHMT (a), K226M bsSHMT (b) and K226Q bsSHMT (c).

Curve E: bsSHMT or K226M or K226Q bsSHMT.

Curve E + Gly: bsSHMT and Lys mutants in presence of 50 mM Gly.

Curve E+Gly+FTfH: bsSHMT and Lys mutants in presence of 50 mM Gly and 1 mM FTfH.

Stopped-flow studies were carried out to monitor the rate of formation of quinonoid intermediate on addition of Gly at 495 nm for both bsSHMT and Lys mutants. The rates at 495, 412, 425 and 343 nm were measured to monitor the formation of QI, external aldimine and gem-diamine, respectively. The rates were determined using stopped-flow spectrophotometer. Rate of formation of quinonoid intermediate on addition of Gly to bsSHMT was measured with 10 and 50 mM Gly and at different time points (5, 50 and 200 s). Table 1.3 shows the rate of formation of QI at different time point with varying concentration of Gly for bsSHMT-Gly binary complex at 495 nm. Fig 1.10 shows the spectra obtained on addition of 10 or 50 mM Gly upto 50 s. It can be seen from the Table 1.3 and Fig 1.10 that, varying concentration of Gly did not alter the rate drastically. However the reaction was not completed within 50 s and this suggestion was supported by the data in Fig 1.10 which shows, that this curve did not reach a plateau. Increasing the time range to 200 s resulted in a typical graph which shows a plateau (Fig 1.11). However the rates obtained were similar to that at 50 s range. The rate at which curve reached steady-state was considered as final rate (0.06 s^{-1}) upon addition of Gly (50 mM) at 495 nm (Fig 1.11).

Rate of formation of external aldimine and gem-diamine

The rate of formation of external aldimine at 425 nm via gem-diamine intermediate (343 nm) on addition of Gly (50 mM) to bsSHMT was measured. Table 1.4 summarizes the rate of formation of external aldimine and gem-diamine at different time point. Fig 1.12 and 1.13 represent the rate of of gem-diamine and external aldimine respectively. The reaction was completed within 0.5 s and curve reached plateau. A further increase in the reaction time to 50 or 500 s, an insignificant change was observed. Experiments were repeated at least 6 times to obtain a consistent rate for the reaction at 343 and 425 nm. The rate varied over a large range and hence the results were not satisfactory and consistent. Since both the reactions are very fast, rates could not be measured.

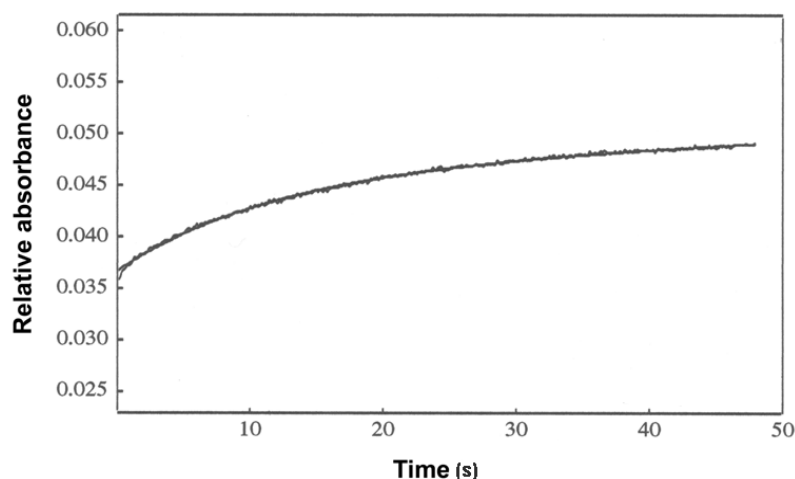


Fig 1.10: The increase in absorbance for 50s at 495 nm when the bsSHMT was mixed with 10 or 50 mM Gly in the stopped-flow spectrophotometer. bsSHMT (10 mg ml^{-1}) in 50 mM potassium phosphate buffer, pH 7.4, containing 1 mM EDTA, 1 mM 2-ME was used for the reaction.

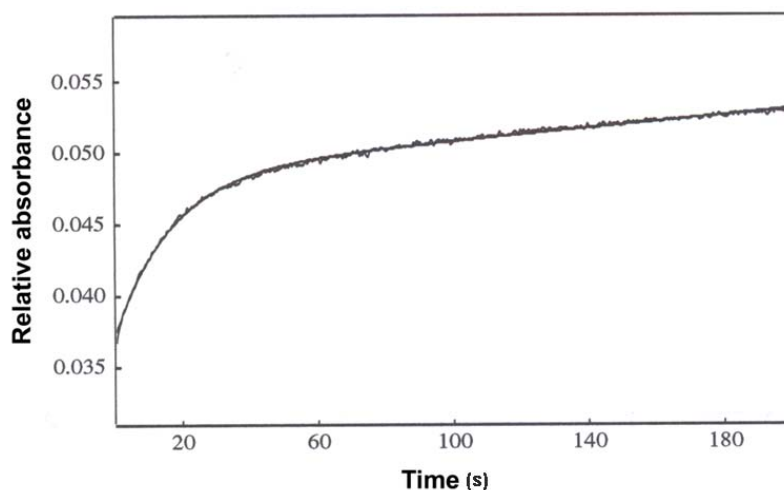


Fig 1.11: The increase in absorbance for 200s at 495 nm when bsSHMT was mixed with 10 or 50 mM Gly in the stopped-flow spectrophotometer. The reaction was measured for 200 s. An increase in the scan time to 200 s resulted in a typical hyperbolic curve. bsSHMT (10 mg ml^{-1}) in 50 mM potassium phosphate buffer, pH 7.4, containing 1 mM EDTA, 1 mM 2-ME was used in the reaction.

Table 1.3: The rate for the formation of quinonoid intermediate at 495 nm for bsSHMT-Gly binary complex with varying concentration of Gly and different time points.

Time (s)	Rate (s^{-1})	Gly (mM)	Remark (\uparrow at 495 nm)
50	$8.6 \pm 1.7 \times 10^{-3}$	10	Curve failed to reach plateau
50	$8.7 \pm 1.8 \times 10^{-3}$	50	
200	$6.2 \pm 6.1 \times 10^{-4}$	10	Curve reached plateau
200	$5.9 \pm 5.6 \times 10^{-5}$	50	

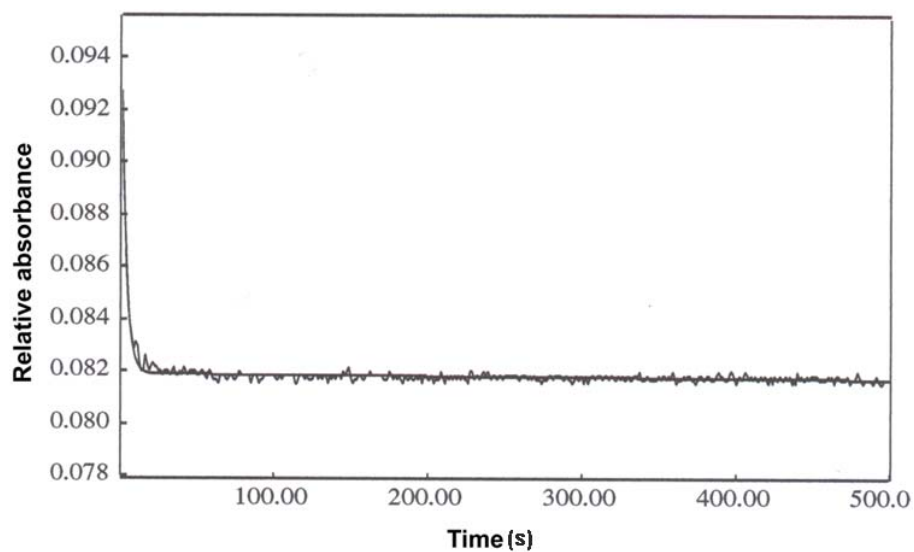


Fig 1.12: The decrease in absorbance at 343 nm on mixing bsSHMT with 50 mM Gly in the stopped-flow spectrophotometer. bsSHMT (10 mg ml^{-1}) in 50 mM potassium phosphate buffer, pH 7.4, containing 1 mM EDTA, 1 mM 2-ME was rapidly mixed with 50 mM Gly. (Rate constant $328 \pm 6 \text{ s}^{-1}$).

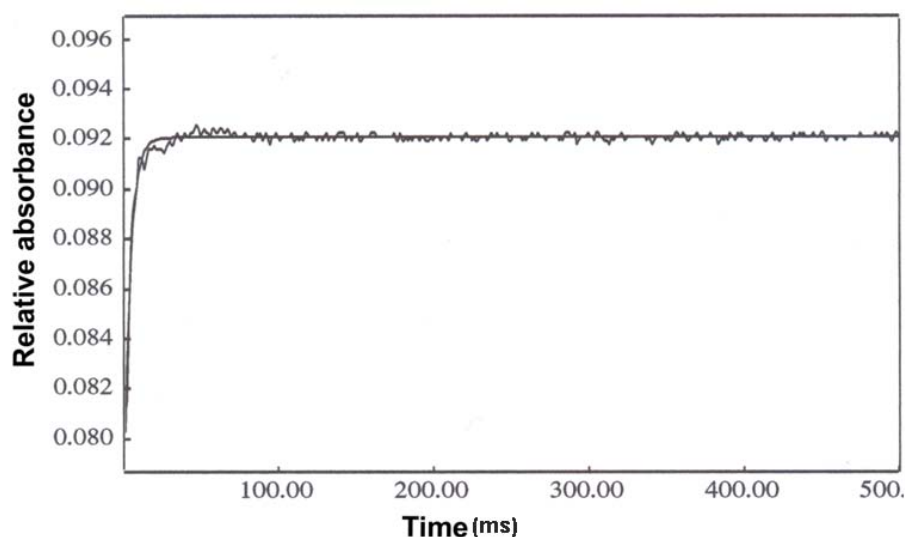


Fig 1.13: The increase in absorbance at 425 nm on mixing bsSHMT with Gly in the stopped-flow spectrophotometer. bsSHMT (10 mg ml^{-1}) in 50 mM potassium phosphate buffer, pH 7.4, containing 1 mM EDTA, 1 mM 2-ME was used flowed against 50 mM Gly. (Rate constant $245 \pm 5 \text{ s}^{-1}$).

The rate of formation of the quinonoid intermediate on addition of Gly to K226M and K226Q bsSHMT

The rate of formation of quinonoid intermediate in the case of Lys mutants was monitored using 50 mM Gly. It can be seen from the Fig 1.8 that, there was no QI formation at 495 nm on addition of Gly to both the Lys mutants. A small rate ($2 \times 10^{-4} \text{ s}^{-1}$) was observed with a standard error of $\pm 9.8 \times 10^{-5}$. This rate was considered as insignificant as there was no change in the relative absorbance (Fig 1.14). Similar results were obtained for K226Q bsSHMT; though the time of reaction was increased to 100 s (Fig 1.14).

The rate of formation of external aldimine and gem-diamine on addition of Gly to K226M bsSHMT and K226Q bsSHMT

The spectral studies suggested a shift in λ_{max} from 412 to 425 nm on addition of Gly to K226M bsSHMT (Fig 1.8 b). Unlike in bsSHMT, this mutant had distinct λ_{max} difference between external and internal aldimine. It was of interest to monitor the changes at 412 and 425 nm. The result represented in Table 1.5 and Fig 1.15 suggests that, K226M and K226Q bsSHMT did not show a good rate at 412 and 425 nm. A relative decrease in the curve was expected for K226M bsSHMT at 412 nm. The reaction was monitored till 500 s (Fig 1.15) to obtain a good curve and rate; however K226M bsSHMT showed a small increase with an insignificant rate. The absorbance change either at 412 or 425 nm was not sufficient to obtain satisfactory rates (Table 1.5). The experiments were performed several times. Similar results were obtained for K226Q bsSHMT; hence it was difficult to measure the rate of formation of an external aldimine and gem-diamine.

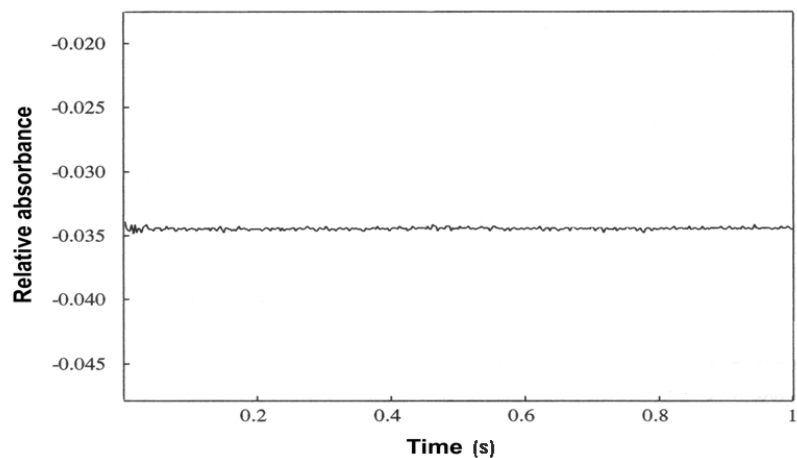


Fig 1.14: The stopped-flow scan at 495 nm upon addition of 50 mM Gly to K226M bsSHMT. K226M bsSHMT (10 mg ml^{-1}) in 50 mM potassium phosphate buffer, pH 7.4, containing 1 mM EDTA, 1 mM 2-ME was used for the reaction. Both the Lys mutants gave similar results hence only K226M bsSHMT is represented.

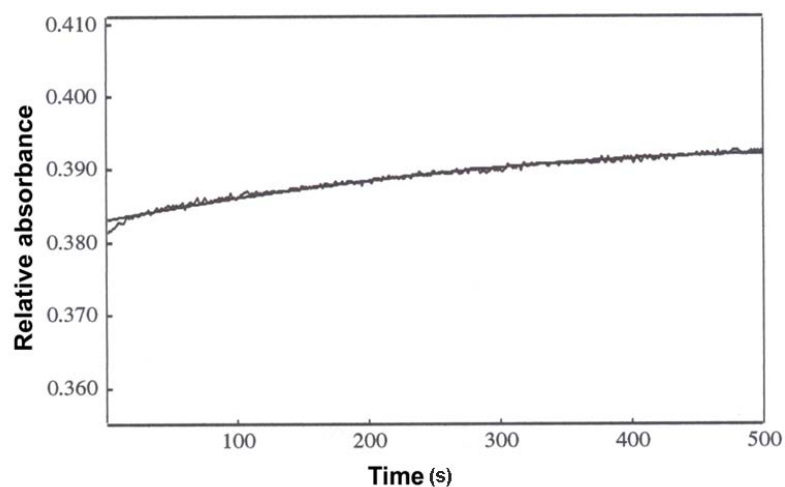


Fig 1.15: The stopped-flow scan at 412/425 nm for the formation of external aldimine upon addition of 50 mM Gly to K226M/K226Q bsSHMT. K226M bsSHMT (10 mg ml^{-1}) in 50 mM potassium phosphate buffer, pH 7.4, containing 1 mM EDTA, 1 mM 2-ME was used for the reaction. Since K226Q bsSHMT gave a similar result, only the scan for K226M bsSHMT is given to avoid repetition.

Table 1.4: The rate of formation of external aldimine and gem-diamine on addition of Gly to K226M bsSHMT.

Since the reaction did not reach a clear plateau, calculations of the rates were performed by taking cut off time as closer to the plateauing curve as possible.

Enzyme	Wavelength (nm)	Time (s)	Rate (s⁻¹)
K226M	412	0.5	$4.90 \pm 0.15 \times 10^{-4}$
		180	$1.28 \pm 0.05 \times 10^{-3}$
	425	0.5	$8.10 \pm 0.27 \times 10^{-4}$
		180	$1.30 \pm 0.05 \times 10^{-3}$
K226Q	412	100	$5.31 \pm 0.01 \times 10^{-2}$
	425	100	$5.54 \pm 0.02 \times 10^{-2}$

Rates for the enhanced formation of the quinonoid intermediate

The bsSHMT-Gly binary complex, on addition of THF results in the formation of a quinonoid intermediate at 495 nm. This reaction takes place within the mixing time of the spectrophotometer (Fig 1.8 a). It is well known that addition of THF enhances the rate of reaction and drives equilibrium towards the quinonoid intermediate from external aldimine. Rates of this reaction were determined using stopped-flow spectrophotometer as described in methods section. Rates were measured at different times viz, 0.05 to 500 s. The experiments were repeated four times to obtain consistent rates and averages of rates obtained are presented. The rates measured at 495 nm with different time scales are summarized in Table 1.6.

It can be seen from the Fig 1.16 and 1.17 that, interaction of THF with bsSHMT-Gly binary complex could be in two phases, initial fast phases and a second slow phase. Rates were measured for both initial fast phase and second slow phase. Fig 1.16 shows initial fast phase, Fig 1.17 shows the late slow phase with a decrease and Fig 1.18 shows the final slow phase increase. Fig 1.19 shows all the phases of the reaction. These experiments were repeated several times and the consistent observation was that an initial rapid increase was followed by slow phase. The entire reaction was monitored for 500 s at 495 nm to confirm the fast and slow reactions. The rate of over all reaction was 0.08 s^{-1} . However, both the Lys mutants did not show any enhanced rate upon addition of THF (Fig 1.20).

Fig 1.20 shows a comparison of the rates for the formation of quinonoid intermediate in the bsSHMT and Lys mutant, upon addition of THF to Gly-binary complexes. Only initial fast rate is compared and plotted in the graph. An analogue of THF, FTTHF interacts with the quinonoid intermediate generated during the SHMT reaction with Gly. It can be seen from Fig 1.9 that the wild-type enzyme, upon interaction with Gly-FTTHF, yielded the characteristic quinonoid intermediate with a maximum absorbance at 495 nm, and a rate constant of 0.08 s^{-1} . The mutant enzyme did not show any absorbance change at 500 nm (Fig 1.9 b, c).

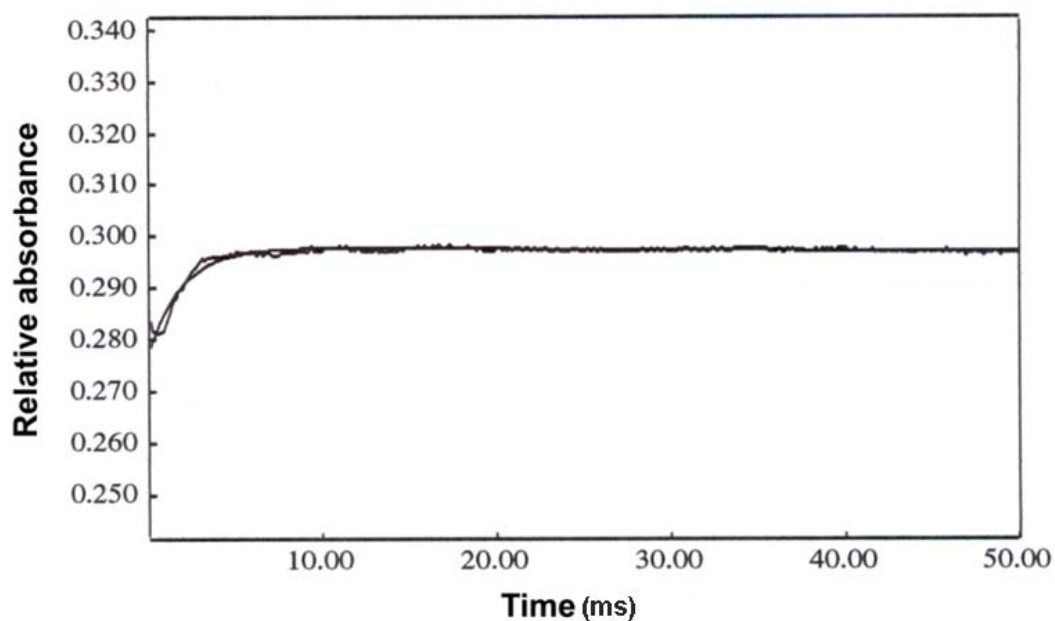


Fig 1.16: The initial increase in absorbance at 495 nm when the bsSHMT (10 mg ml^{-1})-Gly (50 mM) was mixed with THF ($70 \text{ }\mu\text{M}$) in stopped-flow spectrophotometer and relative absorbance measured for 50 ms. All the experiments were carried out in 50 mM potassium phosphate buffer, pH 7.4, containing 1 mM EDTA, 1 mM 2-ME.

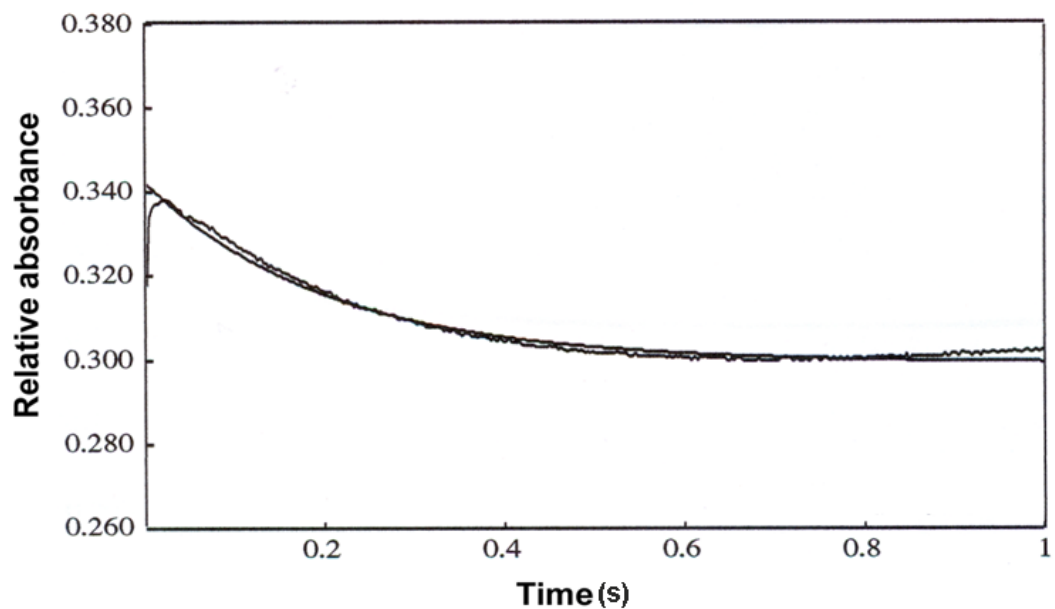


Fig 1.17: The decrease in absorbance at 495 nm on mixing bsSHMT (10 mg ml^{-1})-Gly (50 mM) with THF ($70 \text{ }\mu\text{M}$) in stopped-flow spectrophotometer and the reaction was measured for 1 s. All the experiments were carried out in 50 mM potassium phosphate buffer, pH 7.4, containing 1 mM EDTA, 1 mM 2-ME.

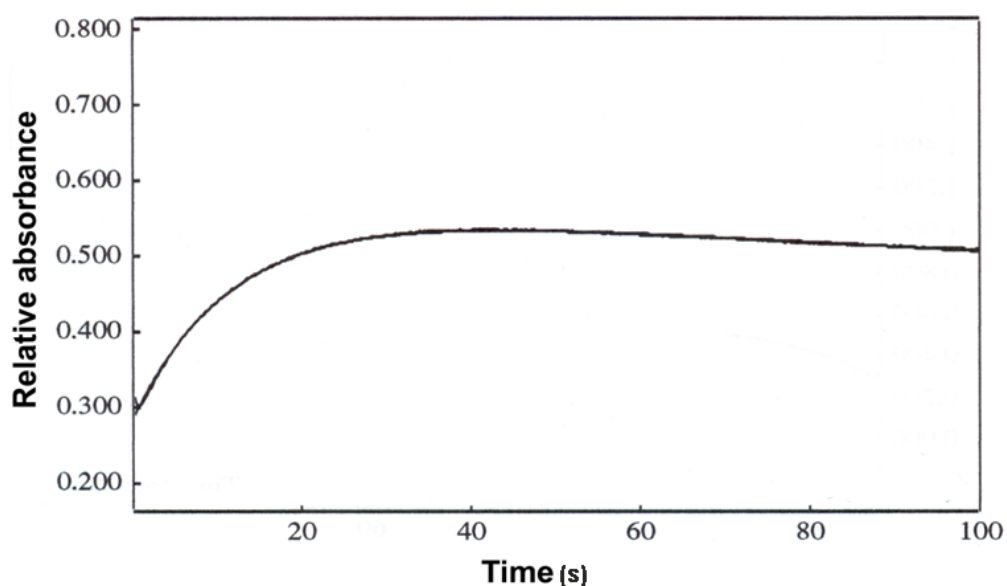


Fig 1.18: The final increase in absorbance at 495 nm on mixing of bsSHMT (10 mg ml^{-1})-Gly (50 mM) with THF ($70 \text{ }\mu\text{M}$) in the stopped-flow spectrophotometer and relative absorbance measured for 100 s. All the experiments were carried out in 50 mM potassium phosphate buffer, pH 7.4, containing 1 mM EDTA, 1 mM 2-ME.

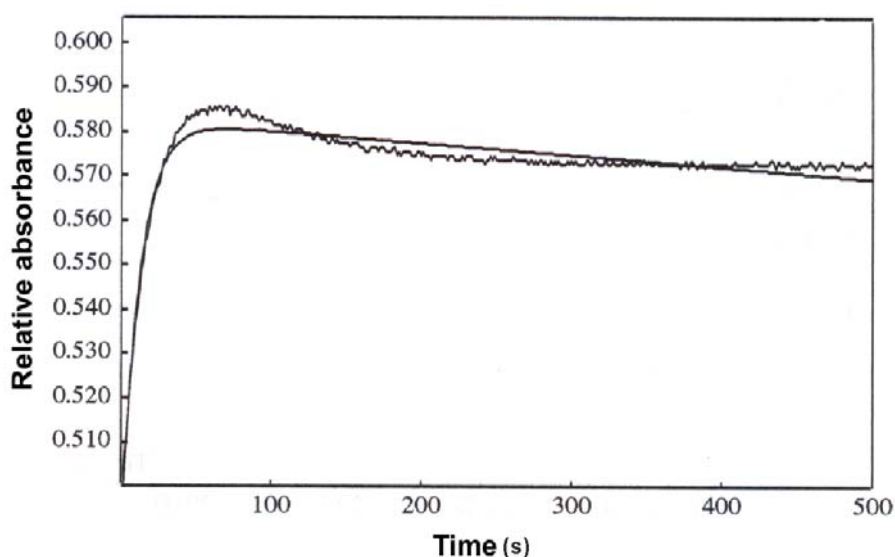


Fig 1.19: A graphical representation of the overall reaction on addition of THF to bsSHMT-Gly binary complex, showing initial fast and a slow phase. The reaction was monitored till 500 s to confirm the over all rate. All the experiments were carried out in 50 mM potassium phosphate buffer, pH 7.4, containing 1 mM EDTA, 1 mM 2-ME. The solid line shows the best fit curve, the observed line is wavy.

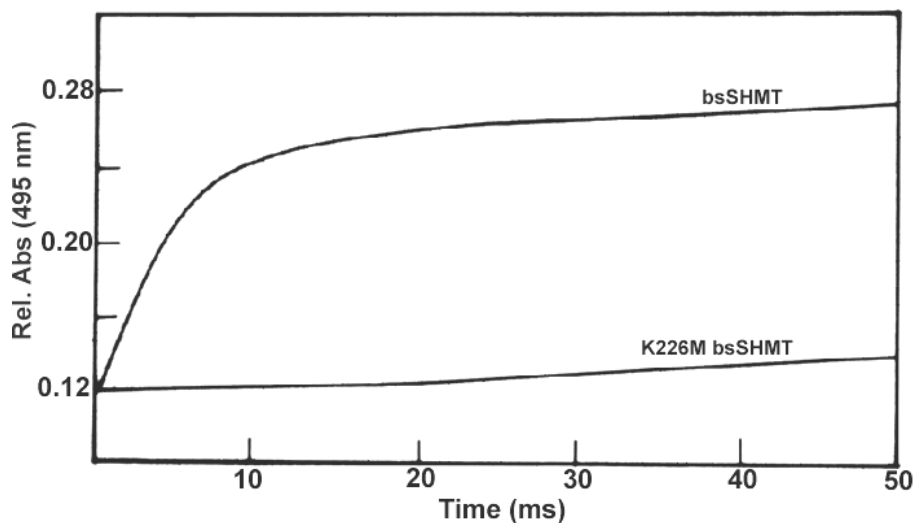


Fig 1.20: A graphical comparison of the formation of the quinonoid intermediate upon addition of THF to bsSHMT and Lys mutant Gly binary complexes. (Only data with K226M is represented as similar observations were made with K226Q bsSHMT).

Table 1.5: The rate for enhanced formation of quinonoid intermediate on addition of THF to bsSHMT-Gly complex.

Since the reaction did not reach a clear plateau, calculations of the rates were performed by taking cut off time as closer to the plateauing curve as possible.

Wavelength (495 nm)	Time (s)	Rate (s^{-1})
Initial increase (\uparrow)	0.05	340 ± 10
Decrease (\downarrow)	1.0	4.8 ± 0.1
Late increase (\uparrow)	50	$7.8 \pm 0.1 \times 10^{-2}$
Late increase (\uparrow)	100	$8.4 \pm 0.1 \times 10^{-2}$
Late increase (\uparrow)	500	$8.0 \pm 0.1 \times 10^{-2}$

Interaction with aminoxy compounds

The PLP Schiff's base is disrupted by a strong nucleophile like $\text{NH}_2\text{-OH}$, aminoxy compounds such as MA, AAA, etc., were potent inhibitors of the tetrameric SHMT (Baskaran *et al.*, 1989b; Acharya *et al.*, 1991; Jagath *et al.*, 1997a). It was of interest to examine the effect of these compounds on the dimeric bsSHMT. Earlier observation on SHMT showed that MA reacts with the internal aldimine to generate a characteristic intermediate absorbing at 388 nm before the formation of the oxime product (Acharya *et al.*, 1991).

The interaction of MA with bsSHMT resulted in the disappearance of internal aldimine at 425 nm and the formation of an intermediate with maximum absorbance at 388 nm (Fig 1.21 a). On addition of 10 mM of MA to K226M and K226Q bsSHMT, it failed to show any change in absorbance at 412, 388, and 325 nm, indicating that PLP at the active site of the mutant was incapable of interacting with MA (Fig 1.21 b).

The rate of formation of intermediate and the final oxime with MA on reaction with bsSHMT was monitored by stopped-flow kinetics. A rapid decrease in absorbance at 425 nm (30 s), increase at 388 nm (30 s), a slow decrease at 388 nm and an increase at 325 nm (50 s) was observed with bsSHMT on addition of MA (Fig 1.21a).

The rate of disruption of the internal aldimine (as monitored by decrease in optical density at 425 nm) and the formation of the intermediate absorbing at 388 nm was 1.6 s^{-1} (Fig 1.22). The intermediate was converted to the oxime product with the absorbance maximum at 325 nm with a rate constant of 0.004 s^{-1} (Fig 1.23). Stopped-flow studies of Lys mutant on addition of MA did not show change in relative absorbance at 425, 388 and 325 nm (Fig 1.24).

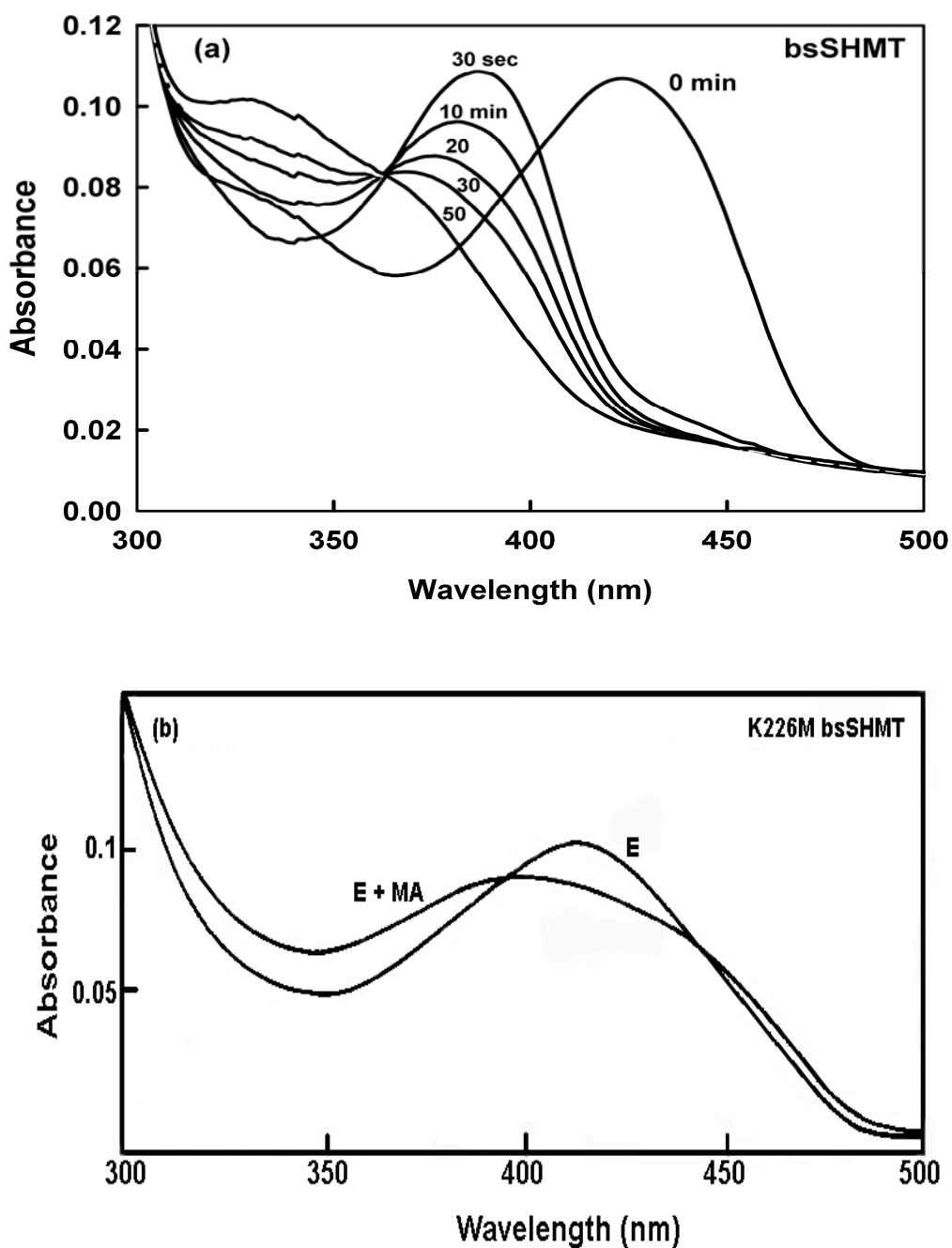


Fig 1.21: Interaction of MA with bsSHMT and K226M bsSHMT.

(a) To bsSHMT (1 mg ml^{-1}) in 50 mM potassium phosphate buffer, pH 7.4, containing 1 mM EDTA, 1 mM 2-ME (curve E); 2 mM MA was added, and the spectra were recorded. The figure shows the formation of an intermediate with absorbance maximum at 388 nm prior to formation of the product oxime absorbing at 325 nm. The isobestic point is seen at 360 nm.

(b) There were no spectral changes on addition of 10 mM MA to K226M bsSHMT (curve E + MA). The mutant enzyme (1 mg ml^{-1}) is represented as (curve E).

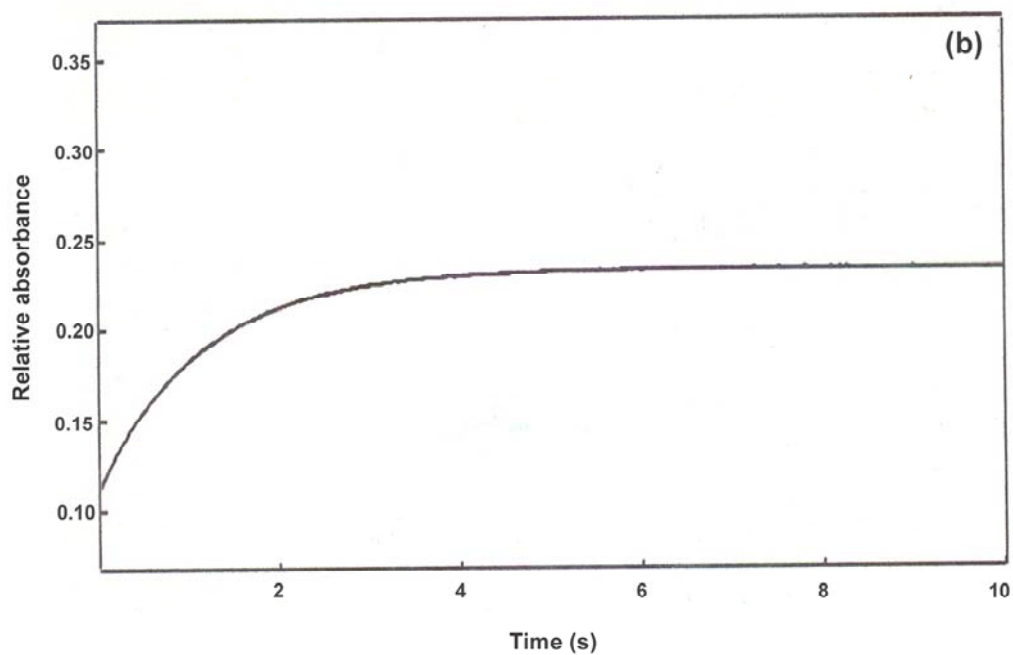
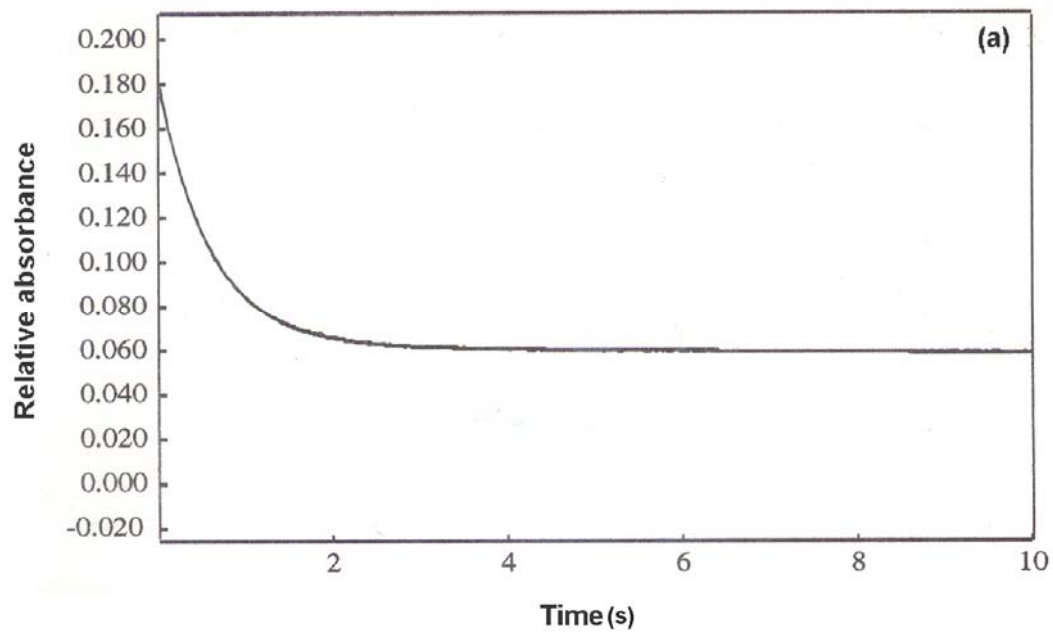


Fig 1.22: The relative absorbance changes of bsSHMT at (a) 425 and (b) 388 nm on addition of MA.

All the experiments were carried out in 50 mM potassium phosphate buffer, pH 7.4, containing 1 mM EDTA, 1 mM 2-ME.

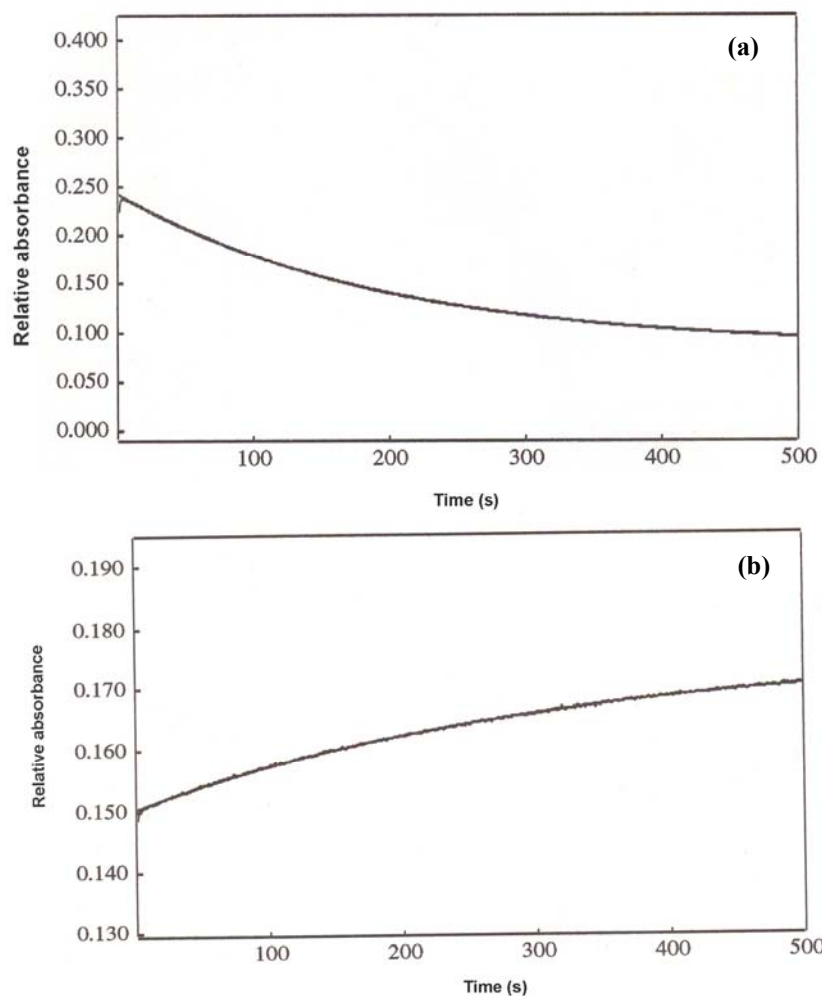


Fig 1.23: The relative absorbance changes on addition of MA to bsSHMT at two different wavelengths (a) 388 and (b) 325 nm.

(a) The decrease in relative absorbance at 388 nm, (b) The increase at 325 nm was monitored for 500 s. All the experiments were carried out in 50 mM potassium phosphate buffer, pH 7.4, containing 1 mM EDTA and 1 mM 2-ME.

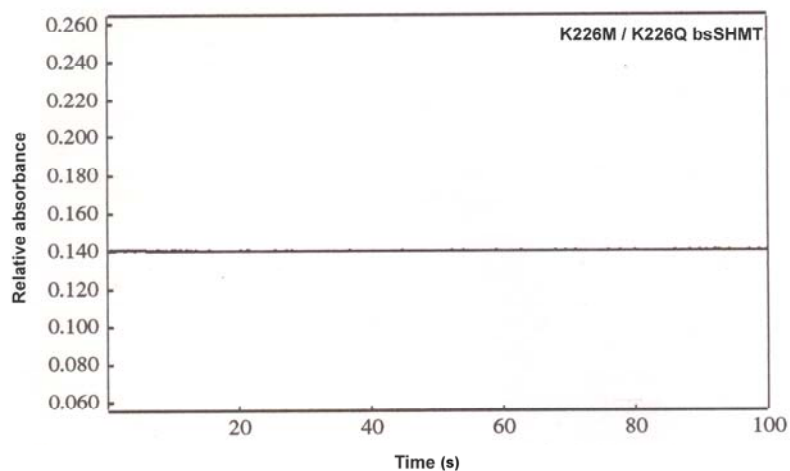


Fig 1.24: Interaction of K226M and K226Q bsSHMT with of 10 mM of MA.
The reaction was monitored at 412, 425, 388 and 325 nm similar to that of bsSHMT.

Crystal structures of K226M bsSHMT and its complexes

Internal aldimine of K226M bsSHMT

The overall structures of the Lys mutants are very similar to that of the wild-type enzyme (Fig 1.25 a). K226M and K226Q bsSHMT show a rms deviation of 0.14 Å and 0.15 Å, respectively, when compared with the wild-type enzyme. The mutation did not induce any gross conformational changes in the protein molecule. Active sites of both the mutants are essentially similar to that of the wild-type enzyme. However, an interesting positional change was observed in the orientation of the PLP ring in the mutant protein structure compared to wild-type bsSHMT (Fig 1.25 b). The PLP ring in the mutant protein structure showed a rotation of approximately 16° around the C₅-C_{5'} bond of PLP, compared to the bsSHMT internal aldimine.

L-Ser/Gly external aldimine of K226M and K226Q bsSHMT

The crystals of the complexes of K226M and K226Q bsSHMT with Ser/Gly were obtained by crystallization in the presence of 10 mM Ser/Gly in the drop as described in methods section. The complexes (L-Ser/Gly) of the K226M and K226Q revealed the presence of the bound substrate in the active site of the enzyme (Fig 1.26). The orientation of the PLP ring and the conformation of the substrate in the active site are very similar to that of external aldimine form of the wild-type enzyme.

The PLP ring in the structure of K226M bsSHMT was rotated by 16° when compared to bsSHMT internal aldimine. K226M bsSHMT in presence of L-Ser, substrate (L-Ser) undergoes a further rotation of approximately 9° to form external aldimine. The change in orientation of Y61 (Fig 1.26) was similar to that observed in bsSHMT-Ser complex (Trivedi *et al.*, 2002).

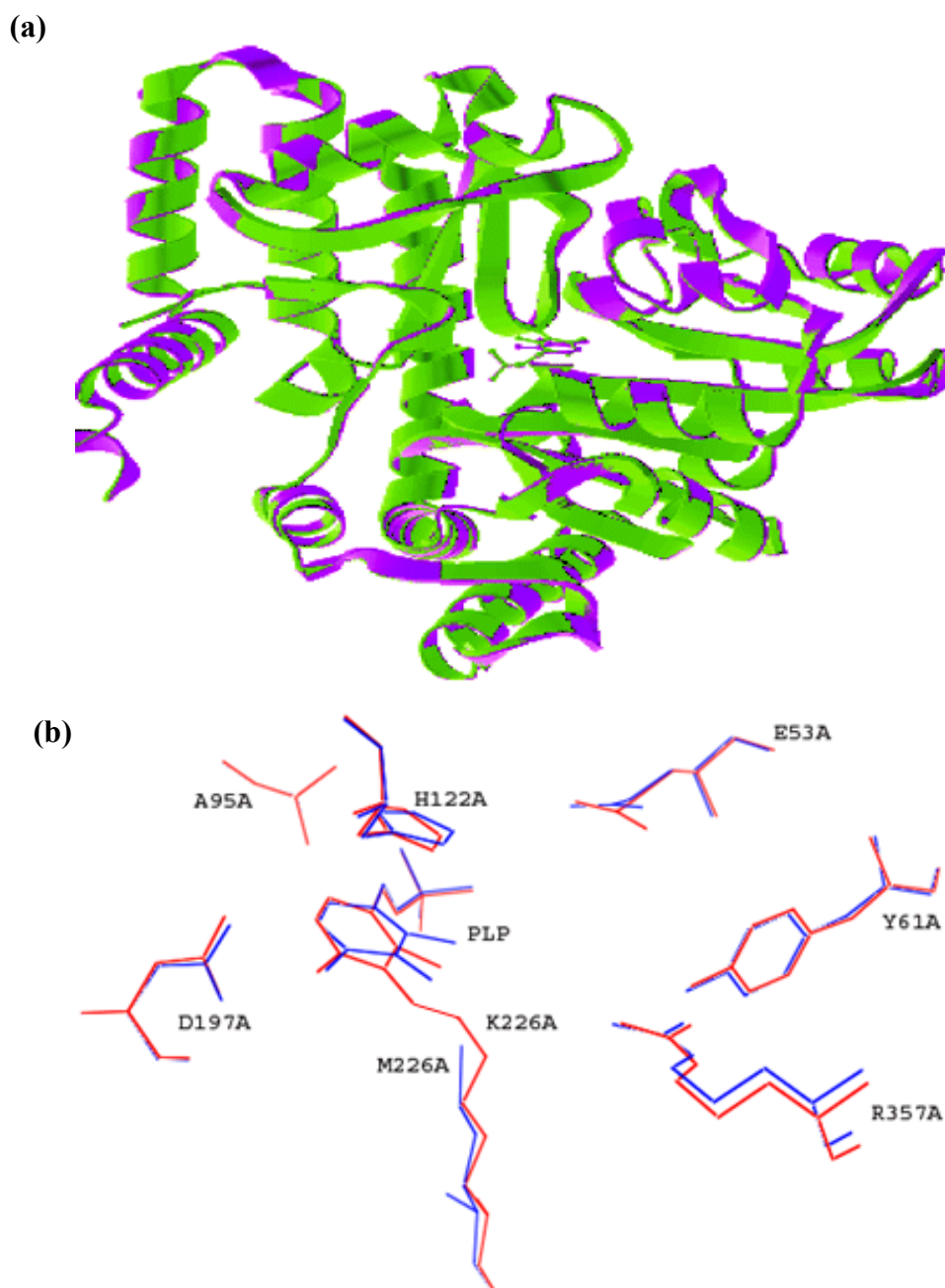


Fig 1.25: The comparison of crystal structures of bsSHMT and K226M bsSHMT.

(a) The structures of bsSHMT (earlier work) and K226M bsSHMT (this study) are shown as a ribbon diagram and overlaid on each other. The PLP molecule is shown in ball and stick representation. Colour: bsSHMT in magenta and K226M bsSHMT, green.

(b) An active site overlay of bsSHMT and K226M bsSHMT showing the change in orientation of the PLP ring. Colour: The structure of bsSHMT, blue and K226M bsSHMT in red.

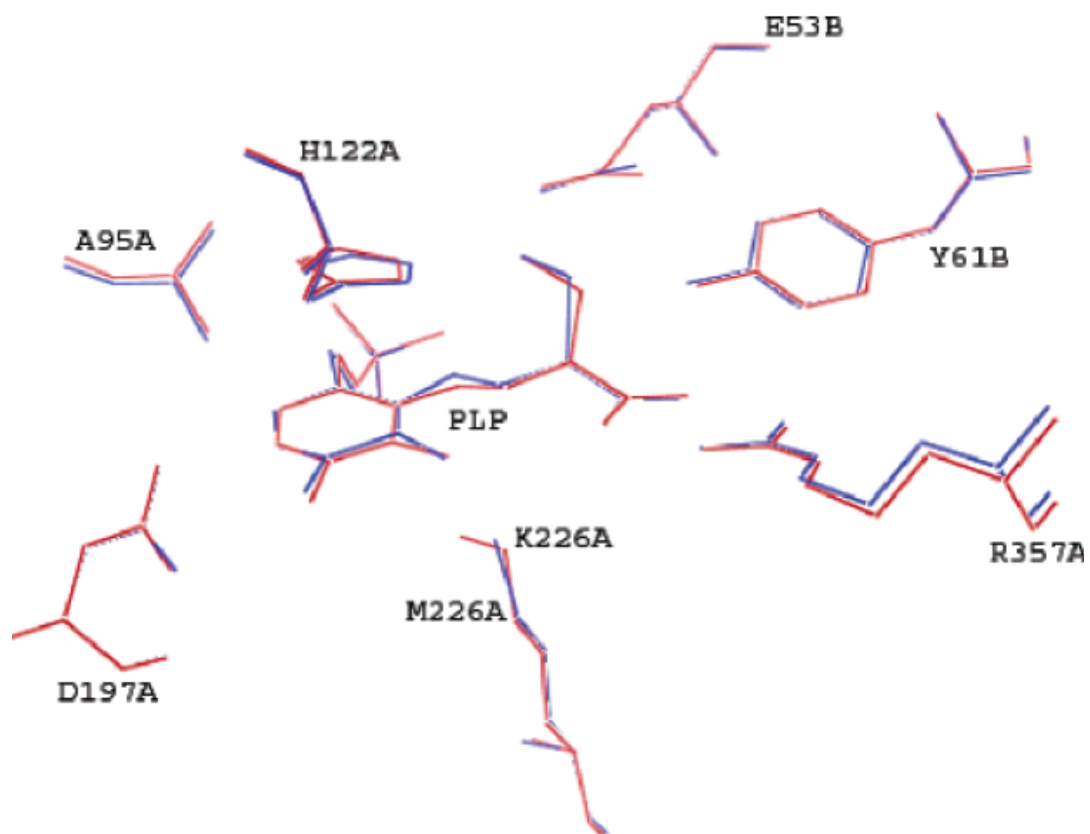


Fig 1.26: An overlay of L-Ser external aldimine structures of bsSHMT and K226M bsSHMT. Colour: bsSHMT-Ser external aldimine complex in red and K226M bsSHMT serine external aldimine complex in blue.

Discussion

The biochemical and structural studies on SHMT from various sources have implicated several amino acid residues, such as Lys, 226, Glu 53, Arg 357, and His 122 in the catalytic mechanism of the enzyme (numbering according to the primary sequence of bsSHMT, (Jala *et al.*, 2002). Active site Lys, Glu, His have been implicated in proton abstraction (Ziak *et al.*, 1990; Jala *et al.*, 2000; Talwar *et al.*, 2000a; Szebenyi *et al.*, 2004) and Arg (Fratte *et al.*, 1994; Jagath *et al.*, 1997a; Jala *et al.*, 2003a) plays an important role in substrate binding. However, mutational analysis of His (Jagath *et al.*, 1997b) and biochemical and structural studies on Glu residue suggest that these residues were probably not involved in the proton abstraction step of catalysis (Jala *et al.*, 2000; Trivedi *et al.*, 2002). On the basis of earlier biochemical and X-ray crystallographic studies on SHMT, retroaldol cleavage and direct displacement mechanisms and a combination of the two mechanisms were proposed for the THF-dependent cleavage of L-Ser catalyzed by SHMT (Schirch, 1982; Trivedi *et al.*, 2002; Schirch and Szebenyi, 2005).

Mutational analysis of the Lys residue, which anchors PLP, has been carried out in several PLP-enzymes (Ziak *et al.*, 1990; Toney and Kirsch, 1991a; Schirch *et al.*, 1993a; Ziak *et al.*, 1993; Gentry-Weeks *et al.*, 1995; Malashkevich *et al.*, 1995a; Rege *et al.*, 1996; Talwar *et al.*, 1997; Osterman *et al.*, 1999; Chen and Frey, 2001; Phillips *et al.*, 2004). The results presented in this chapter, describes the isolation, purification and biochemical characterization of K226M and K226Q bsSHMT as well as the three-dimensional structures of the unliganded and substrate-bound forms. Mutant clones were over expressed and purified. K226M bsSHMT, as isolated contained PLP, in spite of the absence of Lys (Table 1.2). However, K226Q bsSHMT as isolated had only 50% of PLP compared to bsSHMT. It is interesting to recall the observations with eSHMT Lys mutants, which were also dimers. K229Q eSHMT was isolated with a full complement of PLP but bound to the substrate as an external aldimine. K229H eSHMT did not contain PLP as an external aldimine (Schirch *et al.*, 1993a). In contrast, the mutation of Lys 256 in scSHMT resulted in the disruption of the tetramer to dimer with concomitant loss of PLP (Talwar *et al.*, 1997; Jala *et al.*, 2003b). THF-dependent cleavage of L-Ser was completely abolished in both K226M and K226Q bsSHMT. However, THF-independent cleavage was drastically affected,

but not completely abolished (Table 1.2). These results suggest that proton abstraction step is significantly not affected by the mutation of Lys.

The studies with AAT revealed that the Lys mutant enzymes were either completely inactive or showed very low levels of activity depending on the nature of the substitutions for Lys. Mutation to Ala, Arg, or Cys resulted in an inactive enzyme (Malcom and Kirsch, 1985; Ziak *et al.*, 1990; Toney and Kirsch, 1991a). Mutation of Lys of AAT to His retained 0.1% activity compared to the wild-type enzyme. These observations were interpreted to suggest that the active site Lys amino group was serving as the base to remove the α -proton of the substrate in forming the quinonoid intermediate. Such a conclusion was also supported by the three-dimensional structure of the mutant AATs suggests that, Lys plays an important role as proton abstractor in conjugation with a water molecule. However, the authors also suggested that a suitable polar residue such as His, perhaps in conjunction with a water molecule, can to a large extent replace Lys 258 (Ziak *et al.*, 1993). On the other hand, K229H and K229R eSHMT mutants were inactive, whereas the K229Q mutant was isolated with bound substrate and catalyzed a single turnover reaction but did not show steady-state catalytic activity. After a detailed examination, it was suggested that the Lys mutations in eSHMT had probably affected the product release step of catalysis in the THF-dependent cleavage of L-Ser (Schirch *et al.*, 1993a). Our results are not in agreement with this explanation as no detectable activity was observed with K226M and K226Q bsSHMT (Table 1.2).

Spectral studies of K226M bsSHMT suggest that mutant enzyme had an altered absorbance maximum at 412 nm (Fig 1.8 b); however the λ_{\max} for K226Q bsSHMT was similar to that of bsSHMT (Fig 1.8 c). The absorbance maximum at 412 nm for K226M bsSHMT mutant could be due to the aldehyde from the PLP in the active site environment (free PLP absorbs at 388 nm). Far-UV CD studies and crystal structure of K226M and K226Q bsSHMT suggest that, the mutation did not induce any gross conformational changes in the protein molecule. A change in orientation change in PLP ring (16°) was observed in K226M bsSHMT structure (Fig 1.25 b). It is interesting to recall that the active site Lys mutants of AAT also showed a similar change in the orientation of the PLP ring (Malashkevich *et al.*, 1995a). The

structures of the mutant enzymes clearly demonstrate that PLP could bind even in the absence of a covalent bond with Lys. However, the orientation of the PLP ring seems to be affected by the disruption of the Schiff's base. The bathochromic shift from 390 to 412 nm in the mutant could be due to altered interactions of the enzyme with PLP, especially in the absence of the Lys residue. These altered interactions could be responsible for the change in the orientation of the PLP ring by 16° observed in the crystal structure of the mutant enzyme, compared to the internal aldimine structure of bsSHMT. The rate of interaction with MA also suggests that, the change in active site environment in the case of K226M bsSHMT (Fig 1.21 b and Fig 1.24). Neither of the Lys mutants nor their Gly external aldimine complexes showed any change in absorbance at 412, 388, and 325 nm indicating that PLP at the active site of the mutant was incapable of interacting with MA.

The crystal structure of the ternary complex of mcSHMT also showed a rotation of 16° of the PLP ring compared to the orientation of PLP in the internal aldimine (Fig 1.25 b). The orientation of PLP in these structures is similar to the position of PLP in the gem-diamine form (Szebenyi *et al.*, 2000). Similarly, structures of Lys mutants of AAT revealed a rotation of the PLP ring of 16° compared to the wild-type enzyme. The PLP ring in the structure of K226M bsSHMT with the substrate undergoes a further rotation of approximately 9° compared to the unliganded structures of K226M and K226Q bsSHMT (Fig 1.26). These observations imply that orientation of PLP is a crucial feature in catalysis.

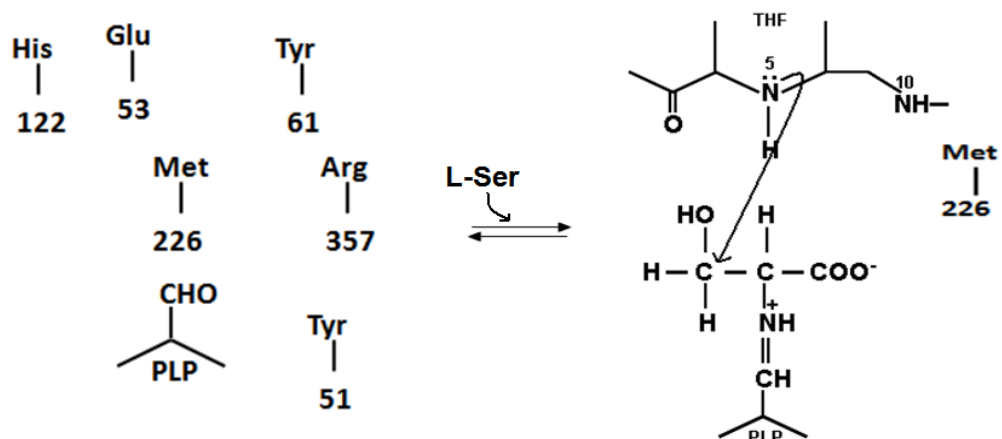
Addition of L-Ser/Gly to K226M bsSHMT resulted in a shift in the absorbance maximum from 412 to 425 nm, suggesting that PLP at the active site has the ability to react with the substrate and form an external aldimine complex (Fig 1.8 b, c). K226Q bsSHMT showed a small decrease at 425 nm on addition of substrates. However, in the case of K229Q eSHMT, on the basis of the spectral and kinetic studies, it has been reported that the enzyme was isolated with bound substrate (Schirch *et al.*, 1993a). However, the Lys mutant structures of bsSHMT (Fig 1.25 b) clearly demonstrate that there was no density attributes to the bound substrate. Binary complexes solved in presence of either of the substrates forms a clear external aldimine (Fig 1.26). The orientation of the PLP ring and the amino acid substrate in the crystal structure of the external aldimine forms of K226M and K226Q bsSHMT

were very similar to their corresponding orientation in the external aldimine form of the wild-type enzyme. The conformation of the PLP ring in the structure of unliganded mutant SHMTs appears to be that of gem-diamine form, whereas the orientation of the PLP in the substrate-bound form of the mutant SHMTs appears to be in the external aldimine conformation, with a rotation of approximately 25° compared to the wild-type enzyme.

Addition of THF to bsSHMT-Gly complex results in formation of a quinonoid intermediate and this process occurs in milliseconds (Fig 1.8, Table 1.3). A similar increase in absorbance at 495 nm, upon addition of THF, was observed in all SHMTs (Schirch and Ropp, 1967). Stopped-flow studies on the rate of formation of quinonoid intermediate on addition of THF/FTHF suggest that enhanced quinonoid intermediate was not observed with the substrates in the mutant enzyme (Fig 1.14). The absence of significant increase in absorbance at 495 nm, upon addition of Gly and THF/FTHF, suggested that the THF-mediated proton abstraction was affected by mutation of K226 to Met or Gln. The schematic representation of the mechanism (Scheme 1.1) suggests the possible step at which mutation has been affected bsSHMT catalysis. K226M bsSHMT was isolated with PLP and had an absorbance maximum at 412 nm (structure I, Fig 1.8 b). The orientation of PLP was changed by 16° in the absence of Schiff's base. Upon reaction with L-Ser it is converted to external aldimine (structure II) absorbing at 425 nm. The orientation of PLP is changed by 25° from the initial orientation (structure I). Attack of N5 of THF on C_β of L-Ser leads to bond cleavage resulting in the formation of quinonoid intermediate (structure III), this step is affected due to mutation of Lys residue in the forward reaction where L-Ser is the substrate (Scheme 1.1a, structure III). In the reverse reaction where Gly is used as a substrate, Lys mutants can form a small amount of quinonoid intermediate on addition of THF. However, further enhanced quinonoid intermediate formation in presence of THF is affected in Lys mutants (Scheme 1.1 b, structure III). It is well established that formation of the external aldimine proceeds through gem-diamine intermediate (343 nm) (16°). It is clear that the mutation does not affect either binding of PLP or its conversion to the substrate external aldimine complex (Fig 1.26).

Scheme 1.1: Schematic representation of the role of Lys 226 in reaction catalyzed by bsSHMT with L-Ser and Gly.

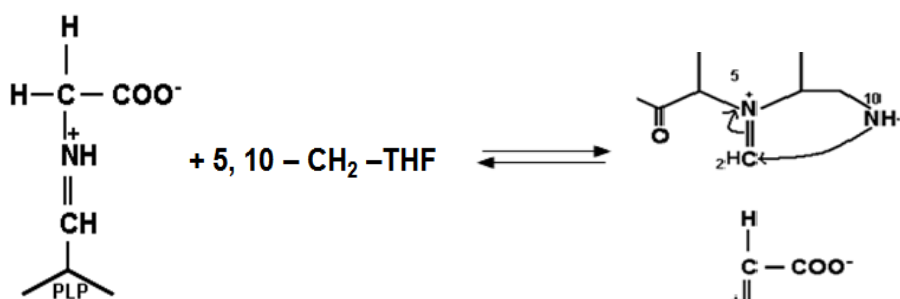
(a) Reaction with L-Ser



I
PLP at the active site of
K226M bsSHMT (412 nm)
PLP is rotated by 16°

II
L-Ser external aldimine
(425 nm)
PLP is rotated by 25°

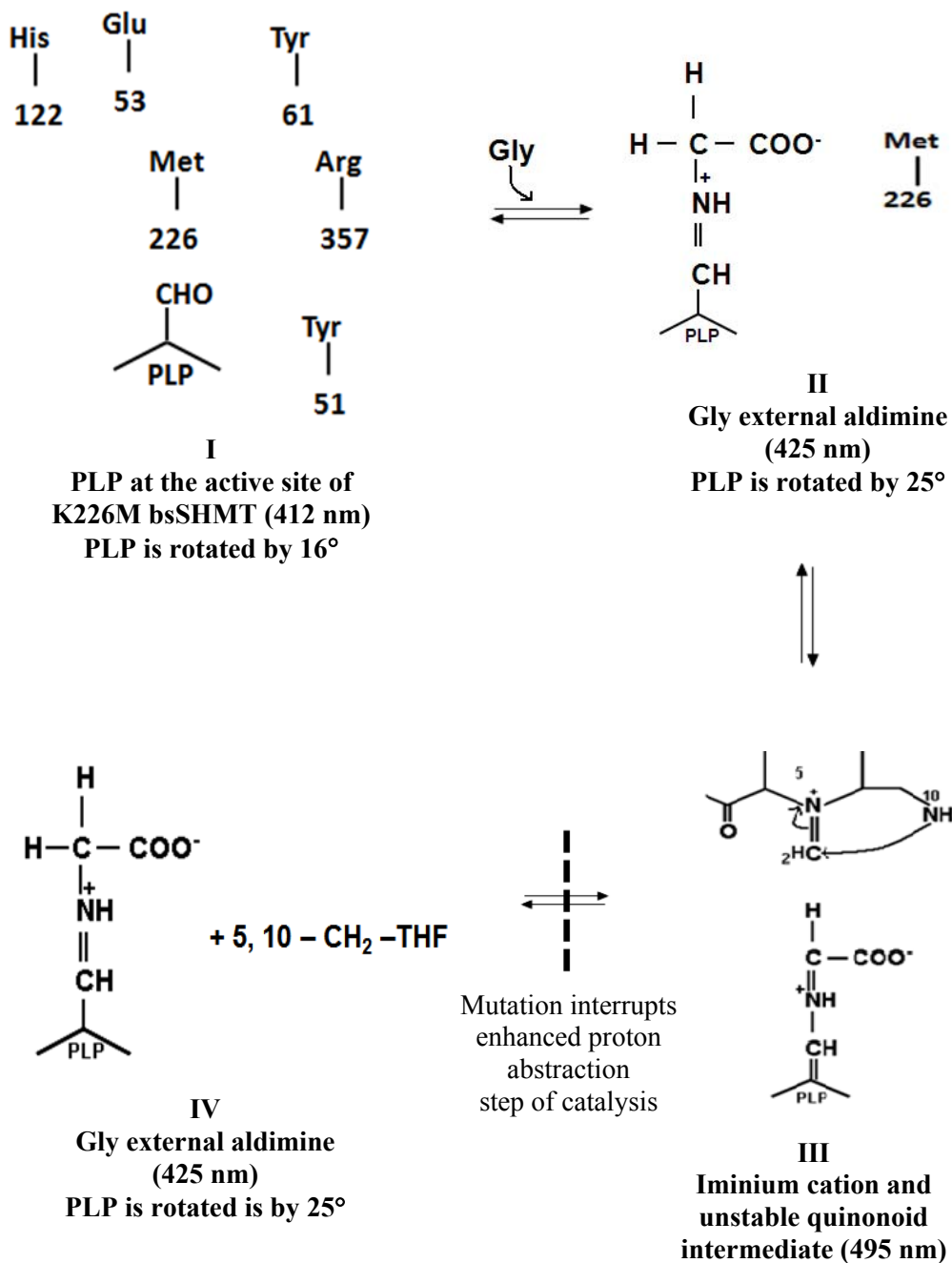
The step blocked
 by mutation



IV
Gly external aldimine
(425 nm)
PLP is rotated by 25°

III
Iminium cation and
unstable quinonoid
intermediate (495 nm)

(b) Reaction with Gly



However, the conversion of the external aldimine (PLP -25°) structure II to the quinonoid intermediate is affected (structure III). This could be an additional reason for the absence of enhanced proton abstraction. The orientation of PLP in the quinonoid intermediate with the product Gly, appears to be in the gem-diamine form. In the structure of the ternary complex of the mcSHMT as well bsSHMT, the PLP orientation is similar to that seen in geminal diamine complex (Szebenyi *et al.*, 2000). In the absence of the $-NH_2$ group of Lys, the conversion of the external aldimine to product quinonoid intermediate, where the PLP orientation is similar to that of gem-diamine, that is, the change in orientation of PLP from 25° to 16° , may not be possible. This in turn could lead to shifting of equilibrium towards the L-Ser external aldimine form.

In view of the lack of even a single turnover and the absence of bound H_2O at the active site, it can be suggested that Lys 226 plays a crucial role in bsSHMT catalysis with L-Ser as a substrate (Scheme 1.1a: conversion of structure II to structure III). In the reverse reaction Lys mutants were capable of forming a small amount of quinonoid intermediate on addition of THF to bsSHMT-Gly binary complex (structure IV). Results obtained in this study suggest that, K226 plays an important role in enhanced quinonoid intermediate formation on addition of THF (Scheme 1.1b: conversion of structure III to structure IV). In order for the product to be formed, $C_\alpha-C_\beta$ bond cleavage should be concurrent with the conversion of the enzyme from the external aldimine form of the substrate to the gem-diamine form of the product prior to the release of the product and the formation of the internal aldimine (structure I). The orientation of PLP changes from 25° in the external aldimine form to 16° in the quinonoid intermediate, and the quinonoid intermediate is stabilized by the interactions of Lys at the active site. In the absence of the $-NH_2$ group of Lys, the conversion of the external aldimine to product quinonoid intermediate, where the PLP orientation is similar to that of gem-diamine, that is, the change in orientation of PLP from 25° to 16° , may not be possible. This in turn could lead to shifting of equilibrium towards the substrate external aldimine form (L-Ser form). Further, the interactions of Lys 226 with residues such as Tyr 51 and Thr 223 have been implicated in the conversion of the enzyme from one form to another (Trivedi *et al.*, 2002). These interactions do not exist in K226M bsSHMT, and

therefore, the conversion of substrate external aldimine to quinonoid intermediate (which is in an orientation similar to that of gem-diamine) is not possible.

The results presented in this chapter establish the correlation between the biochemical and structural properties of Lys 226 mutants of bsSHMT. It is clear that the mutation does not affect either binding of PLP or its conversion to the substrate external aldimine complex. However, the conversion of PLP external aldimine (PLP-25°) to the quinonoid intermediate is affected. The quinonoid intermediate with the product Gly appears to be in the gem-diamine form. Thus K226 is responsible for flipping of PLP from one orientation to another, which is accompanied by C_α-C_β bond cleavage, and for the THF-mediated enhanced C_α proton abstraction in the reverse reaction. The crystal structure of Lys mutants and their substrate complexes were determined for the first time. These results suggest that Lys is not the crucial proton abstractor in the reaction as envisaged by earlier workers. A search for a residue that could function as a proton abstractor was extended to other possible residues at the active site. One such residue is Glu 53, and the results of investigations with mutation of Glu 53 are presented in the next chapter.

Chapter 2

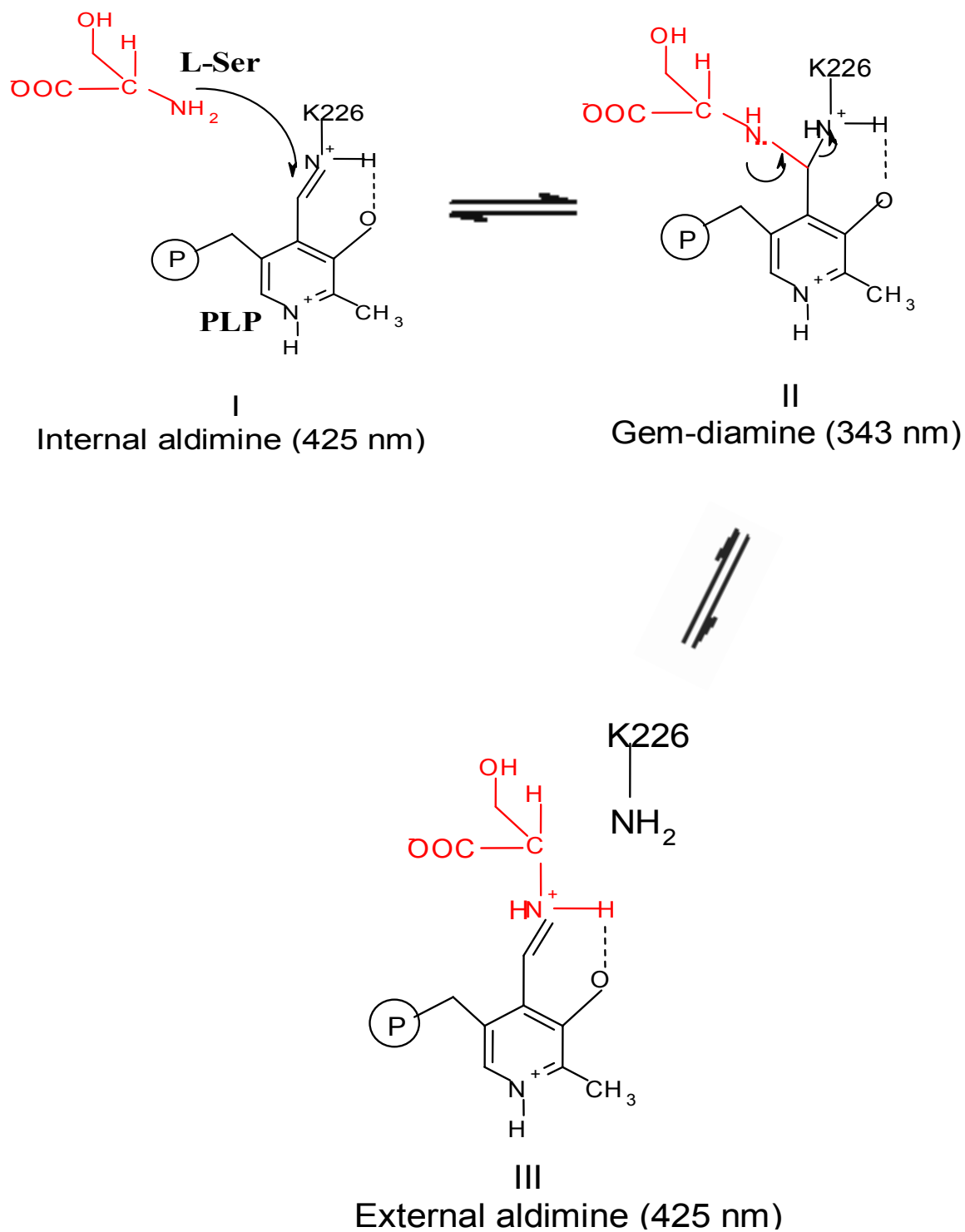
The involvement of glutamate 53 in
binding of L-serine and folate, and
conversion of bsSHMT from
'open' to 'closed' form

An outstanding characteristic of enzymes is their specificity for substrates and their ability to catalyze defined chemical reactions. However, some enzymes are able to carry out one or more types of reactions. Enzyme catalysis is related to binding of the substrate to defined areas or pockets of the protein in a specific conformation. The conformation of the enzyme-substrate complex is determined by the interaction between protein and substrate, each imposing conformational constraints on the other. Following this event, interaction of the substrate(s) with active site residues leads to catalysis.

Amino acid substrates bind to vitamin B₆-enzymes by forming a Schiff's base with the enzyme-bound PLP. The conversion of the substrate to product proceeds via several covalent reaction intermediates with defined spectral properties. The unique spectral properties of the intermediates in PLP-enzymes provide a convenient handle for identifying them and for analyzing the kinetics of their formation and decomposition. Most of the PLP-enzymes exist in their resting state as a Schiff's base which is referred to as an "internal aldimine" (John, 1995) (Scheme 2.1-I, bsSHMT is taken as a representative enzyme for depicting external aldimine formation).

The reaction is initiated by the binding of amino acid (or other substrates) to enzyme, forming a Schiff's base between the L-Ser and the PLP. In the next step, substrate displaces ϵ -amino group of Lys to form an "external aldimine" (Scheme 2.1-III, L-Ser is shown as representative of amino acid). It has been suggested that a gem-diamine intermediate in which α -amino group of substrate and ϵ -amino group of active site Lys are linked to PLP, is formed prior to the formation of external aldimine (Scheme 2.1-II) which is an obligatory step in the reaction mechanism of PLP-enzymes (Scheme 2.1) (John, 1995).

Scheme 2.1: Formation of L-Ser-external aldimine from internal aldimine via a gem-diamine intermediate. (bsSHMT is taken as a representative enzyme for depicting external aldimine formation)



SHMT has been isolated from several sources and in recent years the crystal structures of the enzyme and its complexes with substrates and inhibitors have been elucidated to high resolution (Renwick *et al.*, 1998; Scarsdale *et al.*, 1999; Scarsdale *et al.*, 2000; Szebenyi *et al.*, 2000; Trivedi *et al.*, 2002; Szebenyi *et al.*, 2004).

Crystal structure of the binary complex of bsSHMT-Ser suggests that Glu 53 is within hydrogen bonding distance with hydroxyl group of L-Ser (Fig 2.1a). Ternary complex of bsSHMT-Gly-FTHF suggests that Glu 53 has an interaction with formyl oxygen and N10 of FTHF (Fig 2.1b) (Trivedi *et al.*, 2002).

Based on the crystal structures and biochemical studies several mechanisms have been proposed for SHMT catalysis. Earlier, retroaldol cleavage mechanism was proposed for the catalysis of all 3-hydroxy amino acids by SHMT (Schirch, 1982; Schirch and Szebenyi, 2005). On the basis of bsSHMT-Ser binary complex, and ternary complex of bsSHMT-Gly-FTHF (Fig 2.1b) a direct displacement mechanism was proposed (Trivedi *et al.*, 2002). However, recently a combination of the classical retroaldol cleavage and direct displacement mechanism was proposed on the basis of biochemical and structural studies on E74Q rcSHMT (Szebenyi *et al.*, 2004).

The poor resolution in the crystal structures of E74Q rcSHMT and its substrate complexes failed to provide clear and conclusive information on the role of the Glu residue. In an effort to resolve this ambiguity, biochemical properties, 3D structure of E53Q bsSHMT, its binary complexes with Gly, L-Ser, L-*allo* Thr and the ternary complex with Gly and FTHF were determined and examined and represented in this chapter.

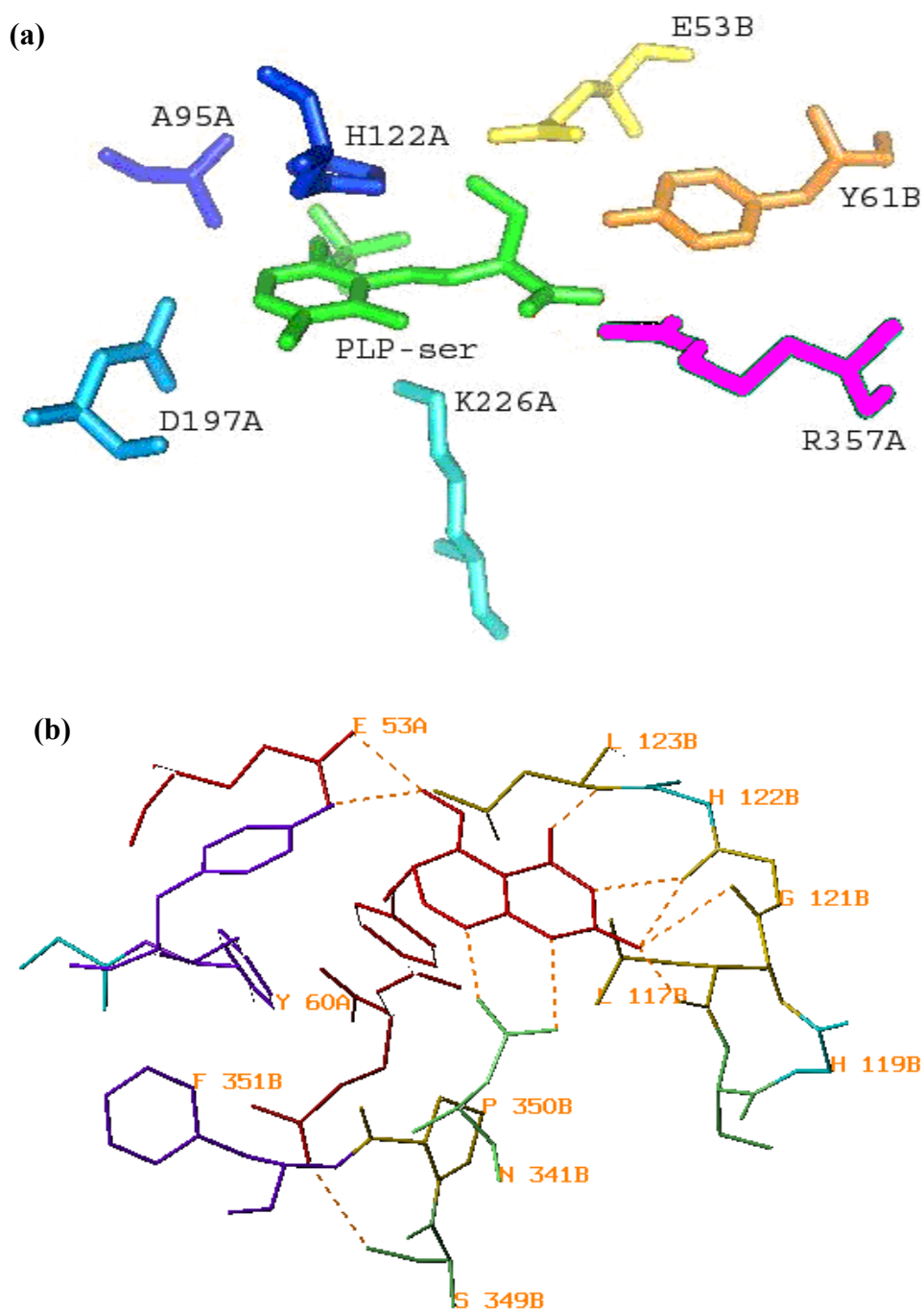


Fig 2.1: The crystal structure of bsSHMT-Ser and bsSHMT-Gly-FTHF complexes.

(a) L-Ser binding site with amino acids involved in catalysis. PLP-Ser aldimine is shown in green (Trivedi *et al.*, 2002).

(b) The active site region in the monomer A of the bsSHMT ternary complex showing the key residues interacting with FTHF. The figure was prepared by molscript. A, B after amino acids indicates subunit from which it comes. The active site residues are contributed from both the subunit A and B (Trivedi *et al.*, 2002).

Results

Expression and purification of E53Q bsSHMT

E53Q bsSHMT mutant construct was generated, transformed into *E. coli* BL21 (DE3) pLysS strain, overexpressed and purified according to the procedure described for bsSHMT in methods section. The purified protein showed a single band on SDS-PAGE analysis and a sub unit molecular weight of 45 kDa (Fig 2.2). The yield of the E53Q bsSHMT (45-50 mg L⁻¹) was similar to that obtained for bsSHMT.

Catalytic properties of bsSHMT and E53Q bsSHMT

THF-dependent cleavage of L-Ser

The THF-dependent cleavage of L-Ser was determined as described in methods section. bsSHMT catalyzes the THF-dependent conversion of L-Ser to Gly and 5, 10-CH₂ THF with a specific activity of 5.9 units (Table 2.1). The activity in the absence of THF was 10,000 fold lower compared to the activity in its presence. Mutation of Glu 53 leads to a complete loss of THF-dependent activity. When the mutant enzyme concentration was increased by 1000-fold (1 mg ml⁻¹) in the assay the amount of activity observed was insignificant. This observation suggests that E53 is essential for the THF-dependent cleavage of L-Ser.

THF-independent cleavage of L-Ser

THF-independent cleavage of L-Ser was also carried out with bsSHMT and E53Q bsSHMT. The standard radioactive assay using L-[3-¹⁴C] Ser was carried out in the absence of THF with varying concentrations of E53Q bsSHMT from 0.01 to 1 mg. The THF-independent cleavage of L-Ser could be measured only with higher concentrations of E53Q bsSHMT (1 mg or above) and bsSHMT did not show any cleavage of L-Ser in the absence of THF. Data are summarized in Table 2.1.

THF-independent cleavage of E53Q bsSHMT and bsSHMT

In addition to THF-dependent cleavage, SHMT also catalyses the THF-independent conversion of L-*allo* Thr to Gly and acetaldehyde. The THF-independent activity of E53Q bsSHMT with L-*allo* Thr as substrate had increased by 1.5 fold (Table 2.1). The K_m and specific activity values for L-*allo* Thr with bsSHMT

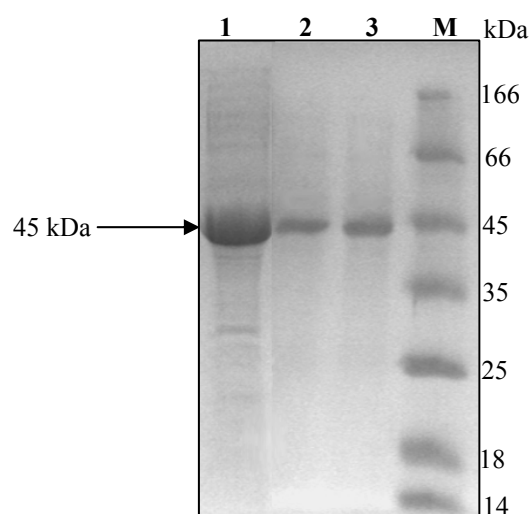


Fig 2.2: SDS-PAGE (12%) analysis of the fractions obtained during the purification of E53Q bsSHMT.

M: markers (kDa), β -galactosidase 166; bovine serum albumin 66.2; ovalbumin 45; lactate dehydrogenase 35; restriction endonuclease Bsp981 25; β -lactoglobulin 18.4; lysozyme 14.4); Lane 1: E53Q bsSHMT crude extract (Total cell lysate or soluble fraction) (25 μ g); Lane 2: DEAE-cellulose eluted fraction (10 μ g); Lane 3: purified E53Q bsSHMT (10 μ g).

Table 2.1: Kinetic constants for bsSHMT and E53Q bsSHMT.

Enzyme	Specific activity (L-Ser) ¹ (μ mol/min/mg)		K_m (mM)		Specific activity ² (μ mol/min/mg)
	+ THF	- THF	L-Ser	L- <i>allo</i> Thr	L- <i>allo</i> Thr
bsSHMT	5.9	8×10^{-4}	0.9	0.8	0.6
E53Q	NA	15×10^{-4}	NA	9.5	1.0

¹ expressed as μ mol of HCHO $\text{min}^{-1} \text{mg}^{-1}$ when L-Ser and THF were used as substrates.

² expressed as μ mol of NADH oxidized $\text{min}^{-1} \text{mg}^{-1}$ with L-*allo* Thr as substrate.

NA- Activity not detectable.

were 0.8 mM and 0.65 $\mu\text{mol mg}^{-1}$, respectively, and 9.5 mM and 1.1 $\mu\text{mol mg}^{-1}$, respectively, with E53Q bsSHMT. These observations are in general agreement with those of (Jala *et al.*, 2000) and (Szebenyi *et al.*, 2004) which suggested no change and a 4-fold increase in the activity L-*allo* Thr respectively. Interestingly THF-independent cleavage of L-Ser was also enhanced by nearly two fold (Table 2.1)

Crystal structure of E53Q bsSHMT internal aldimine

Crystals of E53Q bsSHMT were obtained by vapour diffusion hanging drop method as described in methods section and according to the procedure standardized earlier (Trivedi *et al.*, 2002) for bsSHMT. Though the overall structure of E53Q bsSHMT was similar to that of bsSHMT (rms deviation 0.10 Å), differences were seen only in the vicinity of the mutated residue. The side chain of Q53 in E53Q bsSHMT was in a different conformation compared to that of E53 in bsSHMT internal aldimine. This change in the conformation induces changes in the side chain conformation of two near-by Tyr's 60 and 61 (Fig 2.3). The plane of phenyl ring of Y60 in E53Q is almost perpendicular to that observed in bsSHMT. In comparison, the shift is less in case of Y61 (~18°). However, the orientation of PLP in E53Q bsSHMT (Fig 2.3) was identical to that of bsSHMT.

Crystal structure of E53Q bsSHMT in presence of L-*allo* Thr

Attempts were made to crystallize bsSHMT and E53Q bsSHMT in the presence of L-*allo* Thr. A procedure similar to that described earlier (Trivedi *et al.*, 2002) for obtaining binary complex was adopted. L-*allo* Thr (10 mM) was used in the crystallization condition. It can be seen from the Fig 2.4 that, though bsSHMT and E53Q bsSHMT were co-crystallized with L-*allo* Thr, only Gly bound to PLP was observed at the active site. This observation suggested that L-*allo* Thr was cleaved to Gly during crystallization (5-10 days). The increase in the activity with L-*allo* Thr (Table 2.1) is consistent with the observation of only Gly bound at the active site when E53Q bsSHMT was co-crystallized with L-*allo* Thr. The density for acetaldehyde formed in the cleavage was not seen in the crystal structure. However in E53Q bsSHMT-Gly(L-*allo* Thr) carboxylate of Gly is in two conformations (Fig 2.4a).

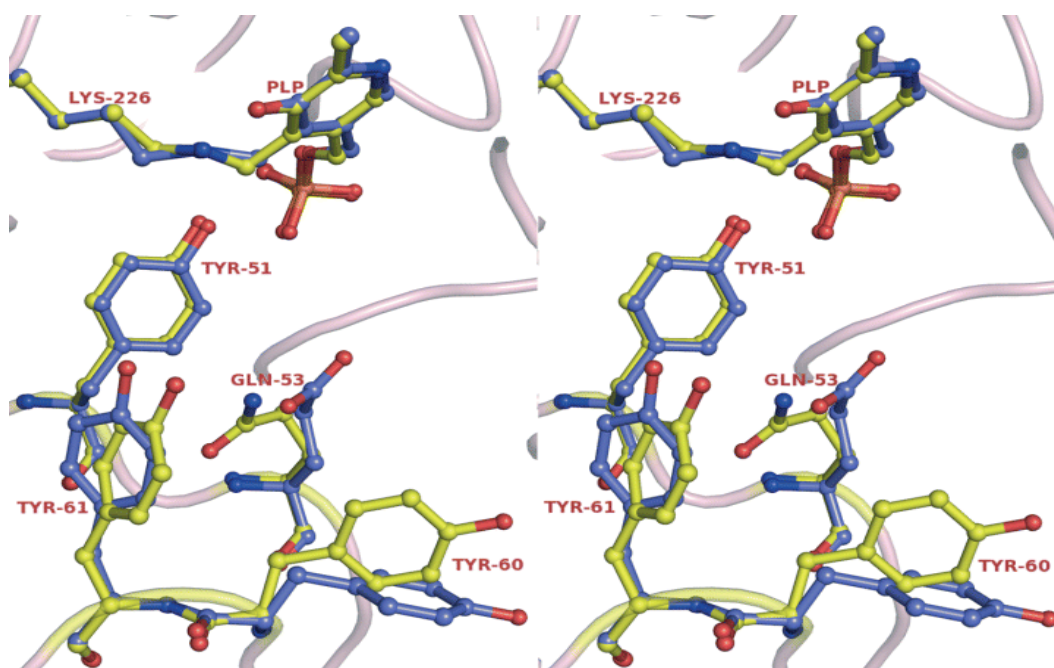


Fig 2.3: A stereo diagram of E53Q bsSHMT showing active site residues. Conformation of residues Y51, E53, Y60, Y61 and Schiff's base (PLP covalently linked to K226) in E53Q bsSHMT mutant (Yellow) with respect to bsSHMT (Blue). Y51 and the Schiff base are in the same orientation in E53Q bsSHMT and bsSHMT, whereas the orientations of E53, Y60 and Y61 have changed.

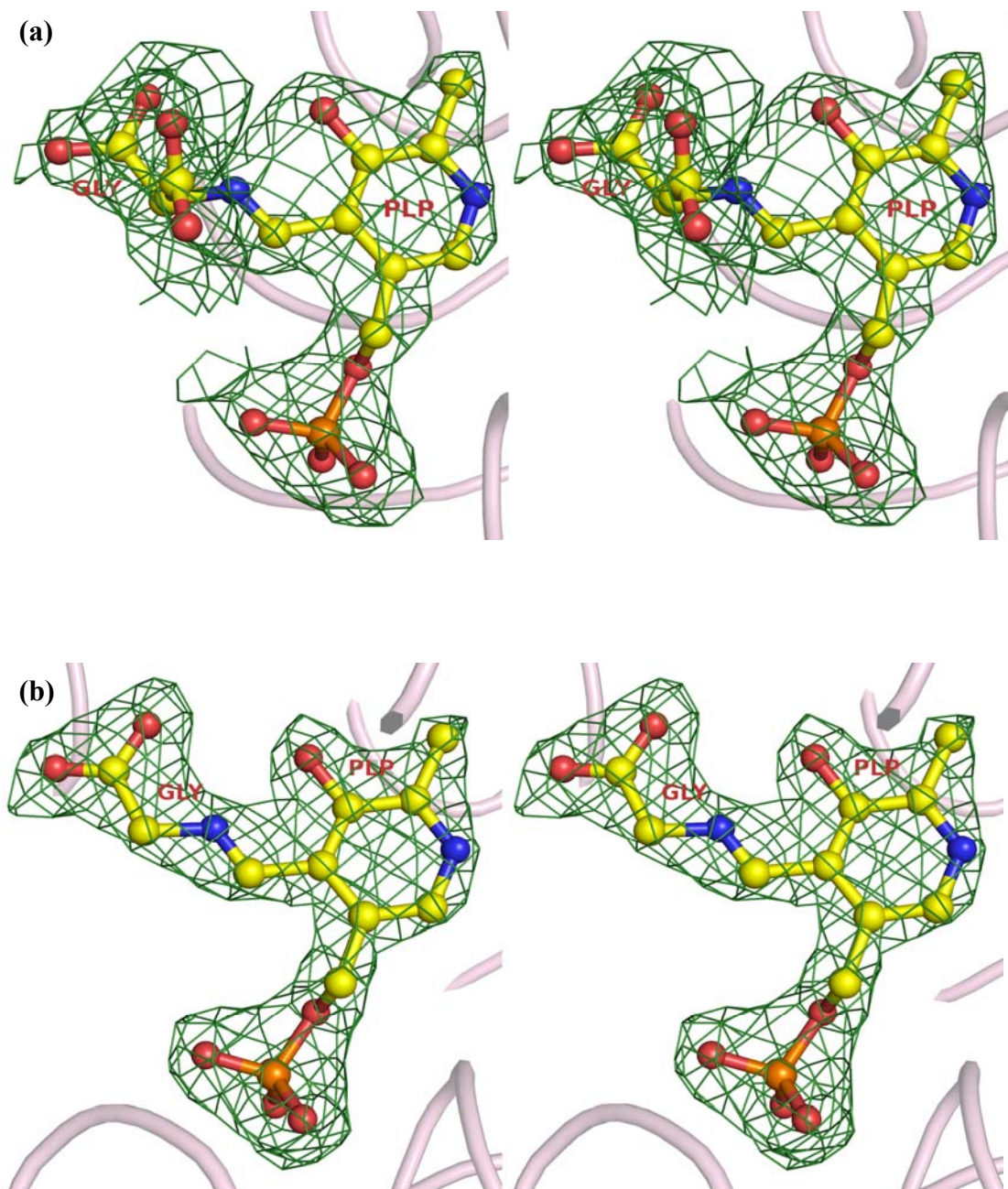


Fig 2.4: A stereo view of electron density maps showing Gly external aldimine in E53Q and bsSHMT.

(a) Stereo view of electron density showing Gly external aldimine of E53Q bsSHMT. The structure was obtained by adding *L-allo* Thr, suggesting Gly carboxylate is in two conformations.

(b) Stereo view of electron density showing Gly external aldimine of bsSHMT obtained by adding *L-allo* Thr. Gly is seen in only one conformation.

Cleavage of L-*allo* Thr to Gly and acetaldehyde requires several proton transfers. L-*allo* Thr was modeled into the active site of bsSHMT-Ser complex after removing L-Ser. An examination of this model reveals that in addition to E53, NE2 atom of H122 is in close proximity (2.82 Å) from OH group of L-*allo* Thr. On the basis of modeled structure, it could be suggested that H122 could also be a residue involved in one of the proton abstraction steps in the reaction with L-*allo* Thr. However, it has been reported that *erythro* and *threo* forms of L-Thr are poor substrates compared to L-*allo* Thr (Scarsdale *et al.*, 1999). The model building studies show that -OH group of erythro is not properly positioned for proton abstraction by H122. It is likely that Y61, which undergoes large movements when the enzyme forms complexes with ligands, is involved in proton abstraction from the L-*allo* Thr and/or the protonation of Gly quinonoid intermediate to the external aldimine.

Studies on E53Q bsSHMT binary and ternary complexes

Spectral studies in presence of L-Ser or L-Ser and THF/FTHF

In bsSHMT, THF markedly enhances the amount of distribution of the internal aldimine, gem-diamine, external aldimine and quinonoid intermediates in equilibrium (Jala, 2002). This property provides a convenient handle to distinguish between the reactions of the enzyme with L-Ser and Gly as well as mutant and wild-type enzyme. E53Q bsSHMT exhibited the characteristic absorbance maximum at 425 nm indicating the presence of an internal aldimine.

Addition of L-Ser showed a small decrease of absorption at 425 nm, probably suggesting the formation of an external aldimine (Fig 2.5a). Further addition of THF or FTHF to E53Q bsSHMT-Ser binary complex showed a small increase in the absorption at 495 nm and 500 nm, respectively, indicating formation of quinonoid intermediate to same extent as bsSHMT (Fig 2.5a). It is interesting to recall that with bsSHMT, a quinonoid intermediate was not observed when folate derivatives were added to L-Ser external aldimine (Fig 2.5b). The small amount of THF-independent reaction with L-Ser that generates Gly and its subsequent reaction is probably responsible for the quinonoid intermediate observed in the mutant enzyme (Table 2.1).

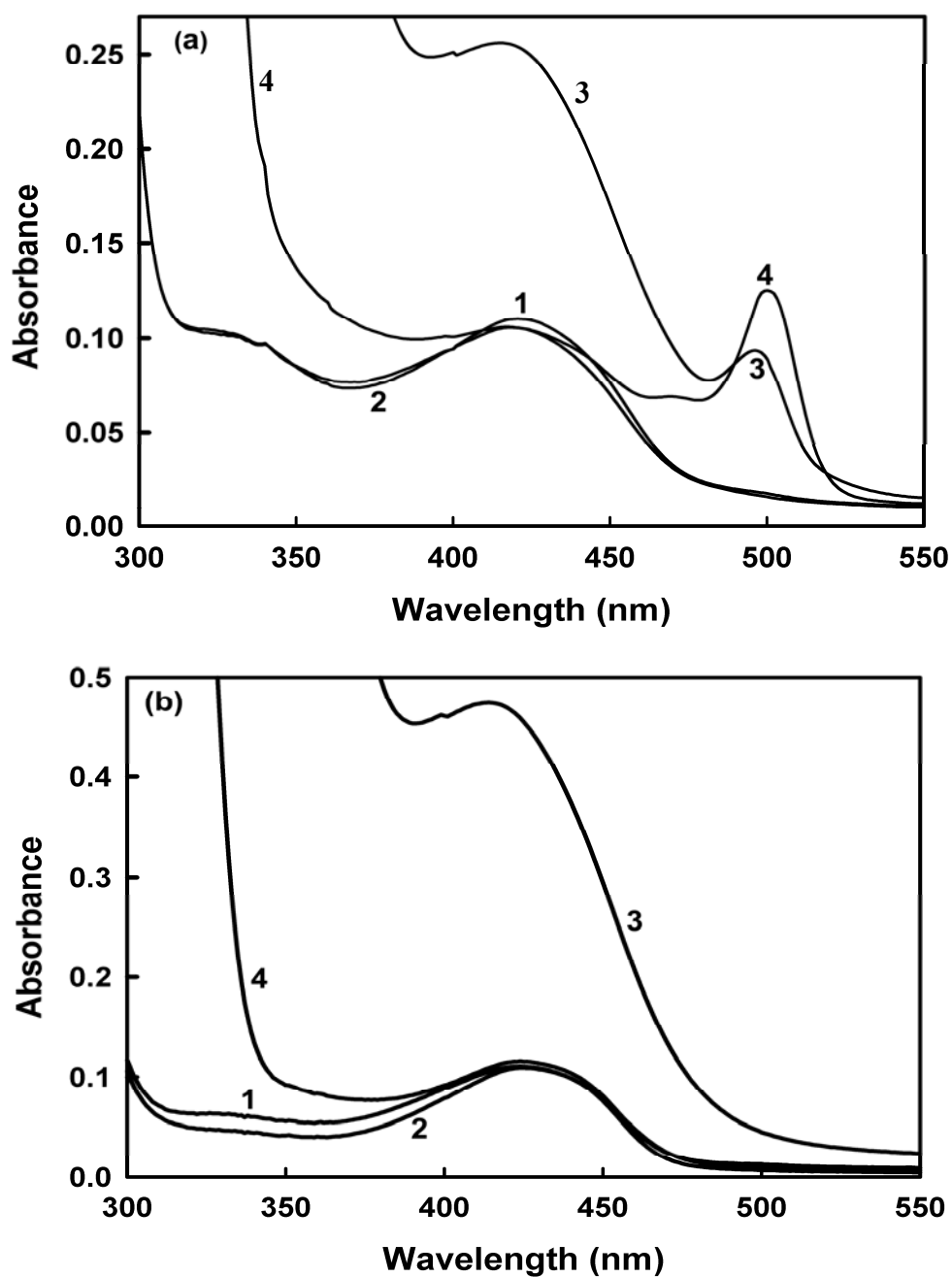


Fig 2.5: Absorbance changes on the addition of L-Ser, L-Ser + THF/FTHF to bsSHMT and E53Q bsSHMT.

(a) Curve 1: E53Q bsSHMT (1mg ml^{-1}). Curve 2: in presence of L-Ser (50 mM). Curve 3: E53Q bsSHMT + L-Ser and THF (1.8mM). Curve 4: E53Q bsSHMT + L-Ser and FT HF ($100\ \mu\text{M}$).

(b) Curve 1: bsSHMT (1mg ml^{-1}). Curve 2: in presence of L-Ser (50 mM). Curve 3: bsSHMT + L-Ser and THF (1.8mM). Curve 4: bsSHMT + L-Ser and FT HF ($100\ \mu\text{M}$). All the spectral studies were carried out in 50 mM potassium phosphate buffer, pH 7.4, containing 1 mM EDTA, 1 mM 2-ME.

Formation of the quinonoid intermediate in E53Q bsSHMT-L-Ser (Fig 2.5a) requires an incubation of 10 min. This observation was supported when THF-independent cleavage of L-Ser was carried out with bsSHMT and E53Q bsSHMT. The standard radioactive assay using L-[3-¹⁴C] Ser was carried out in the absence of THF and varying concentrations of E53Q bsSHMT from 0.01 to 1 mg was used for the assay (Table 2.1). The THF-independent cleavage of L-Ser could be measured only with higher concentrations of E53Q bsSHMT (1 mg or above) and bsSHMT did not show any cleavage of L-Ser in the absence of THF (Table 2.1).

Interestingly all spectral studies are carried out at 1 mg ml⁻¹ concentration. Hence, it is possible that the formation of quinonoid intermediate could be due to THF-independent cleavage of L-Ser to Gly at higher enzyme concentration used in crystallography experiments. However, it is important to note that THF-dependent cleavage of L-Ser is 10⁶ fold higher when compared THF-independent cleavage of L-Ser (Table 2.1), highlighting the importance of THF in SHMT catalysis. Presence of THF enhances the rate of formation of quinonoid intermediate and shifts the equilibrium towards the formation of quinonoid intermediate and thereby enhancing the rate of C_α-C_β bond cleavage (Scheme 2.2).

Visible CD changes in bsSHMT or E53Q bsSHMT in presence of L-Ser and Gly

As the internal and external aldimine of SHMTs have similar visible absorbance spectra (Fig 2.5), CD studies were carried out to examine the formation of external aldimine. Visible CD spectrum of bsSHMT and E53Q bsSHMT was recorded in the range of 300-550 nm as described in methods section. Addition of L-Ser (50 mM) to bsSHMT causes a significant decrease in its molar ellipticity at 425 nm (Fig 2.6 a). On the other hand, addition of L-Ser to E53Q bsSHMT causes only a small change (Fig 2.6 b), suggesting that this external aldimine is spectrally different from that of the bsSHMT-Ser complex. The visible CD spectrum of the bsSHMT-Gly (50 mM) showed a minor decrease compared to the decrease seen on addition of L-Ser to bsSHMT (Fig 2.7 a). However, the E53Q bsSHMT-Gly did not show a significant decrease in molar ellipticity on addition of Gly (Fig 2.7 b).

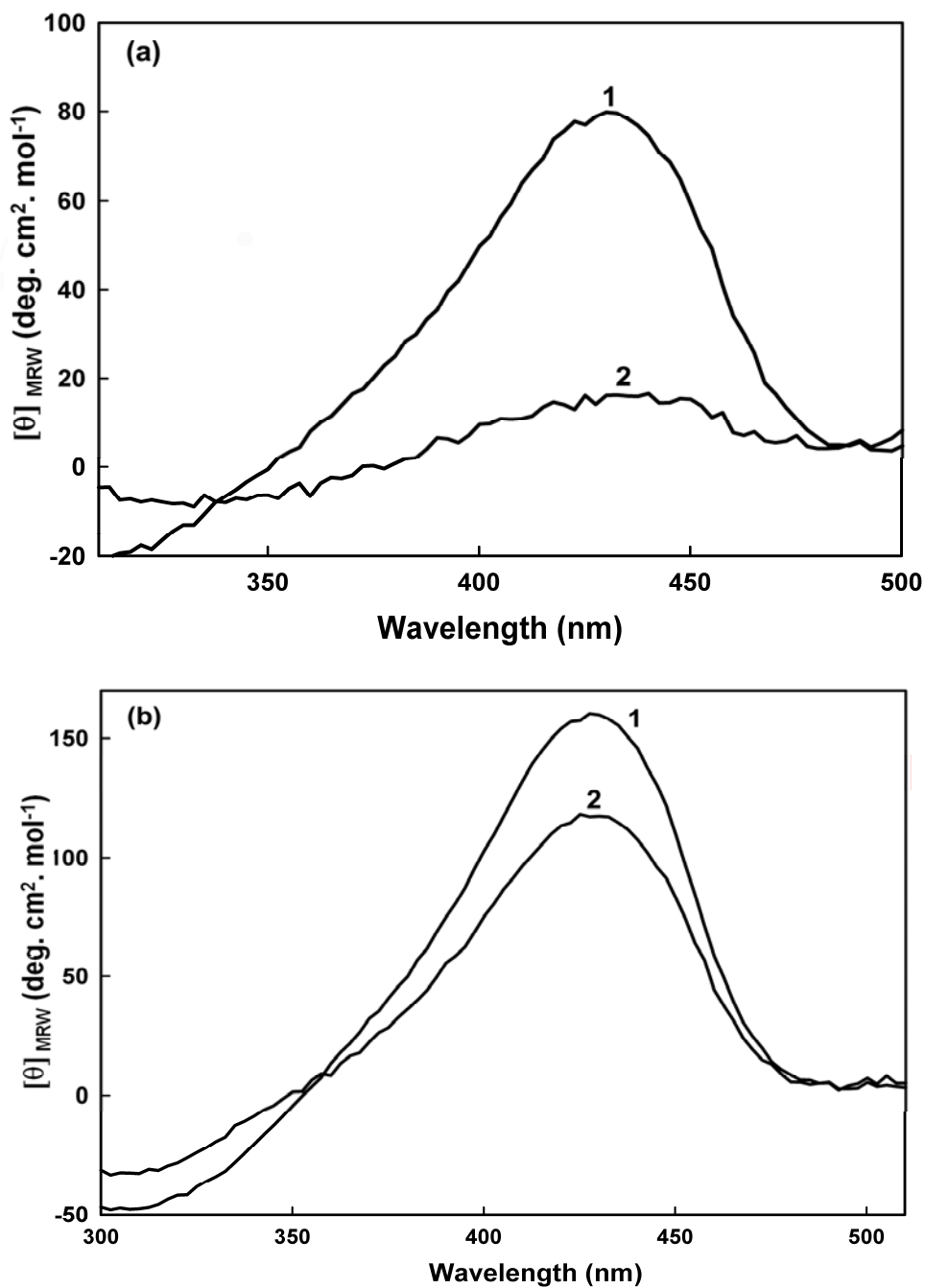


Fig 2.6: The visible CD spectrum of bsSHMT and E53Q bsSHMT with L-Ser.
(a) Curve 1: The spectrum of bsSHMT (1 mg ml^{-1}) recorded in the range of 300-550 nm. Curve 2: in presence of L-Ser (50 mM) to bsSHMT.
(b) Curve 1: The spectrum of E53Q bsSHMT (1 mg ml^{-1}) recorded in the range of 300-550 nm. Curve 2: in presence of L-Ser (50 mM) to E53Q bsSHMT.

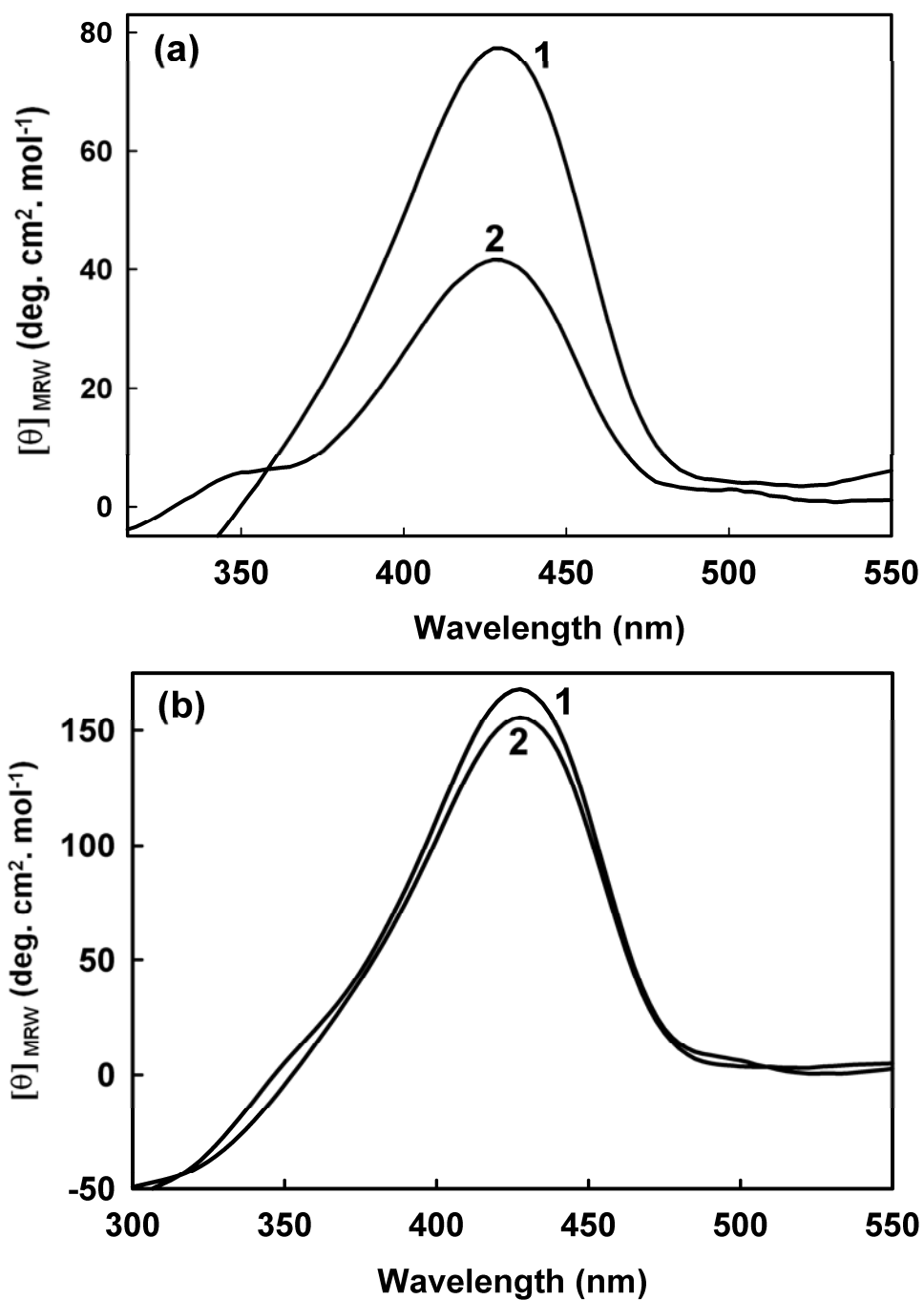


Fig 2.7: The visible CD spectra of bsSHMT and E53Q bsSHMT with Gly.
(a) Curve 1: The spectrum of bsSHMT (1 mg ml^{-1}) recorded in the range of 300 - 550 nm. Curve 2: in presence of Gly (50 mM) to bsSHMT.
(b) Curve 1: The spectrum of E53Q bsSHMT (1 mg ml^{-1}) recorded in the range of 300-550 nm. Curve 2: in presence of Gly (50 mM) to E53Q bsSHMT.

Thermal denaturation of E53Q bsSHMT in the presence and absence of L-Ser/Gly

It has been suggested that the binding of L-Ser to SHMT in the open form leads to its conversion to the closed form facilitates the THF-enhanced reaction with L-Ser (Picot *et al.*, 1991). The apparent T_m values for bsSHMT and E53Q bsSHMT were determined as described in methods section, by measuring absorbance at 287 nm in 50 mM potassium phosphate buffer, pH 7.4, containing 1 mM EDTA, 1 mM 2-ME upon heating the sample from 30-90°C. As in other SHMTs, the addition of L-Ser (100 mM) enhances the thermal stability of the bsSHMT from 65 to 80°C. Gly (100 mM), on the other hand, is unable to cause this change (Table 2.2). Addition of L-Ser to E53Q bsSHMT does not cause the expected enhancement of thermal stability.

Crystal structure of E53Q bsSHMT in presence of L-Ser

Crystals of E53Q bsSHMT-Ser/Gly binary complex were obtained as described in methods section,. The structure of E53Q bsSHMT in complex with L-Ser (E53Q bsSHMT-Ser) shows that, the side chain conformations of Q53 in the mutant and E53 in bsSHMT-Ser complexes are similar except for OE1 and NE2 atoms. No significant changes in the conformation of residues Y60, Y61 and PLP orientation are observed in the mutant in comparison with bsSHMT-Ser. However, the side chain hydroxyl of bound L-Ser is in two positions (Fig 2.8a). The first position is identical to that of bsSHMT-Ser complex. In the second position, Ser-OG has a weak hydrogen bonding interaction with OG of S172 (3.59 Å) and a water molecule (3.46 Å). Apart from these changes near the active site, a small movement of the main chain is also observed in some solvent exposed regions such as 83–87 (0.2–0.4 Å) and 237–242 (0.4 –0.7 Å) (not shown in the figure).

Crystal structure of E53Q bsSHMT in presence of Gly

Crystals of E53Q bsSHMT-Gly binary complex were obtained as described in methods section. The most significant difference in the structure is observed in the case of the bound Gly. The carboxylate group of Gly is in two distinct conformations in E53Q bsSHMT-Gly. In one conformation, the carboxylate group forms hydrogen bonds with R357, as in bsSHMT-Gly (Trivedi *et al.*, 2002). In the second

conformation, the carboxylate forms hydrogen bonds with NE2 of Q53 (3.34 Å) and NE2 of H122 (3.32 Å). When the carboxylate is in the conformation found more predominantly i.e., towards R357, a water molecule with an occupancy of 0.6 is present close to the position corresponding to the second conformation of the carboxylate group (Fig. 2.8 b). The hydrogen bonding between Q53 and the second conformation of carboxylate of Gly found in E53Q bsSHMT-Gly is less likely to occur in the wild type enzyme. The water molecule with partial occupancy is stabilized by its interaction with OG of S172 (3.2 Å) and another water molecule (2.76 Å).

Table 2.2: The apparent T_m (°C) values for bsSHMT and E53Q bsSHMT in the presence and absence of L-Ser and Gly.

Enzyme	Apparent T_m (°C)		
	No ligand	L-Ser (100 mM)	Gly (100 mM)
bsSHMT	65 ± 1	80 ± 1	65 ± 1
E53Q	72 ± 1	71 ± 1	71 ± 1

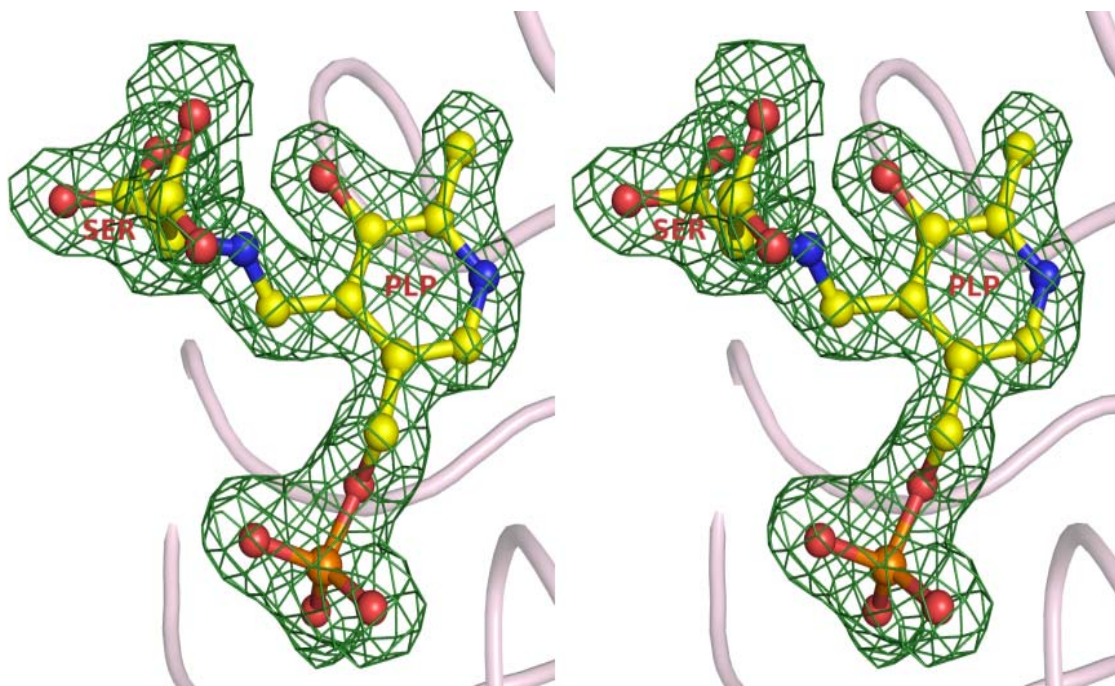


Fig 2.8 (a): A stereo diagram illustrating electron density corresponding to PLP and L-Ser in E53Q bsSHMT-Ser. The two conformations of side chain of L-Ser are shown.

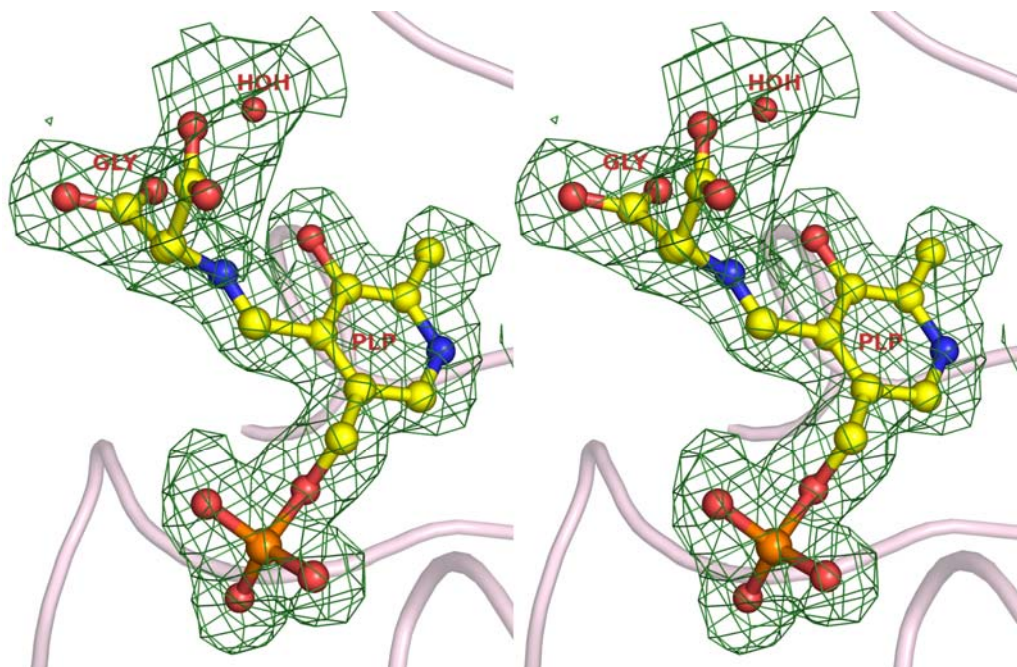


Fig 2.8 (b): A stereo diagram illustrating electron density corresponding to PLP and Gly in E53Q-Gly complex. Carboxylate of Gly shows two conformations as seen in E53Q-Gly(L-*allo* Thr). A water molecule is present close to the second conformation of carboxylate.

Spectral studies in presence of Gly or Gly and THF/FTHF

Reaction intermediates formed can be monitored spectrally on addition of Gly, Gly-THF/FTHF to bsSHMT. It was of interest to study identifying the step at which reaction has been arrested due to the mutation. Both bsSHMT and E53Q bsSHMT showed an absorbance maximum at 425 nm in the range of 300-550 nm. Addition of Gly (50 mM) resulted in a small decrease in the absorption at 425 nm and a corresponding increase at 495 nm, indicating the presence of a small amount (10%) of quinonoid intermediate. Similar spectral changes were observed in the case of E53Q bsSHMT on addition of Gly. Further addition of THF or FTHF to bsSHMT/E53Q bsSHMT-Gly complex showed an increase in the absorbance significantly at 495 nm and 500 nm, respectively (Fig 2.9), depicting the conversion of a significant fraction of the enzyme to the quinonoid form.

The structure of the ternary complex of bsSHMT with Gly and FTHF showed that the glutamate residue is involved in the interaction of the formyl oxygen of -CHO and N10 of pyridine ring (Fig 2.1 b). It could be hypothesized that the absence of these interactions might make the ternary complex less stable. It was, therefore, of interest to examine the stability of quinonoid intermediate. Both bsSHMT and E53Q bsSHMT ternary complexes formed upon addition of FTHF (100 μM) to 1 mg ml⁻¹ of bsSHMT or E53Q bsSHMT in 50 mM potassium phosphate buffer, pH 7.4, containing 1 mM EDTA, 1 mM 2-ME and incubated for 10 min. These mixtures were dialyzed against 50 mM potassium phosphate buffer, pH 7.4, containing 1 mM EDTA, 1 mM 2-ME (50 mM potassium phosphate pH 7.4 containing 1 mM EDTA and 1 mM 2-ME) but devoid of Gly and FTHF. At intervals of 1 h the contents of the dialysis bags were removed and spectra recorded. Significant decrease in the amount the ternary complex of was observed as mentioned by the decrease in the quinonoid intermediate peak at 500 nm during this period (1, 2, 3 and 4h), with concomitant appearance of a peak at 425 nm (Fig 2.10). At the end of 4 h of dialysis the quinonoid intermediate peak had almost disappeared, suggesting that FTHF had dissociated from the complex and distribution of the intermediates was altered in the case of the E53Q bsSHMT-Gly-FTHF ternary complex. However, a similarly treated bsSHMT-Gly-FTHF complex did not show any change even after dialyzing for 4 h (Table 2.3).

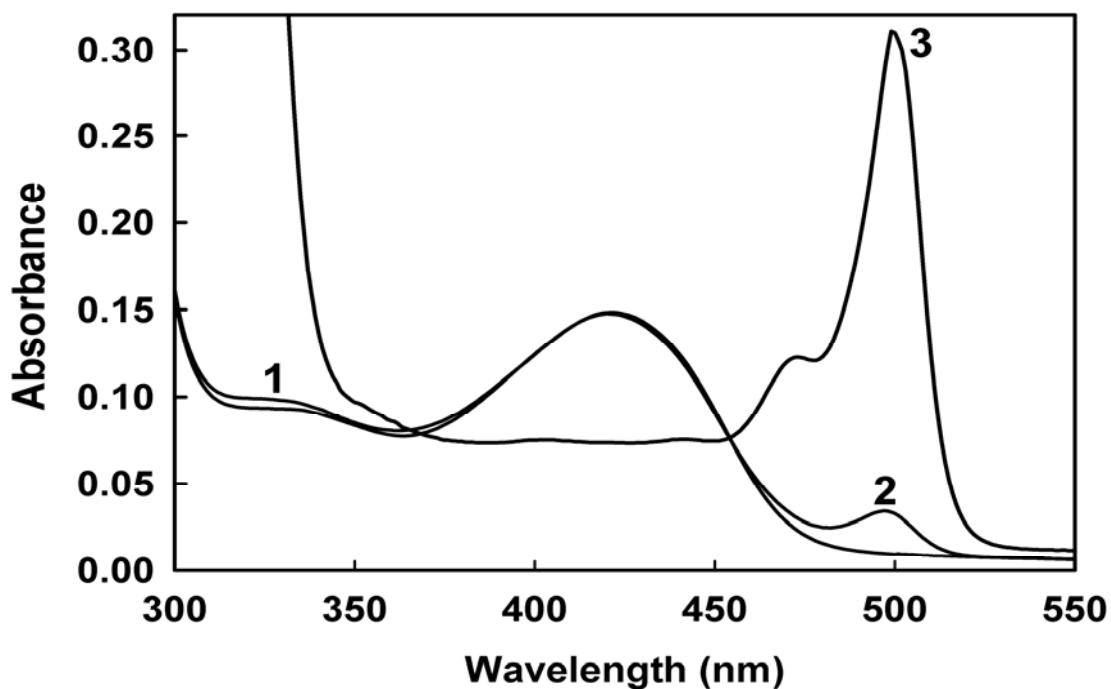


Fig 2.9: The absorbance changes on the addition of Gly, Gly + THF/FTTH to bsSHMT or E53Q bsSHMT.
 Curve 1: bsSHMT or E53Q bsSHMT (1 mg ml^{-1}) in 50 mM potassium phosphate buffer, pH 7.4, containing 1 mM EDTA, 1 mM 2-ME.
 Curve 2: in presence of 50 mM Gly.
 Curve 3: Addition of THF (1.8 mM) or FTTH (100 μM) to bsSHMT or E53Q binary complexes.

Table 2.3: The time course for the disappearance of quinonoid intermediate.

The changes were measured at 500 nm for quinonoid intermediate and appearance of external aldimine at 435 nm on addition of FTHF to the binary complex of bsSHMT and E53Q bsSHMT.

Time (h)	Enzyme			
	bsSHMT		E53Q	
	Absorbance value at 500 nm	425 nm	Absorbance value at 500 nm	425 nm
0	0.35	0.03	0.22	0.04
1	0.34	0.03	0.13	0.06
2	0.34	0.03	0.09	0.07
3	0.34	0.03	0.03	0.08

The time course of the loss of absorbance at 500 nm of the ternary complex of bsSHMT and E53Q bsSHMT were determined by using 1 mg ml⁻¹ of the both wild-type and mutant enzyme binary complex with Gly (50 mM) in 50 mM potassium phosphate buffer, pH 7.4, containing 1 mM EDTA, 1 mM 2-ME. The spectral changes were recorded on addition of FTHF (500 μM) and maximum absorbance was observed at 500 nm. This complex was dialyzed against 50 mM potassium phosphate buffer, pH 7.4, containing 1 mM EDTA, 1 mM 2-ME and spectra were recorded for observing absorbance maxima (500 nm) at different time interval (1, 2, 3 and 4 h). The data obtained are summarized in Table 2.3. The time course of loss of absorbance at 500 nm of the ternary complex of the mutant enzyme is in agreement with the observations recorded in Fig 2.10.

The dissociation constant (k_d) of FTHF for E53Q bsSHMT-Gly was determined from double reciprocal plots of the change in the absorbance at A₅₀₀ nm versus FTHF concentration at different fixed concentrations of Gly. A replot of the Y intercept versus concentration of Gly gave the k_d values for FTHF. A similar experimental approach was used to determine the k_d for folate derivatives in the case of rcSHMT (Schirch and Ropp, 1967). The k_d value for E53Q bsSHMT-Gly was 25 μM compared to 10 μM for bsSHMT-Gly.

PLP content of the dialyzed samples of bsSHMT and E53Q bsSHMT were measured after 4 h. (Fig 2.11). Spectrum of bsSHMT/E53Q bsSHMT (1 mg ml⁻¹) in 50 mM potassium phosphate buffer, pH 7.4, containing 1 mM EDTA, 1 mM 2-ME was recorded in the range of 300 -550 nm. Addition of 0.1N NaOH results in formation of a new peak at 388 nm which corresponds to λ_{max} of free PLP in both the cases. The amount of PLP was calculated was 1 mol per mol of subunit for both bsSHMT and E53Q bsSHMT (Fig 2.11).

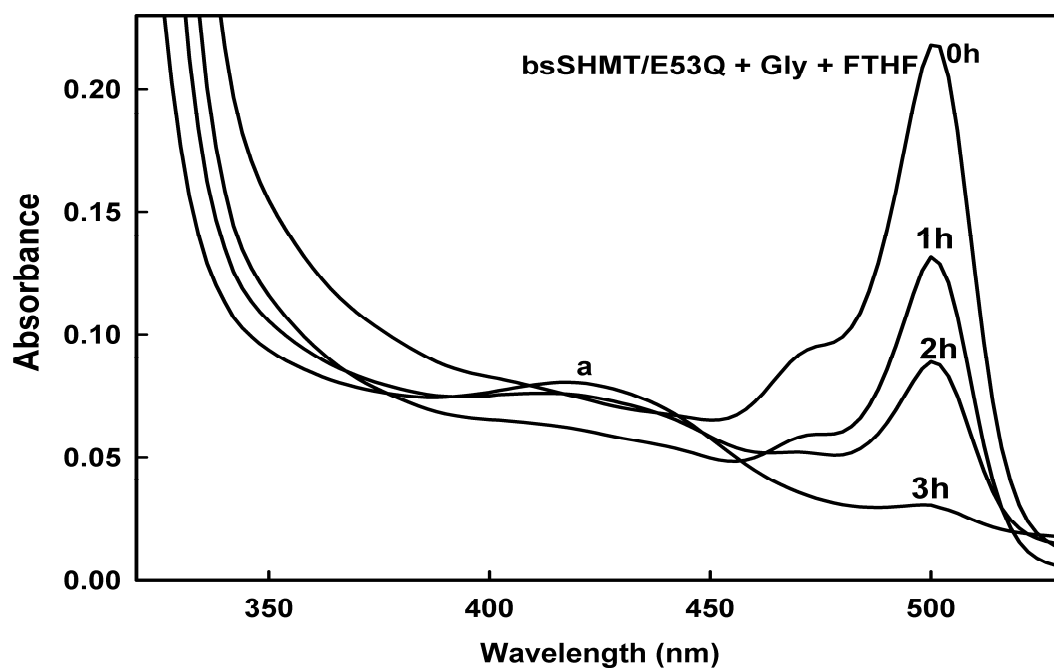


Fig 2.10: The time course of disappearance of quinonoid intermediate in E53Q bsSHMT and bsSHMT ternary complexes.

Curve 0h: The spectrum of bsSHMT-Gly-FTHF (1 mg ml^{-1} bsSHMT, 50 mM Gly, $500 \text{ }\mu\text{M}$ FTHF) and E53Q bsSHMT-Gly (FTHF) had absorbance maximum at 500 nm . Spectra were recorded after 1, 2 and 3 h of dialysis, respectively.

Curve 0h: bsSHMT quinonoid intermediate generated at 500 nm was unchanged after dialysis for 3 h. E53Q bsSHMT-Gly (FTHF) showed a significant decrease was observed in the quinonoid intermediate peak (500 nm) with concomitant appearance of a peak at 425 nm (curve a).

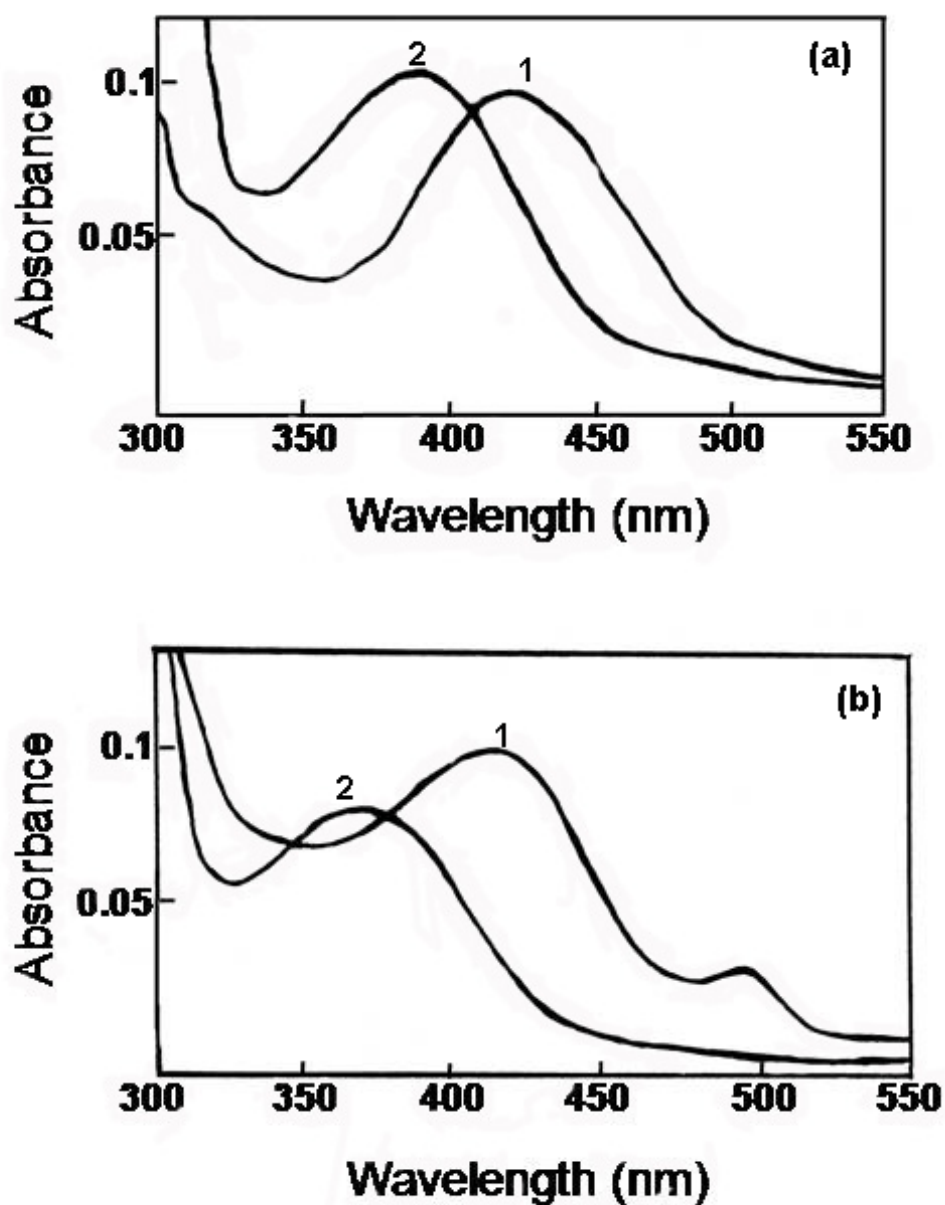


Fig 2.11: PLP content of bsSHMT and E53Q bsSHMT ternary complexes after dialysis.

(a) bsSHMT (1 mg ml^{-1}) in 50 mM potassium phosphate buffer, pH 7.4, containing 1 mM EDTA, 1 mM 2-ME (curve 1); on addition of 0.1N NaOH (curve 2).

(b) E53Q bsSHMT-Gly-FTHF (1 mg ml^{-1}) dialyzed against the buffer not containing Gly (curve 1); on addition of 0.1 N NaOH (curve 2).

Stopped flow studies

Rate of formation of quinonoid intermediate

The pre-steadystate kinetics of the formation of the quinonoid complex for bsSHMT and E53Q bsSHMT with Gly or Gly and THF/FTHF were monitored using stopped-flow spectrophotometer as described in methods section. The change in the amplitude for bsSHMT in 50 s was 0.002 and the rate constant was 0.08 s^{-1} . Addition of THF to bsSHMT-Gly binary complex enhanced both the amplitude (0.15 AU) and the rate constant to 340 s^{-1} (scanned for 50 ms) respectively. In the case of E53Q bsSHMT change in the amplitude on addition of Gly was 0.03 and the rate constant was 9.0 s^{-1} . On addition of THF both the amplitude and the rate constant were decreased to 0.01 and 2.2 s^{-1} , respectively. One possible reason for the decrease in rate could be that the absorbance changes measured at equilibrium, when as the kinetic data determine the turnover of an enzyme catalyzed reaction. The situation where FTHF is added to binary complex of the E53Q bsSHMT or the bsSHMT is very similar to that described above (Table 2.4).

Table 2.4: The rate constants for formation of quinonoid intermediate on addition of Gly, Gly + THF/FTHF to bsSHMT or E53Q bsSHMT.

Enzyme	Gly (495 nm)		Gly + THF (495 nm)		Gly + FTHF (500 nm)	
	ΔA	Rate (s^{-1})	ΔA	Rate (s^{-1})	ΔA	Rate (s^{-1})
bsSHMT	0.002	$8 \pm 0.1 \times 10^{-2}$	0.15	340 ± 8	0.76	$8 \pm 0.05 \times 10^{-2}$
E53Q	0.030	9.0 ± 0.2	0.01	2.2 ± 0.2	0.38	$9 \pm 0.05 \times 10^{-2}$

It is pertinent to mention that FTHF is a slow tight binding inhibitor (Stover and Schirch, 1991) and it is not surprising that the rate is slower than that for THF which is the substrate for the enzyme in the forward reaction (L-Ser +THF), enhances quinonoid formation with Gly in the reverse reaction.

Crystal structure of E53Q bsSHMT in presence of Gly and FTHF

Attempts to crystallize E53Q bsSHMT in the presence of Gly and FTHF yielded orthorhombic crystals with E53Q bsSHMT-Gly instead of E53Q bsSHMT-Gly-FTHF ternary complex and the density for FTHF could not be traced in the crystal structure. PLP in this complex was trapped in a gem-diamine form covalently bonded to both the active site Lys and the substrate, Gly amino group (Fig 2.12). Gem-diamine is an intermediate formed in the inter-conversion of the enzyme between internal and external aldimine forms (Scheme 2.1) (Dunathan, 1966). The orientation of PLP in E53Q bsSHMT-Gly(FTHF) complex is closer to that of bsSHMT-Gly-FTHF complex (Fig 2.14) than its orientation in the internal or external aldimine structures of mutant or wild-type enzymes (Trivedi *et al.*, 2002). This is consistent with the earlier observation that the orientation of PLP in the ternary complex of mcSHMT is similar to the PLP in the gem-diamine form (Szebenyi *et al.*, 2000).

However, the present structure does not contain density for FTHF. The similarity in the orientation of PLP to that of the wild-type ternary complex and absence of FTHF in the crystal structure suggests that there is an initial binding of FTHF leading to an alteration in the orientation of PLP and subsequently, FTHF falls off from the active site (Fig 2.10) and the enzyme complex is locked in this conformation. The differences between the structures of this complex and Gly external aldimine (Fig 2.13) suggest that the changes induced by initial binding of FTHF are retained, even though FTHF is absent in the final structure (Fig 2.13).

Another interesting observation in the structure of E53QbsSHMT-Gly(FTHF) is that the phosphate group of PLP is in two conformations (Fig 2.12). The interactions in the first conformation are similar to those described for the bsSHMT-Gly-FTHF (Fig 2.14). The second conformation is stabilized mainly by hydrogen bonding to atoms from the symmetry related subunit. One of the phosphate oxygen atoms in this conformation is held by hydrogen bonding interaction with the phenolate oxygen of Y51, N of G257 and NE2 of Q53 of the symmetry related subunit.

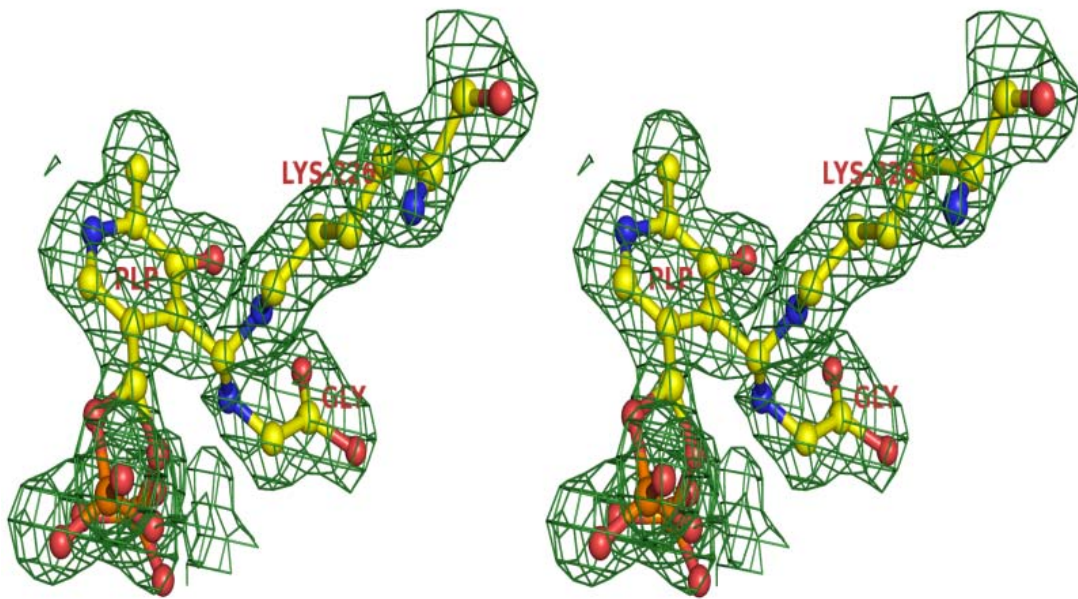


Fig 2.12: A stereo diagram illustrating electron density corresponding to the gem-diamine formed in E53Q bsSHMT in the presence of Gly and FTHF. Phosphate group of PLP is in two conformations

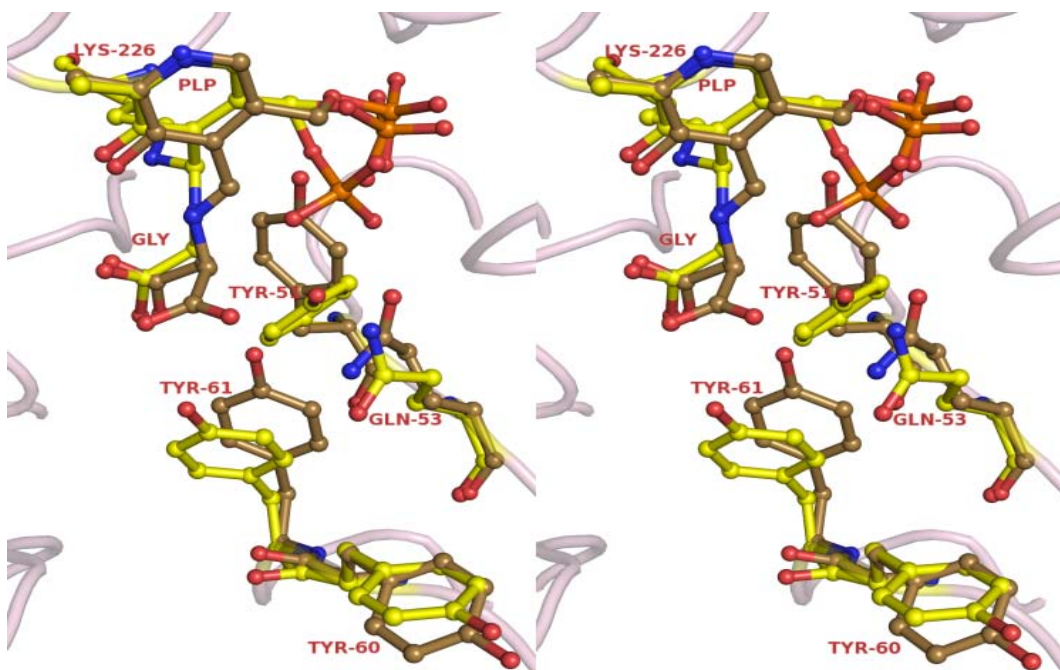


Fig. 2.13: A superposition of residues Y51, E53, Y60 and PLP in E53Q bsSHMT-Gly(FTHF) (yellow) and E53Q bsSHMT-Gly (brown).

Another oxygen atom is held by hydrogen bonding to NE2 of H122 and phenolate oxygen of Y51 of the symmetry related subunit. The third oxygen is hydrogen bonded to a water molecule and NE2 of H122. The new position of the phosphate group induces a displacement in position of Y51. As Y51 moves to the position occupied earlier by Y61, a corresponding movement is also found in Y61 (Fig 2.14). In all other complexes of E53Q bsSHMT, OH of Y51 interacts with OP2 of PLP (Fig 2.10, 2.13, 2.13).

As the orientation of Y51 is different in this complex, a water molecule compensates for this interaction. There are also small main chain movements in the regions 83–87, 237–244, 255–258 and 385–394. Most of these regions are solvent exposed and are not directly related to the active site or site of mutation. The overall structure (other than the changes described above) of E53QbsSHMT-Gly(FTHF) overlaps better with bsSHMT-Gly (rmsd = 0.15 Å) than with the A or B subunits of bsSHMT-Gly-FTHF with which it has rmsd of 0.41 and 0.44 Å, respectively.

Although the density for FTHF is not seen in E53Q bsSHMT-Gly(FTHF), the orientation of PLP (gem-diamine) in this complex is very similar to that of wild-type ternary complex (Fig 2.12, 2.14). Visible circular dichroic (CD) spectra of bsSHMT/E53Q bsSHMT (1 mg ml⁻¹) + Gly (50 mM) + FTHF (500 μM) were recorded in the range of 300–550 nm. The visible CD spectrum of E53Q bsSHMT in the presence of Gly and FTHF showed a band at 343 nm, suggesting the presence of the gem-diamine form of E53Q bsSHMT (Fig 2.15). The crystal structure of E53Q-Gly (FTHF) also showed that PLP is indeed in the gem-diamine form and the FTHF is not bound.

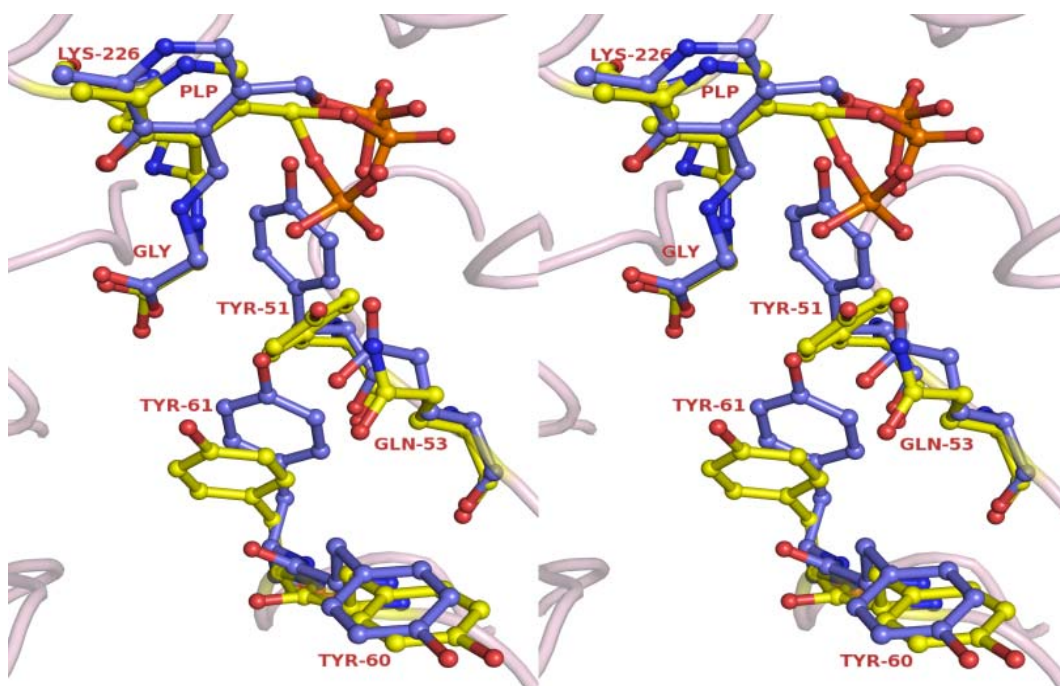


Fig 2.14: A superposition of residues Y51, E53, Y60 and PLP in E53Q bsSHMT-Gly(FTHF)(yellow) and bsSHMT-Gly-FTHF(blue).

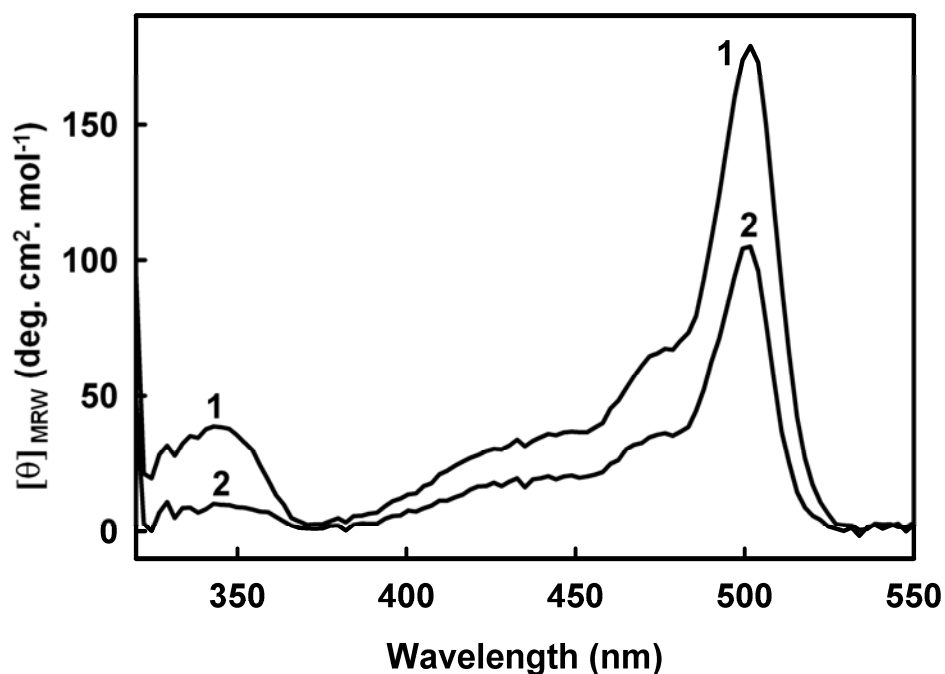


Fig 2.15: Visible CD spectra of bsSHMT-Gly-FTHF and E53Q bsSHMT-Gly(FTHF).

Curve 1: The CD spectrum of the ternary complex of the E53QbsSHMT (1 mg ml⁻¹ enzyme, 50 mM Gly, 500 μM FTHF). Curve 2: ternary complex of bsSHMT.

Enzyme memory in E53Q bsSHMT ternary complex

These results shown in the Fig 2.12, 2.14 on E53Q bsSHMT-Gly(FTHF) complex are reminiscent of the phenomenon called “enzyme memory”. It has been performed that some enzymes retain the conformation of the final E + P (Enzyme + Product) complex for a period of time even after the product has dissociated from the enzyme. This new enzyme conformation is different from the resting enzyme forms. Interaction of the substrate with this new conformation can set up a different kinetic path way of the reaction, with some similarity with the original kinetic path way (Jagannatha Rao, 1982).

The kinetic methods of analysis have been suggested for examining this phenomenon. The E53Q bsSHMT was treated with Gly-FTHF and dialyzed as described above (Fig 2.10) and the kinetic analysis was carried out with dialyzed enzyme with the re-addition of Gly-FTHF. bsSHMT (1 mg ml⁻¹) was incubated with 10 mM Gly and varying concentrations of FTHF (0 - 400 μM), for 1 min and absorbance at 500 nm was measured. The reciprocal of A₅₀₀ was plotted against the reciprocal of FTHF concentration. bsSHMT (10 mg) was incubated with 10 mM Gly and 500 μM FTHF for 5 min and then dialyzed against 50 mM potassium phosphate buffer, pH 7.4, containing 1 mM EDTA, 1 mM 2-ME to remove Gly and FTHF. Such an enzyme (1 mg ml⁻¹) was once again incubated with Gly (10 mM) and different concentrations of FTHF as in and the absorbance was measured at 500 nm as described in previous experiment. The double reciprocal plot (1 / A₅₀₀ versus 1 / [FTHF]) for the dialyzed enzyme is shown in Fig 2.16. A similar procedure was used for E53Q bsSHMT also. As shown in Fig 2.16 a, the double reciprocal plot for the formation of quinonoid intermediate as a function of FTHF concentration is different for E53Q bsSHMT. The mutant enzyme was treated with Gly-FTHF and dialyzed as described above and the kinetic analysis was carried out with dialyzed enzyme with the re-addition of Gly-FTHF. The two forms of enzymes bind to FTHF with different slopes (before dialysis 104 ± 10; after dialysis 234 ± 15). In contrast, for bsSHMT, the slopes were similar before (21 ± 2) and after dialysis (33 ± 3). If the lines were parallel then it would suggest that E53Q bsSHMT has no enzyme memory and that the two forms before and after dialysis were kinetically similar.

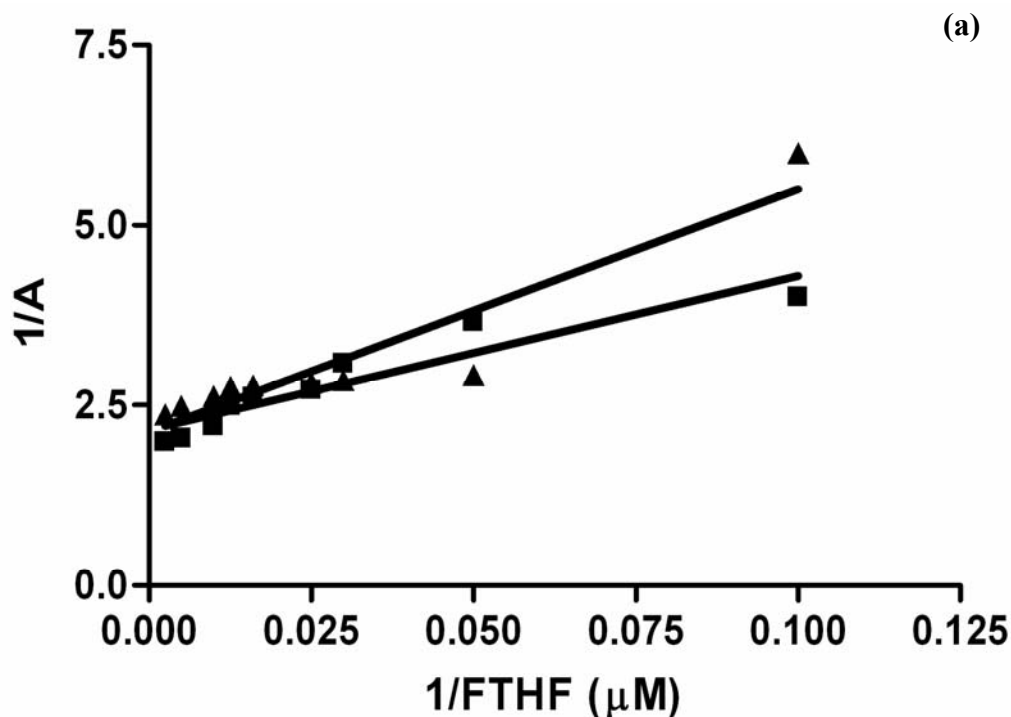


Fig 2.16 (a): Double reciprocal plots for the formation of quinonoid intermediate before and after dialysis of bsSHMT-Gly-FTHF and E53Q bsSHMT-Gly(FTHF).

(a) The reciprocal of A_{500} was plotted against the reciprocal of FTHF concentration (■). bsSHMT (1 mg ml^{-1}) was incubated with 10 mM Gly and varying concentrations of FTHF (0 - 400 μM). The double reciprocal plot ($1/A_{500}$ versus $1/[\text{FTHF}]$) for the dialyzed enzyme is shown as (▲). bsSHMT (10 mg) was incubated with 10 mM Gly and 500 μM FTHF for 5 min and then dialyzed against 50 mM potassium phosphate buffer, pH 7.4, containing 1 mM EDTA, 1 mM 2-ME not containing Gly and FTHF. Such an enzyme (1 mg ml^{-1}) was once again incubated with Gly (10 mM) and different concentrations of FTHF.

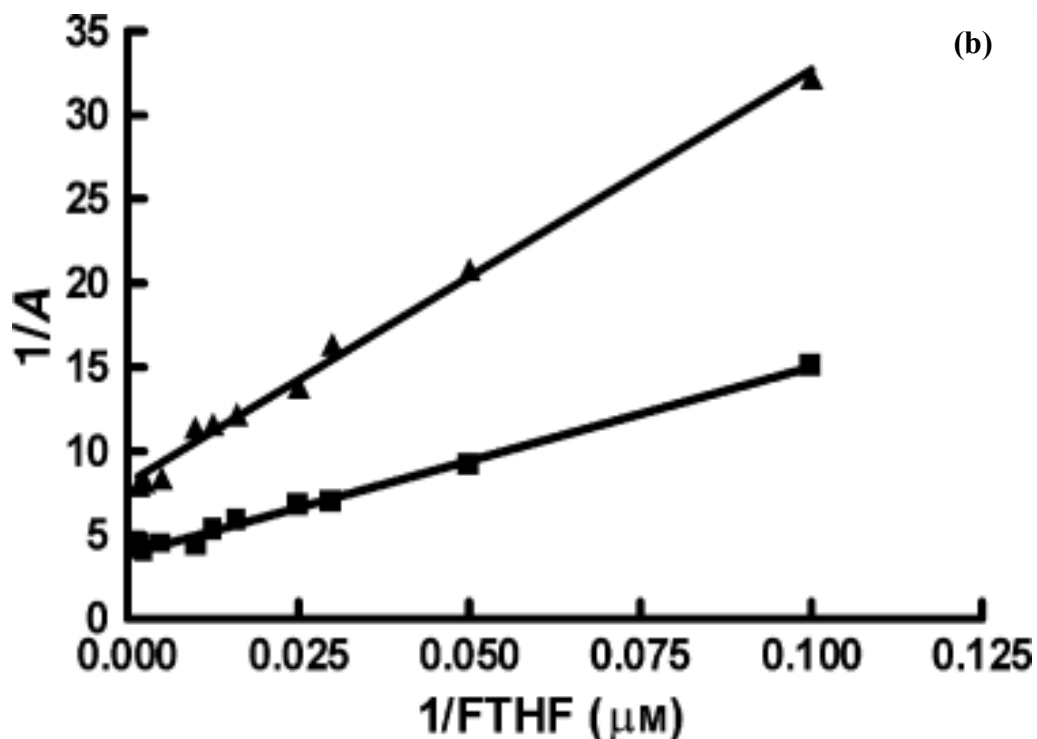


Fig 2.16 (b): The reciprocal of A_{500} was plotted against the reciprocal of FTHF concentration (■). E53Q bsSHMT (1 mg ml^{-1}) was incubated with 10 mM Gly and varying concentrations of FTHF (0 - 400 μM), for 1 min and absorbance at 500 nm was measured). The double reciprocal plot ($1 / A_{500}$ versus $1 / [\text{FTHF}]$) for the dialyzed enzyme is shown by (▲). The enzyme (10 mg) was incubated with 10 mM Gly and 500 μM FTHF for 5 min and then dialyzed against 50 mM potassium phosphate buffer, pH 7.4, containing 1 mM EDTA, 1 mM 2-ME devoid of Gly and FTHF. Such an enzyme was once again incubated with Gly (10 mM) and different concentrations of FTHF as in and the absorbance was measured at 500 nm.

However, as the slopes were significantly different for E53Q bsSHMT. This suggests that the enzyme conformation previously exposed to Gly and FTHF is different from that before exposure. These results suggest that E53Q bsSHMT exhibits enzyme memory.

E53Q-Gly-FTHF complex was prepared as described earlier and the visible CD spectrum was recorded in the range of 300-550 nm (Fig 2.17). The complex was dialyzed against buffer not containing Gly or FTHF. The visible CD spectrum was recorded. It is evident from the Fig 2.17 that the absorbance maxima at 495 nm decreased with time and there was a concomitant increase at 425 nm accompanied by a decrease at 343 nm. These results suggest that E53Q ternary complex was unstable. The experiment described above was carried out in an identical manner using bsSHMT and showed no change in the molar ellipticity at 495, 425 and 343 nm, suggesting that the bsSHMT ternary complex was stable.

It was hypothesized that presence of Gly in the dialysis buffer may help in keeping the enzyme in gem-diamine form for longer duration. Considering this point in view, the above described experiment was repeated in 50 mM potassium phosphate buffer, pH 7.4, containing 1 mM EDTA, 1 mM 2-ME containing 50 mM Gly. It can be seen from the Fig 4.18 that presence of Gly indeed increased the decomposition time of quinonoid intermediate from 45 to 90 min or in other words slowed down the dissociation of the gem-diamine (Fig 2.18).

Further, the dialyzed mutant ternary complex was subjected to NaCNBH₃ reduction to identify the presence of PLP-Lys Schiff's base. In the case of dialyzed E53Q bsSHMT the reduction time was increased by 40 min unlike for the undialyzed E53Q bsSHMT which was reduced in 7 min (Fig 2.19). These observations suggested that, PLP at the active site of dialyzed mutant enzyme is probably in an altered environment.

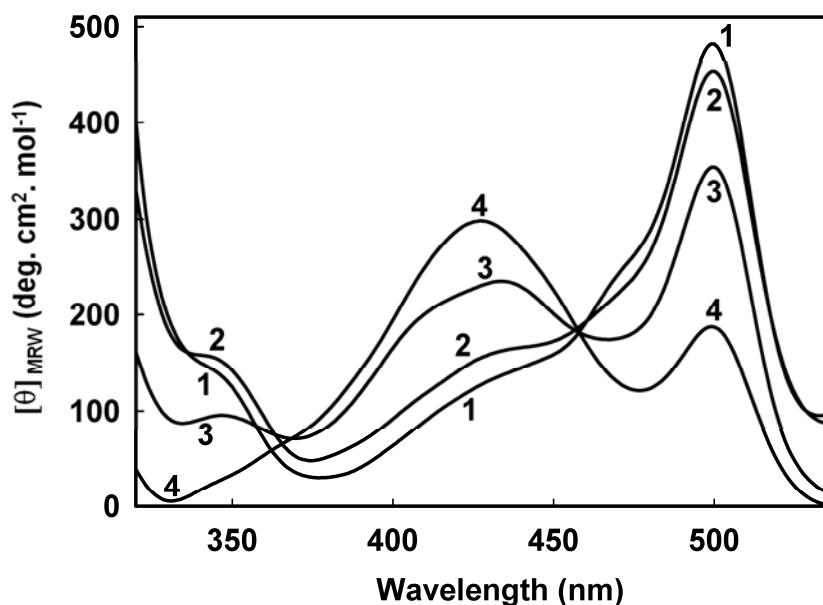


Fig 2.17: The visible CD spectrum of E53Q bsSHMT-Gly-FTHF ternary complex depicting the formation and decomposition of gem-diamine on dialysis. Curve 1: E53Q bsSHMT-Gly-FTHF ternary complex in 50 mM potassium phosphate buffer, pH 7.4, containing 1 mM EDTA, 1 mM 2-ME. Curve 2: Spectra were recorded 15 min after dialysis against same buffer devoid of Gly. Curve 3: after 30 min. Curve 4: after 45 min. The isobestic point was seen at 460 nm.

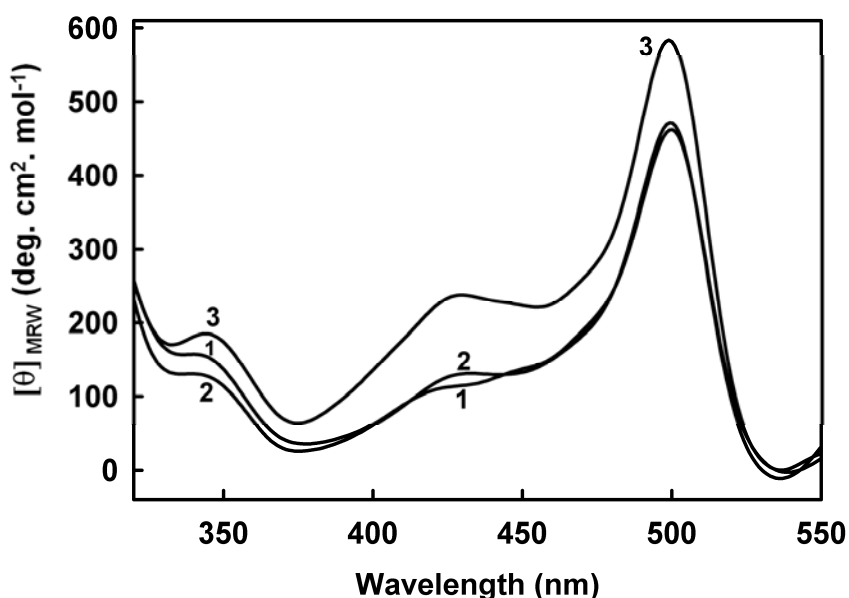


Fig 2.18: The visible CD spectrum of E53Q bsSHMT-Gly-FTHF ternary complex dialyzed against 50 mM potassium phosphate buffer, pH 7.4, containing 1 mM EDTA, 1 mM 2-ME containing Gly (50 mM) for different time intervals.

E53Q bsSHMT ternary complex 20 min after dialyzing against final buffer containing 50 mM Gly (curve 1); after 50 min (curve 2) and after 90 min (curve 3).

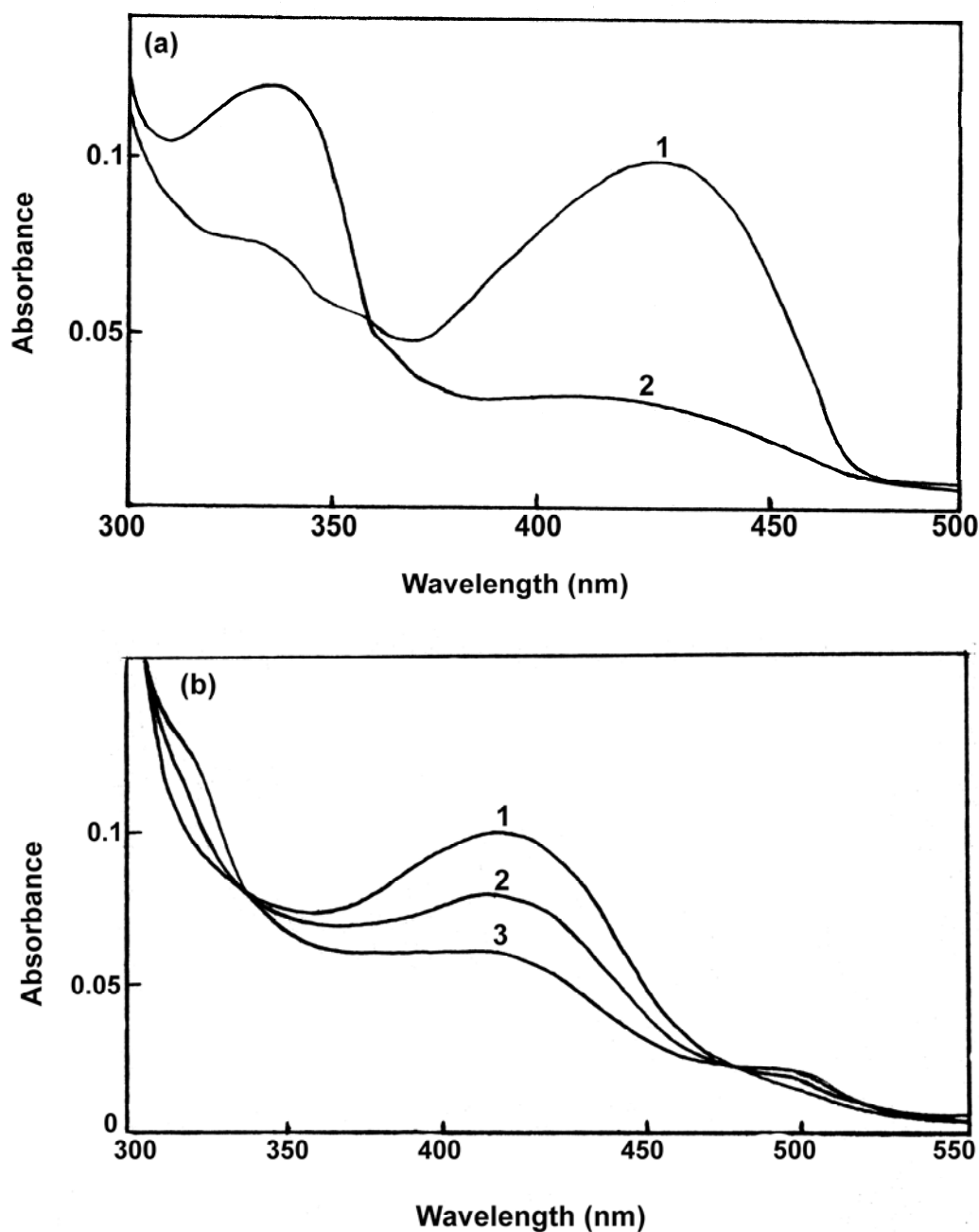


Fig 2.19: Reduction of undialyzed E53Q bsSHMT and dialyzed E53Q bsSHMT with NaCNBH_3 .

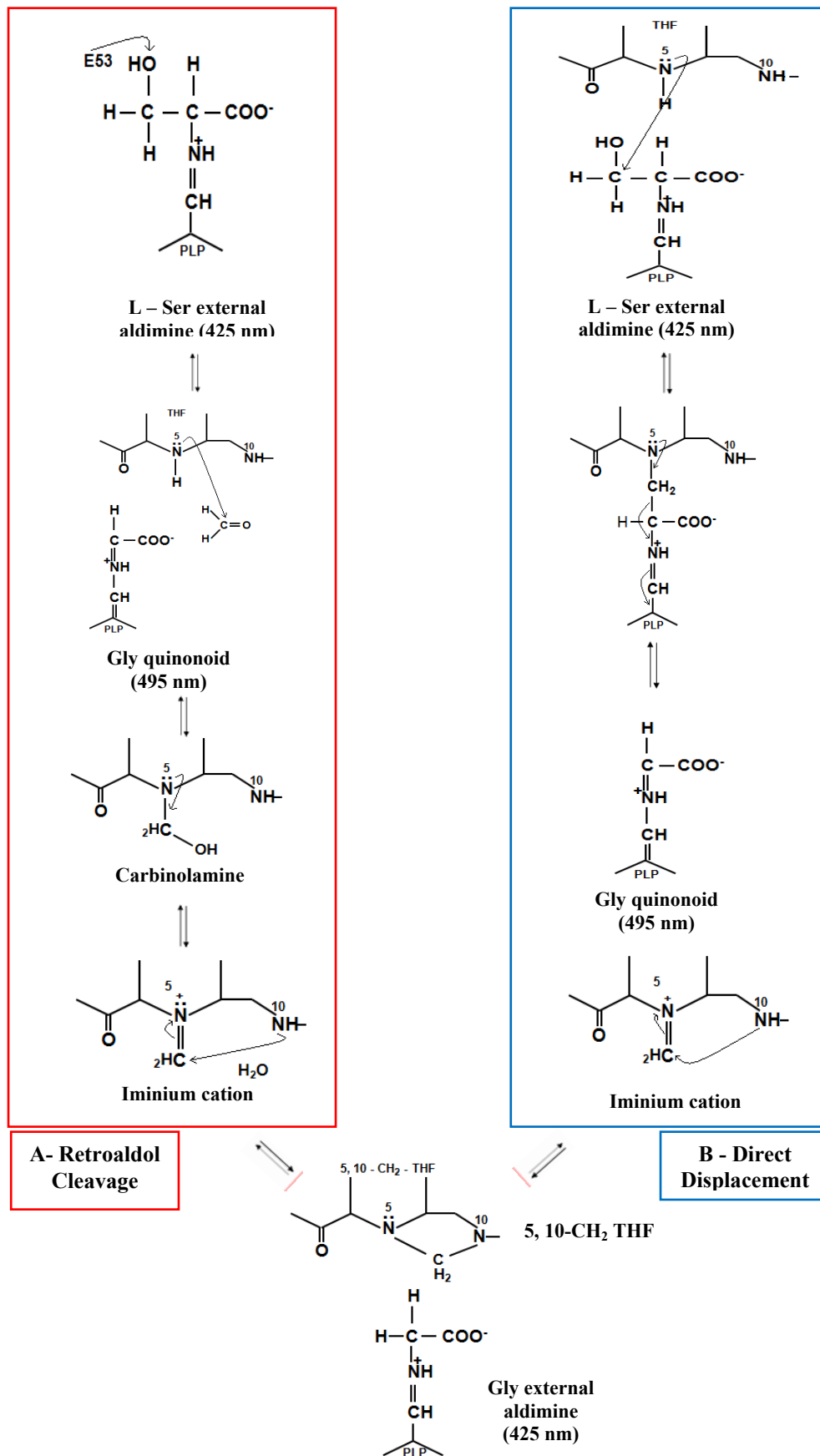
(a) E53Q bsSHMT (1 mg ml^{-1}) in 50 mM potassium phosphate buffer, pH 7.4, containing 1 mM EDTA, 1 mM 2-ME (curve 1), on addition of 0.4 mM NaCNBH_3 and incubated for 7 min (curve 2). The isobestic point was seen at 360 nm.

(b) E53Q bsSHMT ternary complex ($1 \text{ mg ml}^{-1} + 50 \text{ mM Gy} + 500 \text{ }\mu\text{M FTHF}$) dialyzed in 50 mM potassium phosphate buffer, pH 7.4, containing 1 mM EDTA, 1 mM 2-ME devoid of Gly (curve 1); 20 min after addition of 0.4 mM NaCNBH_3 (curve 2); after 40 min for dialyzed E53Q bsSHMT (curve 3).

Discussion

The biochemical and crystal structures of SHMT, its substrate and inhibitor complexes from various sources enabled the proposal of a retroaldol or direct displacement mechanism for SHMT catalysis (Schirch, 1982; Trivedi *et al.*, 2002; Szebenyi *et al.*, 2004; Schirch and Szebenyi, 2005). The classical retroaldol cleavage mechanism (Scheme 2.2 A) is initiated by a proton abstraction from the hydroxymethyl group of L-Ser by a base at the active site, resulting in the formation of Gly quinonoid intermediate and release of formaldehyde. N5 of THF reacts with formaldehyde to form 5-hydroxymethyl THF carbinolamine complex. This intermediate undergoes an elimination reaction to give 5-iminium cation. N10 of THF attacks the iminium cation to give N5, N10-CH₂ THF which is released from the enzyme. This mechanism was based on the assumption that free formaldehyde, in spite of its small size does not rotate at the active site and does not react with other amino acid residues at the active site. In addition to a base at the active site for the abstraction of hydroxyl proton, anti-periplanar geometry of the atoms is required for the catalysis to occur. Of the two groups that could serve as bases for abstracting proton (E53 and H122 in bsSHMT) as indicated by the structure (Fig 2.1 a). E53 was present in its protonated form as the crystal structure of L-Ser binary complexes (Jala *et al.*, 2000; Scarsdale *et al.*, 2000; Trivedi *et al.*, 2002), suggesting that it could be involved in the proton abstraction step of catalysis. Mutation of H147 in scSHMT corresponding to H122 in bsSHMT, led only to a partial loss of enzyme activity, indicating that it could not be the residue abstracting the proton (Jagath *et al.*, 1997b).

An unfavorable geometry and the absence of a base at the active site and an examination of crystal structure of bsSHMT-Ser complex shed new insights into the catalytic mechanism. A direct transfer mechanism was suggested for the reaction catalyzed by SHMT (Scheme 2.2 B) (Trivedi *et al.*, 2002). This proposal envisages a direct nucleophilic displacement of L-Ser hydroxymethyl group by N5 of the THF with a loss of water to form a complex in which the THF, L-Ser and PLP are covalently linked. This is followed by cleavage of the α - β carbon to generate quinonoid intermediate and the N-5 iminium cation. Since free formaldehyde is not an intermediate, the reaction shown in Scheme 2.2 should proceed with complete stereo specificity.

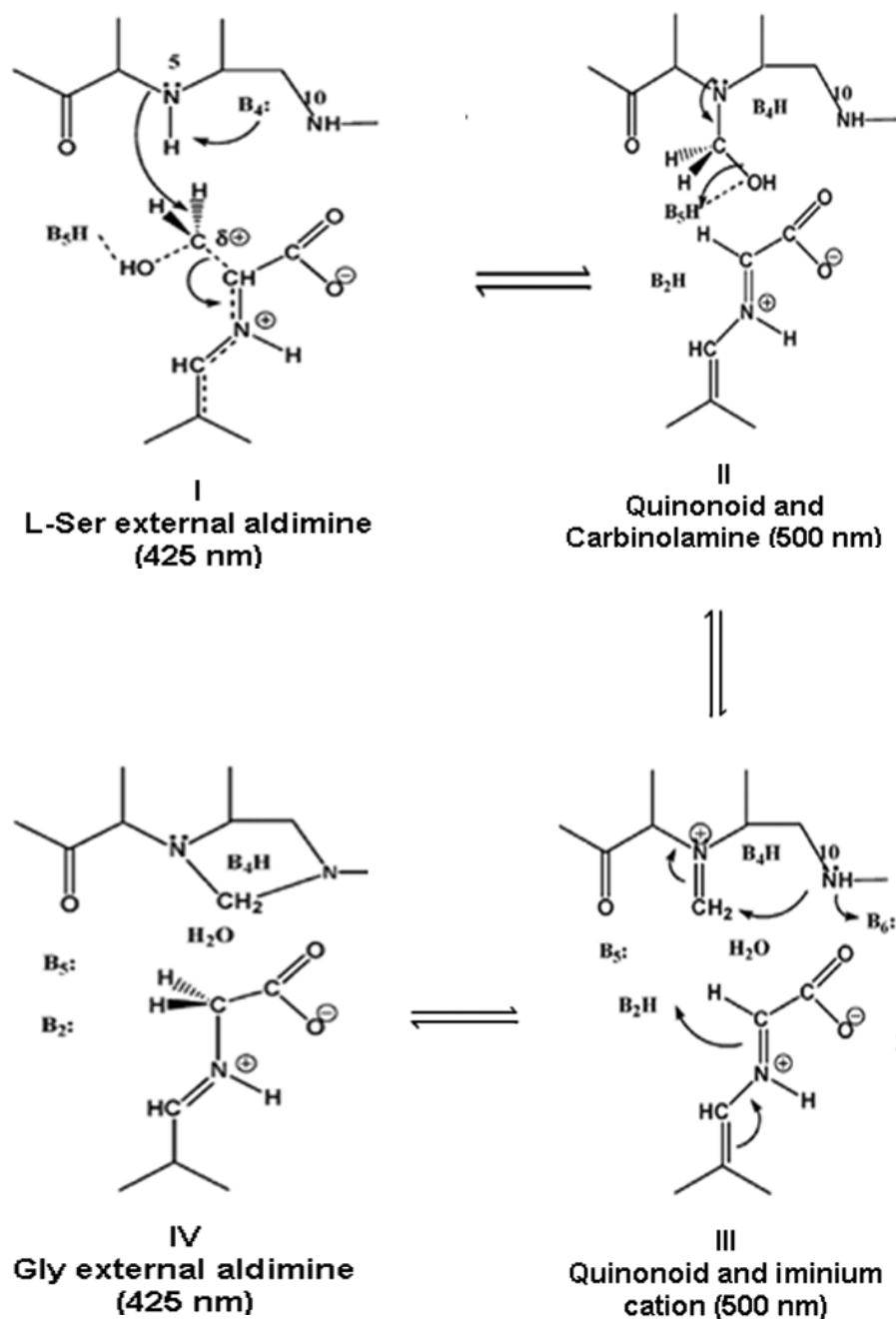


Scheme 2.2: Retroaldol (shown in red) and direct displacement mechanisms (shown in blue) proposed for SHMT catalysis. The basis of the above hypothesis is drawn from the data of Jordan and Akhtar, 1970; Trivedi *et al.*, 2002).

However, biochemical and structural studies on E74Q rcSHMT suggest a combination of the classical retroaldol cleavage and direct displacement mechanism (Scheme 2.3) (Szebenyi *et al.*, 2004). In the revised mechanism, suggests that, the highly polarized C3 of serine is attacked by N5 of THF, cleaving the C2-C3 bond to generate N5-CHOH-THF (carbinolamine intermediate) and the quinonoid complex of Gly. In this mechanism, the preferred direction for the nucleophilic attack by N5 on C3 of L-Ser is opposite of the C3-C2 bond; that is the N5-C3-C2 angle should be close to 180°. N5 is much closer to being properly positioned for such an SN2 attack on C3 of serine (in which the Gly anion is eliminated) than for the attack (in which the L-Ser hydroxyl is eliminated). The breakage of the C2-C3 bond (creating a formaldehyde intermediate) preceding formation of the N5-C3 bond.

Szebenyi *et al.* (2004), also suggest that nucleophilic mechanism requires a proton donor (general acid), at the active site to aid on the breaking of O γ -C3 bond, rather than a strong base. As Glu 75 is protonated and it is well suited for this role. It was suggested that, Glu 75 acts as an acid in retroaldol cleavage of all 3-hydroxy amino acids in spite of enhanced cleavage of L-Ser in the absence of THF and L-*allo* Thr. Studies on the Lys mutants of bsSHMT have provided evidence favoring the direct displacement mechanism.

Results presented in this chapter show that, mutation of E53 to Q drastically affects the THF-dependent L-Ser cleavage. It can be seen from Table 2.1 that, the mutation of E53 to Q completely abolished the THF-dependent cleavage of L-Ser. Increasing the enzyme concentration or reaction time did not increase this activity. Earlier studies with scSHMT and rcSHMT had indicated the loss of activity by 400 and 500-fold, respectively when this residue was mutated (Jala *et al.*, 2000; Szebenyi *et al.*, 2004). A small amount of THF-independent cleavage of L-Ser was observed in the case of E53Q bsSHMT. However, bsSHMT failed to show THF-independent cleavage of L-Ser. It was observed that the THF-independent cleavage of L-Ser in E53Q bsSHMT was negligible when compared to THF-dependent cleavage of L-Ser in bsSHMT. In case of rcSHMT, where, it was claimed that THF-independent activity with L-Ser was enhanced by mutation, the activity assay was beset with many limitations. For example, it was mentioned that HCHO, one of the products of the reaction was inactivating the enzyme and the amount of HCHO formed was in



Scheme 2.3: A concerted mechanism which, combines retroaldol and nucleophilic displacement mechanisms. (Reproduced from Szebenyi *et al.*, 2004)

nano moles, where as the amount of HCHO formed in the THF-dependent reaction was in micro moles. In addition, very high concentration of enzyme was required for determining this activity. In view of these limitations it is difficult to speculate on the mechanism of the reaction and role of E75 on the basis of this data (Szebenyi *et al.*, 2004). However, THF-independent cleavage of L-*allo* Thr was increased by 1.5 fold in E53Q bsSHMT (Table 2.1). A similar increased activity has been reported in the case of E75Q rcSHMT (4 fold). These observations are in general agreement with those of (Jala *et al.*, 2000; Trivedi *et al.*, 2002; Szebenyi *et al.*, 2004) suggesting no change in the activity or a 4-fold increase in the activity. The increased activity of L-*allo* Thr could be due to the replacement of the charged Glu by neutral Gln.

E53Q bsSHMT is capable of forming an internal aldimine with λ_{\max} of 425 nm (Fig 2.5 a and 2.9 b. Spectral studies in presence of L-Ser suggest that the E53Q bsSHMT is capable of forming an external aldimine (Fig 2.5 a). However, decrease in molar ellipticity on addition of L-Ser to E53Q bsSHMT-Ser was not seen as in the case of bsSHMT, suggesting that the formation of external aldimine is affected (Fig 2.6). This was confirmed by the absence of the increase in the thermal stability on addition of L-Ser to the mutant enzyme (Table 2.2) suggesting that ‘open’ to ‘closed’ conformational change was taking place although an external aldimine is formed. The enhancement of thermal stability is a characteristic feature of the SHMT-Ser binary complexes. This has been ascribed to the conversion of the enzyme from an ‘open’ form to a ‘closed’ form. This observation was supported by peptide bond exchange studies, thermal studies and CD studies (Schirch *et al.*, 1991). However, unlike in the case of AAT (Picot *et al.*, 1991), this conformational change is not obvious in crystal structure of SHMT (Trivedi *et al.*, 2002). It is, therefore, not surprising that the absence of conversion from ‘open’ to ‘closed’ form (in which THF-dependent cleavage of L-Ser occurs) is affected by the mutation which resulted in complete loss of THF-dependent cleavage of L-Ser.

It is also well known that the THF-independent reaction takes place in the open form and as such this reaction is unaffected by the mutation. In addition to the above observations, E53Q bsSHMT-Ser binary complex shows the presence of hydroxyl group in two conformations (Fig 2.8), which corroborates the observation

that, E53Q bsSHMT does not have the correct orientation of –OH group in L-Ser binary complex. This could be a strong reason for inefficient binding of L-Ser. It is well known that, glutamate interacts with the –OH of L-Ser at the active site.

This interaction is lost upon mutation, resulting in two distinct orientations of –OH of L-Ser. Addition of THF/FTHF to E53Q bsSHMT gave small peak absorbing at 495 nm (Fig 2.5a). It suggests that mutant enzyme is able to form a quinonoid intermediate. However, the small amount of THF-independent reaction with L-Ser in E53Q bsSHMT was observed only when the mutant enzyme concentration was increased by 100 fold (1 mg ml^{-1}). Spectral studies of mutants were carried out at 1 mg ml^{-1} concentration. The observed quinonoid intermediate in case of spectral studies could be due to Gly generated by THF-independent cleavage of L-Ser. The Gly (product of THF-independent cleavage of L-Ser) reacts with THF/FTHF resulting in the formation of the quinonoid intermediate observed in the mutant enzyme (Fig 2.5 a).

Mutation of glutamate does not affect the formation of the quinonoid intermediate when the THF/FTHF and Gly are added to E53Q bsSHMT. This suggests that glutamate residue is not very essential for the formation of the quinonoid intermediate from Gly and for its enhancement by THF/FTHF. The formation of the quinonoid intermediate requires abstraction of a proton from the α -carbon atom of the bound Gly. Dialysis experiments (Fig 2.10) and dissociation constants (2.5-fold higher) for FTHF suggests that, the affinity of FTHF to mutant binary complex was low when compared to bsSHMT. This could be due to loss of interaction of N10 and formyl oxygen of FTHF with the glutamate which is lost upon mutation. This suggests that glutamate plays an important role in folate binding.

Results obtained upon examining the structure of the mutant enzyme determined in the presence of Gly and FTHF [E53QbsSHMT-Gly(FTHF)] were interesting. E53Q bsSHMT in the presence of Gly and FTHF yielded orthorhombic crystals rather monoclinic as seen in bsSHMT-Gly-FTHF complex and the density for FTHF could not be traced in the crystal structure. PLP in this complex was trapped in a gem-diamine form covalently bound to both the active site Lys and the added Gly amino group (Fig 2.12). Gem-diamine is an intermediate formed in the

inter-conversion of the enzyme between internal and external aldimine forms (Scheme 2.1). The orientation of PLP in E53Q bsSHMT-Gly(FTHF) complex is closer to that of bsSHMT-Gly-FTHF than its orientation in the internal or external aldimine structures of mutant or wild-type enzymes (Fig 2.13, 2.14). This is consistent with the earlier observation that the orientation of PLP in the ternary complex of mcSHMT (Szebenyi *et al.*, 2000) is similar to the PLP in the gem-diamine form. However, the present structure does not contain any density for FTHF (Fig 2.13).

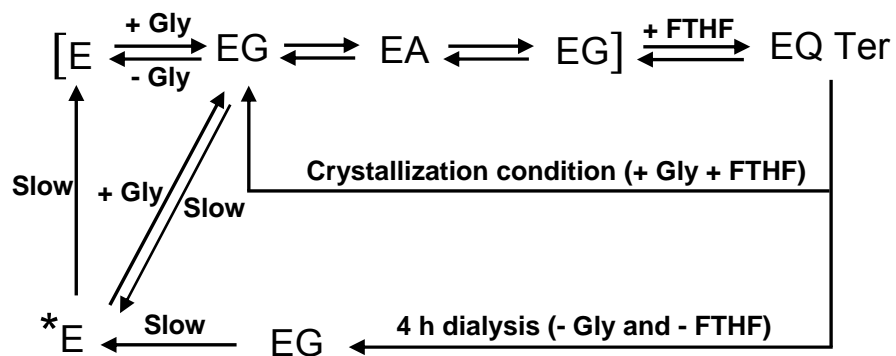
The similarity in the orientation of PLP to that of the wild-type ternary complex and absence of FTHF in the crystal structure suggests that there is an initial binding of FTHF leading to an alteration in the orientation of PLP and subsequently, FTHF falls off from the active site due to its decreased affinity in the absence of E53, leaving behind the enzyme in the gem-diamine form. The differences between the structures of this complex and Gly external aldimine (Fig 2.13) suggest that the changes induced by initial binding of FTHF are retained, even though FTHF is absent from the final structure. This observation was supported by visible CD spectrum of E53Q bsSHMT ternary complex showing the formation of gem-diamine at 343 nm (Fig 2.15). It is pertinent to point out the gem-diamine is an obligate intermediate in all PLP catalysis (Dunathan, 1966).

These observations indicate that binding of FTHF causes a change at the active site of mutant though it falls off from the active site, suggesting mutant enzyme exhibits a phenomenon known as “enzyme memory”. A phenomenon wherein binding of ligands caused conformational changes in the enzyme molecules and even after removal of ligands, such imprints of ligand binding were retained by the enzyme. Whitehead (1970) coined the term “enzyme memory”, to express the idea that the enzyme “recalls” for a while the conformation stabilized by the substrate.

Rabin (1967) proposed that a monomeric flexible one-substrate enzyme, (that is an enzyme exhibiting conformation changes upon substrate binding) can exhibit a non- Michaelian kinetics, or a so-called regulatory, behavior. The basic idea of scheme is that the enzyme conformation which is released at the end of the catalytic

step is different from the initial one and this conformation slowly reverts to that of the free enzyme. Deviations from Michaelian behavior thus appear to be a consequence of different affinity of two conformations of the monomeric enzyme towards the substrate. The early evidence of “enzyme memory” was based on the kinetic studies of wheat-germ hexokinase (Jacques *et al.*, 1974; Jean, 1977). Detailed studies were done on ascorbate oxidase (Katz and Westley, 1979) and protease subtilisin to understand phenomenon of enzyme memory. This ligand induced enzyme memory was extended to stability, affinity, and substrate specificity of protease subtilisin (Yennawar *et al.*, 1995). They have provided a structural explanation for enzyme memory in non-aqueous solvents. One of the important kinetic evidences for the occurrence of enzyme memory is the demonstration of significant variation of acceptor double reciprocal slopes with variation in donor substrate. In the case of ascorbate oxidase (Katz and Westley, 1979) observed, changes in the slope in the double reciprocal plot with three different donor substrates demonstrating enzyme memory. The double reciprocal plots of bsSHMT ternary complex and E53Q bsSHMT-Gly-(FTHF) complex, indeed suggest that, mutant enzyme exhibits enzyme memory (Fig 2.16). These observations are reminiscent of enzyme memory observed in kinetic experiments with plant aspartate synthase, hexokinase (Jacques *et al.*, 1974; Jean, 1977) and ascorbate oxidase (Katz and Westley, 1979). Scheme 2.4 represents the probable mechanism for enzyme memory exhibited by E53Q bsSHMT. E53Q bsSHMT in presence of Gly forms gem-diamine (EG), external aldimine (EA) and quinonoid intermediate (EQ), all the intermediates are in equilibrium. On addition of FTHF to Gly binary complex equilibrium is shifted in favor of quinonoid intermediate in ternary complex (EQ Ter). However, mutation of Glu residue to Gln abolishes the interaction of Glu with N10 and oxygen of CHO (Fig 2.1); hence FTHF can no longer bind as efficiently as it does to bsSHMT (Fig 2.10).

In the crystallization conditions, presence of Gly may drive the mutant enzyme to be in gem-diamine form. These suggestions were supported by dialysis in presence of Gly in 50 mM potassium phosphate buffer, pH 7.4, containing 1 mM EDTA, 1 mM 2-ME (Fig 2.18). It showed that the enzyme was stabilized as a gem-diamine complex.



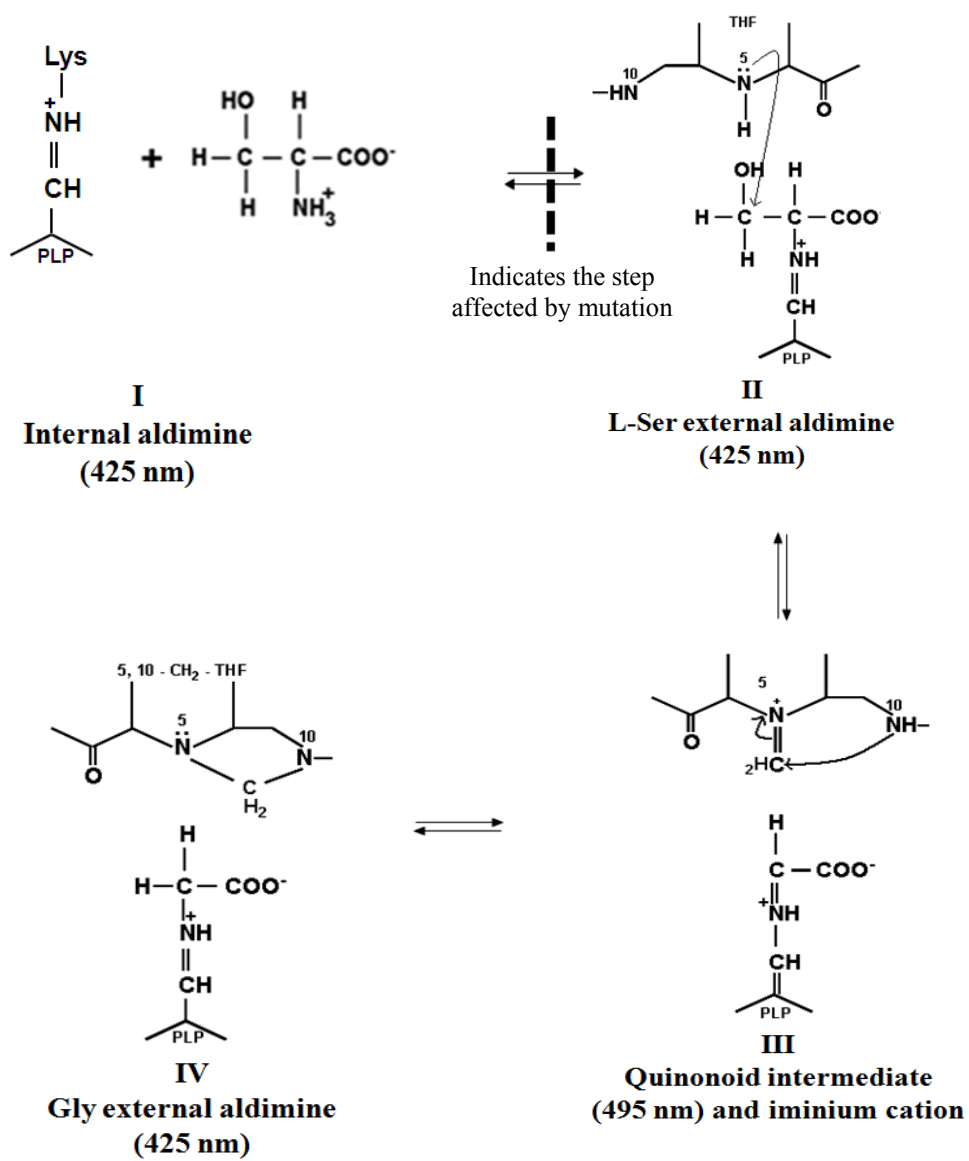
Scheme 2.4: Probable mechanism for E53Q bsSHMT exhibiting enzyme memory.

E – E53Q bsSHMT; EG – E53Q bsSHMT gem-diamine; EA – E53Q bsSHMT Gly external aldimine; EQ – E53Q bsSHMT Gly quinonoid intermediate; EQ Ter - E53Q bsSHMT ternary complex with Gly + FTTHF; *E – E53QbsSHMT after dialysis in new conformation as proposed from the data.

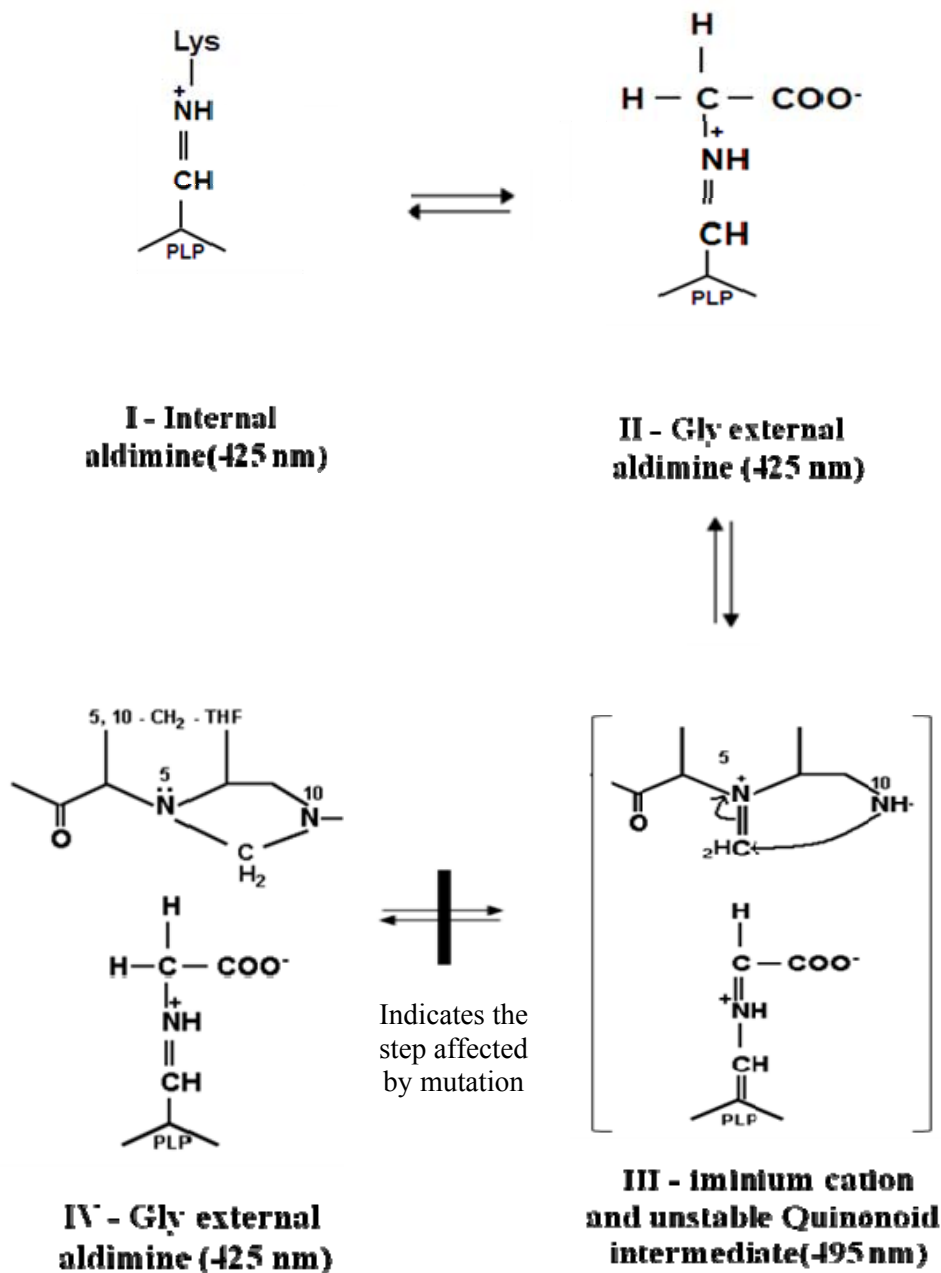
Visible CD studies and decreased affinity of FTHF to E53Q bsSHMT-Gly complex suggest initial binding of FTHF followed dissociation leaving behind gem-diamine form of E53Q bsSHMT. The E53Q bsSHMT-Gly(FTHF) in gem-diamine form retains its conformation for considerable time and slowly dissociates to an external or internal aldimine (Fig 2.17).

In order to enhance the rate of dissociation of FTHF the mutant ternary complex was dialyzed. The mutant gem-diamine (EG) complex slowly dissociates to its internal aldimine form, which is conformationally different (*E) form the native enzyme (E). This enzyme is very slowly converted to the native internal aldimine (E). This proposal was supported by increased time for NaCNBH₃ reduction (Fig 2.19) for the dialyzed enzyme. Addition of Gly to dialysis buffer did not increase the amount of gem-diamine, however helped in keeping the mutant enzyme in gem-diamine form for longer duration (Fig 2.17, 2.18). The mutant enzyme in new conformation (*E) could react with Gly to give gem-diamine could react with different kinetic constants and follow the normal kinetic pathway or may slowly return to its original form (E). Rates of conversion of E53Q bsSHMT form [EG] to *E and *E to [E] could not be measured because of the slow conformational changes at the active site and absence of a convenient spectral handle. Difference in the slope for before and after dialysis (Fig 2.15) supports the fact of enzyme being in different conformation of the mutant and wild-type enzyme. However, more experiments are needed to confirm enzyme memory in this system. Results presented suggest that, phenomenon of enzyme memory is exhibited only with mutant enzyme as a result of its inefficient FTHF binding to E53Q-Gly binary complex. This is the first instance of such a phenomenon observed in structural studies.

The nucleophilic attack mechanism for cleavage of L-Ser by SHMT envisages direct attack of N5 of THF on the C_β of L-Ser. E53 positions the bound amino acid for such an attack by suitable interactions with other active site residues. In addition, E53 also interacts with the formyl oxygen and N10 of FTHF. Therefore it is not surprising that the mutation has affected the hydrogen-bonding network involving key residues such as Y60 and Y61 and the interaction with R357, which anchors the carboxyl group of the substrate as seen in the crystal structures. Scheme 2.5 and 2.6 shows the role of E53 in forward and reverse reaction catalyzed by SHMT.



Scheme 2.5: Schematic representation of the role of E53Q bsSHMT in SHMT catalyzed reverse reaction with L-Ser. As proposed from the data.



Scheme 2.6: Schematic representation of the role of E53Q bsSHMT in SHMT catalyzed reaction with Gly. As proposed from the data.

A consequence of these changes is the complete loss of THF-dependent physiological reaction with L-Ser. However THF-independent reaction is not reduced. The loss of interactions of the Glu residue with the formyl oxygen and N10 of FTHF in the mutant enzyme weakens the interactions with THF/FTHF. Consequently, FTHF dissociates and the mutant enzyme and crystallizes in the gem-diamine form. Formation of a quinonoid intermediate, gem-diamine complex and a slow dissociation of FTHF indicate that E53Q bsSHMT exhibits enzyme memory. This is the first instance of such a phenomenon observed in structural studies.

The results presented in this chapter, clearly indicates that Glu 53 is not involved in the postulated proton abstraction step in the hydroxymethyltransferase reaction of L-Ser. However, the THF-dependent cleavage is lost upon this mutation for other reasons (conversion from 'open' to 'closed' form and proper positioning of L-Ser for attack by N5 of THF). The THF-independent cleavage of 3-hydroxy amino acids and proton abstraction from Gly is unaffected. It was therefore necessary to identify the residues at the active site, which is involved in the proton abstraction. In the next chapter the results of such a study on two likely candidates namely Y61 and Y51 are presented in detail.

Chapter 3

The role of tyrosine residues in cofactor binding and elucidation of mechanism for the tetrahydrofolate-independent cleavage of L-*allo* threonine

Most reactions in both organic chemistry and enzymology are catalyzed by either acid-base mechanisms. Amino acid residues at the active site provide important functional group for enzyme catalysis including proton acceptors and donors. Amino acids which have ionizable side chains have the capacity to act as catalysts at the active site. The potential catalytic groups are the β -carboxyl of Asp, γ -carboxyl of Glu, imidazole of His, thiol of Cys, hydroxyl of Tyr, ϵ -amino group of Lys, guanidino group of Arg and hydroxyl of Ser and Thr.

SHMT in addition to THF-dependent cleavage of L-Ser catalyzes the THF-independent cleavage of 3-hydroxy amino acids and transamination (Malkin and Greenberg, 1964; Schirch and Jenkins, 1964a, b; Chen and Schirch, 1973; Ulevitch and Kallen, 1977a, b, c). A detailed mechanism has been proposed for THF-dependent cleavage of L-Ser based on the biochemical and X-ray structures (Schirch, 1982; Trivedi *et al.*, 2002; Szebenyi *et al.*, 2004; Schirch and Szebenyi, 2005). Although extensive studies have been carried out on the mechanism of THF-dependent reaction of SHMT, not much is known about the mechanism of THF-independent cleavage of 3-hydroxy amino acids. Although it has been proposed that, it proceeds by a similar mechanism (Schirch, 1982; Schirch and Szebenyi, 2005). Several studies have shown that THF-dependent conversion of L-Ser to Gly is completely abolished on mutation of specified residues (Schirch *et al.*, 1993a; Jagath *et al.*, 1997a; Jagath *et al.*, 1997b; Contestabile *et al.*, 2000; Jala *et al.*, 2000; Talwar *et al.*, 2000a; Jala *et al.*, 2003a; Szebenyi *et al.*, 2004). However, the THF-independent cleavage of L-*allo* Thr was enhanced several fold or retained similar to the activity of wild-type enzyme (Jagath *et al.*, 1997b; Contestabile *et al.*, 2000; Jala *et al.*, 2000; Szebenyi *et al.*, 2004). There are very few examples of mutations affecting 3-hydroxy amino acid cleavage. These include Arg (Fratte *et al.*, 1994; Jagath *et al.*, 1997a; Jala *et al.*, 2003a), which is involved in binding of substrate carboxyl group and His 230 which is involved in PLP-binding. In the case of H230 mutation to Y did not result in complete loss of THF-independent activity (Talwar *et al.*, 2000a).

The results presented in the previous chapters suggest that E53 and K226 (numbering as per bsSHMT) are not involved in proton abstraction step of catalysis.

From the observations, it is evident that, the cleavage of 3-hydroxy amino acids may occur by a mechanism different from the classical retroaldol cleavage. In addition, it has not been possible to pinpoint the residue involved in the protonation/deprotonation in both the mechanisms. Fig 3.1 depicts the geometry of the active site of bsSHMT-Ser external aldimine highlighting the residues that could be involved in catalysis (Trivedi *et al.*, 2002). Stereo diagram of bsSHMT-Ser active site shows the Schiff base between PLP and amino group of L-Ser. Residues from the same subunit are represented in yellow colour and those from the other subunit are in green colour. E53 and H122 interact with -OH of L-Ser, Y51 interacts with the phosphate group of PLP and Y61 is close to C β of L-Ser (Trivedi *et al.*, 2002)

Sequence comparison of SHMT from various sources revealed that Y51, Y60 and Y61 (numbering according to bsSHMT sequence) are well conserved (Jala *et al.*, 2002). In the internal aldimine structure of bsSHMT, the hydroxyl group of Y51 was found to interact with the phosphate group of PLP and the side chain of Y61 is hydrogen bonded to R357 (2.7 Å) and it points away from E53 (5 Å). In the external aldimine structure, Y61 points towards E53 approaching its side chain carboxylate group and C β of the bound ligand, L-Ser (2.8 Å) (Trivedi *et al.*, 2002). The residue corresponding to Y61 of bsSHMT in scSHMT (Y82) (Jala *et al.*, 2000) and eSHMT (Y65) were mutated to F earlier (Contestabile *et al.*, 2000). Studies on these mutants have suggested that this residue might be involved in proton abstraction, stabilization of the quinonoid intermediate and conversion of an open to closed form of the enzyme (Contestabile *et al.*, 2000).

In this chapter we have examined the mechanism of THF-independent cleavage of 3-hydroxy amino acids by SHMT. The biochemical properties of Y51F, Y61A and Y61F bsSHMT were examined. In addition, the three dimensional structures of Y61A and Y51F with substrates, especially L-*allo* Thr were also analyzed. The results presented in this chapter, enable us to propose a possible mechanism for SHMT catalyzed THF-independent reaction which is different from the classical retroaldol cleavage mechanism.

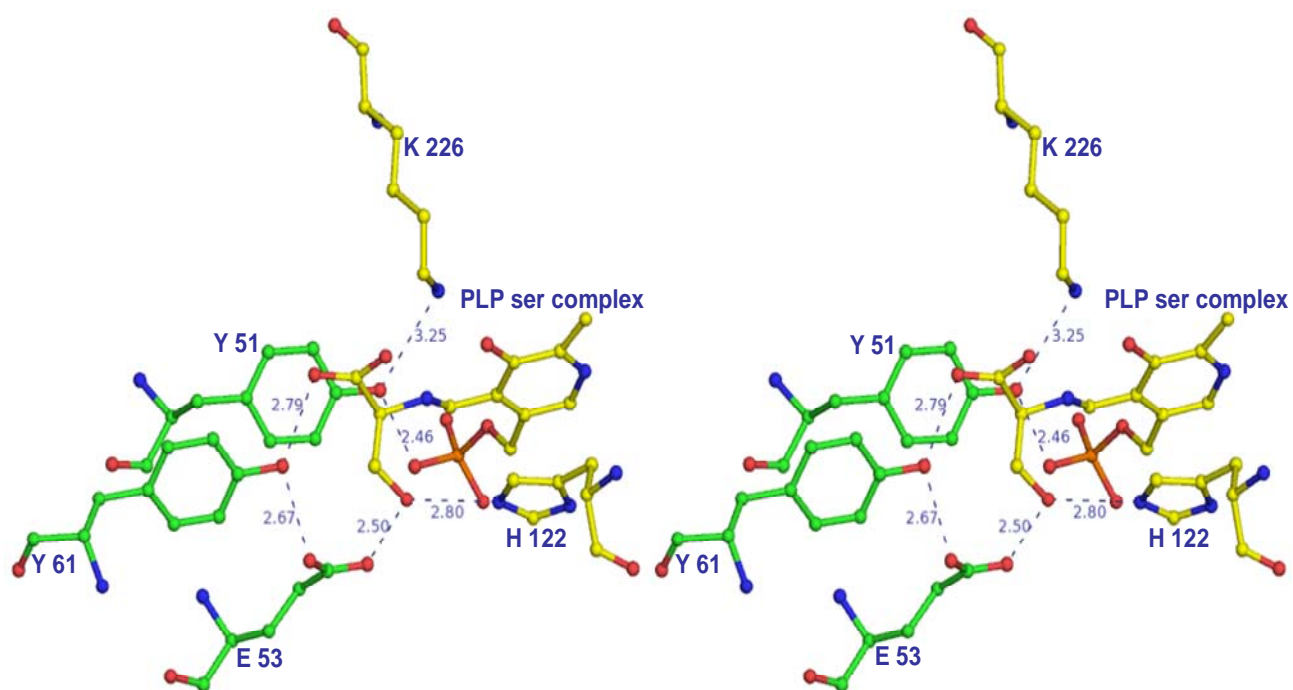


Fig 3.1: Active site geometry of bsSHMT-Ser complex depicting the possible residues involved in catalysis. Figure was generated using the structural data solved from Trivedi et al., (2002) using PyMOL software (DeLano, 2002).

Results

Overexpression and purification of Tyr mutants

Generation of Y51F, Y61F and Y61A bsSHMT mutants, overexpression and purification of the mutants were carried out according to the procedure described in methods section. The fractions obtained during the purification were analyzed by SDS-PAGE (Fig 3.2). The purified Y51F, Y61F, and Y61A bsSHMT were nearly homogeneous and corresponding to the expected molecular weight of 45 kDa.

PLP content and catalytic activity of Y51F, Y61A and Y61F bsSHMTs

The purified Y51F and Y61F bsSHMTs were pale yellow in colour and the PLP content was estimated as described in methods. The PLP content was 0.2 mol/mol in Y51F and 0.6 mol/mol of subunit in Y61F bsSHMT, compared to 1 mol/mol of subunit in bsSHMT. PLP content of Y61A bsSHMT was similar to that of the bsSHMT. Addition of 200 μ M of PLP to the Y51F and Y61F bsSHMTs (1 mg ml⁻¹) in 50 mM potassium phosphate buffer, pH 7.4, containing 1 mM EDTA, 1 mM 2-ME followed by incubation at 4°C for 45 min and dialysis against same buffer not containing PLP restored the PLP content to one mol per mol of subunit. These observations suggest that PLP content could be restored completely upon reconstitution. All further experiments were carried out with the reconstituted enzyme which has 1mol of PLP per mol of subunit.

THF-dependent cleavage assay

The assay was performed according to the procedure mentioned in methods section, except for the concentrations of protein used for the assay. For bsSHMT, 1 μ g of protein and for all the Tyr mutants varying concentrations of protein (10-1000 μ g) in 50 mM potassium phosphate buffer, pH 7.4, containing 1 mM EDTA, 1 mM 2-ME were used. bsSHMT catalyzes the THF-dependent conversion of L-Ser to Gly and 5, 10-CH₂THF with a specific activity of 5.0 U/mg. THF-dependent cleavage of L-Ser was completely abolished in Tyr mutants (Table 3.1). Increasing the protein concentration of mutant enzyme to 1 mg compared to 1 μ g for bsSHMT did not result in any measurable activity.

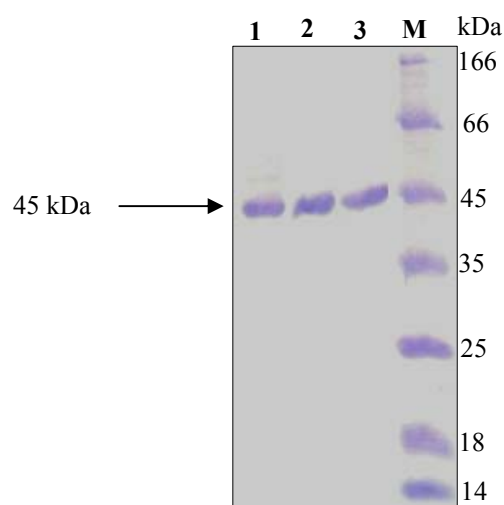


Fig 3.2: SDS-PAGE profile of Y51F, Y61A and Y61F bsSHMT.

M: markers (kDa): β -galactosidase 166; bovine serum albumin 66.2; ovalbumin 45; lactate dehydrogenase 35; restriction endonuclease Bsp981 25; β -lactoglobulin 18.4; lysozyme 14.4); Lane1: purified Y51F bsSHMT (10 μ g); Lane 2: purified Y61F bsSHMT (10 μ g); Lane 3: purified Y61A bsSHMT (10 μ g).

Table 3.1: Enzymatic activities of bsSHMT and its Tyr mutants.

Enzyme	Specific activity (L-Ser) ^a	Specific activity (L- <i>allo</i> Thr) ^b	Transamination (D-Ala) ^c s ⁻¹
bsSHMT	5.0	0.65	0.04
Y51F	NA	NA	NA
Y61F	NA	NA	NA
Y61A	0.05	0.03	NA

a – expressed as μ moles of HCHO/min/mg when L-Ser and THF were used as substrates

b - expressed as μ moles of CH₃CHO/min/mg with L-*allo* Thr as substrate

c - Pseudofirst order rate constant

NA - No activity detectable

THF-independent cleavage of bsSHMT and Y51F, Y61F and Y61A bsSHMT

Apart from THF-dependent interconversion of L-Ser to Gly, SHMT can also catalyses the THF-independent conversion of L-*allo* Thr to Gly and acetaldehyde. The THF-independent L-*allo* Thr cleavage by bsSHMT, Y51F, Y61F and Y61A bsSHMT was carried out. Protein concentrations used in the assay were as follows, for bsSHMT 50 μg and for all the Tyr mutants, varying concentration of protein (10-500 μg) in 50 mM potassium phosphate buffer, pH 7.4, containing 1 mM EDTA, 1 mM 2-ME was used. Except for the protein concentration, rest of the assay was carried out according to the procedure described in methods section. No measurable activity was detected with L-*allo* Thr, when the assay was performed with the Tyr mutants under conditions similar to that of bsSHMT (50 μg). However, on increasing the mutant enzyme concentration 100-fold, a barely detectable level of activity could be measured for Y61A bsSHMT. Transamination with D-Ala was monitored for bsSHMT and all Tyr mutants as described in methods section. Protein concentration of 1 mg ml^{-1} was used for both wild-type and mutant enzymes. D-Ala (100 mM) was added to enzyme and spectra were recorded for different time intervals in the range of 300-550 nm. Transamination reaction with D-Ala was completely abolished in all the mutants. Results of activity measurements are summarized in Table 3.1.

Spectral studies on bsSHMT, Y51F, Y61F and Y61A bsSHMT internal aldimine

Absorption spectrum of all Tyr mutants and bsSHMT (1 mg ml^{-1}) were recorded in 50 mM potassium phosphate buffer, pH 7.4, containing 1 mM EDTA, 1 mM 2-ME. The visible absorption spectrum of Y61A bsSHMT was similar to that of wild-type enzyme with maximal absorbance at 425 nm (Fig 3.3). This corresponds to the λ_{max} (425 nm) of the internal aldimine form of the enzyme. In contrast, Y51F and Y61F bsSHMT mutants showed a λ_{max} at 396 nm, (Fig 3.3). Since Y51F and Y61F bsSHMT showed a λ_{max} different from that of the wild-type enzyme, the mode of PLP-interaction in Y51F and Y61F was further examined. NaCNBH₃ specifically reduces an internal aldimine to a secondary amine which has the distinct λ_{max} at 325 nm.

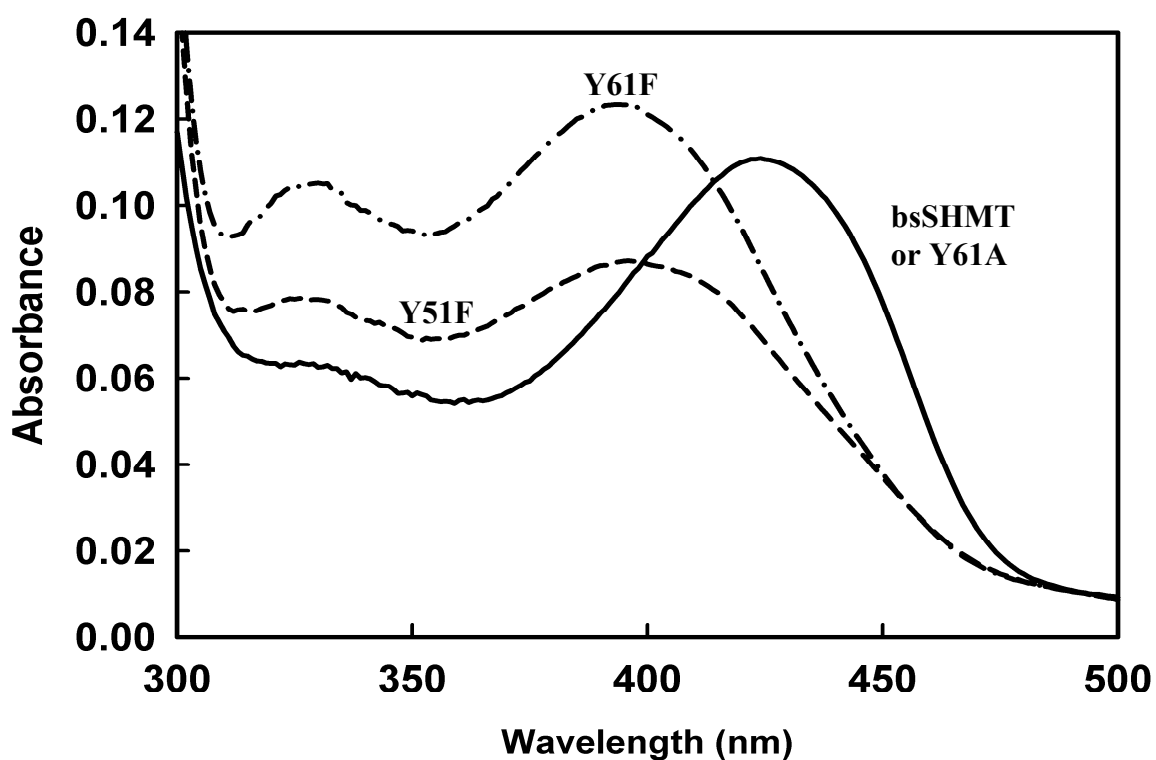


Fig 3.3 An overlay of internal aldimine spectra of bsSHMT, Y51F, Y61F and Y61A.

All the spectra were recorded in 50 mM potassium phosphate buffer, pH 7.4, containing 1 mM EDTA, 1 mM 2-ME at 1 mg ml⁻¹ of protein concentration.

The visible spectrum of Y51F and Y61F was recorded in 50 mM potassium phosphate buffer, pH 7.4, containing 1 mM EDTA, 1 mM 2-ME at 1 mg ml⁻¹ concentration. NaCNBH₃ (1 mM) was added to the enzymes and spectra were re-recorded. With bsSHMT (1 mg ml⁻¹), the reaction proceeds to completion in 5 min (Fig 3.4a). Although Y51F and Y61F bsSHMT could be reduced by NaCNBH₃, the time required for completion of the reaction was 30 min (Fig 3.4b).

In addition to NaCNBH₃ reduction, interaction with inhibitors like MA, have also been used to examine the changes in the active site environment of PLP-enzymes (Jala *et al.*, 2003a). Spectrum of bsSHMT and Tyr mutants (1 mg ml⁻¹) was recorded in 50 mM potassium phosphate buffer, pH 7.4, containing 1 mM EDTA, 1 mM 2-ME (Fig 3.5). MA (2 mM and 10 mM) was added to bsSHMT and Y51F bsSHMT, respectively and spectra recorded in the range of 300-500 nm. Addition of MA to bsSHMT results in its conversion to an oxime absorbing at 325 nm through an intermediate absorbing at 388 nm. The intermediate (λ_{\max} 388 nm) is formed within 30 s of the addition of MA to bsSHMT and the overall reaction takes 20 min for completion. This intermediate was suggested to be PLP (Fig 3.5a) (Baskaran, 1989; Acharya *et al.*, 1991). It is known that any disruption at the active site results in the loss of this intermediate and direct conversion of the PLP-Schiff's base to the oxime. In all the three mutants, addition of MA resulted in the formation of the oxime in approximately the same time (20 min) as in the case of bsSHMT.

However, the peak at 388 nm corresponding to the formation of the intermediate was not observed when MA (10 mM) was added to all Tyr mutants (Fig 3.5 b, c and d). The rate constants for the formation of oxime were measured using stopped-flow spectrophotometer as described in methods section. The spectrum was monitored at 396, 425, 388, and 325 nm. The rate constant for the conversion of the bsSHMT internal aldimine to the intermediate form was observed to be 1.6 s⁻¹ and the rate of conversion of the intermediate to the final product was 4x10⁻³ s⁻¹. The formation of oxime in the mutants occurred with similar rate constants of 5 x10⁻³ s⁻¹ for Y51F, 2 x10⁻³ s⁻¹ for Y61F and 1 x10⁻³ s⁻¹ for Y61A bsSHMT.

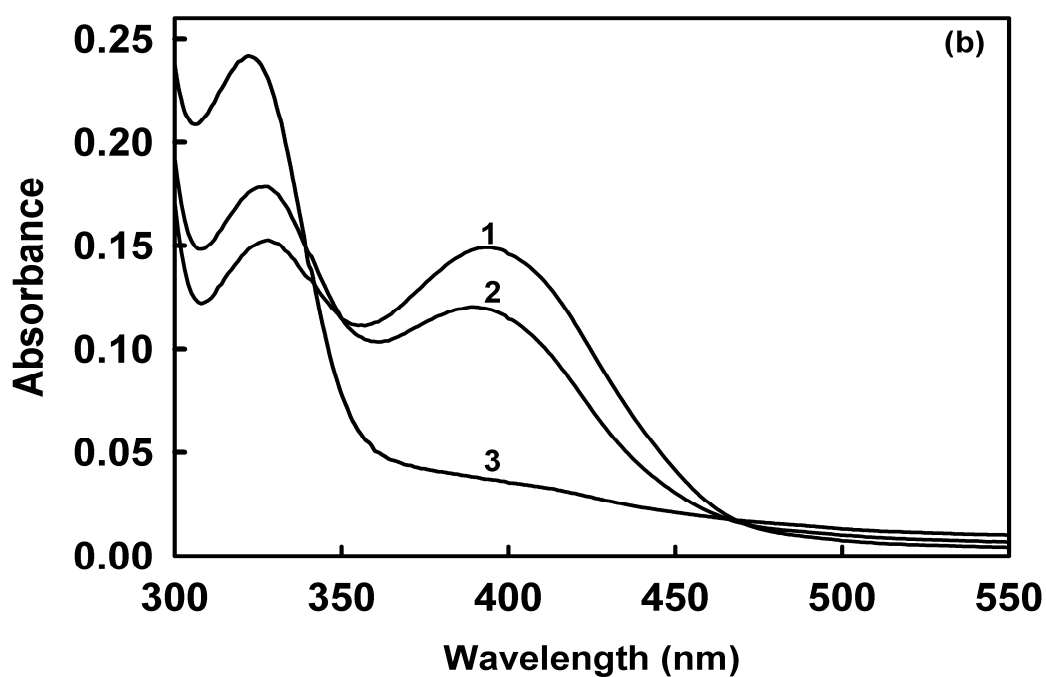
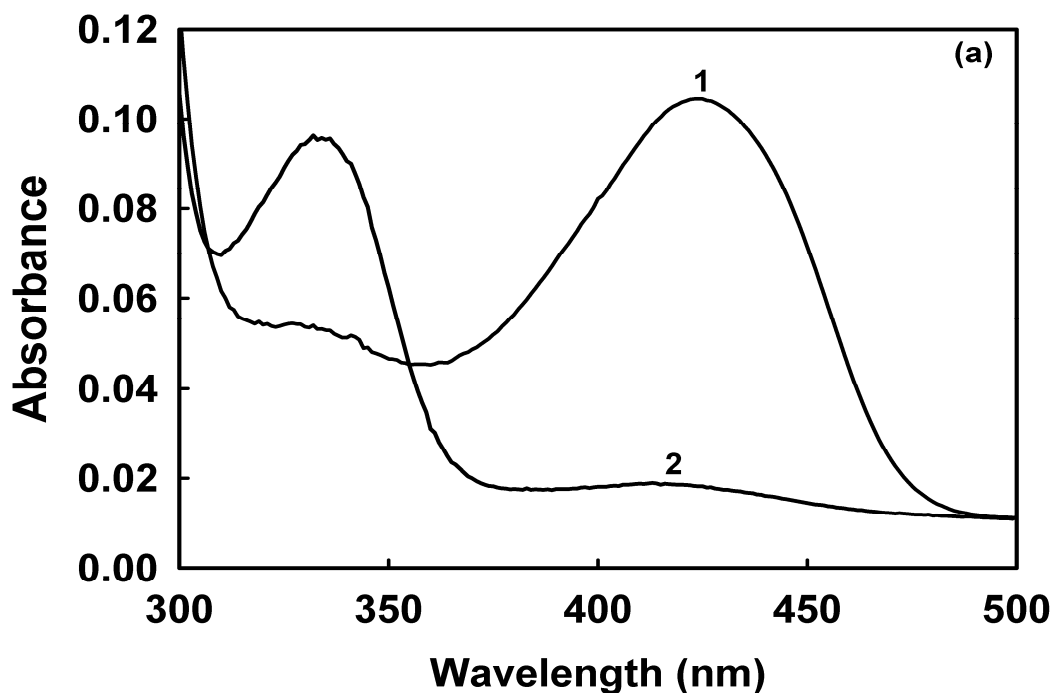


Fig 3.4: The reduction of bsSHMT and Y51F bsSHMT by NaCNBH₃.

(a) Curve 1: bsSHMT untreated (1mg ml⁻¹) in 50 mM potassium phosphate buffer, pH 7.4, containing 1 mM EDTA, 1 mM 2-ME. Curve 2: 5 min after addition of NaCNBH₃ (1 mM).

(b) Curve 1: Y51F bsSHMT untreated (1mg ml⁻¹) in 50 mM potassium phosphate buffer, pH 7.4, containing 1 mM EDTA, 1 mM 2-ME. Curve 2: 5 min after addition of NaCNBH₃ (1 mM). Curve 3: after 30 min.

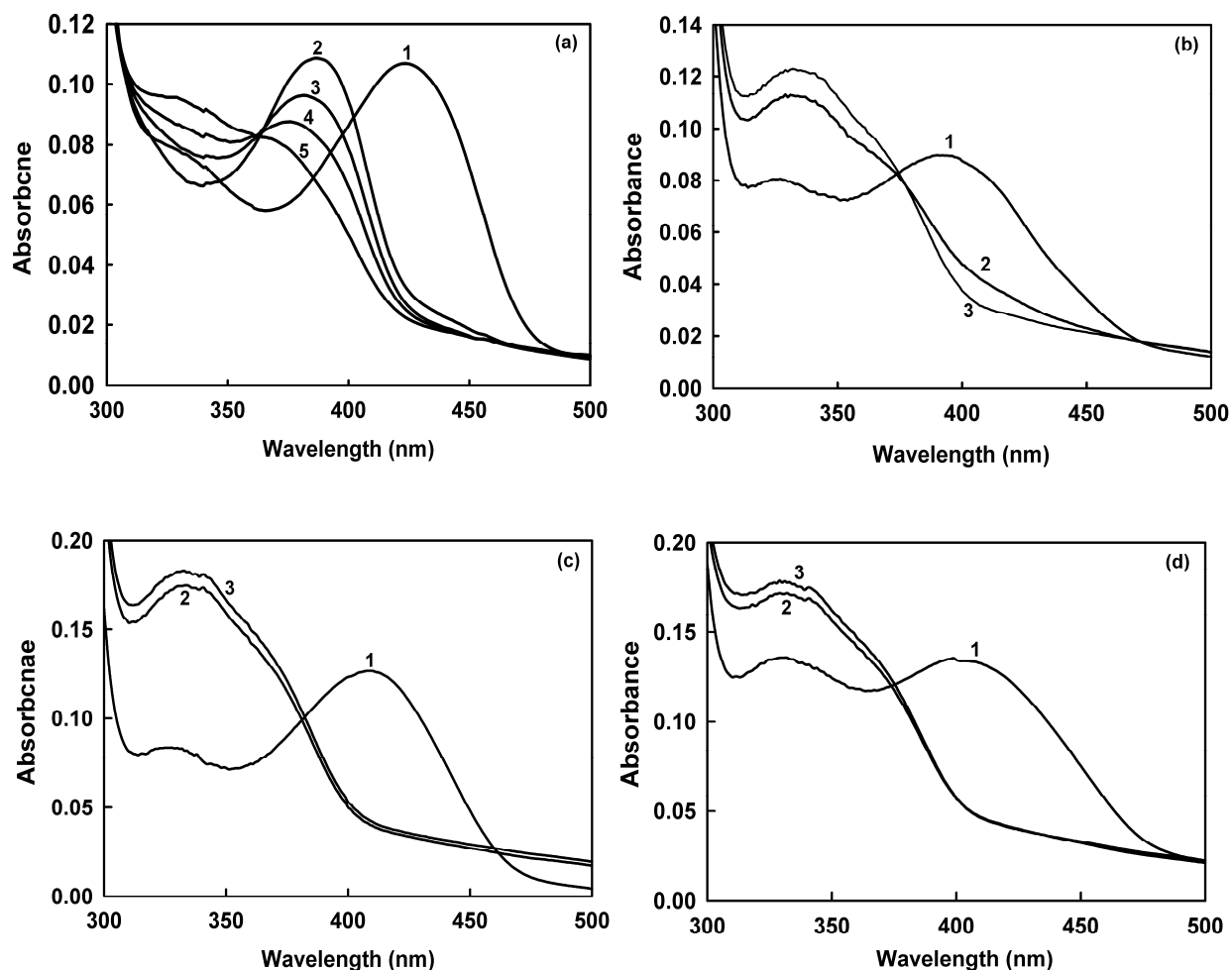


Fig 3.5: Interactions of bsSHMT and Tyr mutants with MA.

(a) Curve 1: The spectrum of bsSHMT (1 mg ml^{-1}) in 50 mM potassium phosphate buffer, pH 7.4, containing 1 mM EDTA, 1 mM 2-ME. Curve 2: in presence of 2 mM MA and the spectra were recorded after 30 s. Curve 3: 10 min. Curve 4: after 20min and curve 5: 30 min.

(b) Curve 1: The spectrum of Y51F bsSHMT (1 mg ml^{-1}) in 50 mM potassium phosphate buffer, pH 7.4, containing 1 mM EDTA, 1 mM 2-ME. Curve 2: on addition of MA (10 mM). Curve 3: after 20 min.

(c and d) Curve 1: The spectra were recorded for Y61F and Y61A bsSHMT (1 mg ml^{-1}) in 50 mM potassium phosphate buffer, pH 7.4, containing 1 mM EDTA, 1 mM 2-ME. Curve 1: upon addition of MA (10 mM). Curve 2: after 5 min, and curve 3 shows after 20 min.

Crystal structures of Y51F and Y61A bsSHMT

Crystals of Y51F and Y61A bsSHMT were obtained as previously standardized (Trivedi *et al.*, 2002). The superposition of all C_α atoms for the overall internal aldimine structures of Y51F and Y61A bsSHMTs are very similar to that of bsSHMT with an rms deviation of 0.11 and 0.19 Å. In bsSHMT, Y51 hydroxyl forms a hydrogen bond with the phosphate oxygen of PLP. In Y51F bsSHMT, this interaction is lost and the phenyl plane of F51 is rotated by 75° when compared to that of Y51. PLP is easily lost from Y51F due to this mutation. A water molecule is present in Y51F bsSHMT at the position corresponding to the OH of Y51.

The change in the orientation of F51 in the mutant induces a corresponding change in the orientation of the phenyl ring of Y61 by about 85° (Fig 3.6). A smaller change (18°) is also observed in the orientation of Y60. However, this change in orientation is probably due to the change in ψ angle for the Y60-Y61 peptide unit by about 26°. There is a small change in the orientation of E53, no other significant changes were observed in Y51F bsSHMT. In spite of these changes, the orientation of PLP in Y51F bsSHMT is the same as that of bsSHMT. Most of the observed changes appear to result from the loss of stabilizing interactions due to Y to F mutation.

In Y61A bsSHMT, the orientation of PLP is different by about 11° along N1-C3 axis when compared to that of bsSHMT (data not shown). However, there is no change in λ_{\max} of this mutant (425 nm, Fig 3.3). Also, there are no significant changes in the orientation of residues E53, Y51 and Y60 when compared to the bsSHMT. In contrast, the spectral changes are minimal in Y61A bsSHMT when compared to the Y51F and Y61F bsSHMT.

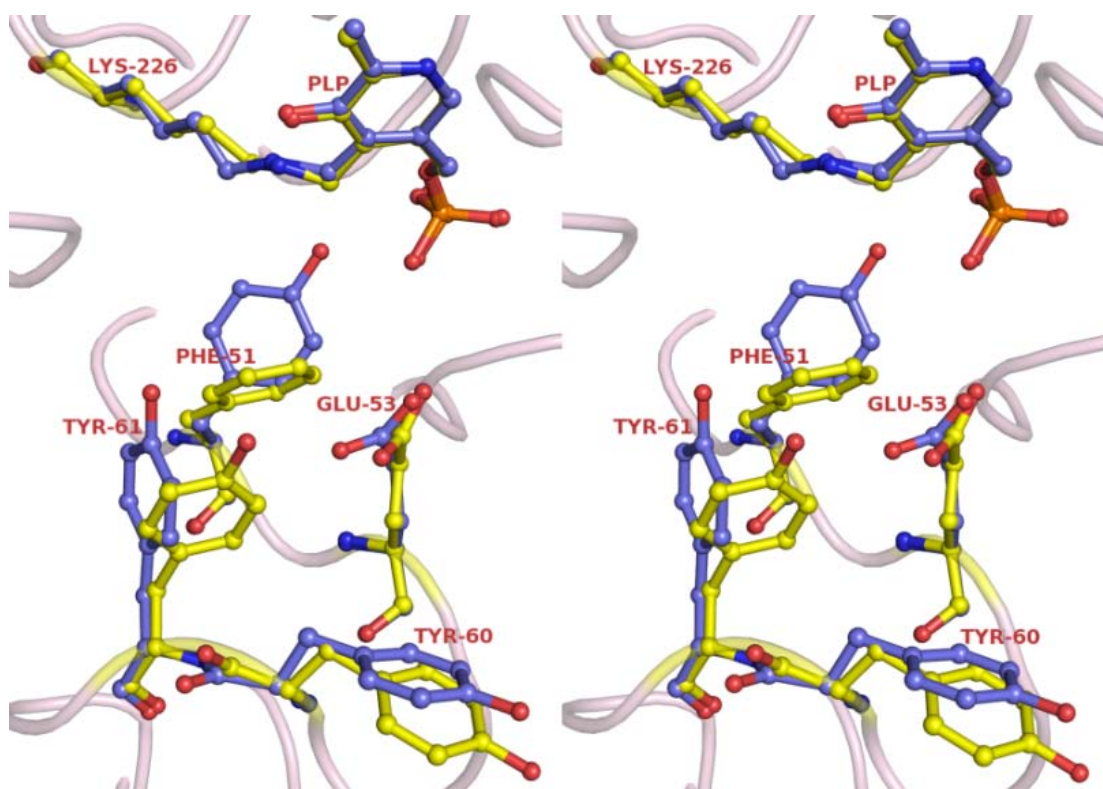


Fig 3.6: A superposition of the active sites of bsSHMT (blue) and Y51F bsSHMT (yellow) showing the differences in conformation of residues Y51 of wild-type and F51 of the mutant, E53, Y60 and Y61.

Spectral studies of bsSHMT and Tyr mutants on addition of D-Ala, L-Ser and Gly

Transamination reaction with D-Ala was examined by monitoring spectral changes in the enzyme absorbance at 425 nm on addition of 100 mM D-Ala using bsSHMT (1 mg ml⁻¹) and 200 mM for Tyr mutants in 50 mM potassium phosphate buffer, pH 7.4, containing 1 mM EDTA, 1 mM 2-ME at 37°C. In the case of bsSHMT, reaction with D-Ala resulted in a time-dependent decrease at 425 nm and a concomitant increase in absorbance at 325 nm due to the formation of PMP (Fig 3.7 a). The change in absorbance values at 425 nm were used to calculate pseudofirst order rate constant for bsSHMT for D-Ala. Y51F, Y61F and Y61A bsSHMT did not react at 100 mM D-Ala. Increase in D-Ala (200 mM) concentration did not change the spectral pattern for Tyr mutants (Fig 3.7 b, c and d). The increase in period of incubation to 30 or 60 min did not result in any reaction. These results suggest that mutation has completely affected the THF-independent activity and the mutants were inactive.

Addition of L-Ser or Gly to Y51F and Y61F bsSHMT resulted in a shift of λ_{\max} from 396 nm to 412 nm (Fig 3.8 c). There was no change in the λ_{\max} when these ligands were added to Y61A bsSHMT (Fig 3.8 d). Addition of THF or FTfH to Gly external aldimine of bsSHMT converts a large fraction of the molecules to the quinonoid form which maximally absorbs at 495 nm (Fig 3.8 b). However, addition of L-Ser and L-Ser +THF/FTfH does not show the formation of quinonoid intermediate (Fig 3.8 a). Unlike bsSHMT, addition of THF or FTfH to the Gly external aldimine of Y51F and Y61F bsSHMT's did not show any absorbance change at 495 nm (Fig 3.8 c), while Y61A bsSHMT showed a barely detectable peak at 495 nm (0.8% of that seen with bsSHMT) (Fig 3.8 d). This suggests that the formation of the quinonoid intermediate is affected in all the three mutants.

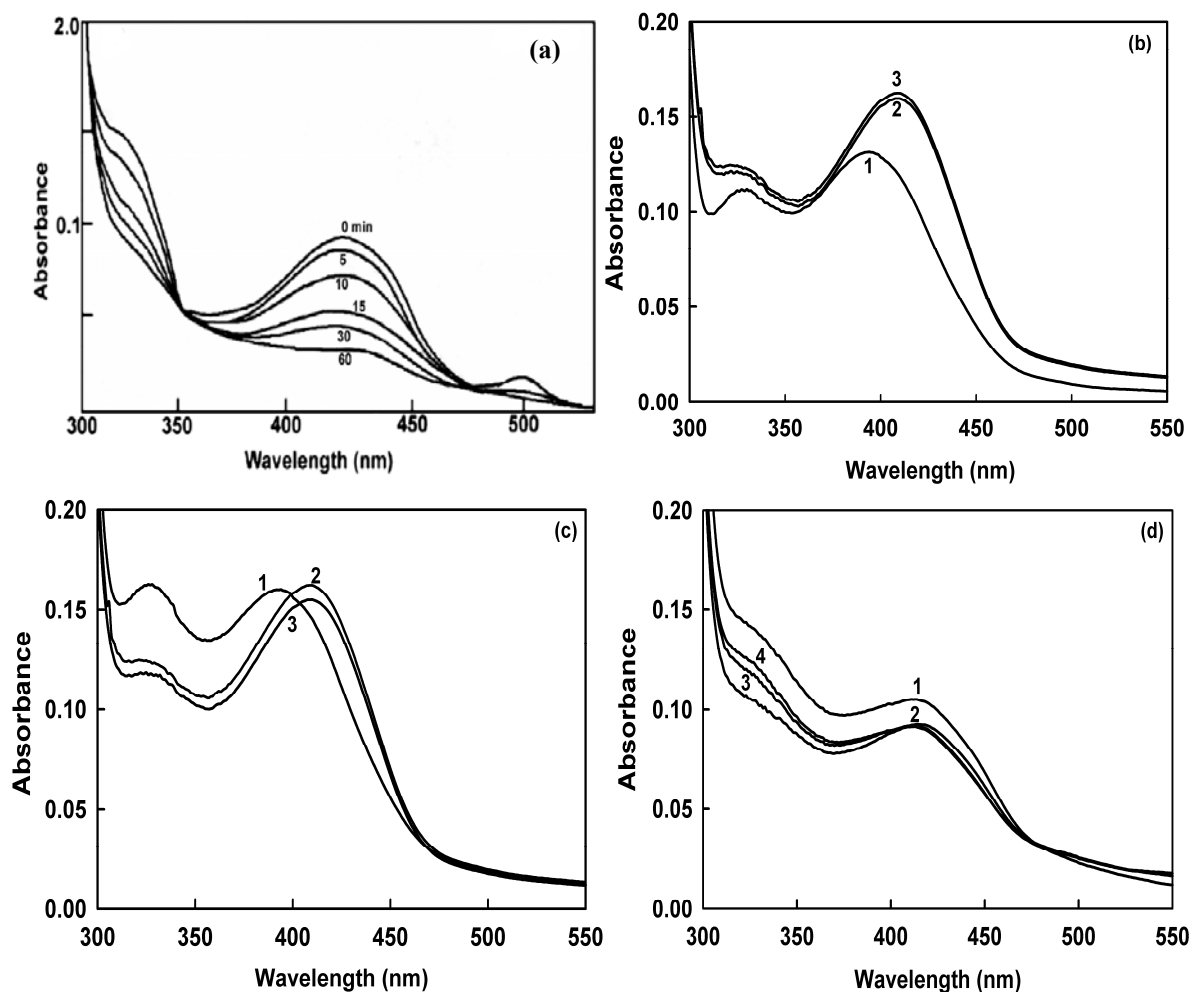


Fig 3.7: Transamination reaction catalyzed by bsSHMT and Tyr mutants.

(a) D-Ala (100 mM) was added to bsSHMT (1 mg ml^{-1}) and spectra were recorded at 37°C in 50 mM potassium phosphate buffer, pH 7.4, containing 1 mM EDTA, 1 mM 2-ME at the time intervals shown in the figure. The isobestic point can be seen at 350 nm (This Fig 3.7a is the same as Fig 1.6 and is shown here for comparison).

(b) Curve 1: Y51F bsSHMT (1 mg ml^{-1}) in 50 mM potassium phosphate buffer, pH 7.4, contains 1 mM EDTA, 1 mM 2-ME. Curve 2: 30 min after addition of D-Ala (200 mM) and curve 3: 60 min.

(c) Curve 1: Y61F bsSHMT (1 mg ml^{-1}) in 50 mM potassium phosphate buffer, pH 7.4, containing 1 mM EDTA, 1 mM 2-ME. Curve 2: 30 min after addition of D-Ala and curve 3: 60 min.

(d) Curve 1: Y61A bsSHMT (1 mg ml^{-1}) in 50 mM potassium phosphate buffer, pH 7.4, containing 1 mM EDTA, 1 mM 2-ME; after addition of 200 mM of D-Ala the time at which the spectra was recorded were 10 min (curve 2); 30 min (curve 3); 60 min (curve 4). All the experiments were carried out at 37°C . Spectra were recorded at in the range of 300-550 nm.

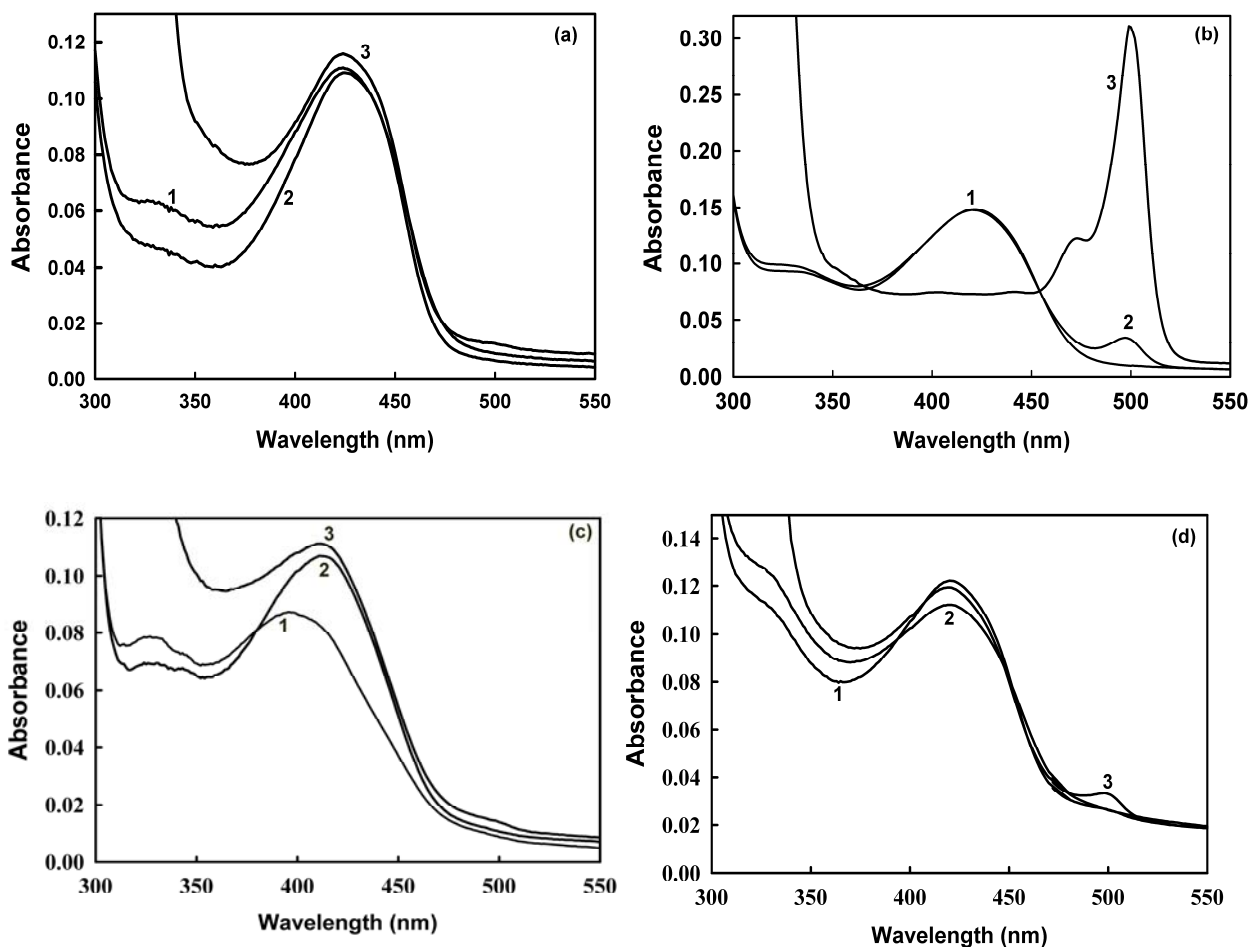


Fig 3.8: The spectral changes on addition of L-Ser/Gly and Gly + THF/FTHF to bsSHMT, Y51F, Y61F and Y61A bsSHMT.

(a) Curve 1: Spectrum of bsSHMT (1 mg ml^{-1}) in 50 mM potassium phosphate buffer, pH 7.4, containing 1 mM EDTA, 1 mM 2-ME. Curve 2: in presence of 50 mM L-Ser. Curve 3: in presence of 1.8 mM THF/1 mM FTTHF.

(b) Curve 1: Spectrum of bsSHMT 1 mg ml^{-1} in 50 mM potassium phosphate buffer, pH 7.4, containing 1 mM EDTA, 1 mM 2-ME. Curve 2: in presence of 50 mM Gly. Curve 3: addition of 1.8 mM THF/1 mM FTTHF to Gly binary complex.

(c) Curve 1: Spectrum of Y51F / Y61F bsSHMT 1 mg ml^{-1} in 50 mM potassium phosphate buffer, pH 7.4, containing 1 mM EDTA, 1 mM 2-ME. Curve 2: addition of 50 mM L-Ser/Gly. Curve 3: further addition of 1.8 mM THF/1 mM FTTHF.

(d) Curve 1: Spectrum of Y61A bsSHMT 1 mg ml^{-1} in 50 mM potassium phosphate buffer, pH 7.4, containing 1 mM EDTA, 1 mM 2-ME. Curve 2: on addition of 50 mM Gly; curve 2: further addition of 1.8 mM THF/1 mM FTTHF.

The visible CD ellipticity maximum at 425 nm of bsSHMT is reduced upon the formation of external aldimine with L-Ser or Gly (Jala *et al.*, 2000). The visible CD spectrum of bsSHMT and all Tyr mutants (1 mg ml⁻¹) were recorded in 50 mM potassium phosphate buffer, pH 7.4, containing 1 mM EDTA, 1 mM 2-ME in the range of 300-550 nm. The spectral changes on addition of L-Ser/Gly (50 mM) were also monitored. Y61A bsSHMT exhibited an ellipticity maxima at 425 nm (Fig 3.9 a), similar to that of bsSHMT (Fig 3.9 b). No ellipticity was observed in the visible region with Y51F or Y61F bsSHMT mutants (Fig 3.9 a).

Addition of L-Ser (50 mM) to Y61A bsSHMT caused a decrease in ellipticity at 425 nm (Fig 3.9 c), as similar to that seen with bsSHMT (Fig 3.9 b). This observation suggests that Y61A can form an external aldimine. Unlike in bsSHMT and Y61A bsSHMT, Y61F and Y51F bsSHMT did not show any change in their spectra on addition of L-Ser (Fig 3.9 d). However, addition of Gly to Y51F bsSHMT results in the appearance of a peak at 343 nm. This peak indicates the formation of a gem-diamine (Fig 3.9 d).

Crystal structures of L-Ser and Gly binary complex

Crystal structures of Y51F and Y61A bsSHMT in presence of L-Ser and Gly were determined as described in methods. Although the overall structure of Y51F bsSHMT-Gly is very similar to that of bsSHMT-Gly with an rms deviation of 0.15 Å for the superposition of all C_α atoms, significant differences were observed in the PLP orientation and ligand binding properties. In Y51F bsSHMT-Gly complex, PLP is found in its gem-diamine form which is consistent with the observation of visible CD ellipticity maximum at 333 nm (Fig 3.9 d). However, the density connecting PLP to Gly is weaker compared to PLP-Lys (Fig 3.10) also, only the carboxyl of Gly has good density. These observations coupled with spectroscopic studies suggest that the structure corresponds to gem-diamine form. The conformations of F51, Y60, Y61 and E53 are very similar in Y51F and Y51F bsSHMT-Gly, although they are different from those seen in wild-type internal and external aldimines.

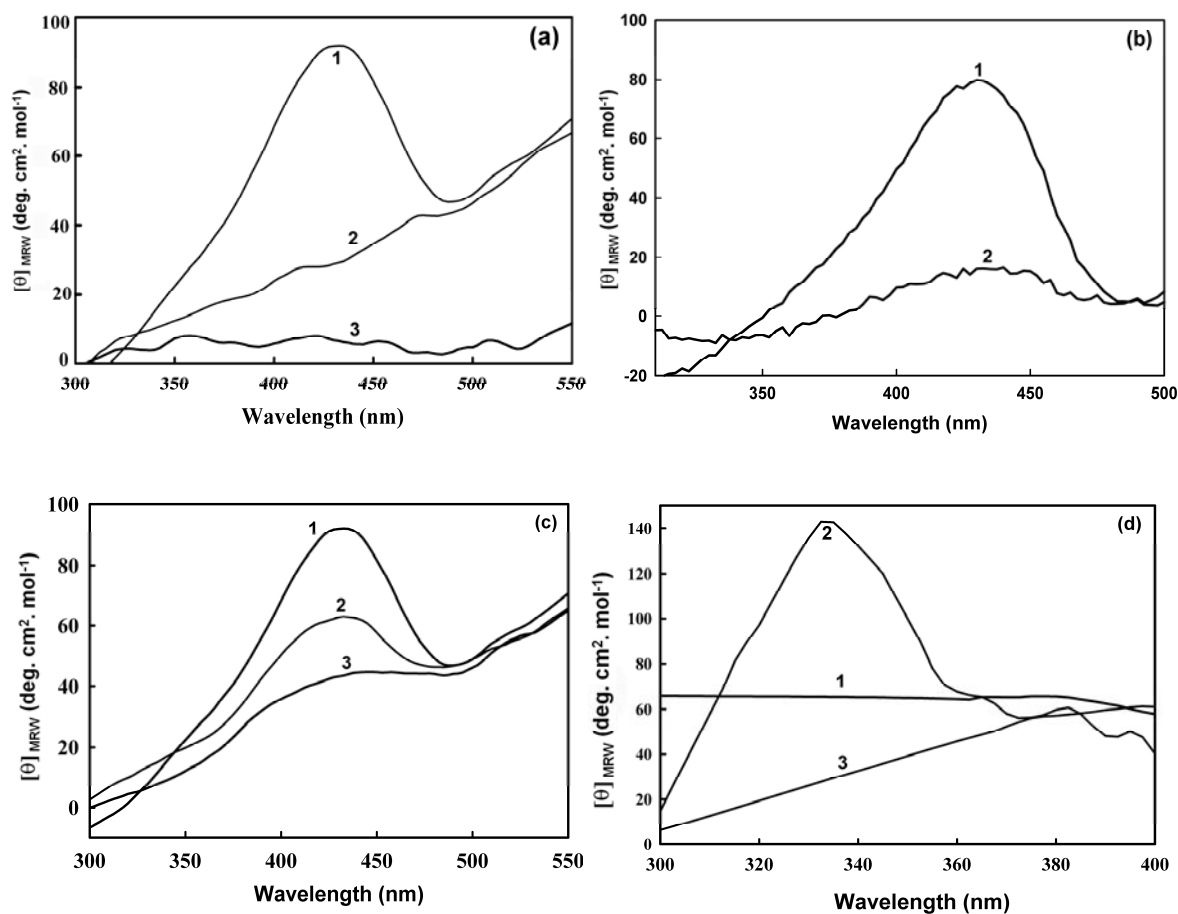


Fig 3.9: The visible CD spectrum of bsSHMT and Tyr mutants and changes on addition of L-Ser and Gly.

(a) Curve 1: Spectrum of Y61A; curve 2: Y61F; curve 3: Y51F recorded in 50 mM potassium phosphate buffer, pH 7.4, containing 1 mM EDTA, 1 mM 2-ME in the range of 300 to 550 nm with 1 mg ml^{-1} concentration.

(b) Curve 1: The visible CD spectrum of bsSHMT recorded in the range of 300 to 500 nm at 1 mg ml^{-1} concentration. Curve 2: in presence of L-Ser (50 mM) to bsSHMT.

(c) Curve 1: Visible CD spectrum of Y61A bsSHMT (1 mg ml^{-1}). Curve 2: and in presence of L-Ser (50 mM). Curve 3: on addition of Gly. Spectra were recorded in the range of 300 to 550 nm in 50 mM potassium phosphate buffer, pH 7.4, containing 1 mM EDTA, 1 mM 2-ME.

(d) Curve 1: The visible CD spectrum of Y51F bsSHMT (1 mg ml^{-1}). Curve 2: in presence of Gly (50 mM). Curve 3: on addition of 50 mM L-Ser. Spectra were recorded in the range of 300 to 400 nm in 50 mM potassium phosphate buffer, pH 7.4, containing 1 mM EDTA, 1 mM 2-ME.

Another interesting observation was that the phosphate group of PLP had two distinct conformations (Fig. 3.10). The additional conformation may be attributed to the loss of hydrogen bonding between Y51F and the phosphate oxygen. A few water molecules could be fitted with partial occupancy close to the oxygen atoms of the original phosphate

In Y61A bsSHMT-Gly complex, Gly is bound to PLP as an external aldimine. The position of Gly and orientation of PLP are very similar to those of bsSHMT-Gly complex. The crystal structures of Y51F and Y61A bsSHMT-Ser complex showed that L-Ser forms a clear external aldimine with PLP. The conformations of F51 and Y61 in Y51F bsSHMT-Ser are similar to those of Y51F bsSHMT-Gly. The external aldimine may be stabilized by interactions of L-Ser hydroxyl with E53 and surrounding water molecules.

Crystal structure of L-allo Thr binary complex

Crystal structure of Y51F and Y61A bsSHMT-L-*allo* Thr were obtained by co-crystallizing the mutants with 10 mM L-*allo* Thr. A similar procedure was followed for obtaining the L-*allo* Thr binary complexes as that of L-Ser/Gly complexes (Trivedi *et al.*, 2002). In bsSHMT, L-*allo* Thr is cleaved to Gly and hence the density corresponding to only Gly was observed when the crystals were obtained in presence of L-*allo* Thr. The most interesting observation made in Tyr mutants is that an intact L-*allo* Thr is bound to PLP and it forms an external aldimine. Except for the bound ligand, the structures of Y51F and Y61A bsSHMT L-*allo* Thr complexes (Fig 3.11 and 3.12) are very similar to that of bsSHMT-Gly(L-*allo* Thr) (crystals of bsSHMT obtained in the presence of L-*allo* Thr) with an rms deviation of 0.11 and 0.19 Å, respectively. The position and orientation of L-*allo* Thr is similar to that of L-Ser in Y51F and Y61A bsSHMT-Ser complexes with O γ interacting with E53 and H122 (Fig 3.9). C γ of L-*allo* Thr has a hydrophobic interaction with the side chain of S172.

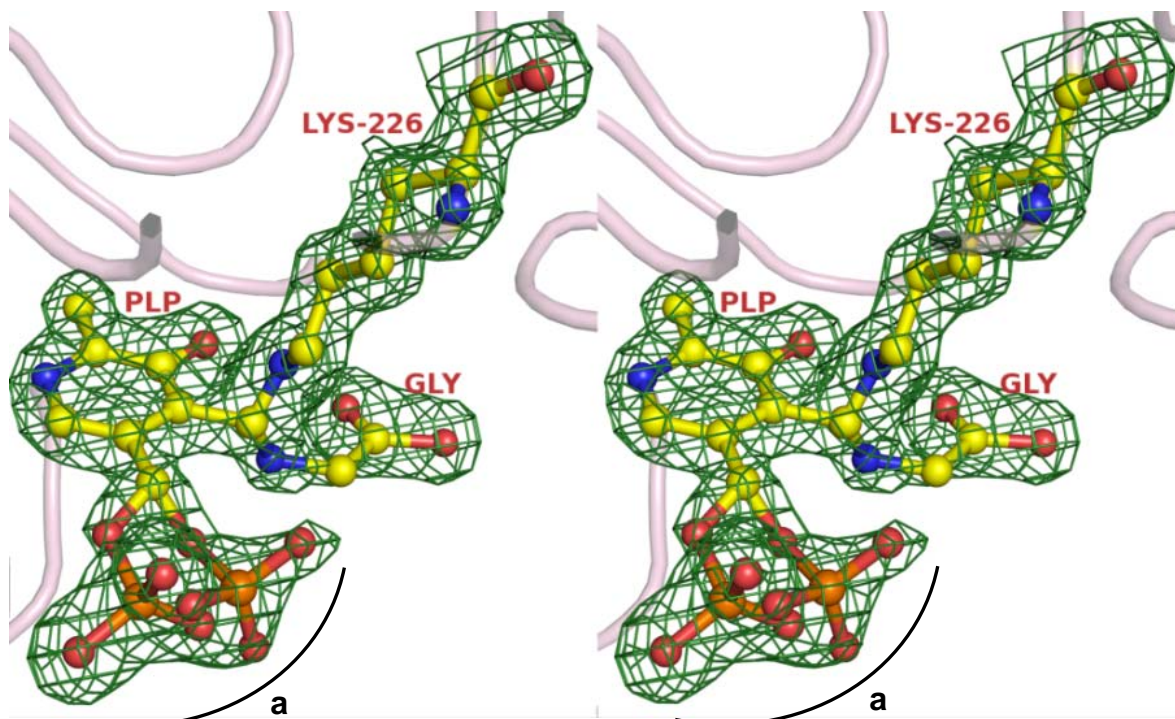


Fig 3.10: A stereo diagram showing an electron density for gem- diamine in Y51F bsSHMT-Gly complex.

PLP is bonded to both Lys 226 and Gly amino groups. The phosphate group (a in diagram) can have the flexibility of being present in the either of the two multiple conformation.

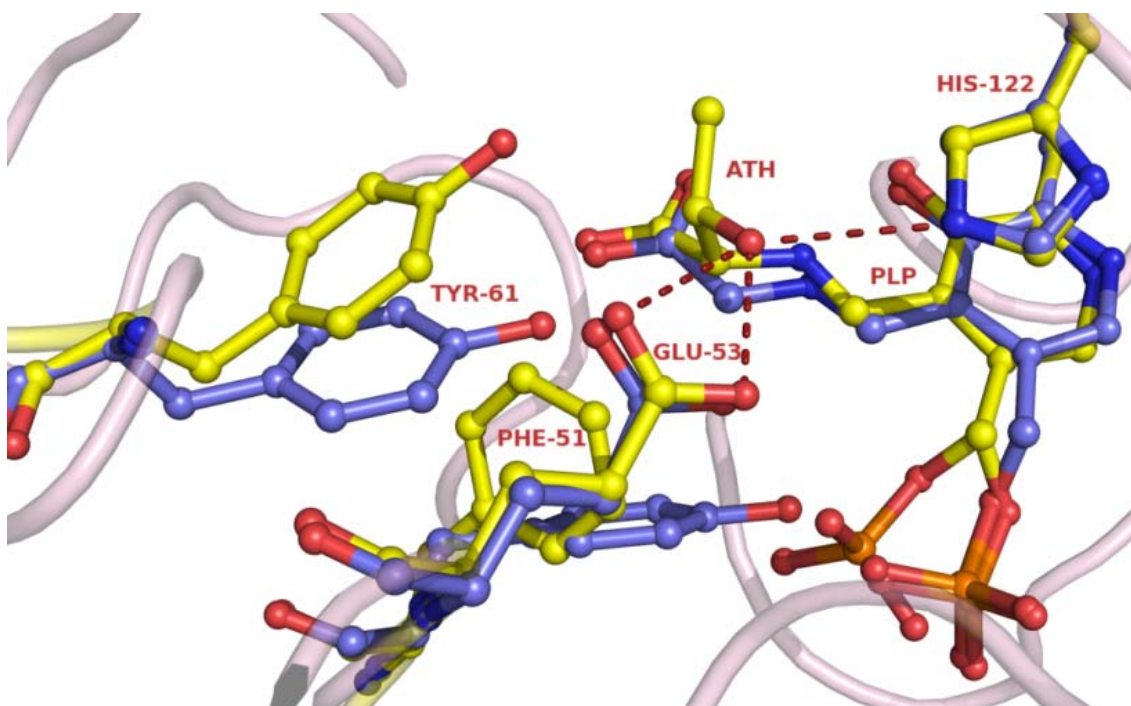


Fig 3.11: A superposition of Y51F bsSHMT (yellow) and bsSHMT (blue) complexes obtained in the presence of *L-allo* Thr.

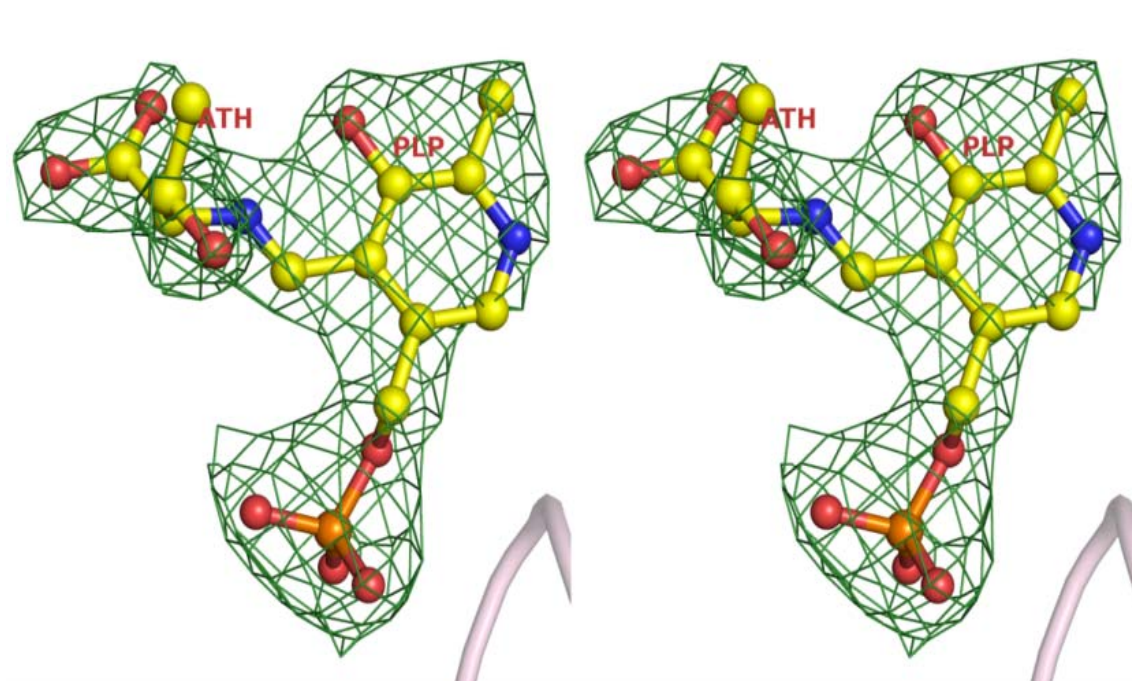


Fig 3.12: The electron density corresponding to *L-allo* Thr in Y61A bsSHMT.

In Y51F bsSHMT-*allo* Thr complex (Fig 3.11), the phosphate of PLP is in two conformations as in Y51F bsSHMT-Gly. In Y61A bsSHMT, the density for the side chain of *L-allo* Thr is weaker when compared to that of Y51F bsSHMT-*allo* Thr. These are the first two mutant structures of SHMT in which *L-allo* Thr is bound to PLP as an external aldimine and is not further converted to Gly and acetaldehyde. Mutation of Y51 and Y61 leads to the loss of THF-independent reaction. Therefore, these residues might be directly involved in *L-allo* Thr to Gly conversions.

Discussion

It was proposed that, the classical retroaldol mechanism for the cleavage of 3-hydroxyl amino acids begins with an abstraction of hydroxyl proton either by Glu or His at the active site (Schirch, 1982; Szebenyi *et al.*, 2004). In addition to the hydroxyl proton, active site Lys and Tyr residues have been invoked as C_α proton abstractors in several PLP-dependent enzymes, such as AAT (Ziak *et al.*, 1990; Toney and Kirsch, 1991b; Ziak *et al.*, 1993), 5-aminolevulinate synthase (Tan *et al.*, 1998) and alanine racemase (Sun and Toney, 1999). Structural and mutational analysis of active site Lys mutant, K226M bsSHMT (Chapter 1), H147 and E74Q scSHMT (Jagath *et al.*, 1997b; Jala *et al.*, 2000) demonstrated that these residues were not involved in hydroxyl or C_α proton abstraction (Contestabile *et al.*, 2000). As evident from the structure of bsSHMT and its substrate complexes (Fig 3.2), Y51 and Y61 are the other possible candidates for C_α proton abstraction.

Both Y51 and Y61 were mutated to Y51F, Y61A and Y61F bsSHMT. Mutations result in a complete loss of THF-dependent and -independent activities (Table 3.1) the only example of loss of both the activities of SHMT. Mutation of Y51 drastically affected the binding of PLP, possibly as a consequence of a change in the orientation of the phenyl ring in Y51F bsSHMT. Y51F bsSHMT, as isolated has less amount of PLP suggesting that mutation has weakened the PLP-enzyme interaction. However, the mutant enzyme could be completely reconstituted with PLP. NaCNBH₃ reduction and MA interaction with Y51F bsSHMT suggest that the mutants were able to interact with MA without forming an intermediate. This observation suggests that the accessibility of the Schiff's base to the reducing agent is affected due to the mutation. Interaction of MA with Tyr mutants also supports this

observation. These results suggest that the mutant enzymes are in internal aldimine form, however, the environment of PLP is different from that of bsSHMT. As a result of this change there was an alteration in the λ_{\max} of the internal aldimine (396 nm) of Y51F bsSHMT (Fig 3.3). A similar change in PLP-orientation was also observed in Y121F mutant of ALS (Tan *et al.*, 1998), K258H AAT (Ziak *et al.*, 1993) K226M bsSHMT (Chapter 1), K229R eSHMT (Schirch *et al.*, 1993a, b). The loss of characteristic ellipticity maximum at 425 nm for Y51F bsSHMT (Fig 3.9 a) and absence of intermediate (Fig 3.7 b) upon interaction with MA. Similar spectral changes are observed in Y61F bsSHMT. Since this mutant enzyme did not crystallize in spite of many efforts, the related structural changes could not be ascertained.

Spectral studies on addition of L-Ser/Gly+THF suggest that all the Tyr mutants were incapable of forming a quinonoid intermediate (Fig 3.8 c, d). Visible CD studies on Y61A bsSHMT suggest that Y61A bsSHMT is capable of forming an external aldimine structure (Fig 3.9 c). This conclusion is also supported by the X-ray structures of the binary complexes of Y61A bsSHMT with L-Ser and Gly. However, visible CD studies of Y51F bsSHMT in presence of Gly suggest the formation of a gem-diamine (Fig 3.9 d). This observation was also confirmed by Gly binary structure of Y51F bsSHMT, which suggest that the density connecting PLP-Gly is weaker, compared to PLP-Lys (Fig 3.10). In addition, only the carboxyl of Gly has good density.

In addition to these observations phosphate group of PLP is in two distinct conformations (Fig 3.10). As a result of these changes, PLP orientation is different in Y51F bsSHMT-Gly when compared to that of wild-type internal and Gly external aldimines. The plane of the pyridine ring is rotated by about 22° along the C2-N1 axis. As a consequence, the C5A atom of PLP moves by 1.66 Å. The change in the orientation of PLP and the conformation of F51, Y60, Y61 and E53 could lead to the Gly being present predominantly in the gem-diamine form.

Mechanism of THF-independent cleavage of L-allo Thr by bsSHMT

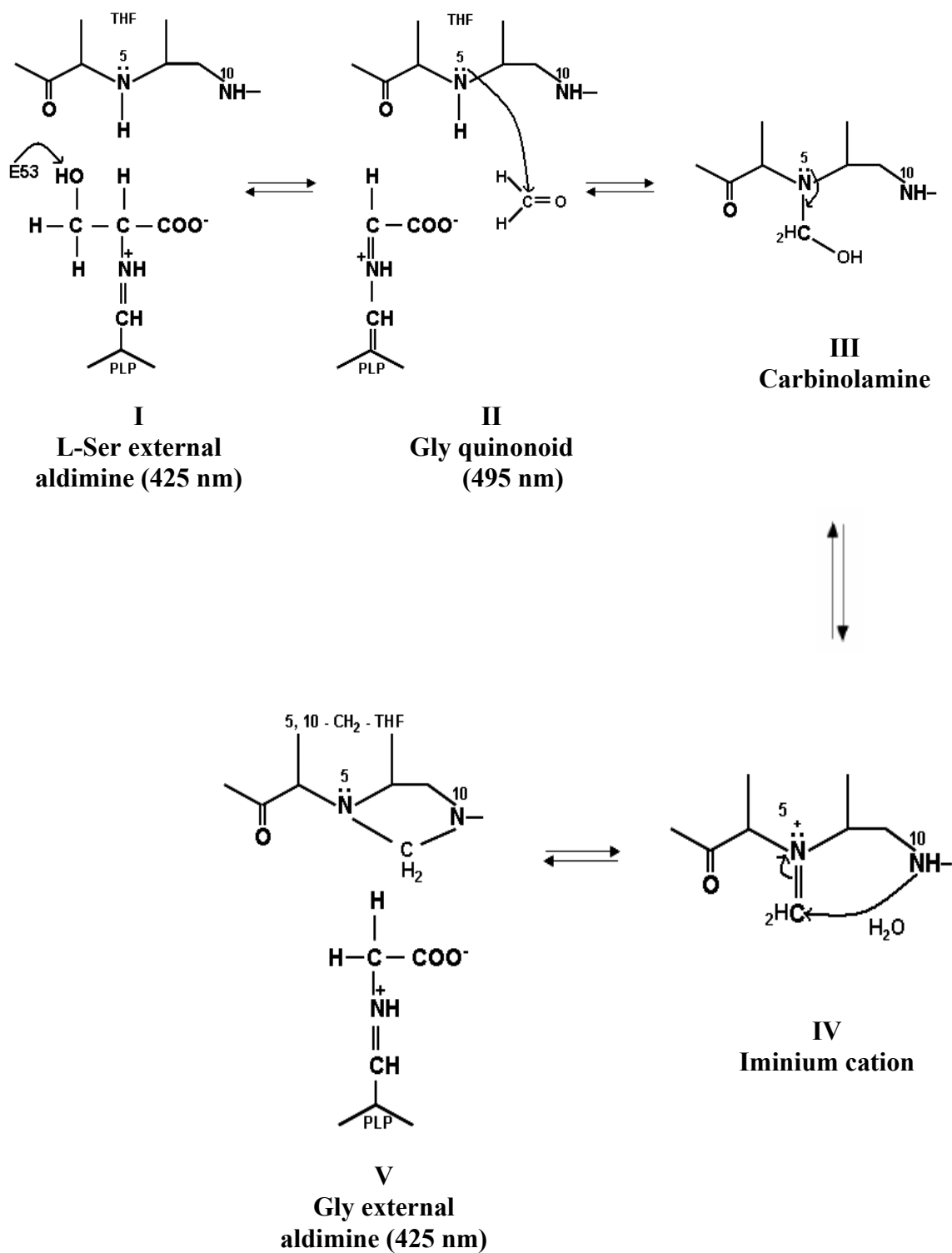
It has been proposed that the conversion of L-Ser to Gly by SHMT takes place in the presence of THF by a direct displacement mechanism (Trivedi *et al.*, 2002) (Scheme 3.1). The cleavage of L-*allo* Thr to Gly is THF-independent. The main difference between L-Ser and L-*allo* Thr is the substitution of C_β - hydrogen in L-Ser by a methyl group in L-*allo* Thr. It was proposed earlier that the THF-independent conversion of β-hydroxy amino acids such as L-*allo* Thr by SHMT takes place by a retroaldol cleavage mechanism (Scheme 3.1c) (Schirch and Szebenyi, 2005). In this mechanism, the first step is an abstraction of proton from the side chain hydroxyl group. The crystal structure of bsSHMT-Ser complex suggests that H122 and E53 are well positioned for abstracting the proton (Trivedi *et al.*, 2002).

Mutation of either H122 or E53 in bsSHMT did not affect the cleavage of L-*allo* Thr, although the physiological activity of SHMT was completely abolished (Jagath *et al.*, 1997b; Jala *et al.*, 2000). This shows that neither H122 nor E53 are involved in the abstraction of the proton from the side chain hydroxyl group. Superposition of bsSHMT-Gly-FTHF ternary complex with Y51F and Y61A bsSHMT L-*allo* Thr complex shows that the additional methyl group at C_β is in severe steric clash with FTHF molecule. This may prevent binding of FTHF/THF to SHMT, when L-*allo* Thr external aldimine is formed and the cleavage occurs in the absence of THF.

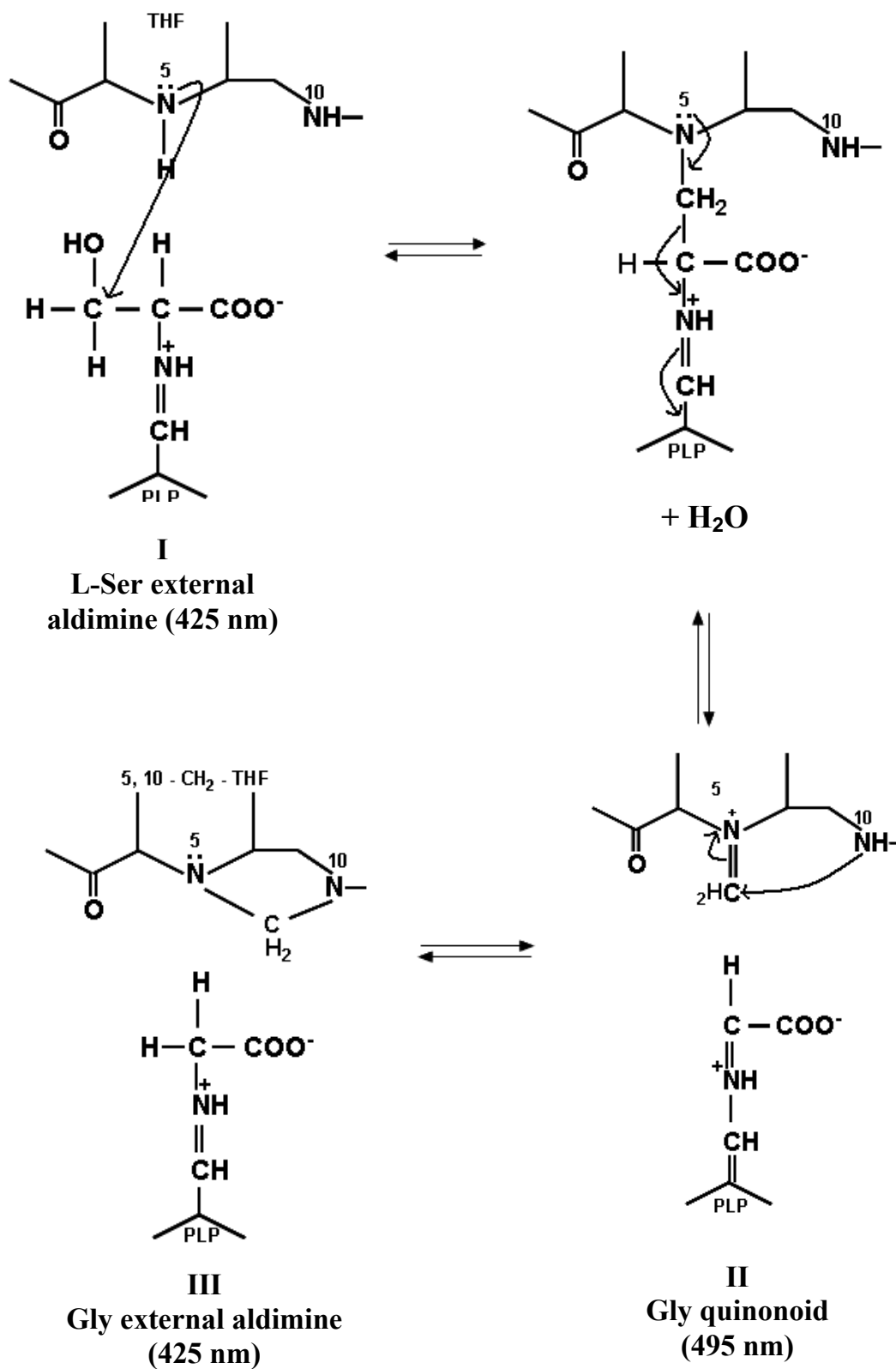
Earlier studies have shown that there is a linear relationship between the rate of THF-independent cleavage of β-substituted substrates and hydration equilibria of the product aldehyde, demonstrating that the cleavage is accelerated by the presence of electron donating substituent at C_β (Webb and Matthews, 1995). It was shown that amongst all β-hydroxy amino acid substrates, L-Ser and α-methyl-L-Ser are the slowest reactants (10⁵ fold slower) for SHMT in the absence of THF (Chapter 2, Table 2.1) (Webb and Matthews, 1995). However, the question that still remains unanswered is why Y61 cannot abstract C_α proton from L-Ser when THF is not present. The OH of L-Ser has a lower radius than CH₃ group of L-*allo* Thr, which facilitates higher hydration. This makes C_α-C_β bond energetically stable and hence the removal of C_α proton by Y61 would be unfavorable.

Scheme 3.1: Reaction mechanisms proposed for THF-dependent cleavage of L-Ser and THF-independent cleavage of 3-hydroxy amino acids by SHMT.

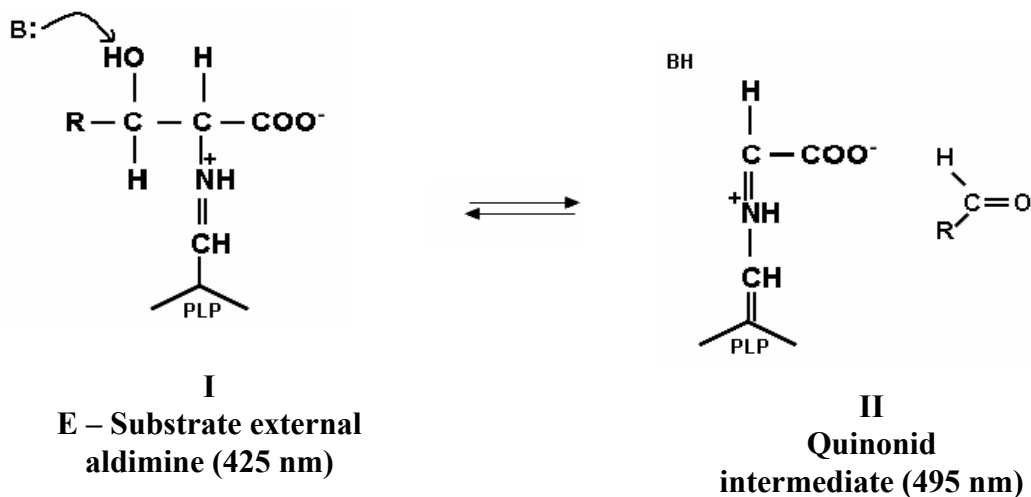
(a) Retroaldol mechanism. The wavelength maximum is shown next to the intermediate in the scheme such as 425, 495 nm.



Scheme 3.1 (b): Direct displacement mechanism. The wavelength maximum is shown next to the intermediate in the scheme such as 425, 495 nm.

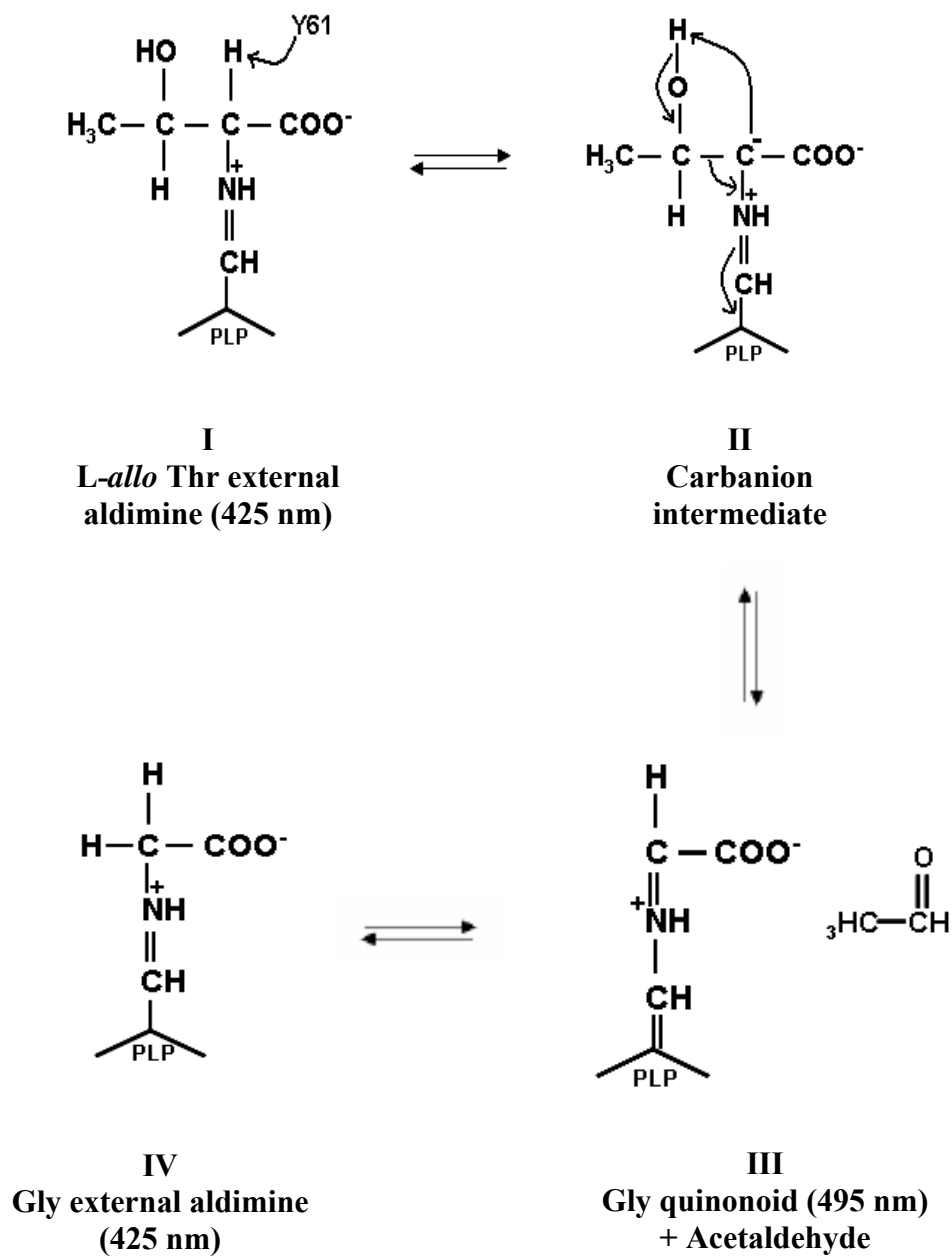


Scheme 3.1 (c): Retroaldol mechanisms proposed for the cleavage of 3-hydroxy amino acids. The wavelength maximum is shown in parenthesis. B is the unprotonated amino acid base and BH is the protonated amino acid base at the active site.



The studies presented here show that mutation of either Y51 or Y61 affects the THF-independent cleavage of *L-allo* Thr (Table 3.1). Examination of the active site geometry in bsSHMT (Fig 3.1) and Y51F and Y61A mutants show that Y51 and Y61 are not placed suitably for the removal of proton from the hydroxyl group of *L-allo* Thr. However, they may have a role in abstracting proton from the C_α atom of *L-allo* Thr. The hydroxyl group of Y51 is at a distance of 3.6 Å and 3.8 Å from C_α of Gly and Ser, respectively, in bsSHMT. Of the two residues, Y51 is unlikely to be involved in proton abstraction from C_α of the bound ligand due to its larger distance and improper geometry. In contrast, the OH of Y61 is at a distance of 3.3 Å and 3.2 Å from C_α of Gly and Ser, respectively. Y61 may be therefore involved in C_α proton abstraction in the THF-independent reaction. Y51 to F mutation leads to a change in the orientation of Y61 and increases the distance between the OH of Y61 and C_α of the ligand. In Gly, L-Ser and *L-allo* Thr complexes of Y51F bsSHMT, the OH of Y61 and C_α of bound ligand are at distances 4.97, 4.39 and 4.39 Å, respectively. This might lead to the loss of *L-allo* Thr cleavage activity of Y51F bsSHMT. It may therefore, be concluded that Y51 is important for PLP binding and proper positioning of Y61, while Y61 is involved in the abstraction of the proton from C_α carbon of *L-allo* Thr. Based on these observations a possible mechanism for SHMT catalyzed cleavage of *L-allo* Thr is proposed (Scheme 3.2).

In this mechanism (Scheme 3.2), after the formation of *L-allo* Thr external aldimine (I), the cleavage is triggered by the abstraction of C_α proton by Y61 leading to the formation of a carbanion intermediate (II). This is followed by an internal rearrangement of proton from the side chain hydroxyl group of *L-allo* Thr to C_α and concomitant cleavage of C_α-C_β bond. This bond cleavage leads to the release of acetaldehyde leaving behind Gly quinonoid intermediate (III). Reprotonation of QI at C4 converts it into Gly external aldimine (IV). This is followed by the nucleophilic attack of ε - amino group of active site Lys on Gly external aldimine leading to the internal aldimine and release of Gly. These results suggest that the catalysis of 3-hydroxy amino acids could proceed via abstraction of C_α proton rather than the hydroxyl proton by Y61 of bsSHMT.



Scheme 3.2: Proposed mechanism for cleavage of L-*allo* Thr by bsSHMT.

Chapter 4

The interaction of bsSHMT with
inhibitors from extracts of various
spices

SHMT is an important enzyme of the thymidylate synthase cycle (Fig I.17) and it plays a crucial role in the inter-conversion of folate coenzymes. It catalyzes the formation of 5, 10-methylene THF, which serves as a key intermediate in the biosynthesis of methionine, thymidylate, purines and formyl t-RNA (Matthews and Drummond, 1990). Increase in the activity, altered kinetics of SHMT in the neoplastic tissues along with enhanced DNA synthesis has suggested that SHMT might be a target for cancer chemotherapy (Bertino *et al.*, 1963; Kumar *et al.*, 1976; Thorndike *et al.*, 1979; Snell, 1984; Renwick *et al.*, 1998; Appaji Rao *et al.*, 2000). It is well established that SHMT is inhibited by several of its substrate (L-Ser/Gly) analogues (Baskaran *et al.*, 1989a; Baskaran *et al.*, 1989b; Acharya *et al.*, 1991; Acharya and Rao, 1992). Most of these interact with the cofactor and the enzyme is inactivated by the formation of an apo-enzyme. The interactions of these compounds have been studied extensively by spectral methods and it has lead to insights into the active site environment. However, the crystal structure of the enzyme complexed with these inhibitors has not been determined so far.

In addition, a few inhibitors have been used to study the differences at the active site environment of wild-type and mutant enzymes (Jala, 2002). MA is one of the good examples, which has been used for such a study. Crystal structures of bsSHMT mutants showed significant changes at the active site, specifically in terms of change in PLP orientation and conformation of the active site residues. Since, MA failed to interact with a few mutants of bsSHMT, AAA was chosen to study differences at the active sites of these mutants. Earlier studies have also suggested that substitution of hydrogen by a -COOH in hydroxylamine (HA) results in increased inhibitory effect (Baskaran *et al.*, 1989b; Acharya *et al.*, 1991). In addition to these studies, screening of new compounds from spices, which are known to have anti-carcinogenic effect, would be useful in the identification of inhibitors. In this chapter an attempt was made to screen the inhibitors for bsSHMT by conventional screening for inhibitors from several spice sources. In addition to this, docking of FTHF analogues which are commercially available were also carried out on the native and ternary complex of bsSHMT to determine the best fit molecule.

Results

The interaction of bsSHMT and its active site mutants with MA

MA was used to study the differences at the active site of wild-type and the mutant SHMTs (Jala, 2002). The interaction of MA with bsSHMT, K226M, K226Q, Y51F, Y61F and Y61A bsSHMT are described in earlier chapters (Chapter 1, 2 and 3). The crystal structure of E53Q bsSHMT also shows changes at the active site. Hence, it was of interest to study the interaction of MA with E53Q bsSHMT. Towards this objective, spectral studies were carried out with bsSHMT/E53Q bsSHMT (1 mg ml^{-1}) and 2 mM MA in 50 mM potassium phosphate buffer, pH 7.4, containing 1 mM EDTA, 1 mM 2-ME. bsSHMT interacts with MA by forming an intermediate at 388 nm (Fig 4.1 a). This intermediate is converted slowly and results in the formation of the final oxime product absorbing at 325 nm. Addition of MA to E53Q bsSHMT (Fig 4.1b) showed a slightly different spectrum compared to all other mutants of bsSHMT. On addition of MA to E53Q bsSHMT, a rapid decrease was observed within 5 min at 425 nm and a concomitant increase at 325 nm. This is followed by slow decrease at 425 nm and a slow increase at 325 nm. The reaction was almost complete by 20 min. Fig 4.1 (b) shows the interaction of E53Q bsSHMT with MA.

Stopped-flow studies

Stopped-flow studies were carried out to measure the rate of disruption of Schiff's base absorbing at 425 nm and the formation of oxime absorbing at 325 nm upon addition of MA to E53Q bsSHMT. Stopped-flow studies were essentially carried out according to the procedure described in methods section. It can be seen from the Fig 4.1 (b) that, E53Q bsSHMT in the normal spectrophotometric studies exhibited an initial rapid decrease (less than 5 min) at 425 nm and further slow decrease up to 20 min. In order to examine the initial fast rate, the reaction was monitored at different time points (5, 10, 50 and 500 s) at 425 nm. Even at 50 s the curve did not reach a plateau. Hence the rate obtained could not be analyzed for the data. Further the reaction was monitored till 500 s. Fig 4.2 shows a typical graph obtained on addition of MA to E53Q bsSHMT. Increase at 325 nm was also measured at different time intervals (50,100 and 200 s). Fig 4.3 shows the formation of an oxime absorbing at 325 nm with a rate of 0.03 s^{-1} .

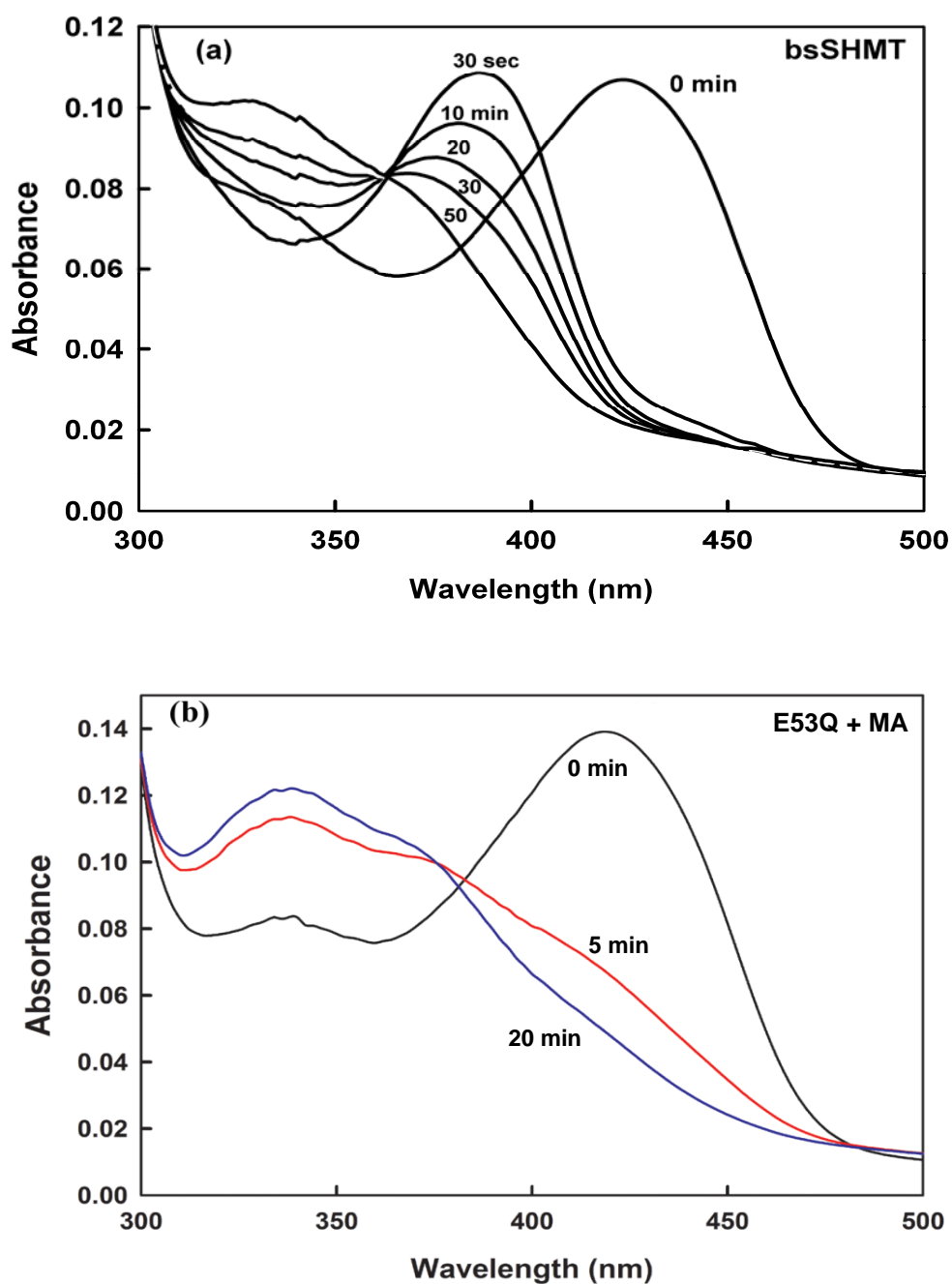


Fig 4.1: The interaction of bsSHMT and E53Q bsSHMT with MA.
 The spectrum of (a) bsSHMT and (b) E53Q bsSHMT (1 mg ml^{-1}) in 50 mM potassium phosphate buffer, pH 7.4, containing 1 mM EDTA, 1 mM 2-ME; MA (2 mM) was added and the spectra recorded at different time intervals.

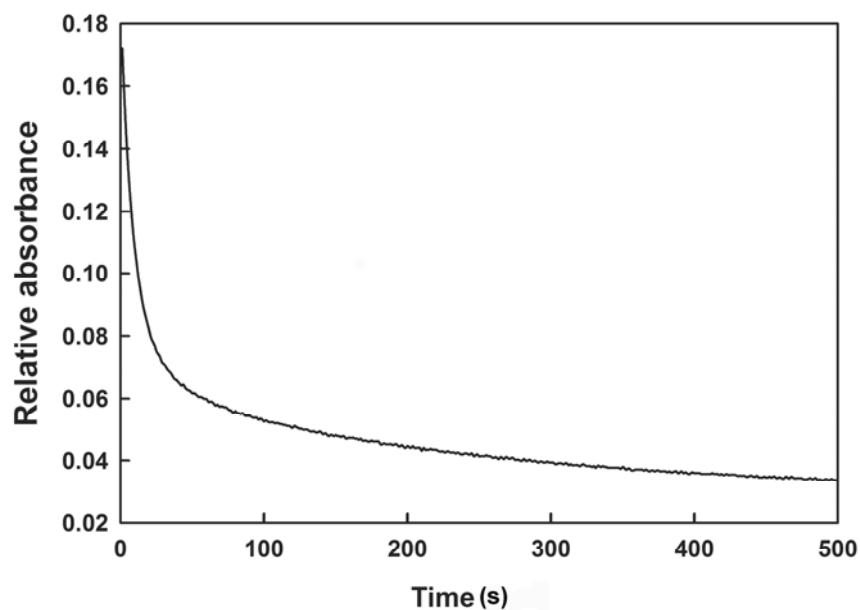


Fig 4.2: The decrease in relative absorbance at 425 nm on addition of MA (2 mM) to E53Q bsSHMT (10 mg ml⁻¹). All reactions were carried out in 50 mM potassium phosphate buffer, pH 7.4, containing 1 mM EDTA, 1 mM 2-ME.

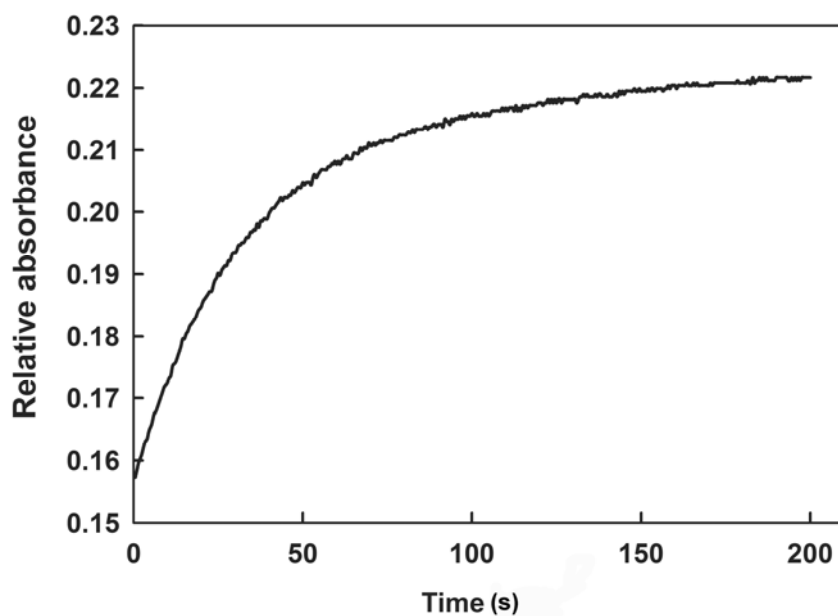


Fig 4.3: The increase in relative absorbance at 325 nm on addition of MA (2 mM) to E53Q bsSHMT (10 mg ml⁻¹). All reactions were carried out in 50 mM potassium phosphate buffer, pH 7.4, containing 1 mM EDTA, 1 mM 2-ME.

The interaction of bsSHMT and its active site mutants with AAA

The interaction of AAA with bsSHMT and its mutants was studied by spectral methods. The spectrum of bsSHMT (1 mg ml⁻¹) in 50 mM potassium phosphate buffer, pH 7.4, containing 1 mM EDTA, 1 mM 2-ME was recorded in the range of 300-550 nm. It can be seen from the Fig 4.4 that the addition of 50 μM of AAA to bsSHMT, results in a disruption of Schiff's base absorbing at 425 nm and formation of an oxime product absorbing at 325 nm.

E53Q and Tyr mutants interaction with AAA was examined. Among all the mutants, only E53Q bsSHMT showed formation of a peak at 388 nm, and slowly converted to its final oxime product (Fig 4.5). Y51F, Y61F and Y61A bsSHMT behaved similarly as of bsSHMT (Fig 4.6). All the spectral studies were carried out in 50 mM potassium phosphate buffer pH 7.4 containing 1 mM EDTA and 1 mM 2-ME.

Spectral and structural studies on the K226M bsSHMT showed that there was a change in the absorption maximum (412 nm) compared to that of bsSHMT. Since K226M bsSHMT failed to interact with MA (10 mM) and it is known that AAA is more reactive compared to MA due to the presence of a -COOH group, it was of interest to study the interaction of AAA with K226M and K226Q bsSHMT.

Spectral changes in the range of 300-550nm were monitored on addition of 10 mM AAA using 1 mg ml⁻¹ of K226M/Q bsSHMT in 50 mM potassium phosphate buffer, pH 7.4, containing 1 mM EDTA, 1 mM 2-ME. K226M bsSHMT reacted very slowly with AAA and the reaction was complete by 1 h. However, in the case of K226Q bsSHMT, a small decrease at 425 nm was observed after 45 min. Both the mutants did not form any intermediate absorbing at 388 nm (Fig 4.5 a, b).

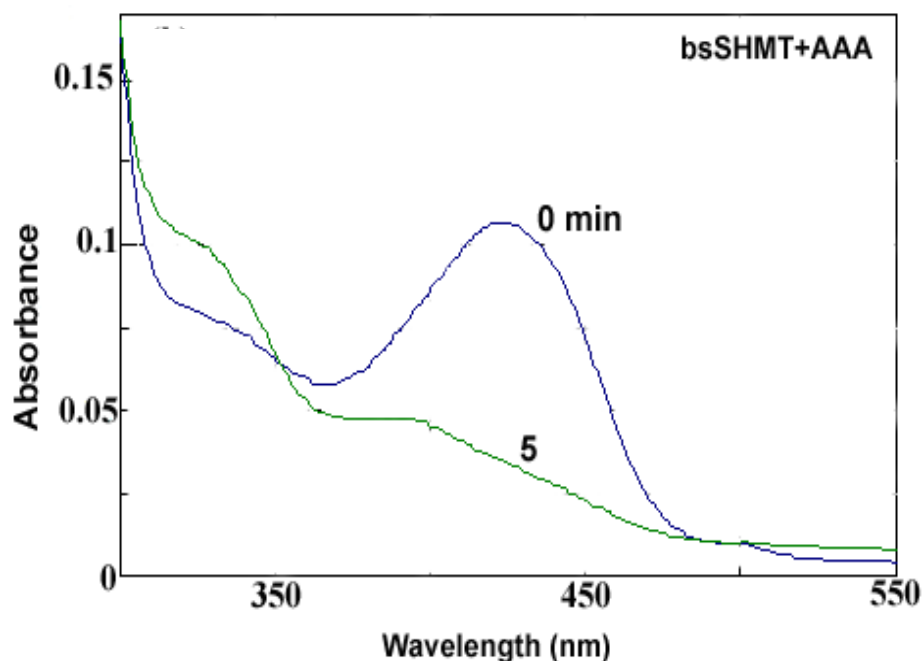


Fig 4.4: The interaction of bsSHMT with AAA.

The spectrum of bsSHMT (1 mg ml^{-1}) was recorded in 50 mM potassium phosphate buffer, pH 7.4, containing 1 mM EDTA, 1 mM 2-ME and 50 μM of AAA was added and the spectra recorded at different time intervals as represented in the figure.

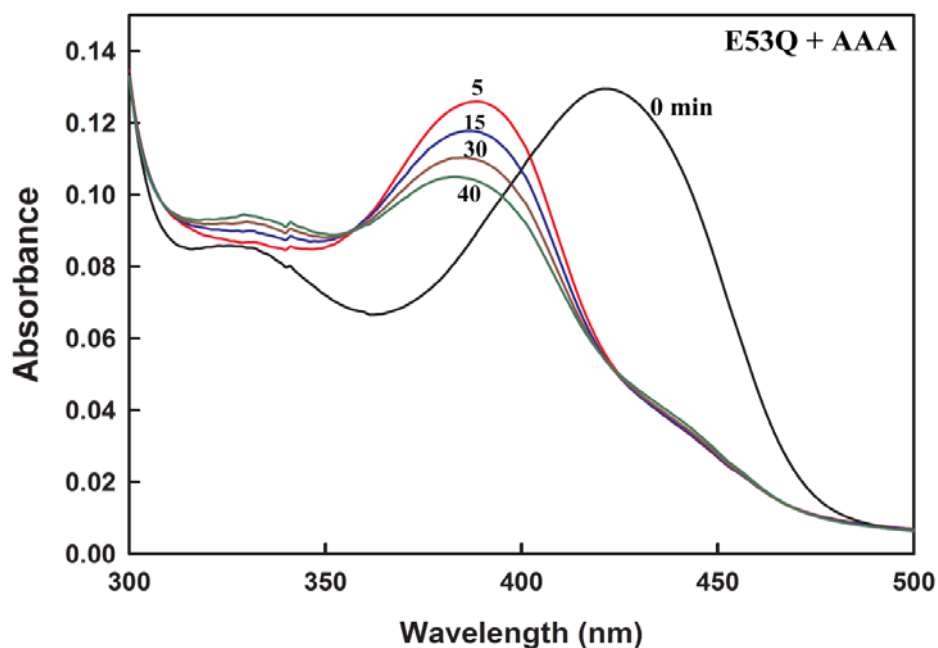


Fig 4.5: The interaction of E53Q bsSHMT with AAA.

The spectrum of E53 bsSHMT (1 mg ml^{-1}) was recorded in 50 mM potassium phosphate buffer, pH 7.4, containing 1 mM EDTA, 1 mM 2-ME (0 min). AAA (0.1 mM) was added and the spectra recorded at different time intervals. The isobestic point was seen at 360 nm.

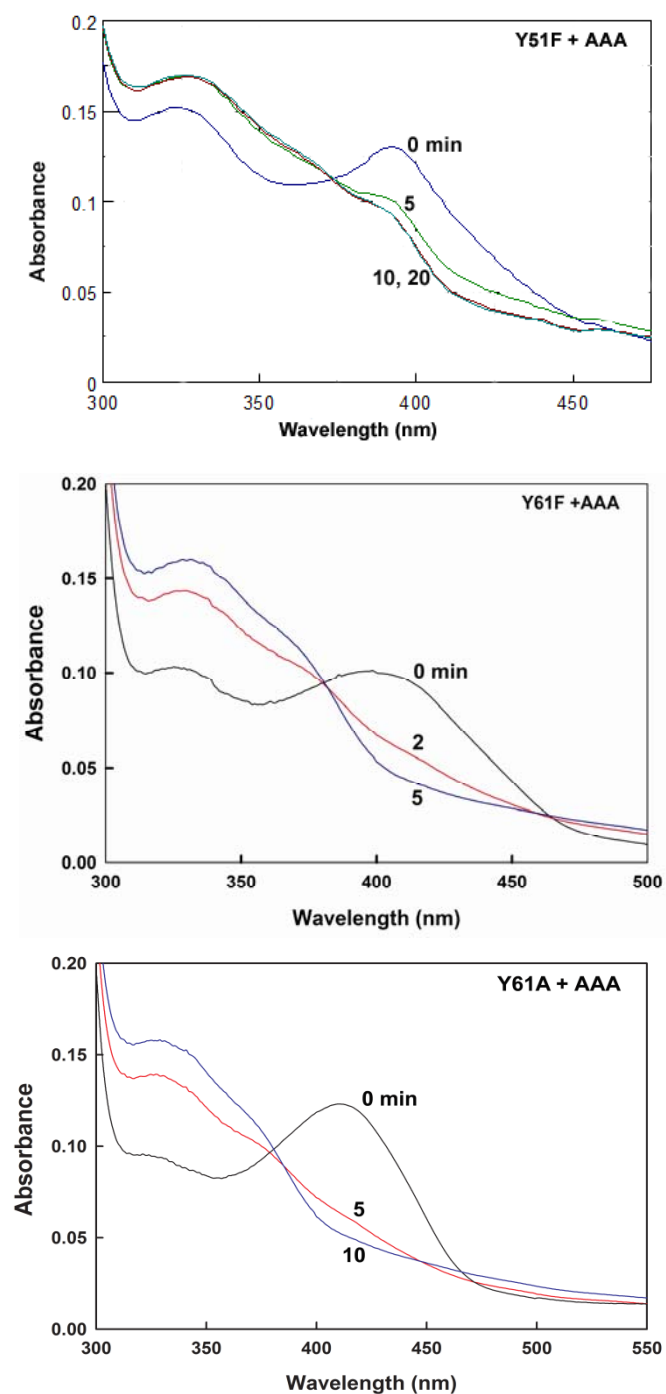


Fig 4.6: The interaction of Y51F, Y61F and Y61A bsSHMT with AAA.
 The spectrum of Y51F, Y61F and Y61A bsSHMT (1 mg ml^{-1}) was recorded in 50 mM potassium phosphate buffer, pH 7.4, containing 1 mM EDTA, 1 mM 2-ME, and 10 mM of AAA was added and the spectra were recorded at different time intervals.

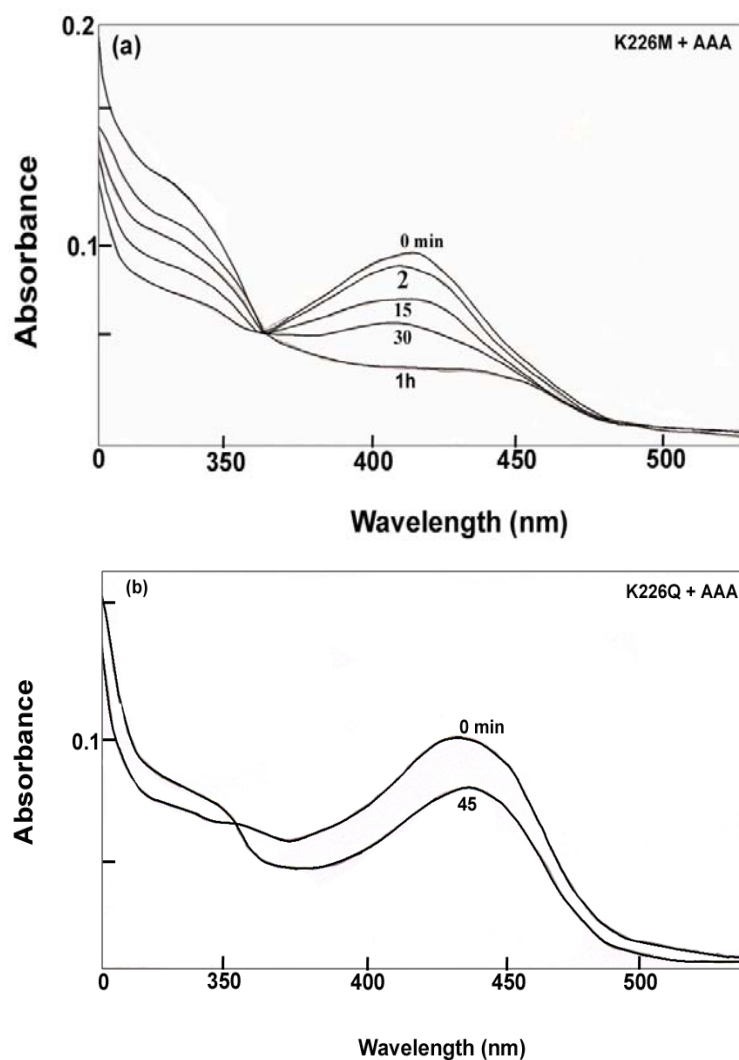


Fig 4.7: The interaction of K226M and K226Q bsSHMT with AAA.

The spectra of K226M and K226Q bsSHMT (1 mg ml^{-1}) were recorded in 50 mM potassium phosphate buffer, pH 7.4, containing 1 mM EDTA, 1 mM 2-ME. AAA (10 mM) was added and the spectra recorded at different time intervals as shown in the figure. The isobestic point in (a) K226M + AAA and (b) K226Q + AAA was at 360 nm.

Stopped-flow studies

The rate constants for the disruption of Schiff's base, formation of the intermediate and its decomposition to the oxime for E53Q bsSHMT were determined. Decrease at 425 and increase at 388 nm was measured at different time points (0.1, 1, and 10 s) with bsSHMT and AAA (0.5mM). At both the wavelengths, plateau was reached within 0.1 s. The rate of disruption of Schiff's base at 425 nm on addition of AAA to bsSHMT was 275 s^{-1} and formation of oxime product at 325 nm was 458 s^{-1} (Fig 4.8 and 4.9)

Stopped-flow studies were carried out with E53Q bsSHMT to obtain the rate constants. The rate of disruption of Schiff's base and the formation of 388 nm intermediate was 13 s^{-1} and 13.9 s^{-1} respectively. The intermediate slowly decomposed with a rate of $4.8 \times 10^{-4} \text{ s}^{-1}$ at 388 nm to final oxime product with a rate of $5.9 \times 10^{-4} \text{ s}^{-1}$ at 325 nm. Representative graphs for all the wavelengths are given (Fig 4.10 - 4.13).

The rate constants calculated for the bsSHMT and E53Q bsSHMT are summarized in Table 4.1. It can be seen from the Table 4.1 that the bsSHMT and AAA reaction was very rapid. On the other hand the rate constants for disruption of Schiff's base of E53Q bsSHMT had decreased considerably explaining the reason for observing intermediate.

Table 4.1: Rate contents for bsSHMT and E53Q bsSHMT on interaction with AAA.

Wavelength (nm)	Rate (s^{-1})	
	bsSHMT	E53Q
425 (↓)	275 ± 5.0	13.0 ± 1.0
388 (↑)	No intermediate	13.9 ± 1.7
388 (↓)	No intermediate	$4.8 \pm 1.2 \times 10^{-4}$
325 (↑)	458 ± 6.0	$5.9 \pm 3.0 \times 10^{-4}$

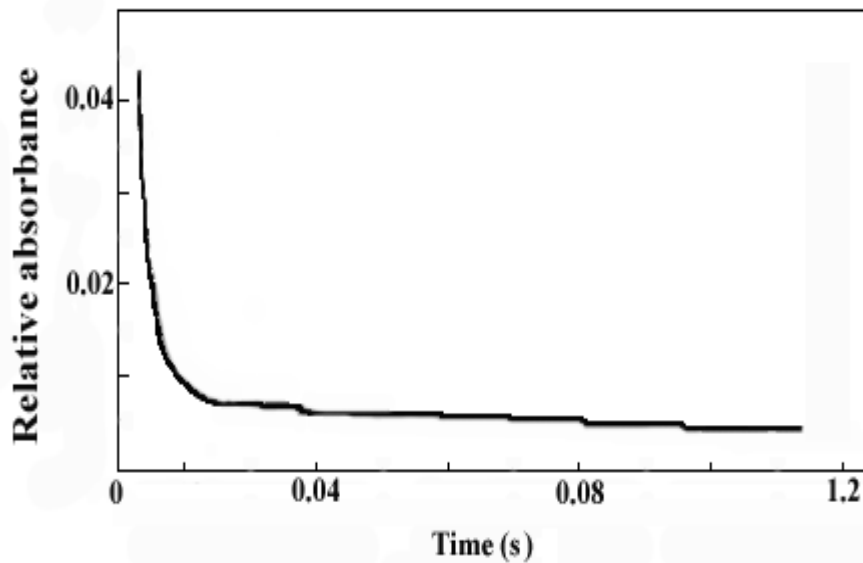


Fig 4.8: The stopped-flow tracings of decrease at 425 nm on addition of AAA (0.5 mM) to bsSHMT (10 mg ml^{-1}). All the experiments were carried out in 50 mM potassium phosphate buffer, pH 7.4, containing 1 mM EDTA, 1 mM 2-ME.

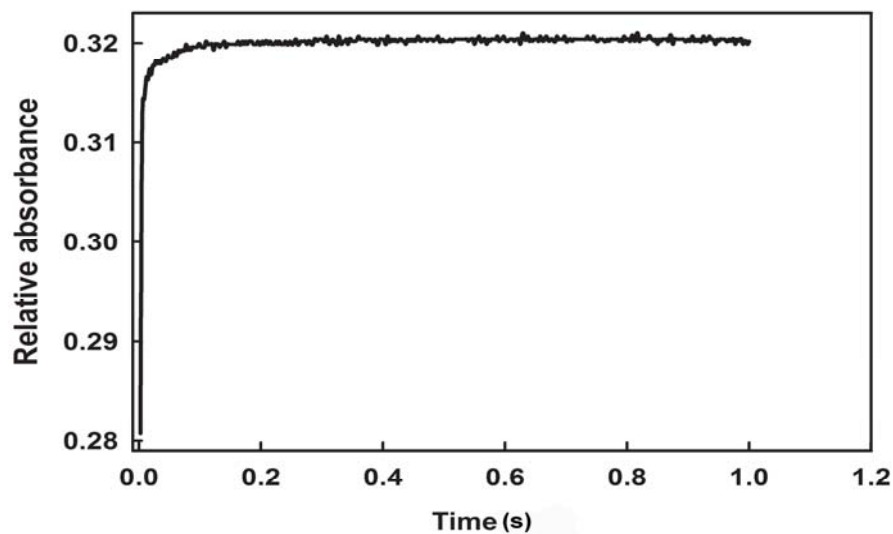


Fig 4.9: The stopped-flow tracings of increase at 325 nm on addition of AAA (0.5 mM) to bsSHMT (10 mg ml^{-1}). All the experiments were carried out in 50 mM potassium phosphate buffer, pH 7.4, containing 1 mM EDTA, 1 mM 2-ME.

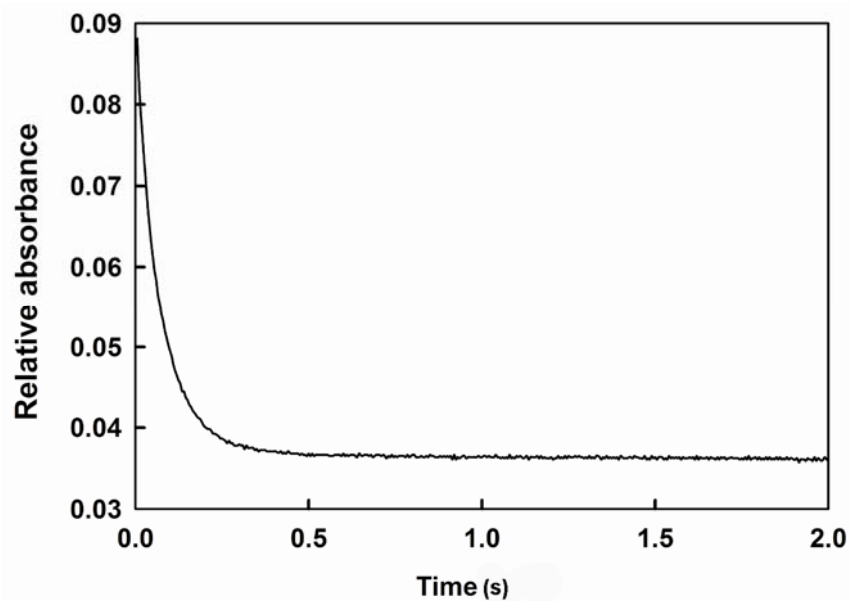


Fig 4.10: The decrease at 425 nm on addition of AAA (0.5mM) to E53Q bsSHMT (10 mg ml⁻¹). All the experiments were carried out in 50 mM potassium phosphate buffer, pH 7.4, containing 1 mM EDTA, 1 mM 2-ME.

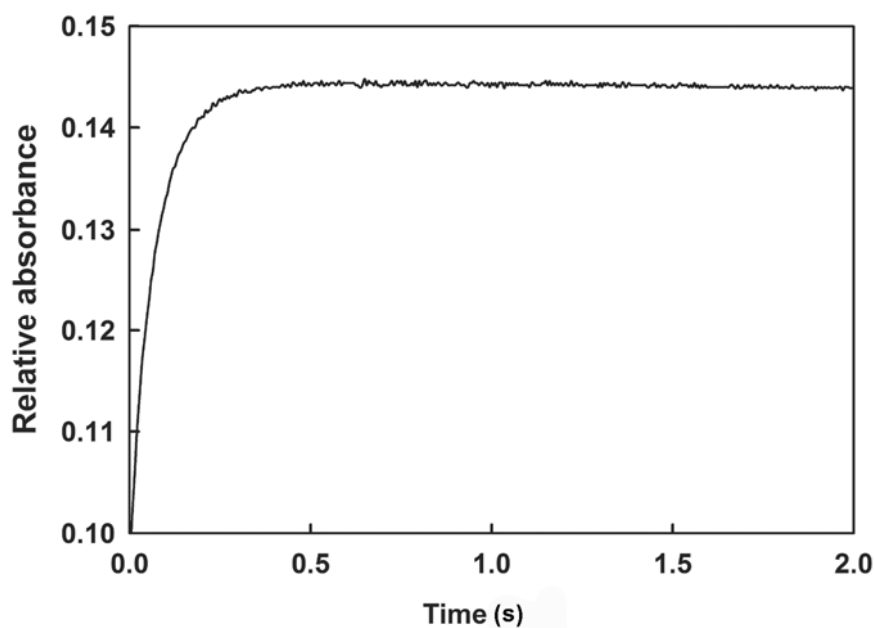


Fig 4.11: The increase at 388 nm on addition of AAA to E53Q bsSHMT AAA (0.5mM) to E53Q bsSHMT (10 mg ml⁻¹). All the experiments were carried out in 50 mM potassium phosphate buffer, pH 7.4, containing 1 mM EDTA, 1 mM 2-ME.

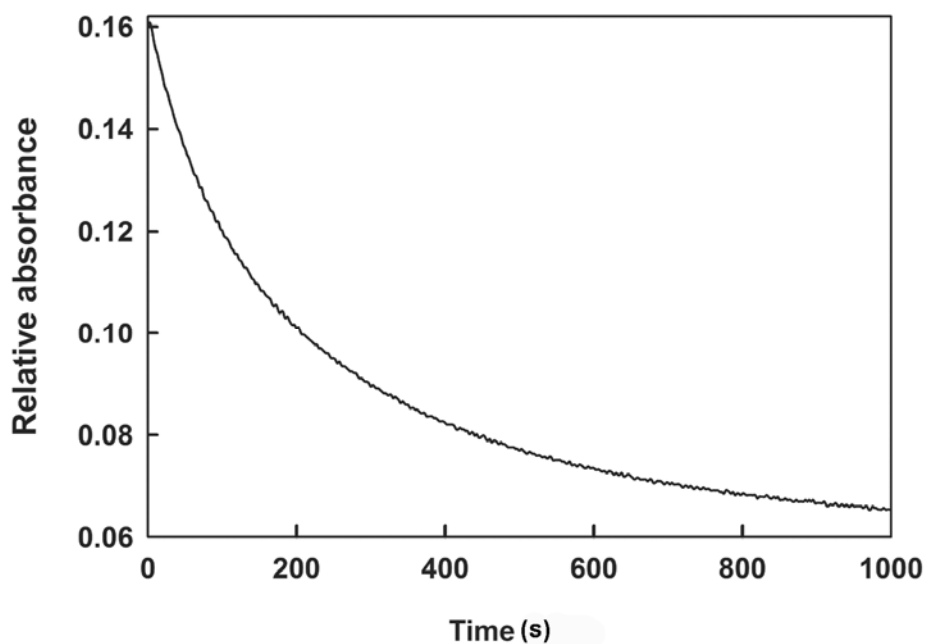


Fig 4.12: The decomposition of intermediate absorbing at 388 nm on addition of AAA (0.5mM) to E53Q bsSHMT (10 mg ml⁻¹). All the experiments were carried out in 50 mM potassium phosphate buffer, pH 7.4, containing 1 mM EDTA, 1 mM 2-ME.

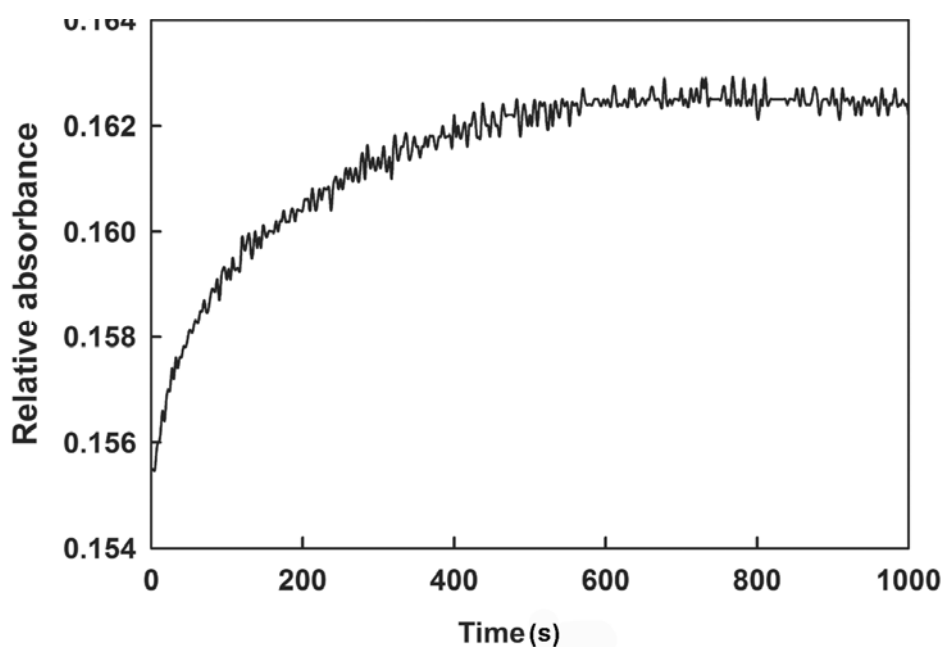


Fig 4.13: The increase at 325 nm on addition of AAA (0.5mM) to E53Q bsSHMT (10 mg ml⁻¹). All the experiments were carried out in 50 mM potassium phosphate buffer, pH 7.4, containing 1 mM EDTA, 1 mM 2-ME.

Studies on other inhibitors of SHMT

Inhibition studies of folate analogues on bsSHMT

In addition to aminoxy compounds, folate analogues have been shown to inhibit SHMT although not very efficiently (Baskaran, 1989). In recent years bioinformatic approaches for indentifying inhibitors have yielded useful lead compounds. It is therefore of interest to examine the fit of these compounds into the bsSHMT structure. Commercially available FTHF analogues from the database were docked on the native and ternary complex of bsSHMT. Table 4.2 summarizes the list of probable inhibitors.

Among the 14 compounds used in docking studies, four water-soluble compounds (SPB, SCR, HTS and RJC – the product code is used for representation of individual compounds). These were selected for further experimental studies. To analyze the inhibitory effect, the compounds were dissolved in water and pH was adjusted to 7.4. bsSHMT (1 µg in 50 mM potassium phosphate buffer, pH 7.4, containing 1 mM EDTA, 1 mM 2-ME) was incubated with 1 mM of each inhibitor for 15 min at 37°C and THF-dependent cleavage assay was carried out as described in methods section.

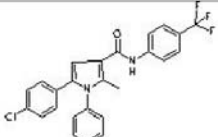
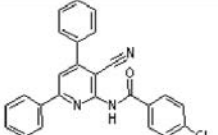
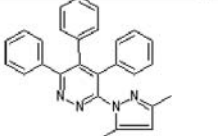
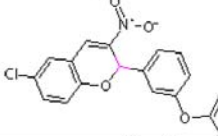
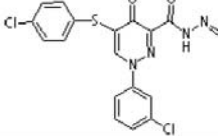
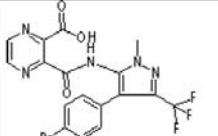
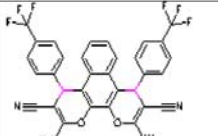
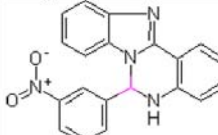
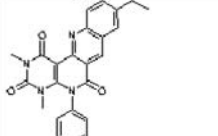
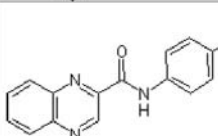
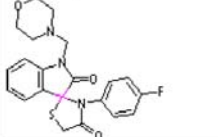
(1) N'-({1-(3-chlorophenyl)-5-[(4-chlorophenyl) thio]-4-oxo-1,4 dihydropyridazin-3-yl}carbonyl)-N,Ndimethylhydrazonoformamide - **(Product code –SPB)**

(2)N-[4-(aminocarbonyl) phenyl]-2-quinoxalinecarboxamide - **(Product code-SCR)**

(3)3-({[4-(4-bromophenyl)-1-methyl-3-(trifluoromethyl)-1Hpyrazol-5-yl] amino} carbonyl) pyrazine-2-carboxylic acid - **(Product code – HTS)**

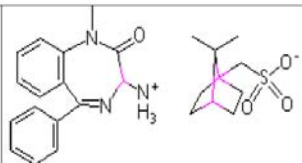
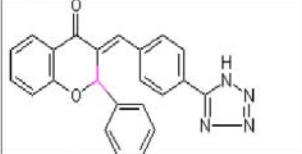
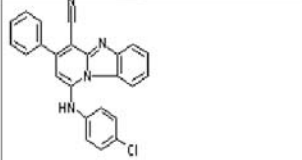
(4) 3-amino-1-methyl-5-phenyl-2, 3- dihydro-1H-1,4-benzodiazepin-2-one (7,7-dimethylbicyclo[2.2.1]hept-1-yl) methanesulfonic acid - **(Product code – RJC)**

Table 4.2: A list of docked folate analogues.

Product name	Structure	Formula	Molecular weight	Product code	Solubility in water
5-(4-chlorophenyl)-2-methyl-1-phenyl-N-[4-(trifluoromethyl)phenyl]-1H-pyrrole-3-carboxamide		C ₂₅ H ₁₈ ClF ₃ N ₂ O	454.8	SP00357	Poor
N1-(3-cyano-4,6-diphenyl-2-pyridyl)-4-chlorobenzamide		C ₂₅ H ₁₆ ClN ₃ O	409.8	RDR03398	Poor
3-(3,5-dimethyl-1H-pyrazol-1-yl)-4,5,6-triphenylpyridazine		C ₂₇ H ₂₂ N ₄	402.4	BTB13493	Poor
6-chloro-3-nitro-2-(3-phenoxyphenyl)-2H-chromene		C ₂₁ H ₁₄ ClNO ₄	379.7	S14129	Poor
N'-({1-(3-chlorophenyl)-5-[(4-chlorophenyl)thio]-4-oxo-1,4-dihydropyridazin-3-yl} carbonyl)-N,N-dimethylhydrazonoformamide		C ₂₀ H ₁₇ Cl ₂ N ₅ O ₂ S	462.3	SPB04054	Good
3-({[4-(4-bromophenyl)-1-methyl-3-(trifluoromethyl)-1H-pyrazol-5-yl]amino} carbonyl)pyrazine-2-carboxylic acid		C ₁₇ H ₁₁ BrF ₃ N ₅ O ₃	470.2	HTS01411	Good
2,11-diamino-4,9-di[4-(trifluoromethyl)phenyl]-4,9-dihydrobenzo[f]pyrano[3,2-h]chromene-3,10-dicarbonitrile		C ₃₂ H ₁₈ F ₆ N ₄ O ₂	604.5	FM00138	Poor
6-(3-nitrophenyl)-5,6-dihydrobenzo[4,5]imidazo[1,2-c]quinazoline		C ₂₀ H ₁₄ N ₄ O ₂	342.3	DP01323	Poor
9-ethyl-2,4-dimethyl-5-phenyl-1,2,3,4,5,6hexahydrobenzo[b]pyrimido[4,5-h][1,6]naphthyridine-1,3,6-trione		C ₂₄ H ₂₀ N ₄ O ₃	412.4	BTB14658	Poor
N-[4-(aminocarbonyl)phenyl]-2-quinoxalinecarboxamide		C ₁₆ H ₁₂ N ₄ O ₂	292.2	SCR00740	Good
N-(Morpholinomethyl)-3-(4-fluorophenyl)spiro(3H-indone-3,2'-thiazolidine-(2,4'-(1H)dione		C ₂₁ H ₂₀ FN ₃ O ₃ S	413.4	S11636	Good

Contd.....

Table 4.2: A list of docked folate analogues. (Continued from prepage)

3-amino-1-methyl-5-phenyl-2,3-dihydro-1H-1,4-benzodiazepin-2-one (7,7-dimethylbicyclo[2.2.1]hept-1-yl)methanesulfonic acid		C ₁₆ H ₁₆ N ₃ O. C ₁₀ H ₁₇ O ₃ S	483.6	RJC03401	Good
2-phenyl-3-[4-(1H-1,2,3,4-tetrazol-5-yl)benzylidene]chroman-4-one		C ₂₃ H ₁₆ N ₄ O ₂	380.4	JFD00174	Poor
1-(4-chloroanilino)-3-phenylpyrido[1,2-a]benzimidazole-4-carbonitrile		C ₂₄ H ₁₅ ClN ₄	394.8	HTS07555	Poor

(The data for this table is obtained form <http://www.maybridge.com>)

It can be seen from the Fig 4.14 that these folate analogues failed to inhibit bsSHMT. The specific activity in the presence of all four compounds was similar to that of bsSHMT. In addition, spectral studies were also carried out to analyze the formation of quinonoid intermediate. For spectral studies bsSHMT (1 mg ml⁻¹ in 50 mM potassium phosphate buffer, pH 7.4, containing 1 mM EDTA, 1 mM 2-ME) was incubated with each of the folate analogues for 15 min and spectra were recorded at 300-550 nm. Further addition of Gly (50 mM) and FTHF (1 mM) resulted in the formation of quinonoid intermediate at 500 nm (data not shown). The above results suggest that the folate analogues were unable to inhibit the enzyme.

An analysis of the procedure used for docking was carried to explain the inability of folate analogues to inhibit bsSHMT. The folate analogues were docked exclusively on a monomer of bsSHMT. SHMT belongs to fold type I family of PLP-dependent enzymes and the active site is situated at the interface of the dimer. Hence, a dimer should have been used as the biological unit for the docking studies. The docking studies were repeated with bsSHMT dimer and the following procedure was employed. Autodock-4 was used for docking studies. Software user manual was available online and the docking procedure followed as described in the manual. The results were analyzed in software available (PyMOL molecular viewer software). Before docking, hydrogens were added to both the macromolecule and the ligand and gasteiger charges were computed. The docking procedure involves initial conversion of both macromolecule and the ligand to a readable format with software (pdbqt format), and further converted to gfp (grid parameter file). LGA (Lamarckian Genetic Algorithm) autodock was performed. The resultant histogram of hits was further used for the analysis using in PyMOL. As a test of the procedure adopted bsSHMT structure (1KKJ) was docked with L-Ser. bsSHMT structure has been solved in presence of L-Ser (1KKP) and Gly+FTHF (1KL2) and the binding sites of the ligands are known (Trivedi *et al.*, 2002). It can be seen from the Fig 4.15 that the docked L-Ser agrees with that of structure solved in presence of L-Ser (1KKP). The Fig 4.15 also shows Glu 53, Lys 226, Tyr 61, His 200 and Arg 357, which are crucial residues at the active site pocket.

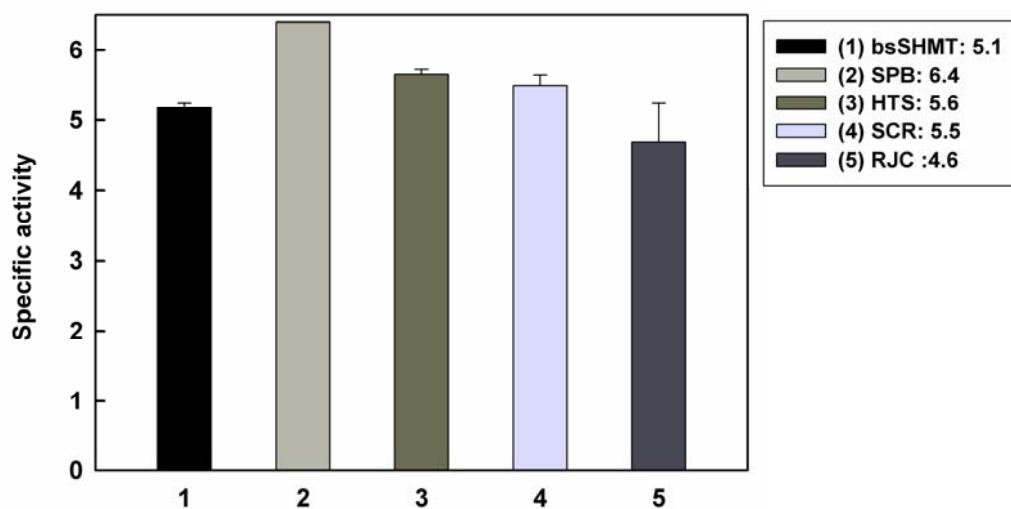


Fig 4.14: Graphical representation for the effect of folate analogues on bsSHMT. Present inhibition is shown in the graph and bsSHMT has been used in the assay as control. Product code is used for representation of individual compounds. Please see page 190 for expansion of abbreviation of compounds. Specific activity unit - $\mu\text{mols of HCHO/min/mg}$

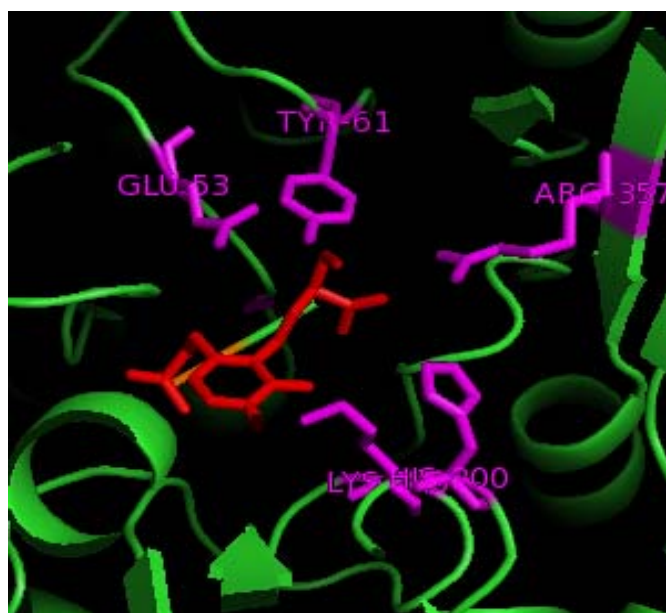


Fig 4. 15: A model representation of bsSHMT active site structure docked with L-Ser.

PLP-L-Ser Schiff's bases represented in red, other active site residues are represented in magenta and bsSHMT in green.

In addition to bsSHMT-Ser, docking of known inhibitors like OADS and TSC was carried out. Table 4.3 and 4.4 represents the results of the docking which depicts the run number and its clustering (runs which represent similar orientation of ligand) with lowest binding energy for OADS and TSC respectively. Total runs were 100. For OADS, runs 44 and 95 show low binding energy are high frequency (total clustering is $34 + 48 = 82$). The results of thiosemicarbazide (Table 4.4) suggest high clustering ($42 + 31$) for two runs. However, the lowest energy corresponds to another run with a frequency of only 2. Further examination shows close similarity in ten docking pattern corresponding to runs 92 and 12. Fig 4.16 shows the docked OADS and active site region of bsSHMT with docked OADS.

In addition to OADS and TSC, an attempt was made to dock MA on bsSHMT. This was not successful as coordinates of MA found in the pdb had unusual features. Fig 4.15 depicts the docked OADS and the active site residues.

Further, docking of N'-({1-(3-chlorophenyl)-5-[(4-chlorophenyl)thio]-4-oxo-1,4-dihydropyridazin-3-yl} carbonyl)-N,N-dimethylhydrazonoformamide-(Product code is SPB) and 3-({[4-(4-bromophenyl)-1-methyl-3-(trifluoromethyl)-1H-pyrazol-5-yl] amino} carbonyl) pyrazine-2-carboxylic acid - (Product code is HTS) did not result in high frequency of clustering for any particular location. Out of 100 runs there were no equivalent results. Fig 4.17 shows the binding of HTS and SPB to bsSHMT. The other folate analogues N-[4-(aminocarbonyl) phenyl]-2-quinoxalinecarboxamide-(Product code is SCR) and 3-amino-1-methyl-5-phenyl-2,3-dihydro-1H-1,4-benzodiazepin-2-one(7,7-dimethylbicyclo [2.2.1]hept-1-yl) methane sulfonic acid (Product code is RJC) also gave similar results.

The binding region of folate analogues on to bsSHMT was similar to that seen in the bsSHMT ternary complex (bsSHMT+Gly+FTHF) (Fig 4.17). The docked folate analogues are found to interact with the known folate binding residues. Fig 4.18 shows the binding region of folate analogue with active site residues and are highlighted. Based on these few results one can not conclusively identify a folate analogue or analogues as a good inhibitor(s).

Table 4.3: Table showing binding energy and cluster rank for OADS.

Cluster Rank	Average Lowest Binding Energy	Run	Number in Cluster
1	- 7.67	44	34
2	- 7.65	95	48
3	- 6.14	40	4
4	-5.94	18	3
5	-5.60	92	4
6	-5.58	9	2
7	-5.48	15	1
8	-5.45	23	2
9	-5.32	67	1
10	-4.80	62	1

Table 4.4: Table showing binding energy and cluster rank for TSC.

Cluster Rank	Average Lowest Binding Energy	Run	Number in Cluster
1	-3.78	97	2
2	-3.76	92	42
3	-3.76	12	31
4	-3.75	99	15
5	-3.75	35	5
6	-3.63	6	1
7	-3.28	41	4

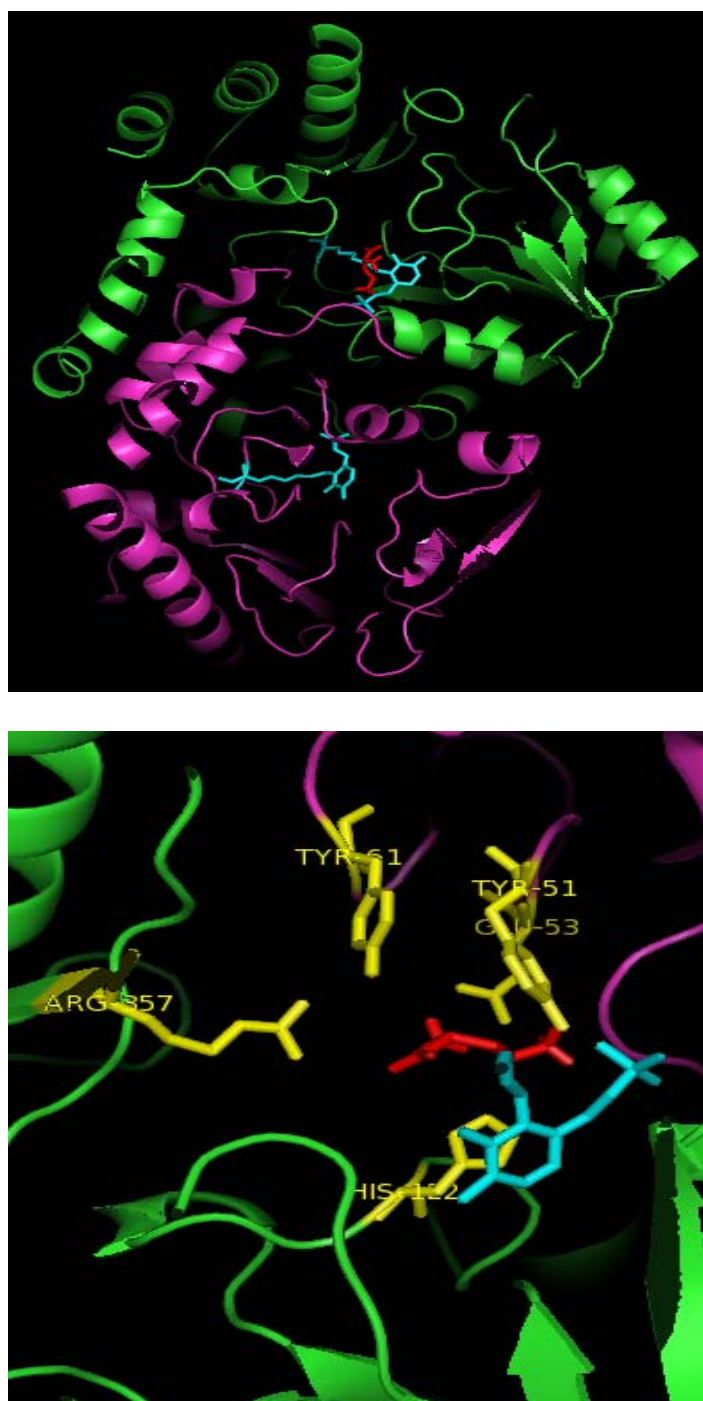


Fig 4.16: (a) An overlay of bsSHMT and docked OADS (b) The active site region of bsSHMT with docked OADS. Figures were prepared using PyMOL software. In both, OADS is represented in red, PLP-Lys Schiff's base in cyan, and the active site residues (Arg 357, Try 61, 51, His 122) colour in yellow.

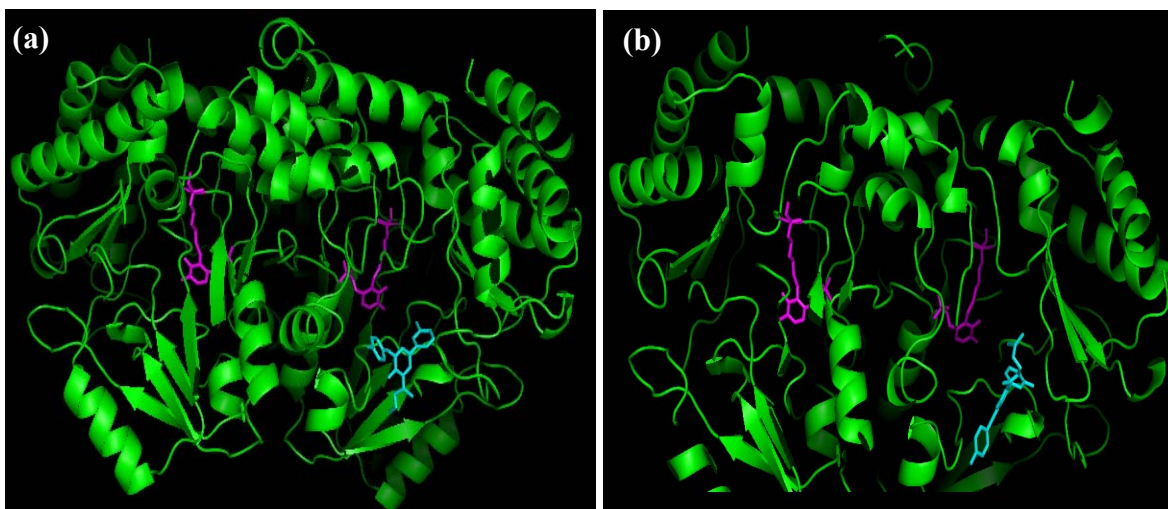


Fig 4.17: An overlay of bsSHMT with docked folate analogues.
 bsSHMT is represented in green in both, PLP-Lys Schiff's base in magenta and
 (a) HTS and (b) SPB in cyan.

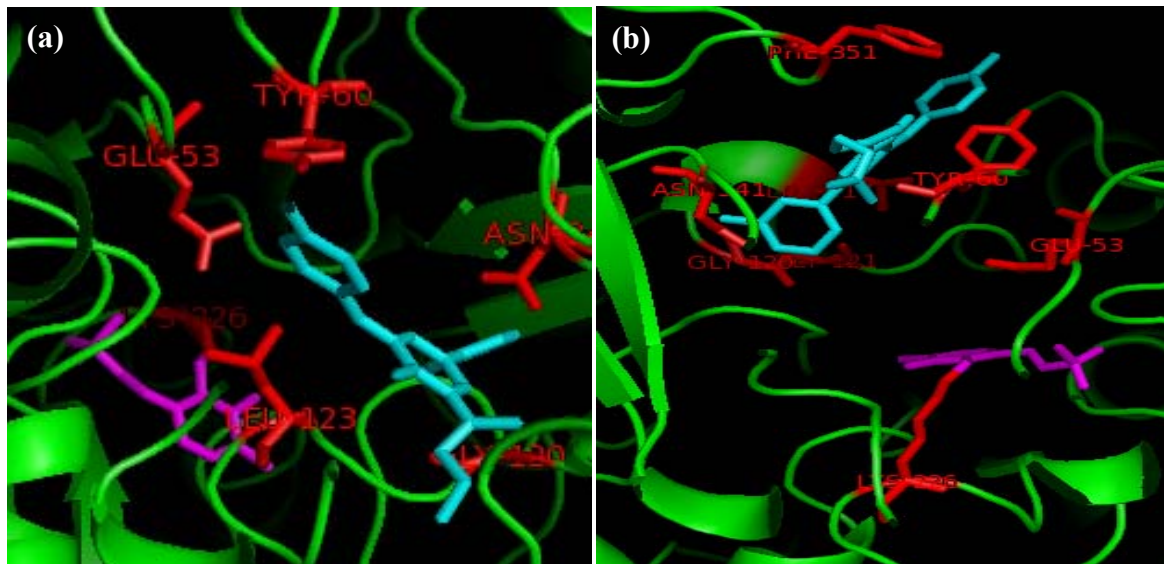


Fig 4.18: The binding region of (a) HTS and (b) SPB on bsSHMT.
 PLP is represented in magenta, both the folate analogues are in cyan, and the active
 site residues are in red.

Preliminary studies on effect of spices extract on the activity of bsSHMT

It is well documented that most of the spices exhibit anti-carcinogenic properties (Rahman, 2003). The anti-carcinogenic activity of spices is mainly due to the bio-active molecules present in the essential oil component of spices. Initial studies were carried out with essential oils of various spices. The essential oil previously extracted from garlic and cumin was used for the assay. These oils were dissolved in a small amount of methanol or dimethyl sulfoxide (DMSO) and volume was made up to 200 μ l using 50 mM potassium phosphate buffer, pH 7. For inhibition assay 1 μ g of bsSHMT and 67 μ l of the essential oil were incubated for 15 min at 37°C. THF-dependent cleavage assay was carried out as described in methods section. Since essential oils were dissolved in DMSO and methanol, both these reagents were kept as controls (67 μ l of DMSO/methanol incubated with 1 μ g of bsSHMT). It can be seen from the Fig 4.19 that DMSO and methanol showed 41 and 28% of inhibition. The effect of essential oil on bsSHMT could not be determined by this method. It is known that L-mimosine inhibits SHMT (Lin *et al.*, 1996). It has been shown that L-mimosine attenuates SHMT transcription by chelating zinc; this in turn causes the disruption of zinc finger transcription factors with the consequent repression of SHMT gene transcription (Oppenheim *et al.*, 2000). L-mimosine was dissolved in 50 mM potassium phosphate buffer, pH 7.4, containing 1 mM EDTA, 1 mM 2-ME and 10 mM was used for the assay. It can be seen from the Fig 4.19 that, L-mimosine failed to inhibit SHMT. Recently it has been shown that, L-mimosine does not inhibit SHMT *in vitro* (Perry *et al.*, 2005; Oppenheim *et al.*, 2000).

Fresh garlic extract and also extracts of other spices were used for the assessing their inhibitory effect. Towards this objective, various spice extracts (pepper, ginger, chilli, and turmeric) were tested for inhibition of bsSHMT. Spice (1 g) was crushed and suspended in 1 ml of water for 10 min. The mix was centrifuged at 10000 rpm for 10 min at 4°C and the supernatant was used for the assay. Each spice extract (67 μ l) was incubated with 1 μ g of bsSHMT for 15 min at 37°C; THF-dependent activity was monitored as described in methods section. It can be seen from the Fig 4.20 that fresh garlic extract shows maximum inhibition of (69%) compared to other selected spices.

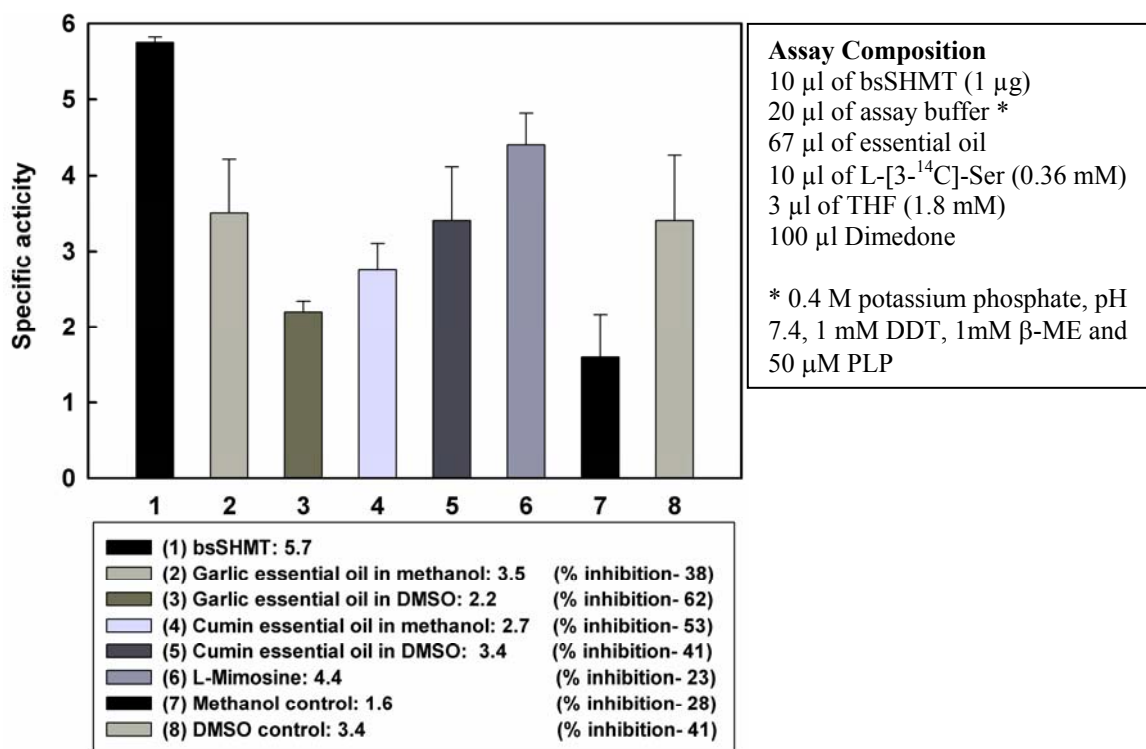


Fig 4.19: The effect of essential oils on bsSHMT activity. Percent inhibition is shown in the graph and bsSHMT has been used in the assay as control. Specific activity unit - μ mols of HCHO/min/mg.

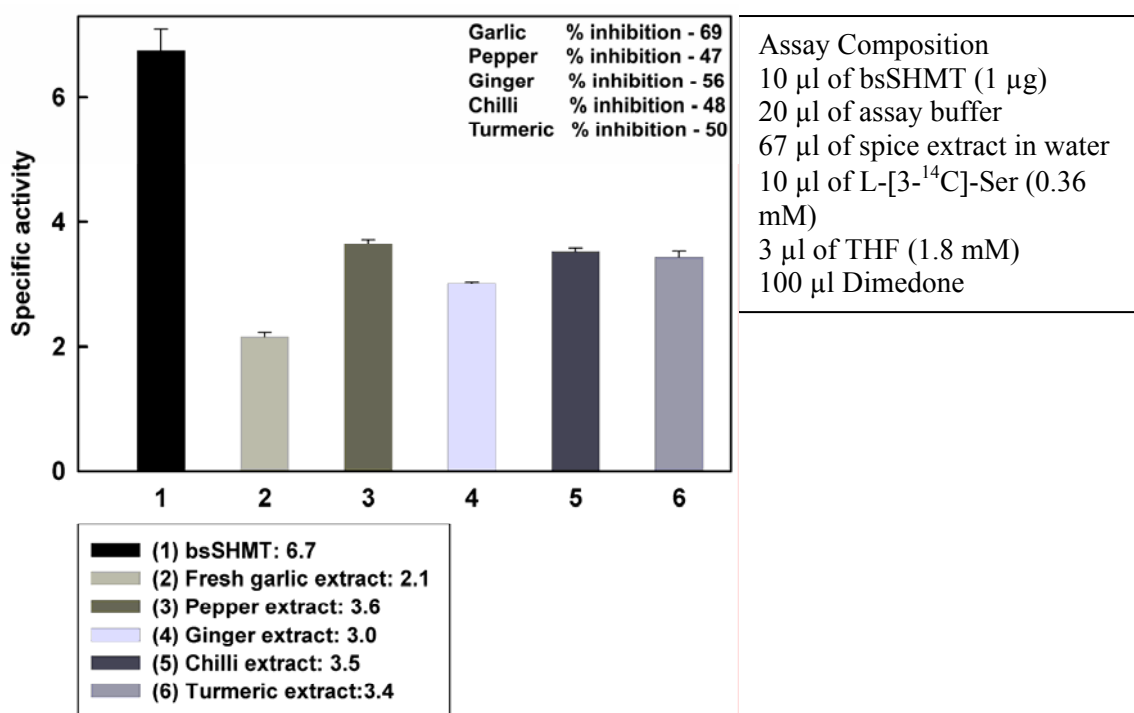


Fig 4.20: The effect of spice extracts on bsSHMT.

Percent inhibition is shown in the graph and bsSHMT has been used in the assay as control. Specific activity unit - μ moles of HCHO/min/mg.

However, the role of proteases present in the extracts could not be ruled out in such a process of incubation with bsSHMT (Fig 4.20). Hence, further experiments were performed with heat-treated garlic extract. The following procedure was used to prepare the extract in 50 mM potassium phosphate buffer, pH 7.4, containing 1 mM EDTA, 1 mM 2-ME. Fresh garlic (1g) was crushed using a pestle and mortar. The entire content was re-suspended in 2 ml of distilled water and boiled in a water bath for 20 min and centrifuged at 12000 rpm for 20 min at 4°C. The supernatant was used for measuring inhibition and the assay was performed as explained earlier.

It can be seen from the Fig 4.21 that heat-treated garlic extract showed 65% inhibition. In the earlier experiment (Fig 4.21), the amount of garlic bio-active components used from extract was small; therefore the concentration of inhibitor(s) in the extract probably minimal. Further, fresh garlic extract was prepared as described in method section. It is evident from the Fig 4.22 that the lyophilized garlic extract inhibited the enzyme by 91%. It was of interest to identify the heat stable compound responsible for bsSHMT inhibition.

Garlic is known to have many organosulfur compounds which are responsible for its biological activity (Rahman, 2003). An examination of the compounds present in garlic suggested that S-allyl Cys, an amino acid derivative, might be the compound responsible for the inhibition (Table I.13). The presence of an amino group in this compound may lead to the formation of Schiff's base with PLP and the presence of an allyl group may help in inhibition.

In this analogy, D-allyl Gly, L-allyl Gly (analogues of allyl Cys) and alliin, which are available commercially, were further examined for the inhibition of bsSHMT. Two different concentrations (1 and 10 mM) of the compounds were used for the assay. In addition, the incubation time was increased from 15 min to 1 h at 37°C. It can be seen from the Fig 4.23 that alliin showed 36 % if inhibition, and all other compounds had no effect.

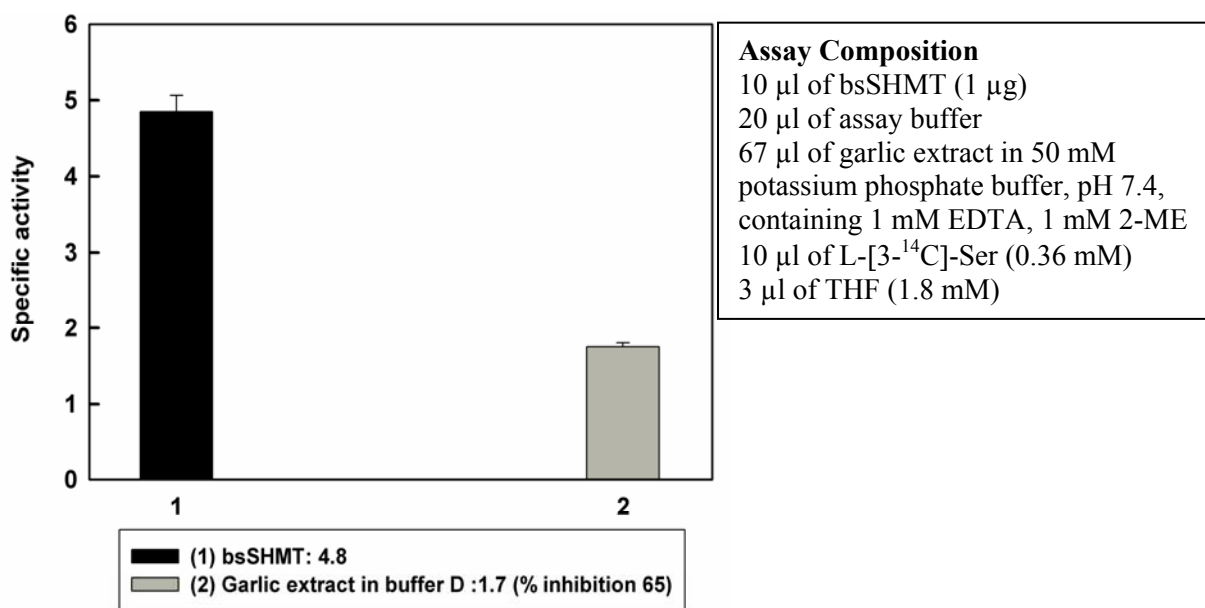


Fig 4.21: An inhibition analysis of bsSHMT activity by with garlic extract. Percent inhibition is shown in the graph and bsSHMT is used as control. Specific activity unit - μ moles of HCHO/min/mg.

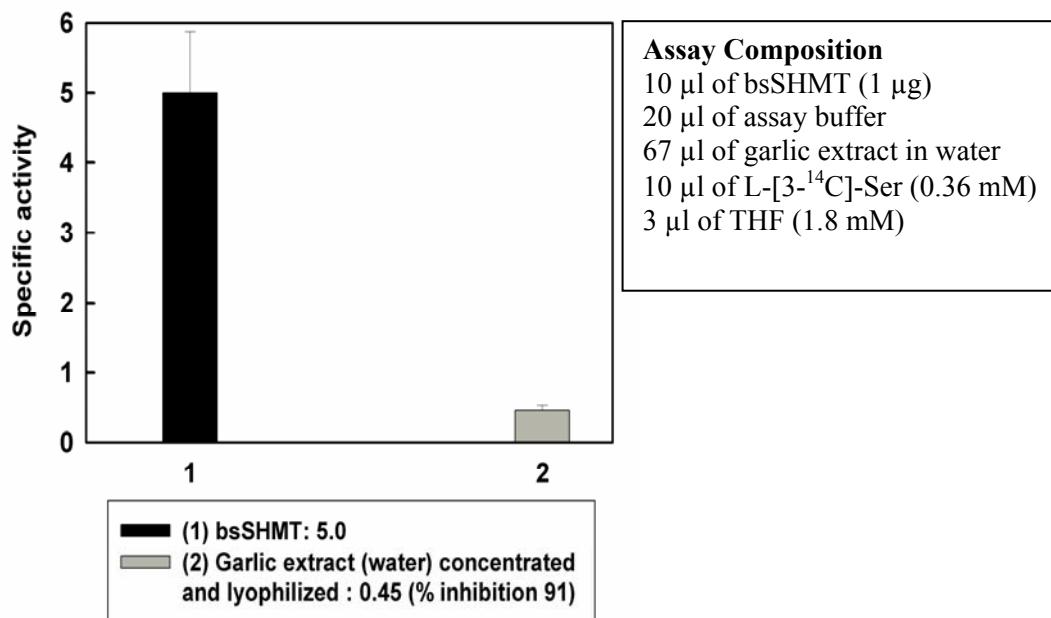


Fig 4.22: An inhibition analysis of bsSHMT activity by water extract of garlic. Percent inhibition is shown in the graph and bsSHMT is used as control. Specific activity unit - μ moles of HCHO/min/mg.

It can be seen from the Fig 4.23, the presence of allyl group in Gly failed to inhibit bsSHMT. Hence, in addition to inhibition studies, docking of alliin, L-allyl Gly and S-allyl Cys onto bsSHMT was carried out to understand the mode of binding. OADS was taken as control as it showed maximum clustering lowest binding energy. Table 4.5 to 4.7 summarizes the clustering rank, binding energy and the number of runs for alliin, L-allyl Gly and S-allyl Cys respectively. It can be seen from the Fig 4.23 that only alliin showed 36 % inhibition and alliin and D/L-allyl Gly failed to inhibit bsSHMT. Hence, it was of interest to analyze the modeled structure of L-allyl Gly, L-allyl Cys and alliin in comparison with OADS. Fig 4.24 shows the mode of binding of OADS, L-allyl Gly, S-allyl Gly and Alliin at the active site of bsSHMT.

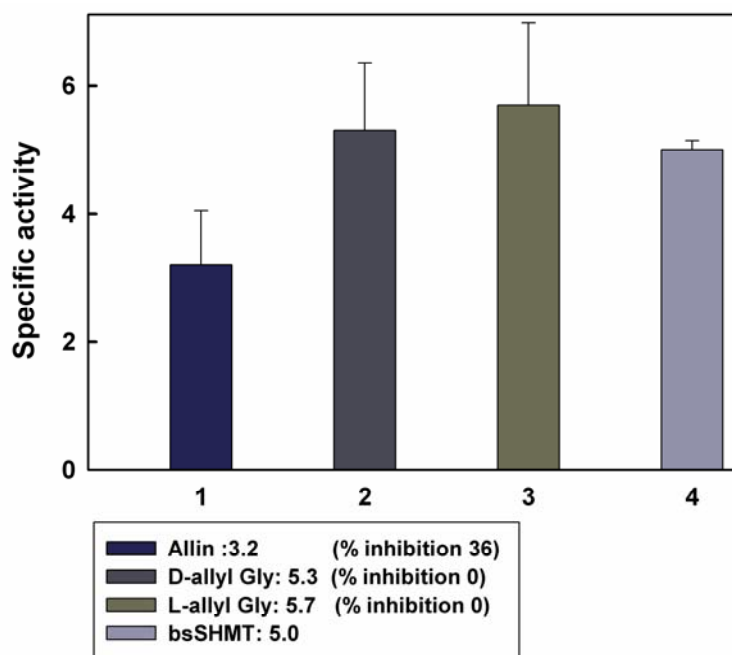


Fig 4.23: An inhibition analysis of bsSHMT with Alliin, D and L-allyl Gly. Percent inhibition is shown in the graph and bsSHMT is used as control. Specific activity unit - $\mu\text{mols of HCHO}/\text{min}/\text{mg}$.

Table 4.5: Table showing binding energy and cluster rank for Alliin.

Cluster Rank	Average Lowest Binding Energy	Run	Number in Cluster
1	-5.59	97	22
2	-5.48	26	13
3	-5.46	93	23
4	-5.46	49	25
5	-5.30	47	4
6	-5.19	70	1
7	-5.17	71	1
8	-5.16	85	2
9	-5.15	64	1
10	-4.73	96	1

Table 4.6: The table showing binding energy and cluster rank for L-allyl Gly.

Cluster Rank	Average Lowest Binding Energy	Run	Number in Cluster
1	-4.91	13	12
2	-4.75	46	27
3	-4.74	11	27
4	-4.73	84	19
5	-4.65	98	1
6	-4.60	95	5
7	-4.60	26	5
8	-4.59	87	1
9	-4.14	63	1
10	-3.88	56	1

Table 4.7: The table showing binding energy and cluster rank for S-allyl Cys.

Cluster Rank	Average Lowest Binding Energy	Run	Number in Cluster
1	-5.16	79	22
2	-5.15	59	16
3	-5.12	57	23
4	-5.11	10	18
5	-5.04	74	5
6	-4.94	51	2
7	-4.83	23	2
8	-5.60	49	1
9	-5.41	3	2
10	-4.38	32	1

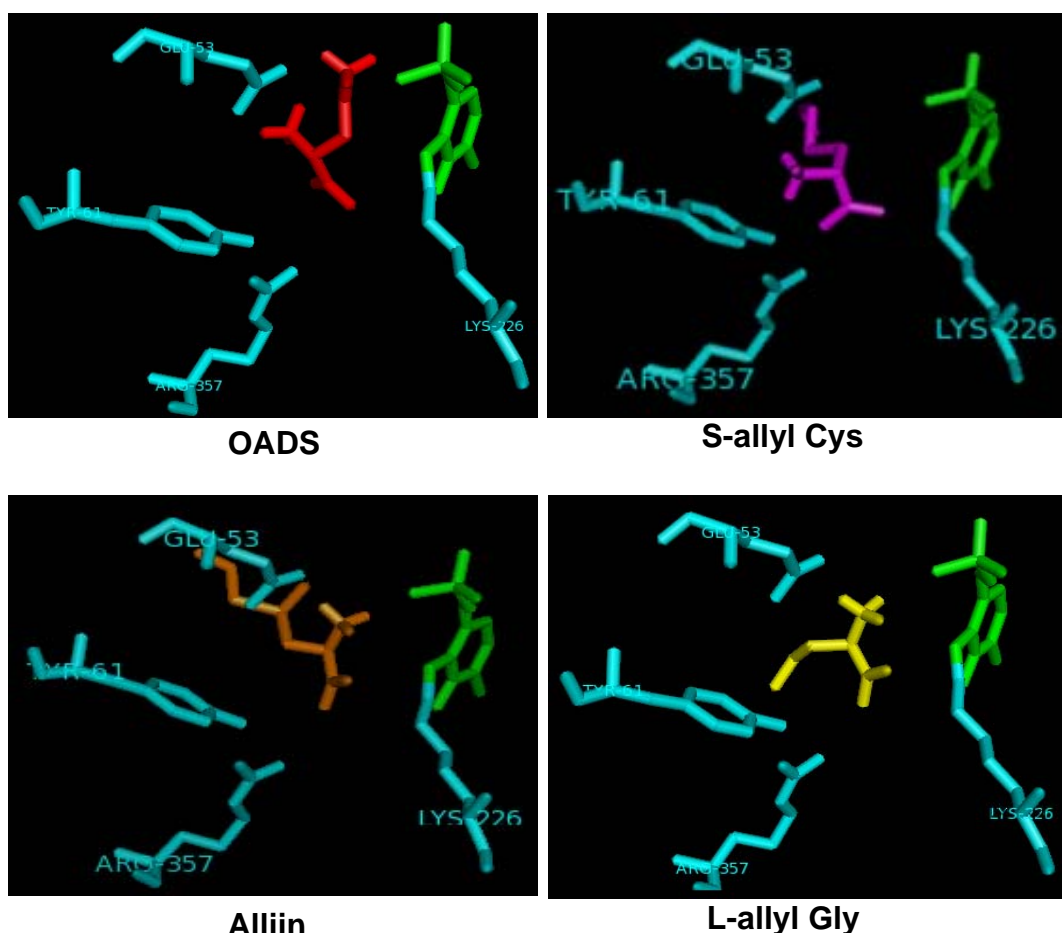


Fig 4.24: An active site of bsSHMT depicting the docked OADS, S-allyl Cys, Alliin and L-allyl Gly.

PLP is represented in green, OADS in red, S-allyl Cys in purple, Alliin in brown, L-allyl Gly in yellow and all other active site residues are in blue.

Discussion

Mutants of bsSHMT showed significant changes at the active site compared to that of wild type enzyme. Inhibitors like MA have been used to study the differences at the active site environment of wild-type and mutant enzymes (Jala, 2002). Since, MA failed to interact with a few mutants of bsSHMT, AAA was chosen to study differences at the active sites of bsSHMT and its mutants. Earlier studies have also suggested that substitution of hydrogen in hydroxylamine (HA) by a -COOH results in increased inhibitory effect (Baskaran *et al.*, 1989b; Acharya *et al.*, 1991).

MA and AAA interacted with the mutant proteins differently. Mutants of bsSHMT (K226M, K226Q, E53Q, Y51F, Y61A and Y61F bsSHMT) failed to form 388 nm intermediate on addition of MA. These results suggest that any change at the active site environment or PLP orientation in bsSHMT could lead to the loss of intermediate formation on interaction with MA. Interaction of K226M and K226Q bsSHMT with AAA suggested that though AAA was more reactive compared to MA, the absence of Schiff's base and a change in the orientation of PLP at the active site in K226M and K226Q bsSHMTs probably resulted in poor binding of AAA at the active site. Unlike MA, AAA could interact with Lys mutants. However, the interaction was very slow in comparison with bsSHMT

Except for E53Q bsSHMT all other mutants (K226M, K226Q, Y51F and Y61F bsSHMT) showed similar interaction pattern with AAA as that of bsSHMT (Fig 4.6 and 4.7). E53Q bsSHMT showed the formation of an intermediate absorbing at 388 nm (Fig 4.5). Stopped-flow studies suggest a drastic decrease in the rate at which AAA interacts with E53Q bsSHMT when compared to bsSHMT (275 s^{-1} to 13 s^{-1}). Interaction of E53 is abolished with AAA as a result of mutation, which in turn affects the rate of reaction or slows down the overall reaction. As a consequence, E53Q bsSHMT is able to form the intermediate at 388 nm when compared to bsSHMT. It is possible that Glu 53 may be the crucial residue involved in binding of AAA as well as in enhancing the rate of the reaction. However, further studies are required to prove the hypothesis. In addition, preliminary docking studies of an oxime over bsSHMT and E53Q bsSHMT suggest that K226, Glu 53, Tyr 51 and 61

are crucial interacting partners (data not shown). Hence mutation of these residues may affect the active site environment which results in the loss of intermediate. Docking of known inhibitors showed efficient binding with bsSHMT. However, commercially available folate analogues failed to inhibit bsSHMT. Though the folate analogues bind to the FTHF binding region in bsSHMT dimer (Fig 4.17 and 4. 18), the lack of uniform clustering for any particular conformation or location of binding may be a cause for the lack of the inhibition.

Inhibition assays carried out using spice extracts suggest that heat-treated garlic water extract was able to inhibit bsSHMT (Fig 4.22). An examination of garlic composition revealed presence of potent organosulfur compounds which may be involved in inhibition (Rahman, 2003). The garlic extract was boiled, to overcome the possible effect of proteases. From the data, S-allyl Cys is one of the amino acid derivative, could be responsible for inhibition of bsSHMT. Alliin gives rise to alliin by the action of allinase enzyme. Alliin is converted to several organosulfur compounds non-enzymatically. S-allyl Cys is formed as a product of this reaction. An attempt was made to purify the end product by reverse phase-HPLC. However, consistent separation of peaks was not observed. Variability in the peak pattern was observed on leaving the sample at room temperature for longer duration. This may be a result of incomplete non-enzymatic reaction of the garlic organosulphur compounds. This suggests that there may be more than one compound in the lyophilized extract. Analogues of S-allyl Cys, D and L-allyl Gly and Alliin failed to inhibit bsSHMT (Fig 4.23). Docking studies with S-allyl Cys, D and L-allyl Gly and Alliin suggest that alliin, L-allyl Gly and S-allyl Cys bind at the active site of bsSHMT with different orientations. However, alliin and L-allyl Gly bind in similar orientation/position which is different from that of OADS. Binding of S-allyl Cys was almost similar to that of OADS. Fig 4.25 shows an overlay of all the compounds on OADS. Hence, it is likely that the extract of garlic may consist of S-allyl Cys as a major component, which may be responsible for the inhibition of bsSHMT. However, further studies need to be carried out with individual components of the garlic extract in various combinations to identify the active component. Further, docking of various compounds from database onto SHMT and studies on a few potential compounds from spices may help in identifying a potent inhibitor for SHMT.

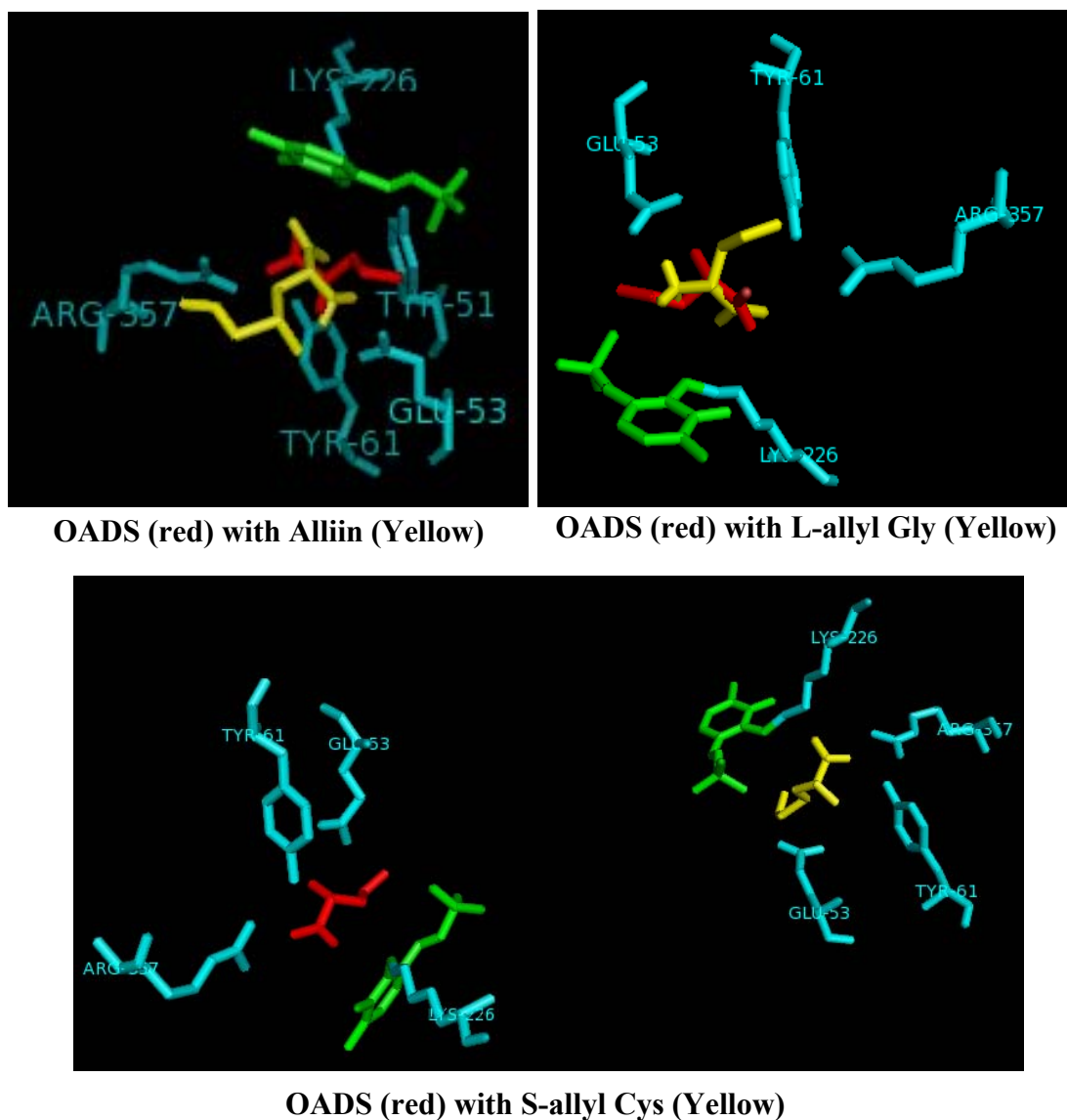


Fig 4.25: An overlay of OADS on Alliin, L-allyl Gly and S-allyl Cys.
 PLP is represented in green and all other active sites are represented in cyan.

SUMMARY AND CONCLUSIONS

A study of enzymes is central to an understanding of biological function. The binding of substrate(s) to an enzyme and its fit at the active site facilitates a multitude of chemical reactions. The mechanism of catalysis include general acid base, covalent and metal ion catalysis. The study of structure-function of enzymes has been central to the elucidation of catalytic mechanisms for biological reactions. In addition to the factors mentioned above, coenzymes which are vitamin derivatives have provided several new insights into biology.

The versatility of PLP and the wide distribution of PLP-dependent enzymes are reflected by the observation that 4% of all catalytic reactions involve this co-enzyme. The availability of biochemical and structural information on more than 140 PLP-enzymes gives a good handle to understand the organization of PLP-enzymes in detail. This information has helped in elucidating the diverse reaction mechanisms of PLP-enzymes. The classification of PLP-enzymes was initially based on the carbon atom involved in the reactions catalyzed. The availability of many primary sequences, three dimensional structures and family profile analyses provided the basis for the present classification. PLP-enzymes are classified into four groups: a) fold type I (α -Family represented by AAT); b) fold type II (β -Family represented by TS); c) fold type III (ALR family) and fold type IV (D-alanine aminotransferase family). SHMT, one of the PLP-enzymes and the subject of this study belongs to the α -family. It links amino acid and nucleotide metabolism. The PLP-dependent enzyme catalyzes many diverse reactions, these include transamination, racemization and decarboxylation. The determinants of substrate specificity are the stereochemical binding of substrate, the conformational changes on binding of substrate, interaction with Arg residues and the changes in hydrogen bond network at the active site.

SHMT catalyzes THF-dependent hydroxymethyltransfer from L-Ser to THF to yield 5, 10-CH₂ THF and Gly. This reaction provides one-carbon fragments for a wide variety of end products in mammalian systems. SHMT being a part of TS cycle, suggested that it could be an alternative target for cancer chemotherapy. SHMT, in addition to L-Ser and Gly inter-conversion, catalyzes cleavage of 3-hydroxy amino acids. L-Thr/L-*allo* Thr cleavage by SHMT results in production of acetaldehyde which is a major flavoring compound in production of fermented dairy products.

Hence SHMT can be used as a starter culture in the manufacture of dairy products. SHMT is used as biocatalysts in the synthesis of β -hydroxy- α -amino acid derivatives.

The objectives of the present investigation are: biochemical characterization of selected residues involved in THF-dependent and -independent reactions; crystallization of the mutant enzymes with their substrate(s)/inhibitor complexes to understand the role of these residues; probe the retroaldol and direct displacement mechanisms for the THF-dependent L-Ser cleavage; establish the mechanism of THF-independent cleavage of 3-hydroxy amino acids by mutation of specific amino acid residues; and study the interaction of chemical inhibitors and compounds from natural sources to understand the role of SHMT in cancer. With these objectives the present investigation was undertaken and results and conclusions are presented out in the form of this thesis entitled “*Structure – Function Relationships in Serine Hydroxymethyltransferase*”.

The present study is divided into four chapters:

Chapter 1: The role of lysine226 in the reaction catalyzed by bsSHMT

Lys residue at the active site of PLP-enzymes in addition to anchoring PLP functions as a proton acceptor or a donor in catalysis. It has been proposed that Lys 229 in eSHMT is crucial for product expulsion, which is a rate determining step of catalysis. Lys 226 of bsSHMT was mutated to Met and Gln, overexpressed and the mutant enzymes were purified. The mutant enzymes contained 1 mol of PLP per mol of subunit suggesting that Schiff's base formation with Lys was not essential for PLP binding. K226M and K226Q bsSHMT were inactive for THF-dependent cleavage of L-Ser. However, cleavage of L-*allo* Thr and transamination reaction was not abolished completely. K226M bsSHMT had distinct λ_{max} of 412 nm and K226Q bsSHMT was similar to that of bsSHMT (425 nm). The crystal structure of K226M bsSHMT revealed that PLP was bound at the active site in an orientation different (16°) from that of the wild-type enzyme. The absence of reaction intermediate at 388 nm on interaction with MA corroborates the suggestion that the active site of K226M bsSHMT was different from that of bsSHMT. Both the Lys mutants were capable of forming an external aldimine; this was also supported by the crystal structure of K226M-Ser/Gly complexes. Spectral studies show the formation of a small amount

of quinonoid intermediate on addition of Gly and THF/FTHF to K226M bsSHMT. However, stopped-flow studies suggested enhanced quinonoid intermediate formed on addition of THF was affected drastically (Fig 1.8b and c). In SHMT, formation of an external aldimine is accompanied by the change in orientation of PLP by 25°. The orientation of PLP in the external aldimine form (25°) changes to 16° during quinonoid intermediate formation. The quinonoid intermediate is stabilized by interactions of Lys at the active site. In the absence of the -NH₂ group of Lys, the conversion of the external aldimine to product quinonoid intermediate, that is, the change in orientation of PLP from 25° to 16°, may not be possible. This in turn could lead to shifting of equilibrium towards the substrate external aldimine form (L-Ser form).

These results show that Lys 226 is responsible for flipping of PLP from one orientation to another, which is accompanied by C_α-C_β bond cleavage. This flip is important in the THF-mediated enhanced C_α proton abstraction from Gly in the reverse reaction.

Chapter 2: The involvement of glutamate 53 of L-serine and folate binding, and conversion of bsSHMT from 'open' to 'closed' form

An examination of the crystal structure of bsSHMT binary and ternary complexes suggested that E53 interacts with L-Ser and FTTHF. Glu 53 was mutated to Gln and structural and biochemical studies were carried out to examine the role of this residue in catalysis. The mutant enzyme was completely inactive for THF-dependent cleavage of L-Ser, whereas there was a 1.5-fold increase in the rate of THF-independent reaction with L-*allo* Thr. Spectral studies showed that E53Q bsSHMT had λ_{max} of 425 nm and the addition of L-Ser/Gly resulted in formation of an external aldimine. The crystal structure of E53Q bsSHMT was similar to that of the wild-type enzyme, except for significant changes at Q53, Y60 and Y61. E53Q bsSHMT binary complex with L-Ser or Gly showed that the side chain of L-Ser and carboxyl of Gly were in two conformations in the respective external aldimine structures. The loss in characteristic decrease in molar ellipticity on addition of L-Ser and loss of enhanced thermal stability suggested that E53Q bsSHMT was unable to undergo a conformational change from 'open' to 'closed' form in which THF-

dependent reaction occurs. Addition of THF/FTHF to E53Q bsSHMT-Gly complex showed the formation of a quinonoid intermediate. Stopped-flow studies were performed to obtain rate constants for the formation of quinonoid intermediate with mutant and wild-type enzymes. However the quinonoid intermediate formed by the mutant enzyme was unstable. Dialysis experiments and dissociation constants (2.5-fold higher) for FT HF suggested that, the affinity for FT HF to mutant binary complex was lower than bsSHMT. This could be due to loss of interaction of N10 and formyl oxygen of FT HF the enzyme. This suggested that Glu plays an important role in folate binding.

The crystal structure of the complex obtained on co-crystallization of E53Q bsSHMT with Gly and FT HF revealed that it exists in a gem-diamine form with an orientation of PLP similar to that of wild-type ternary complex. However, density for FT HF was not observed. The formation of gem-diamine in the above conditions was supported by visible CD spectrum of E53Q bsSHMT ternary complex. The absence of FT HF in the crystal structure and the formation of quinonoid intermediate suggest that there was an initial binding of FT HF to the binary complex of E53Q bsSHMT leading to an alteration in the orientation of PLP. Subsequently, FT HF falls off from the active site leaving behind the gem-diamine complex. The differences between the structures of this complex and Gly external aldimine suggest that the changes induced by initial binding of FT HF are retained, even though FT HF was absent in the final structure. These observations indicate that mutant enzyme exhibits a phenomenon known as “enzyme memory”. In this concept binding of ligands caused conformational changes in the enzyme and even after removal of ligands such imprints of ligand binding were retained by the enzyme. Double reciprocal plots of bsSHMT ternary complex and E53Q bsSHMT-Gly-(FT HF) complex, supports the suggestion that, mutant enzyme exhibits ‘enzyme memory’. This is the first example of structural evidence for ‘enzyme memory’.

The results obtained from these studies suggest that E53 plays an essential role in THF/FT HF binding and in the proper positioning of C_β of L-Ser for direct attack by N5 of THF. It does not have an important role in THF-independent reactions.

Chapter 3: The role of tyrosine residues in cofactor binding and elucidation of mechanism for the tetrahydrofolate-independent cleavage of L-*allo* threonine

Tyr residues play multiple functions in enzyme catalysis. The crystal structure of bsSHMT showed that hydroxyl group of Y51 interacted with the phosphate group of PLP. Binary complex of bsSHMT-Ser showed change in conformation in Y61 on binding of L-Ser. The new conformation Y61 is close to C_β of the bound ligand, L-Ser (2.8 Å). The active site Tyr's was mutated to Y51F, Y61F and Y61A bsSHMT to understand their role in bsSHMT catalysis. Mutation of these residues resulted in a complete loss of THF-dependent and -independent activities. The PLP content of Y51F and Y61F bsSHMT as isolated was 0.2 mol/mol and 0.6 mol/mol of subunit, respectively, compared to 1 mol/mol of subunit in bsSHMT. The mutant enzyme could be completely reconstituted with PLP. However, there was an alteration in the λ_{\max} value of the internal aldimine (396 nm) in the case of Y51F bsSHMT. A decrease in the rate of reduction with NaCNBH₃ and a loss of the intermediate in the interaction with MA suggests that the active site environment is altered in the case of Y51F bsSHMT due to mutation. The mutation of Y51 to F strongly affects the binding of PLP, possibly as a consequence of a change in the orientation of the phenyl ring (75°) in Y51F bsSHMT structure. The results obtained for Y61F were also similar to that of Y51F bsSHMT.

Y61A bsSHMT, as isolated had 1mol/mol of subunit and a λ_{\max} of 425 nm similar to bsSHMT. In addition, Y61A bsSHMT was able to form an external aldimine; this change was supported by enhanced thermal stability of the mutant enzyme on addition of L-Ser. However, the formation of the quinonoid intermediate was hindered. An examination of the active site geometry of bsSHMT and Y51F and Y61A mutants show that Y51 and Y61 are not suitably placed for the removal of the proton from the hydroxyl group of L-*allo* Thr. In bsSHMT, the hydroxyl group of Y51 is at a distance of 3.6 Å and 3.8 Å from C_α of Gly and Ser, respectively. Of the two residues, Y51 is unlikely to be involved in proton abstraction from C_α of the bound ligand due to its longer distance and improper geometry. In contrast, the OH of Y61 is at a distance of 3.3 Å and 3.2 Å from C_α of Gly and Ser, respectively. In Gly, L-Ser and L-*allo* Thr complexes of Y51F bsSHMT, the OH of Y61 and C_α of

bound ligand are at distances 4.97, 4.39 and 4.39 Å, respectively. Y61 therefore may be involved in C_α proton abstraction in the THF-independent reaction.

This might explain the loss of L-*allo* Thr cleavage activity of Y51F bsSHMT. It could therefore, be concluded that Y51 is important for PLP binding and proper positioning of Y61, while Y61 could be involved in the abstraction of the proton from C_α carbon of L-*allo* Thr. Based on these observations, a possible mechanism for SHMT catalyzed cleavage of L-*allo* Thr is suggested.

Chapter 4: The interaction of bsSHMT with specific inhibitors from extracts of various spices

The pivotal role of SHMT in the interconversion of folate coenzymes and its altered kinetic properties in neoplastic tissues suggested that it could be a potential target for cancer chemotherapy. This chapter deals with understanding the interaction of aminoxy compounds with K226M, K226Q, E53Q, Y51F, Y61F and Y61A bsSHMT. MA and AAA interacted with the mutant proteins in different manner. K226M, K226Q bsSHMT did not react with MA and E53Q, Y51F, Y61A and Y61F bsSHMT failed to form 388 nm intermediate on addition of MA. These results suggest that any change at the active site environment or PLP orientation in bsSHMT could lead to the loss of intermediate formation on interaction with MA.

Lys mutants were able to interact with AAA, however the interaction rate was slower compared to bsSHMT suggesting that AAA was a more reactive compared to MA. The absence of Schiff's base and a change in the orientation of PLP at the active site of K226M and K226Q bsSHMTs probably results in poor binding of AAA at the active site. Y51F, Y61F and Y61A bsSHMT showed a similar interaction pattern as that of bsSHMT. Only E53Q bsSHMT showed the formation of an intermediate absorbing at 388 nm on addition of AAA. Stopped-flow studies suggest a drastic decrease in the rate at which AAA interacts with E53Q bsSHMT (13 s⁻¹), when compared to bsSHMT (275 s⁻¹). It is possible that Glu 53 may be the crucial residue involved in binding of AAA as well as in enhancing the rate of the reaction. However, further studies are required to prove this hypothesis.

A fruitful approach of identifying compounds which have anti-carcinogenic effect is to carry out homology modeling and docking of compounds available in several chemical libraries. Homology modeling and docking of commercially available folate analogues were performed. Docking of folate analogues resulted in identification of 14 best compounds of these four water soluble compounds were examined for their ability to inhibit bsSHMT. Activity studies suggested that folate analogues failed to inhibit bsSHMT. In addition to synthetic compounds, naturally occurring compounds from spices that can serve as anti-cancer agents were analyzed for bsSHMT inhibition. The effect of spices such as garlic, ginger, chilli, turmeric extracts was examined. Among all spices, heat-treated and lyophilized garlic extract showed 91% inhibition of bsSHMT. D and L-allyl Gly analogues of substrate L-Ser and S-allyl Cys (probable inhibitor from garlic extract) D and L-allyl Gly, Alliin did not inhibit bsSHMT activity.

Docking studies with S-allyl Cys, D and L-allyl Gly and alliin suggest that alliin, L-allyl Gly and S-allyl Cys bind at the active site of bsSHMT with different orientations. However, alliin and L-allyl Gly bind in similar orientation/position which is different from that of OADS. Binding of S-allyl Cys was almost similar to that of OADS. These results suggest that S-allyl Cys could be a good inhibitor. Chemical synthesis of S-allyl Cys and further activity measurement has to be carried out to demonstrate the inhibition. These results emphasize the importance of examining the naturally occurring and synthetic compounds as possible chemotherapeutic agents.

The results presented in this study re-emphasize the importance of correlating structural information with catalytic function of SHMT. The mutation of Lys 226 demonstrated its role in facilitating the change in orientation of PLP during catalysis. Glu 53 on interaction with L-Ser positions the C_α-C_β bond for attack by N5 of THF, a crucial step in L-Ser cleavage. The loss of efficient binding of FTHF to E53Q bsSHMT-Gly binary complex up on Glu 53 mutation results in the enzyme exhibiting a phenomenon called 'enzyme memory'. Tyr 51 is involved in cofactor binding. Tyr 61 plays an important role in C_α proton abstraction leading to THF-independent cleavage of 3-hydroxy amino acids. These observations prompted a proposal of new mechanism for aldol cleavage of 3-hydroxy amino acids.

References

- Acharya, J.K. (1992) The mechanism of interaction of carbonyl-directed reagents at the active site of sheep liver serine hydroxymethyltransferase, **Ph. D** Thesis, Indian Institute of Science, Bangalore, India.
- Acharya, J.K., Prakash, V., Rao, A.G.A., Savithri, H.S., and Rao, N.A. (1991) Interactions of methoxyamine with pyridoxal-5'-phosphate-schiff's base at the active site of sheep liver serine hydroxymethyltransferase. *Indian J Biochem Biophys*, **28**, 381-388.
- Acharya, J.K., and Rao, N.A. (1992) A novel intermediate in the interaction of thiosemicarbazide with sheep liver serine hydroxymethyltransferase. *J Biol Chem*, **267**, 19066-19071.
- Alastair, A., and Learmonth, M.P. (2002) Protein determination by UV absorption. In J.M. Walker, Ed. *The protein protocols handbook*, **Part 1**. Humana Press Inc Totowa, N J, USA.
- Alder, A.J., Greenfield, N.J., and Fasman, G.D. (1973) Circular dichroism and optical rotatory dispersion of proteins and polypeptides. *Meth Enzymol*, **27**, 675 - 735.
- Alexander, D.C. (1987) An efficient vector-primer cDNA cloning system: Large scale preparation of competent cells. *Meth Enzymol.*, **154**, 41-64.
- Amadasi, A., Bertoldi, M., Contestabile, R., Bettati, S., Cellini, B., di Salvo, M.L., Borri-Voltattorni, C., Bossa, F., and Mozzarelli, A. (2007) Pyridoxal 5'-phosphate enzymes as targets for therapeutic agents. *Curr Med Chem*, **14**, 1291-1324.
- Angelaccio, S., Chiaraluce, R., Consalvi, V., Buchenau, B., Giangiacomo, L., Bossa, F., and Contestabile, R. (2003) Catalytic and thermodynamic properties of tetrahydromethanopterin-dependent serine hydroxymethyltransferase from *Methanococcus jannaschii*. *J Biol Chem*, **278**, 41789-41797.
- Appaji Rao, N., Ambili, M., Jala, V.R., Subramanya, H.S., and Savithri, H.S. (2003) Structure-function relationship in serine hydroxymethyltransferase. *Biochim Biophys Acta*, **1647**, 24-29.
- Appaji Rao, N., Talwar, R., and Savithri, H.S. (2000) Molecular organization, catalytic mechanism and function of serine hydroxymethyltransferase-a potential target for cancer chemotherapy. *Int J Biochem Cell Biol*, **32**, 405-416.
- Baskaran, N. (1989) The mechanism of interaction of O-amino-D-serine and other aminoxy compounds with sheep liver serine hydroxymethyltransferase, **Ph. D**. Thesis, Indian Institute of Science, Bangalore, India.
- Baskaran, N., Prakash, V., Rao, A. G. A., Radhakrishnan, A.N., Savithri, H.S., and Appaji Rao, N. (1989a) Mechanism of interaction of O-amino-D-serine with sheep liver serine hydroxymethyltransferase. *Biochemistry*, **28**, 9607-9612.

- Baskaran, N., Prakash, V., Savithri, H.S., Radhakrishnan, A.N., and Appaji Rao, N. (1989b) Mode of interaction of aminoxy compounds with sheep liver serine hydroxymethyltransferase. *Biochemistry*, **28**, 9613-9617.
- Bertino, J.R., Silber, R., Freeman, M., Alenty, A., Albrecht, M., Gabrio, B.W., and Huennekens, F.M. (1963) Studies on normal and leukemic leukocytes. *Iv*. Tetrahydrofolate-dependent enzyme systems and dihydrofolic reductase. *J Clin Invest*, **42**, 1899-1907.
- Bukin Iu, V., and Sergeev, A.V. (1968) Comparative sensitivity of mouse liver serine-hydroxymethyltransferase to carbonyl reagents and decrease in activity of the enzyme during B6 deficiency. *Biokhimiia*, **33**, 1092-1101.
- Burkhard, P., Rao, G.S., Hohenester, E., Schnackerz, K.D., Cook, P.F., and Jansonius, J.N. (1998) Three-dimensional structure of O-acetylserine sulfhydrylase from *Salmonella typhimurium*. *J Mol Biol*, **283**, 121-133.
- Capelluto, D.G., Hellman, U., Cazzulo, J.J., and Cannata, J.J. (2000) Purification and some properties of serine hydroxymethyltransferase from *Trypanosoma cruzi*. *Eur J Biochem*, **267**, 712-719.
- Chang, W.N., Tsai, J.N., Chen, B.H., Huang, H.S., and Fu, T.F. (2007) Serine hydroxymethyltransferase isoforms are differentially inhibited by leucovorin: Characterization and comparison of recombinant zebrafish serine hydroxymethyltransferases. *Drug Metab Dispos*, **35**, 2127-2137.
- Chaturvedi, S., and Bhakuni, V. (2003) Unusual structural, functional, and stability properties of serine hydroxymethyltransferase from *Mycobacterium tuberculosis*. *J Biol Chem*, **278**, 40793-40805.
- Chaves, A.C., Fernandez, M., Lerayer, A.L., Mierau, I., Kleerebezem, M., and Hugenholtz, J. (2002) Metabolic engineering of acetaldehyde production by *Streptococcus thermophilus*. *Appl Environ Microbiol*, **68**, 5656-5662.
- Chen, D., and Frey, P.A. (2001) Identification of lysine 346 as a functionally important residue for pyridoxal 5'-phosphate binding and catalysis in lysine 2, 3-aminomutase from *Bacillus subtilis*. *Biochemistry*, **40**, 596-602.
- Chen, M.S., and Schirch, L.V. (1973) Serine transhydroxymethylase. A kinetic study of the synthesis of serine in the absence of tetrahydrofolate. *J Biol Chem*, **248**, 3631-3635.
- Christen, P., Kasper, P., Gehring, H., and Sterk, M. (1996) Stereochemical constraint in the evolution of pyridoxal-5'-phosphate-dependent enzymes. A hypothesis. *FEBS Lett*, **389**, 12-14.
- Christen, P., and Mehta, P.K. (2001) From cofactor to enzymes. The molecular evolution of pyridoxal-5'-phosphate-dependent enzymes. *Chem Rec*, **1**, 436-447

- Christen, P., and Metzler, D.E. (1985) *Transaminases*. Wiley: New York; Chichester, USA.
- Ciotti, M.M., and Kaplan, N.O. (1957) Procedures for determination of pyridine nucleotides. *Meth Enzymol*, **3**, 890-899.
- Contestabile, R., Angelaccio, S., Bossa, F., Wright, H.T., Scarsdale, N., Kazanina, G., and Schirch, V. (2000) Role of tyrosine 65 in the mechanism of serine hydroxymethyltransferase. *Biochemistry*, **39**, 7492-500.
- David, D., Rozanne, P., and Olga, A. (1986) Cytidine diphosphate 4-keto-6-dioxy-D-glucose-3-dehydrogenase. D. David, P. Rozanne, and A. Olga, Eds. In *Coenzymes and cofactors, vitamin B6 pyridoxal phosphate-chemical, biochemical and medical aspects*, **1**, p. 392-418. Wiley Interscience, New York, USA.
- Denessiouk, K.A., Denesyuk, A.I., Lehtonen, J.V., Korpela, T., and Johnson, M.S. (1999) Common structural elements in the architecture of the cofactor-binding domains in unrelated families of pyridoxal phosphate-dependent enzymes. *Proteins*, **35**, 250-261.
- DeLano, W.L. (2002) The PyMOL molecular graphics system. DeLano Scientific, San Carlos, CA, USA.
- Dong, Y., Lisk, D., Block, E., and Ip, C. (2001) Characterisation of the biological activity of gamma-glutamyl-semethylselenocysteine: A novel, naturally occurring anticancer agent from garlic. *Cancer Res*, **61**, 2923-2928.
- Dunathan, H.C. (1966) Conformation and reaction specificity in pyridoxal phosphate enzymes. *Proc Natl Acad Sci, USA*, **55**, 712-716.
- Dunn, M.F., Aguilar, V., Brzovic, P., Drewe, W.F., Houben, K.F., Leja, C.A., and Roy, M. (1990) The tryptophan synthase holoenzyme complex transfers indole between the alpha- and beta-sites via a 25-30 Å long tunnel. *Biochemistry*, **29**, 8598-8607.
- Eliot, A.C., and Kirsch, J.F. (2004) Pyridoxal phosphate enzymes: Mechanistic, structural, and evolutionary considerations. *Annu Rev Biochem*, **73**, 383-415.
- Emsley, P., and Cowtan, K. (2004) Coot: Model-building tools for molecular graphics. *Acta Cryst D* **60**, 2126-2132.
- Evande, R., Ojha, S., and Banerjee, R. (2004) Visualization of PLP-bound intermediates in hemeless variants of human cystathionine beta-synthase: Evidence that lysine 119 is a general base. *Arch Biochem Biophys*, **427**, 188-196.
- Finkelstein, J.D., Kyle, W.E., Martin, J.L., and Pick, A.M. (1975) Activation of cystathionine synthase by adenosylmethionine and adenosylethionine. *Biochem Biophys Res Commun*, **66**, 81-87.

- Ford, G.C., Eichele, G., and Jansonius, J.N. (1980) Three-dimensional structure of a pyridoxal-phosphate-dependent enzyme, mitochondrial aspartate aminotransferase. *Proc Natl Acad Sci, USA*, **77**, 2559-2563.
- Franca, T.C., Pascutti, P.G., Ramalho, T.C., and Figueroa-Villar, J.D. (2005) A three-dimensional structure of *Plasmodium falciparum* serine hydroxymethyltransferase in complex with glycine and 5-formyl-tetrahydrofolate. Homology modeling and molecular dynamics. *Biophys Chem*, **115**, 1-10.
- Fratte, S.D., Iurescia, S., Angelaccio, S., Bossa, F., and Schirch, V. (1994) The function of arginine 363 as substrate carboxyl-binding site in *Escherichia coli* serine hydroxymethyltransferase. *Eur J Biochem*, **225**, 395-401.
- Fu, T.F., Boja, E.S., Safo, M.K., and Schirch, V. (2003) Role of proline residues in the folding of serine hydroxymethyltransferase. *J Biol Chem*, **278**, 31088-31094.
- Gentry-Weeks, C.R., Spokes, J., and Thompson, J. (1995) Beta-cystathionase from *Bordetella avium*. Role(s) of lysine 214 and cysteine residues in activity and cytotoxicity. *J Biol Chem*, **270**, 7695-7702.
- Gloss, L.M., and Kirsch, J.F. (1995) Examining the structural and chemical flexibility of the active site base, Lys-258, of *Escherichia coli* aspartate aminotransferase by replacement with unnatural amino acids. *Biochemistry*, **34**, 12323-12332.
- Golberg, J.M., Zheng, J., Deng, H., Chen, Y.Q., Callender, R., and Kirsch, J.F. (1993) The tyrosine-225 to phenylalanine mutation of *Escherichia coli* aspartate aminotransferase results in an alkaline transition in the spectrophotometric and kinetic pK_a values and reduced values of both k_{cat} and k_m . *Biochemistry*, **32**, 8092-8097.
- Graber, R., Kasper, P., Malashkevich, V.N., Sandmeier, E., Berger, P., Gehring, H., Jansonius, J.N., and Christen, P. (1995) Changing the reaction specificity of a pyridoxal-5'-phosphate-dependent enzyme. *Eur J Biochem*, **232**, 686-690.
- Graber, R., Kasper, P., Malashkevich, V.N., Strop, P., Gehring, H., Jansonius, J.N., and Christen, P. (1999) Conversion of aspartate aminotransferase into an L-aspartate beta-decarboxylase by a triple active-site mutation. *J Biol Chem*, **274**, 31203-31208.
- Gutierrez, M.L., Garrabou, X., Agosta, E., Servi, S., Parella, T., Joglar, J., and Clapes, P. (2008) Serine hydroxymethyl transferase from *Streptococcus thermophilus* and L-threonine aldolase from *Escherichia coli* as stereocomplementary biocatalysts for the synthesis of beta-hydroxy-alpha, omega-diamino acid derivatives. *Chemistry*, **14**, 4647-4656.
- Hartman, P.G. (1993) Molecular aspects and mechanism of action of dihydrofolate reductase inhibitors. *J Chemother*, **5**, 369-376.

- Hatefi, Y., Talbert, P.T., Osborn, M.J., and Huennekens, F.M. (1959) *Biochem Prep*, **7**, 89-92.
- Hayashi, H., Inoue, K., Nagata, T., Kuramitsu, S., and Kagamiyama, H. (1993) *Escherichia coli* aromatic amino acid aminotransferase: Characterization and comparison with aspartate aminotransferase. *Biochemistry*, **32**, 12229-12239.
- Henderson, G.B., Murgolo, N.J., Kuriyan, J., Osapay, K., Kominos, D., Berry, A., Scrutton, N.S., Hinchliffe, N.W., Perham, R.N., and Cerami, A. (1991) Engineering the substrate specificity of glutathione reductase toward that of trypanothione reduction. *Proc Natl Acad Sci, USA*, **88**, 8769-8773.
- Huennekens, F.M. (1994) The methotrexate story: A paradigm for development of cancer chemotherapeutic agents. *Adv Enzyme Regul*, **34**, 397-419.
- Huennekens, F.M., Ho, P.P.K., and Scrimgeour, K.G. (1963) Preparations and properties of active formaldehyde and active formate. *Meth Enzymol*, **6**, 806-811.
- Hyde, C.C., Ahmed, S.A., Padlan, E.A., Miles, E.W., and Davies, D.R. (1988) Three-dimensional structure of the tryptophan synthase $\alpha_2 \beta_2$ multienzyme complex from *Salmonella typhimurium*. *J Biol Chem*, **263**, 17857-17871.
- Inoue, K., Kuramitsu, S., Okamoto, A., Hirotsu, K., Higuchi, T., and Kagamiyama, H. (1991) Site-directed mutagenesis of *Escherichia coli* aspartate aminotransferase: Role of Tyr70 in the catalytic processes. *Biochemistry*, **30**, 7796-7801.
- Jacques, R., Jean-Claude, M., and Jean, B. (1974) Regulatory behavior of monomeric enzymes. The mnemonical enzyme concept. *Eur J Biochem*, **49**, 195-208
- Jagannatha Rao, G.S. (1982) Hysteretic regulation of mung bean (*Vigna radiata*) aspartate transcarbamylase and crystal structure of carbamyl aspartic acid, **Ph D**. Indian Institute of Science, Bangalore, India.
- Jagath, J.R. (1997) Molecular insights into the structure and catalytic mechanism of mammalian cytosolic serine hydroxymethyltransferase, **Ph. D**. Thesis, Indian Institute of Science, Bangalore, India.
- Jagath, J.R., Appaji Rao, N., and Savithri, H.S. (1997a) Role of Arg - 401 of cytosolic serine hydroxymethyltransferase in subunit assembly and interaction with the substrate carboxyl group. *Biochem J*, **327**, 877-882.
- Jagath, J.R., Sharma, B., Rao, N.A., and Savithri, H.S. (1997b) The role of His-134, -147, and -150 residues in subunit assembly, cofactor binding, and catalysis of sheep liver cytosolic serine hydroxymethyltransferase. *J Biol Chem*, **272**, 24355-24362.

- Jager, J., Moser, M., Sauder, U., and Jansonius, J.N. (1994) Crystal structures of *Escherichia coli* aspartate aminotransferase in two conformations. Comparison of an unliganded open and two liganded closed forms. *J Mol Biol*, **239**, 285-305.
- Jala, V.R. (2002) Unraveling the structure-function relationships in serine hydroxymethyltransferase: Targeted mutagenesis, **Ph.D.** Thesis, Indian Institute of Science, Bangalore, India.
- Jala, V.R., Ambili, M., Prakash, V., Appaji Rao, N., and Savithri, H.S. (2003a) Disruption of distal interactions of Arg 262 and of substrate binding to Ser 52 affect catalysis of sheep liver cytosolic serine hydroxymethyltransferase. *Indian J Biochem Biophys*, **40**, 226-237.
- Jala, V.R., Appaji Rao, N., and Savithri, H.S. (2003b) Identification of amino acid residues, essential for maintaining the tetrameric structure of sheep liver cytosolic serine hydroxymethyltransferase, by targeted mutagenesis. *Biochem J*, **369**, 469-476.
- Jala, V.R., Prakash, V., Rao, N.A., and Savithri, H.S. (2000) The role of Glu74 and Tyr82 in the reaction catalyzed by sheep liver cytosolic serine hydroxymethyltransferase. *Eur J Biochem*, **267**, 5967-5976.
- Jala, V.R., Prakash, V., Rao, N.A., and Savithri, H.S. (2002) Overexpression and characterization of dimeric and tetrameric forms of recombinant serine hydroxymethyltransferase from *Bacillus stearothermophilus*. *J Biosci*, **27**, 233-242.
- Jean, B., Jacques Ricard and Jean-Claude M. (1977) Enzyme memory: Kinetics and thermodynamics of the slow conformation changes of wheat-germ hexokinase. *Eur J Biochem*, **80**, 593-601.
- Jensen, R.A., and Gu, W. (1996) Evolutionary recruitment of biochemically specialized subdivisions of family I within the protein superfamily of aminotransferases. *J Bacteriol*, **178**, 2161-2171.
- John, R.A. (1995) Pyridoxal phosphate-dependent enzymes. *Biochim Biophys Acta*, **1248**, 81-96.
- Jordan, P.M., and Akhtar, M. (1970) The mechanism of action of serine transhydroxymethylase. *Biochem J*, **116**, 277-286.
- Katz, M., and Westley, J. (1979) Enzymic memory. Steady state kinetic and physical studies with ascorbate oxidase and aspartate aminotransferase. *J Biol Chem*, **254**, 9142-9147.
- Kochhar, S., and Christen, P. (1992) Mechanism of racemization of amino acids by aspartate aminotransferase. *Eur J Biochem*, **203**, 563-569.

- Kolsterman, H.J. (1986) In Coenzymes and cofactors. D. Dolphin, R. Poulson, and O. Avramovic, Eds. John Wiley-Interscience, New York, USA.
- Koshland, D.E. (1970) In "The enzymes". In P.D. Boyer, Ed, **vol 1**, p. 341-396. Academic press, New York, USA.
- Kumar, P.M., North, J.A., Mangum, J.H., and Rao, N.A. (1976) Cooperative interactions of tetrahydrofolate with purified pig kidney serine transhydroxymethylase and loss of this cooperativity in 11210 tumors and in tissues of mice bearing these tumors. *Proc Natl Acad Sci U S A*, **73**, 1950-1953.
- Laemmli, U.K. (1970) Cleavage of structural proteins during the assembly of the head of bacteriophage T4. *Nature*, **227**, 680-685.
- Larry, D.L., and Christopher, D.G. (2005) Composition, stability and bioavailability of garlic products used in a clinical trial. *J Agric Food Chem*, **53**, 6254-6261.
- Laskowski, R.A., McArthur, M.W., Moss, D.S., Thornton, J.M. (1993) PROCHECK: A program to check the stereo-chemical quality of protein structures. *J Appl Cryst*, **26**, 283-291.
- Layne, E. (1957) Spectrophotometric and turbidimetric methods for measuring proteins. *Meth Enzymol*, **3**, 447-454.
- Leartsakulpanich, U., Kongkasuriyachai, D., Imwong, M., Chotivanich, K., and Yuthavong, Y. (2008) Cloning and characterization of *Plasmodium vivax* serine hydroxymethyltransferase. *Parasitol Int*, **57**, 223-228.
- Lin, H.B., Falchetto, R., Mosca, P.J., Shabanowitz, J., Hunt, D.F., and Hamlin, J.L. (1996) Mimosine targets serine hydroxymethyltransferase. *J Biol Chem*, **271**, 2548-2556.
- Lowry, O.H., Rosebrough, N.J., Farr, A.L., and Randall, R.J. (1951) Protein measurement with the folin phenol reagent. *J Biol Chem*, **193**, 265-275.
- Lu, Z., Nagata, S., McPhie, P., and Miles, E.W. (1993) Lysine 87 in the beta subunit of tryptophan synthase that forms an internal aldimine with pyridoxal phosphate serves critical roles in transamination, catalysis, and product release. *J Biol Chem*, **268**, 8727-8734.
- Madison, J.T., and Thompson, J.F. (1976) Threonine synthetase from higher plants: Stimulation by S-adenosylmethionine and inhibition by cysteine. *Biochem Biophys Res Commun*, **71**, 684-691.
- Malashkevich, V.N., Jager, J., Zaik, M., Sauder, U., Gehring, H., Christen, P., and Jansonius, J.N. (1995a) Structural basis for the catalytic activity of aspartate aminotransferase K258H lacking the pyridoxal-5'-phosphate-binding lysine residue. *Biochemistry*, **34**, 405-414

- Malashkevich, V.N., Onuffer, J.J., Kirsch, J.F., and Jansonius, J.N. (1995b) Alternating arginine-modulated substrate specificity in an engineered tyrosine aminotransferase. *Nat Struct Biol*, **2**, 548-553.
- Malcom, B.A., and Kirsch, J.F. (1985) Site-directed mutagenesis of aspartate aminotransferase from *Escherichia coli*. *Biochem Biophys Res Commun*, **132**, 915-921.
- Malkin, L.I., and Greenberg, D.M. (1964) Purification and properties of threonine or *allo*-threonine aldolase from rat liver. *Biochim Biophys Acta*, **85**, 117-131.
- Manohar, R., Rao, A.G.A., and Rao, N.A. (1984) Kinetic mechanism of the interaction of D-cycloserine with serine hydroxymethyltransferase. *Biochemistry*, **23**, 4116-4122.
- Matsui, I., Matsui, E., Sakai, Y., Kikuchi, H., Kawarabayasi, Y., Ura, H., Kawaguchi, S., Kuramitsu, S., and Harata, K. (2000) The molecular structure of hyperthermostable aromatic aminotransferase with novel substrate specificity from *Pyrococcus horikoshii*. *J Biol Chem*, **275**, 4871-4879.
- Matthews, R.B., and Drummond, J.T. (1990) Providing one-carbon units for biological methylations: Mechanistic studies on the serine hydroxymethyltransferase, methylenetetrahydrofolate reductase and methyltetrahydrofolate-homocysteine methyltransferase. *Chem Rev*, **90**, 1275-1290.
- Mehta, P.K., and Christen, P. (2000) The molecular evolution of pyridoxal-5'-phosphate-dependent enzymes. *Adv Enzymol Relat Areas Mol Biol*, **74**, 129-184.
- Miles, E.W. (1991) Structural basis for catalysis by tryptophan synthase. *Adv Enzymol Relat Areas Mol Biol*, **64**, 93-172.
- Mukherjee, M., Sievers, S.A., Brown, M.T., and Johnson, P.J. (2006) Identification and biochemical characterization of serine hydroxymethyl transferase in the hydrogenosome of *Trichomonas vaginalis*. *Eukaryot Cell*, **5**, 2072-2078.
- Murshudov, G.N., Vagin, A.A., and Dodson, E.J. (1997) Refinement of macromolecular structures by the maximum-likelihood method. *Acta Cryst D*, **53**, 240-255.
- Nakagawa, H., Tsuta, K., Kiuchi, K., Senzaki, H., Tanaka, K., Hioki, K., and Tsubura, A. (2001) Growth inhibitory effects of diallyl disulfide on human breast cancer cell lines. *Carcinogenesis*, **22**, 891-897.
- Nelson, R.L. (1982) The comparative clinical pharmacology and pharmacokinetics of vindesine, vincristine and vinblastine in human patients with cancer. *Med Pediatr Oncol*, **10**, 115.

- Okamoto, A., Ishii, S., Hirotsu, K., and Kagamiyama, H. (1999) The active site of *Paracoccus denitrificans* aromatic amino acid aminotransferase has contrary properties: Flexibility and rigidity. *Biochemistry*, **38**, 1176-1184.
- Okamoto, A., Nakai, Y., Hayashi, H., Hirotsu, K., and Kagamiyama, H. (1998) Crystal structures of *Paracoccus denitrificans* aromatic amino acid aminotransferase: A substrate recognition site constructed by rearrangement of hydrogen bond network. *J Mol Biol*, **280**, 443-461.
- Onuffer, J.J., and Kirsch, J.F. (1995) Redesign of the substrate specificity of *Escherichia coli* aspartate aminotransferase to that of *Escherichia coli* tyrosine aminotransferase by homology modeling and site-directed mutagenesis. *Protein Sci*, **4**, 1750-1757.
- Oppenheim, E.W., Nasrallah, I.M., Mastri, M.G., and Stover, P.J. (2000) Mimosine is a cell-specific antagonist of folate metabolism. *J Biol Chem*, **275**, 19268-19274.
- Osterman, A.L., Brooks, H.B., Jackson, L., Abbott, J.J., and Phillips, M.A. (1999) Lysine-69 plays a key role in catalysis by ornithine decarboxylase through acceleration of the schiff base formation, decarboxylation, and product release steps. *Biochemistry*, **38**, 11814-11826.
- Otwinowsky, Z., and Minor, W. (1997) Processing of X-ray diffraction data collected in oscillation mode. *Meth Enzymol*, **276**, 307-326.
- Paiardini, A., Contestabile, R., D'Aguzzo, S., Pascarella, S., and Bossa, F. (2003) Threonine aldolase and alanine racemase: Novel examples of convergent evolution in the superfamily of vitamin B6-dependent enzymes. *Biochim Biophys Acta*, **647**, 214-219.
- Pan, P., Jaussi, R., Gehring, H., Giannatosio, S., and Christen, P. (1994) Shift in pH-rate profile and enhanced discrimination between dicarboxylic and aromatic substrates in mitochondrial aspartate aminotransferase Y70H. *Biochemistry*, **33**, 2757-2760.
- Perry, C., Sastry, R., Nasrallah, I.M., and Stover, P.J. (2005) Mimosine attenuates serine hydroxymethyltransferase transcription by chelating zinc. Implications for inhibition of DNA replication. *J Biol Chem*, **280**, 396-400.
- Peterson, E.A., and Sober, H.A. (1954) Preparation of crystalline phosphorylated derivatives of vitamin B6. *J Am Chem Soc*, **76**, 169-183.
- Phillips, R.S., Chen, H.Y., Shim, D., Lima, S., Tavakoli, K., and Sundararaju, B. (2004) Role of lysine-256 in *Citrobacter freundii* tyrosine phenol-lyase in monovalent cation activation. *Biochemistry*, **43**, 14412-14419.
- Pinto, J.T., and Rivlin, R.S. (2001) Antiproliferative effects of allium derivatives from garlic. *J Nutr*, **131**, 1058S -1060S.

- Picot, D., Sandmeier, E., Thaller, C., Vincent, M.G., Christen, P., and Jansonius, J.N. (1991) The open/closed conformational equilibrium of aspartate aminotransferase. Studies in the crystalline state and with a fluorescent probe in solution. *Eur J Biochem*, **196**, 329-341.
- Rabin, B.Q. (1967) Cooperative effects in enzyme catalysis: A possible kinetic model based on substrate induced conformation isomerization. *Biochem J*, **103**, 22c-23c.
- Rahman, K. (2003) Garlic and aging: New insights into an old remedy. *Age Res Rev*, **2**, 39-56.
- Rao, N.A., Talwar, R., and Savithri, H.S. (2000) Molecular organization, catalytic mechanism and function of serine hydroxymethyltransferase-a potential target for cancer chemotherapy. *Int J Biochem Cell Biol*, **32**, 405-416.
- Rege, V.D., Kredich, N.M., Tai, C.H., Karsten, W.E., Schnackerz, K.D., and Cook, P.F. (1996) A change in the internal aldimine lysine (K42) in *O*-acetylserine sulfhydrylase to alanine indicates its importance in transamination and as a general base catalyst. *Biochemistry*, **35**, 13485-13493.
- Renwick, S.B., Snell, K., and Baumann, U. (1998) The crystal structure of human cytosolic serine hydroxymethyltransferase: A target for cancer chemotherapy. *Structure*, **6**, 1105-1116.
- Rustum, Y.M., Harstrick, A., Cao, S., Vanhoefer, U., Yin, M.B., Wilke, H., and Seeber, S. (1997) Thymidylate synthase inhibitors in cancer therapy: Direct and indirect inhibitors. *J Clin Oncol*, **15**, 389-400.
- Saeed, A., and Young, D.W. (1992) Synthesis of L-beta-hydroxy amino acids using serine hydroxymethyltransferase. *Tetrahedron*, **48**, 2507-2514.
- Sambrook, J., and Russell, D.W. (2001) Molecular cloning: A laboratory manual. Cold Spring Harbour Laboratory Press, Cold Spring, Harbour, NY, USA.
- Sanger, F., Nicklen, S., and Coulson, A.R. (1977) DNA sequencing with chain-terminating inhibitors. *Proc Natl Acad Sci USA*, **74**, 5463-5467.
- Scarsdale, J.N., Kazanina, G., Radaev, S., Schirch, V., and Wright, H.T. (1999) Crystal structure of rabbit cytosolic serine hydroxymethyltransferase at 2.8 Å resolution: Mechanistic implications. *Biochemistry*, **38**, 8347-8358.
- Scarsdale, J.N., Radaev, S., Kazanina, G., Schirch, V., and Wright, H.T. (2000) Crystal structure at 2.4 Å resolution of *E. Coli* serine hydroxymethyltransferase in complex with glycine substrate and 5-formyl tetrahydrofolate. *J Mol Biol*, **296**, 155-168.
- Schirch, D., Delle Fratte, S., Iurescia, S., Angelaccio, S., Contestabile, R., Bossa, F., and Schirch, V. (1993a) Function of the active-site lysine in *Escherichia coli* serine hydroxymethyltransferase. *J Biol Chem*, **268**, 23132-23138.

- Schirch, D., Delle Fratte, S., Iurescia, S., Angelaccio, S., Contestabile, R., Bossa, F., and Schirch, V. (1993b) Serine hydroxymethyltransferase: Role of the active site lysine in the mechanism of the enzyme. *Adv Exp Med Biol*, **338**, 715-718.
- Schirch, L. (1982) Serine hydroxymethyltransferase. *Adv Enzymol Relat Areas Mol Biol*, **53**, 83-112.
- Schirch, L.V.G., and Mason, M. (1963) Serine transhydroxymethylase. A study of the properties of a homogeneous enzyme preparation and of the nature of its interaction with substrates and pyridoxal 5-phosphate. *J Biol Chem*, **238**, 1032-1037.
- Schirch, V., Shostak, K., Zamora, M., and Guatam-Basak, M. (1991) The origin of reaction specificity in serine hydroxymethyltransferase. *J Biol Chem*, **266**, 759-764.
- Schirch, V., and Szebenyi, D.M. (2005) Serine hydroxymethyltransferase revisited. *Curr Opin Chem Biol*, **9**, 482-487.
- Schirch, V.L., and Jenkins, W.T. (1964a) Serine transhydroxymethylase. Properties of the enzyme-substrate complexes of D-alanine and glycine. *J Biol Chem*, **239**, 3801-3807.
- Schirch, V.L., and Jenkins, W.T. (1964b) Serine transhydroxymethylase. Transamination of D-alanine. *J Biol Chem*, **239**, 3797-3800.
- Schirch, V.L., and Ropp, M. (1967) Serine transhydroxymethylase. Affinity of tetrahydrofolate compounds for the enzyme and enzyme-glycine complex. *Biochemistry*, **6**, 253-257.
- Sharma, S., and Bhakuni, V. (2007) Cloning and structural analysis of *Mycobacterium leprae* serine hydroxymethyltransferase. *Protein Expr Purif*, **55**, 189-197.
- Shaw, J.P., Petsko, G.A., and Ringe, D. (1997) Determination of the structure of alanine racemase from *Bacillus stearothermophilus* at 1.9 Å resolution. *Biochemistry*, **36**, 1329-1342.
- Snell, E.E. (1981) Vitamin B-6 analysis: Some historical aspects In methods in vitamin B-6 nutrition. In J.E. Leklum, and R.D. Reynolds, Eds. Plenum press, New York, USA.
- Snell, K. (1984) Enzymes of serine metabolism in normal, developing and neoplastic rat tissues. *Adv Enzyme Regul*, **22**, 325-400.
- Snell, K. (1985) Enzymes of serine metabolism in normal and neoplastic rat tissues. *Biochim Biophys Acta*, **843**, 276-281.

- Snell, K., and Riches, D. (1989) Effects of a triazine antifolate (nsc 127755) on serine hydroxymethyltransferase in myeloma cells in culture. *Cancer Lett*, **44**, 217-220.
- Storici, P., Capitani, G., De Biase, D., Moser, M., John, R.A., Jansonius, J.N., and Schirmer, T. (1999a) Crystal structure of GABA-aminotransferase, a target for antiepileptic drug therapy. *Biochemistry*, **38**, 8628-8634.
- Storici, P., Capitani, G., Muller, R., Schirmer, T., and Jansonius, J.N. (1999b) Crystal structure of human ornithine aminotransferase complexed with the highly specific and potent inhibitor 5-fluoromethylornithine. *J Mol Biol*, **285**, 297-309.
- Stover, P., and Schirch, V. (1991) 5-formyltetrahydrofolate polyglutamates are slow tight binding inhibitors of serine hydroxymethyltransferase. *J Biol Chem*, **266**, 1543-1550.
- Stover, P., Zamora, M., Shoshtak, K., Gautam-Basak, M., and Schirch, V. (1992) *Escherichia coli* serine hydroxymethyltransferase. The role of histidine 228 in determining reaction specificity. *J Biol Chem*, **267**, 17679-17687.
- Studier, F.W., and Moffatt, B.A. (1986) Use of bacteriophage T7 RNA polymerase to direct selective high-level expression of cloned genes. *J Mol Biol*, **189**, 113-130.
- Sugio, S., Petsko, G.A., Manning, J.M., Soda, K., and Ringe, D. (1995) Crystal structure of a D-amino acid aminotransferase: How the protein controls stereoselectivity. *Biochemistry*, **34**, 9661-9669.
- Sun, S., and Toney, M.D. (1999) Evidence for a two-base mechanism involving tyrosine-265 from arginine-219 mutants of alanine racemase. *Biochemistry*, **38**, 4058-4065.
- Sun, S., Zabinski, R.F., and Toney, M.D. (1998) Reactions of alternate substrates demonstrate stereoelectronic control of reactivity in dialkylglycine decarboxylase. *Biochemistry*, **37**, 3865 -3875.
- Sundaram, S.G., and Milner, J.A. (1996a) Diallyl disulfide induces apoptosis of human colon tumor cells. *Carcinogenesis*, **17**, 669-673.
- Sundaram, S.G., and Milner, J.A. (1996b) Diallyl disulfide inhibits the proliferation of human tumor cells in culture. *Biochim Biophys Acta*, **1315**, 15-20.
- Szebenyi, D.M., Liu, X., Kriksunov, I.A., Stover, P.J., and Thiel, D.J. (2000) Structure of a murine cytoplasmic serine hydroxymethyltransferase quinonoid ternary complex: Evidence for asymmetric obligate dimers. *Biochemistry*, **39**, 13313-13323.
- Szebenyi, D.M., Musayev, F.N., di Salvo, M.L., Safo, M.K., and Schirch, V. (2004) Serine hydroxymethyltransferase: Role of Glu75 and evidence that serine is cleaved by a retroaldol mechanism. *Biochemistry*, **43**, 6865-6876.

- Talwar, R., Jagath, J.R., Datta, A., Prakash, V., Savithri, H.S., and Rao, N.A. (1997) The role of lysine-256 in the structure and function of sheep liver recombinant serine hydroxymethyltransferase. *Acta Biochim Pol*, **44**, 679-688.
- Talwar, R., Jagath, J.R., Rao, N.A., and Savithri, H.S. (2000a) His230 of serine hydroxymethyltransferase facilitates the proton abstraction step in catalysis. *Eur J Biochem*, **267**, 1441-1446.
- Talwar, R., Rao, N.A., and Savithri, H.S. (2000b) A change in reaction specificity of sheep liver serine hydroxymethyltransferase. Induction of NADH oxidation upon mutation of His230 to tyr. *Eur J Biochem*, **267**, 929-934.
- Talwar, R., Leelavathy, V., Krishna Rao, J.V., Appaji Rao, N., and Savithri, H.S. (2000c) Role of Pro-297 in the catalytic mechanism of sheep liver serine hydroxymethyltransferase. *Biochem J*, **350**, 849-853.
- Tan, D., Barber, M.J., and Ferreira, G.C. (1998) The role of tyrosine 121 in cofactor binding of 5-aminolevulinic acid synthase. *Protein Sci*, **7**, 1208-1213.
- Taylor, R.T., and Weissbach, H. (1965) A radioactive assay for serine hydroxymethyltransferase. *Anal Biochem*, **13**, 80-84.
- Then, R.L. (1993) History and future of antimicrobial diaminopyrimidines. *J Chemother*, **5**, 361-368.
- Thorndike, J., Pelliniemi, T.T., and Beck, W.S. (1979) Serine hydroxymethyltransferase activity and serine incorporation in leukocytes. *Cancer Res*, **39**, 3435-3440.
- Toney, M., and Kirsch, J.F. (1987) Tyrosine 70 increases the coenzyme affinity of aspartate aminotransferase. A site-directed mutagenesis study. *J Biol Chem*, **266**, 23900-23903.
- Toney, M.D. (2005) Reaction specificity in pyridoxal phosphate enzymes. *Arch Biochem Biophys*, **433**, 279-287.
- Toney, M.D., and Kirsch, J.F. (1991a) The K258R mutant of aspartate aminotransferase stabilizes the quinonoid intermediate. *J Biol Chem*, **266**, 23900-23903.
- Toney, M.D., and Kirsch, J.F. (1991b) Tyrosine 70 fine-tunes the catalytic efficiency of aspartate aminotransferase. *Biochemistry*, **30**, 7456-7461.
- Toney, M.D., and Kirsch, J.F. (1993) Lysine 258 in aspartate aminotransferase: Enforcer of the circe effect for amino acid substrates and general-base catalyst for the 1,3-prototropic shift. *Biochemistry*, **32**, 1471-1479.

- Toney, M.D., Pascarella, S., and De Biase, D. (1995) Active site model for gamma-aminobutyrate aminotransferase explains substrate specificity and inhibitor reactivities. *Protein Sci*, **4**, 2366-2374.
- Trivedi, V., Gupta, A., Jala, V.R., Saravanan, P., Rao, J.G.S., Rao, N.A., Savithri, H.S., and Subramanya, H.S. (2002) Crystal structure of binary and ternary complexes of serine hydroxymethyltransferase from *Bacillus stearothermophilus*: Insights into the catalytic mechanism. *J Biol Chem*, **277**, 17161-17169.
- Tsuruo, T., Iida, H., Naganuma, K., Tsukagoshi, S., and Sakurai, Y. (1983) Promotion by verapamil of vincristine responsiveness in tumor cell lines inherently resistant to the drug. *Cancer Res*, **43**, 808.
- Ulevitch, R.J., and Kallen, R.G. (1977a) Purification and characterization of pyridoxal 5'-phosphate dependent serine hydroxymethylase from lamb liver and its action upon β -phenylserines. *Biochemistry*, **16**, 5342-5350.
- Ulevitch, R.J., and Kallen, R.G. (1977b) Studies of the reactions of lamb liver serine hydroxymethylase with L-phenylalanine: Kinetic isotope effects upon quinonoid intermediate formation. *Biochemistry*, **16**, 5350-5354.
- Ulevitch, R.J., and Kallen, R.G. (1977c) Studies of the reactions of substituted D,L-erythro-beta-phenylserines with lamb liver serine hydroxymethylase. Effects of substituents upon the dealdolization step. *Biochemistry*, **16**, 5355-5363.
- Ura, H., Harata, K., Matsui, I., and Kuramitsu, S. (2001) Temperature dependence of the enzyme-substrate recognition mechanism. *J Biochem*, **129**, 173-178.
- Vacca, R.A., Christen, P., Malashkevich, V.N., Jansonius, J.N., and Sandmeier, E. (1995) Substitution of apolar residues in the active site of aspartate aminotransferase by histidine. Effects on reaction and substrate specificity. *Eur J Biochem*, **227**, 481-487.
- Vacca, R.A., Giannattasio, S., Graber, R., Sandmeier, E., Marra, E., and Christen, P. (1997) Active-site arg --> lys substitutions alter reaction and substrate specificity of aspartate aminotransferase. *J Biol Chem*, **272**, 21932-21937.
- Vatsyayan, R., and Roy, U. (2007) Molecular cloning and biochemical characterization of *Leishmania donovani* serine hydroxymethyltransferase. *Protein Expr Purif*, **52**, 433-440.
- Vidal, L., Calveras, J., Clapes, P., Ferrer, P., and Caminal, G. (2005) Recombinant production of serine hydroxymethyltransferase from *Streptococcus thermophilus* and its preliminary evaluation as a biocatalyst. *Appl Microbiol Biotechnol*, **68**, 489-497.
- Volm, M. (1998) Multidrug resistance and its reversal. *Anticancer Res*, **18**, 2905-2917.

- Watanabe, A., Kurokawa, Y., Yoshimura, T., Kurihara, T., Soda, K., and Esaki, N. (1999a) Role of lysine 39 of alanine racemase from *Bacillus stearothermophilus* that binds pyridoxal 5'-phosphate. Chemical rescue studies of Lys39 --> Ala mutant. *J Biol Chem*, **274**, 4189-4194.
- Watanabe, A., Kurokawa, Y., Yoshimura, T., and Esaki, N. (1999b) Role of tyrosine 265 of alanine racemase from *Bacillus stearothermophilus*. *J Biochem*, **125**, 987-990.
- Webb, H.K., and Matthews, R.G. (1995) 4-chlorothreonine is substrate, mechanistic probe, and mechanism-based inactivator of serine hydroxymethyltransferase. *J Biol Chem*, **270**, 17204-17209.
- Weiner, M.P., Costa, G.L., Schoettlin, W., Cline, J., Mathur, E., and Bauer, J.C. (1994) Site-directed mutagenesis of double-stranded DNA by the polymerase chain reaction. *Gene*, **151**, 119-123.
- White, F.L., and Olsen, K.W. (1987) Effects of cross linking on the thermal stability of hemoglobin. *Arch Biochem Biophys*, **258**, 51-57.
- Whitehead, E. (1970) The regulation of enzyme activity and allosteric transition. *Progress Biophys*, **21**, 321 - 397.
- William, B.P., Raymond, W.R., William, D.E., and Janathan, M. (1994) The anticancer drugs. Eds B.P. William, W.R. Raymond, D.E. William, and M. Janathan, in *The anticancer drugs*, 183-98. Oxford university press, UK.
- Yadav, J.S., Chandrasekhar, S., Ravindra Reddy, Y., and Rama Rao, A.V. (1995) Synthesis of (2R,3S)-3-hydroxy leucine: A constituent of lysobactin. *Tetrahedron*, **51**, 2749-2754.
- Yang, J.T., Wu, C.S., and Martinez, H.M. (1986) Calculation of protein conformation from circular dichroism. *Meth Enzymol*, **130**, 208 - 269.
- Yennawar, H.P., Yennawar, N.H., and Farber, G.K. (1995) A structural explanation for enzyme memory in nonaqueous solvents. *J Am Chem Soc*, **117**, 577-585.
- Young-Joon, S. (2002) Anti-tumor promoting potential of selected spice ingredients with antioxidative and anti-inflammatory activities: A short review. *Food and Chem Toxicol*, **40**, 1091-1097.
- Ziak, M., Jager, J., Malashkevich, V.N., Gehring, H., Jaussi, R., Jansonius, J.N., and Christen, P. (1993) Mutant aspartate aminotransferase (K258H) without pyridoxal-5'-phosphate-binding lysine residue - structural and catalytic properties. *Eur J Biochem*, **211**, 475-484.
- Ziak, M., Jaussi, R., Gehring, H., and Christen, P. (1990) Aspartate aminotransferase with the pyridoxal-5'-phosphate-binding lysine residue replaced by histidine retains partial catalytic competence. *Eur J Biochem*, **181** 329-333.